ANA MARGARIDA DA SILVA VILAS-BOAS

PALYNOLOGY OF THE TRIASSIC - JURASSIC OF THE SILVES GROUP IN PORTUGAL - ITS IMPLICATIONS ON A CHANGING WORLD

UAlg FCT
UNIVERSIDADE DO ALGARVE
FACULDADE DE CIÊNCIAS E TECNOLOGIA

University of Algarve
Faculty of Sciences and Technology
2023

ANA MARGARIDA DA SILVA VILAS-BOAS

PALYNOLOGY OF THE TRIASSIC - JURASSIC OF THE SILVES GROUP IN PORTUGAL - ITS IMPLICATIONS ON A CHANGING WORLD

PhD In Marine, Earth and Environmental Sciences,
Branch Geosciences
Specialty in Geology

Work carried out under the guidance of:

Professor Doutor Paulo Fernandes
(UAlg – Universidade do Algarve)

Doutora Zélia Pereira
(LNEG – Laboratório Nacional de Energia e Geologia)

Professora Doutora Simonetta Cirilli
(UniPG - Università degli Studi di Perugia)

University of Algarve
Faculty of Sciences and Technology
2023

Caption of the photomicrography in the cover:
Cluster *Classopollis torosus* Reissinger, 1950, Pereiros Formation, lower Hettangian, Lower Jurassic, sample LAM 12, Lusitanian Basin

PALYNOLOGY OF THE TRIASSIC - JURASSIC OF THE SILVES GROUP IN PORTUGAL - ITS IMPLICATIONS ON A CHANGING WORLD

Statement of Work Authorship

I declare to be the author of this work, which is unique and unprecedented. Authors and works consulted are properly cited in the text and are included in the listing of references included.

Ana Margarida da Silva Vilas-Boas

Copyright

Aos meus Pais, Irmãos, Avós e Renato.

“I am among those who think that science has great beauty.”

Marie Curie

Acknowledgements/ Agradecimentos

I want to thank all the people who crossed my path and who, in some way contributed to the execution of this work. In particular, to my supervisors Professor Doctor Paulo Fernandes, Doctor Zélia Pereira and Professor Doctor Simonetta Cirilli to whom I address my first words.

I express deep gratitude to my supervisors for all the support they have given me throughout this time and for all the knowledge they have transmitted. I would also like to thank you for the great experience you provided and for never leaving me helpless. They introduced me to new realities and enriched me professionally and personally. Thank you very much for your time, and for being the inspiring people you are. Thank you so much for your trust in me and my work in this big, beautiful world of pollens and spores. To you, my greatest thanks, and may our friendship endure.

Secondly, to the Foundation for Science and Technology for granting me a PhD scholarship (SFRH/BD/144125/2019), essential for this research project.

I would like to thank the facilities at the CIMA-UAlg laboratory, in Faro, LNEG, in São Mamede Infesta, Porto and UniPG, in Perugia, Italy, for welcoming me to their facilities.

To Professor Doutor Luís Vítor Duarte, who, even though he was not directly linked to the Ph.D. project, was the one who "pushed" me into this world of Palynology and was never able to disconnect again. A huge thank you.

To Irene, for helping me with the laboratory preparation of some of the samples.

To Sérgio Sêco, for helping to decipher the geology of the Lusitanian Basin.

To Márcia Mendes, for sharing her extensive palynological knowledge.

To Nuno and Belinha, eternal friends, who, despite the few times we manage to reconcile our lives and manage to meet, are people I know I will never lose in my life.

To Julian Oswald, who was always there to listen and for his friendly words that improved the tensest moments. Even far away, he was always there to tell me something that made me smile!

A toda a minha família que sempre esteve ao meu lado, sempre me apoiou e sempre demonstrou orgulho pela minha jornada. Obrigado a todos!

Aos meus pais e irmãos, pelo apoio e compreensão incondicional. Obrigado pelo vosso carinho e amor. Obrigada a vocês, que sempre acreditaram em mim e na minha capacidade, mesmo quando eu não acreditei. Eu sei que posso contar com vocês para sempre. A vocês dedico esta etapa da minha vida. Sem vocês nada disto teria sido possível. Muito obrigado!

Aos meus avós, por serem simplesmente os melhores avós de todos os tempos.

To Renato Godinho, thank you for the patience and affection you showed in my most complicated and happiest moments. Without you, everything would have been much more complicated. Thank you for being there to give me strength and always with the right word. A huge thank you!

I want to thank everyone who went through this stage in my life, helping me overcome all the difficult moments.

To all of you, my biggest thank you.

Obrigada a todos!

Abstract

The biostratigraphy of the Lusitanian and Algarve basins is based on macrofossils and microfossils (foraminifers, nannofossils, and ostracods). Compared to these works, palynological studies are rare in these basins. Palynomorphs are a powerful biostratigraphic and paleoenvironmental tool, and their research could significantly contribute to the context of the two basins. In this project, the Upper Triassic and Lower Jurassic of the Lusitanian and Algarve basins were studied.

In the Lusitanian Basin, twelve sections were sampled, all in Coimbra and Miranda do Corvo: Lamas I, Lamas II, Castelo Viegas I, Castelo Viegas II, IdealMed, Alto de São João, Parque de Campismo, Sobral Cid, Carvalhais, Redonda, Lordemão and Eiras. A total of 122 samples were collected in these sections and studied in detail.

In the Algarve Basin, fifteen sections were sampled throughout the entire basin: Vale de Fuzeiros, Bengado, International Racetrack of Algarve, Marco, Loulé Rock Salt Mine, Santa Rita, Amorosa, Amado's Beach, Rocha da Pena, Bodega, Barragem do Funcho, Santa Catarina Fonte do Bispo, Fonte da Pedra, Diapiro de Albufeira and Ayamonte. Full amount of 254 samples were collected in these sections and studied in detail.

Six boreholes were sampled: Golfinho-1, Santiago do Cacém-3, Santiago do Cacém-42, Santiago do Cacém-61, Campelos-1, and Lula-1, performing 122 samples collected from these boreholes and studied in detail.

The data obtained in the Lusitanian Basin allowed improving the dating of the units of the Silves Group, from the oldest to the most recent: Conraria Formation, Penela Formation, Castelo Viegas Formation, and Pereiros Formation.

The co-occurrence of typical Norian and Rhaetian palynomorphs, such as *Classopollis meyerianus, Granuloperculatipollis rudis, Patinasporites densus, Vallasporites ignacii, Duplicisporites granulatus, Paracirculina quadruplicis,* and *Praecirculina granifer*, allowed the Conraria Formation, at the base of the Silves

Group, to be dated from the Norian to lower Rhaetian. Based on the palynological content, proposing the informal *Classopollis meyerianus-Granuloperculatipollis rudis* palynozone for the Conraria Formation was possible.

Two informal palynozones are proposed for the Pereiros Formation: *Ischyosporites variegatus-Kraeuselisporites reissingeri* and *Pinuspollenites minimus*. The informal palynozone *Ischyosporites-variegatus-Kraeuselisporites reissingeri* is associated with the upper Rhaetian due to the presence of *Classopollis meyerianus, Classopollis torosus* together with index species of this age, such as *Ischyosporites variegatus, Kraeuselisporites reissingeri,* and *Rhaetipollis germanicus*. The informal palynozone *Pinuspollenites minimus* is defined based in the first occurrence of *Pinuspollenites minimus* and *Perinopollenites elatoides,* accompanied by the dominance of *Classopollis meyerianus* and *Classopollis torosus*, dating from the base of the Hettangian. Therefore, based on the palynological association obtained in these two informal palynozones, it is possible to date the Pereiros Formation as being upper Rhaetian to lower Hettangian and conclude that the Triassic-Jurassic transition occurs at the base of this formation within the informal *Ischyosporites variegatus-Kraeuselisporites reissingeri* palynozone.

The absence of palynological data from the Penela and Castelo Viegas formations due to not favorable lithologies to palynological studies did not allow for a review and improvement in the precision of the age associated with these formations. However, considering their stratigraphic position, sandwiched between the Conraria Formation (Norian – early Rhaetian) and the Pereiros Formation (late Rhaetian – earliest Hettangian), these formations would date, indirectly, from the Rhaetian.

In conclusion, the palynological associations obtained in the Lusitanian Basin made it possible to date the formations of the Silves Group from the Norian to the Hettangian.

To identify the limit between the Triassic and Jurassic in the Lusitanian Basin, new samples were collected in the most basal part of the Pereiros Formation. The palynological content obtained, such as the spores *Calamospora*

tener, Ischyosporites variegatus, Kraeuselisporites reissingeri, and *Porcellispora longdonensis,* and the pollen grains *Alisporites* sp., *Perinopollenites elatoides,* and *Pinuspollenites minimus*, allowed confirming the Hettangian age for the base of this formation. The presence of foraminiferal linings in the basal part of the Pereiros Formation documents, the first marine incursion event that occurred in the Lusitanian Basin. These data allow us to interpret this unit as deposited in an estuary environment and suggest a small marine transgression episode. The middle part of this formation is interpreted as a coastal plain environment dominated by fluvial sedimentation processes recording a small marine regression episode, and the top of Pereiros Formation as an evaporite tidal flat under hot, arid climatic conditions.

In the Algarve Basin, the Silves Group comprehends the units, from the oldest to the most recent: São Bartolomeu de Messines Clays, Silves Sandstones, Silves Marl-Carbonate Evaporitic Complex, and Volcano-Sedimentary Series.

For the first time, it is possible to associate an age interval with the Silves Group, ranging from the early Carnian to the early Hettangian, based on palynomorphs, including the Triassic-Jurassic transition, and to establish paleoenvironmental interpretations.

The most basal part of the Silves Sandstones was sampled, and its palynological association, which comprised *Aulisporites astigmosus, Enzonalasporites vigens, Vallasporites ignacii,* and *Samaropollenites minimus*, allowed the base of this unit to be dated as early Carnian. These data will enable us to interpret that the beginning of sedimentation in the Algarve Basin occurred in the Late Triassic (early Carnian). The co-occurrence of taxa such as *Aulisporites astigmosus, Enzonalasporites vigens, Samaropollenites speciosus* and *Tulesporites briscoensis* (recorded for the first time in Iberia and Europe) indicates a mixture of microfloras with affinities from Central Europe and North America, in the Carnian, this data is consistent with the paleogeographic position of the Iberian Peninsula during the Late Triassic.

The new palynological data from this investigation indicate that the top of the Silves Sandstones unit dates from the late Carnian, the base of the Silves Marl-Carbonate Evaporitic Complex unit dates from the late Carnian and the top of this last unit dates from the late Rhaetian to the early Hettangian. From a paleoenvironmental point of view, the presence and rapid increase of algal spores (*Plaesiodictyon mosellanum* ssp. *variable*, *Plaesiodictyon mosellanum* ssp. *bullatum*, *Botryococcus* spp., and *Ovoidites* sp.) at the base of the Silves Marl-Carbonate Evaporitic Complex unit indicates the transition from alluvial depositional systems (Silves Sandstones) initially, to lacustrine environments, which later changed to arid coastlines. The consistent increase in xerophytic elements (e.g., pollens grains *Alisporites* spp., *Classopollis* spp., *Cerebropollenites* spp., and *Perinopollenites* spp.) indicates a shift to more arid and hot conditions for the top of the Silves Group, being consistent with lithofacies deposited in *sabkha* environment (evaporites).

For the first time, the Triassic-Jurassic transition is described based in palynomorph studies in the Algarve Basin at the top of the Silves Marl-Carbonate Evaporitic Complex in the Loulé Rock Salt Mine. The previous transition occurs in a mudstone layer, with ca. 1 m thick, interspersed with evaporites, and should correspond to a short period of interruption of the evaporite environment.

With this work, we propose an age of the Silves Group in the Lusitanian Basin, from the Norian – early Hettangian, and in the Algarve Basin from the lower Carnian to the early Hettangian, with the identification, for the first time, of the Triassic-Jurassic transition in Portugal.

The new lithostratigraphic schemes of the Silves Group for the Lusitanian and Algarve basins, together with the paleoenvironmental interpretations obtained with this investigation, are a significant contribution to the context of the Late Triassic and Early Jurassic in Portugal, especially for biostratigraphy.

Keywords: Palynology, Triassic, Jurassic, Lusitanian Basin, Algarve Basin, Triassic-Jurassic Boundary.

Resumo

O intervalo de tempo na fronteira Triássico-Jurássico representa uma fase crítica na história da Terra, marcada por mudanças tectónicas e globais: (1) o inicio da fragmentação da Pangeia; (2) grandes quantidades de evaporitos são depositados em áreas extensas de plataformas continentais (por exemplo, Península Ibérica, Norte de África (Buratti and Cirilli, 2007); (3) o clima no Triássico Superior é um dos mais quentes da história da Terra; (4) deposição de "red beds" e (5) sem gelo nas altas paleolatitudes (Hochuli and Vigran, 2010) Este intervalo de tempo está associado a uma das crises bióticas mais severas da história da Terra, a Extinção do Final do Triássico, que causou mudanças na flora e fauna nos ecossistemas continentais, e grandes extinções nos organismos do reino marinho (Whiteside *et al*., 2007; Bonis *et al*., 2010; Lindström, 2016; Lindström *et al*., 2017a, 2017b). O evento de Extinção do Final do Triássico é marcado por mudanças rápidas e abruptas dos paleoambientes e paleoecossistemas, e uma severa perda taxonómica de cerca de 40-73%, sendo considerada a terceira crise biótica mais grave da história da Terra (Lindström *et al*., 2017b). Várias causas explicativas desta crise biótica foram propostas, como por exemplo, os efeitos provocados pelo magmatismo da Província Magmática do Atlântico Central (PMAC), que levaram à subida dos níveis do CO_2 e do SO_2 atmosféricos, causando um agravamento do efeito estufa e um aquecimento global generalizado. Porém, ainda não foi resolvido se as erupções ocorreram antes (Marzoli *et al*., 1999, 2008), durante ou depois da Transição Triássico Jurássico (Whiteside *et al*., 2007). Estudos palinológicos mostraram que o vulcanismo da PMAC começou antes da Transição Triássico Jurássico e, assim, corroboram a hipótese de que essas erupções muito possivelmente influenciaram a crise biótica deste limite (Marzoli *et al*., 2008; Cirilli *et al*., 2009; Cirilli, 2010).

Em Portugal continental, as sucessões sedimentares de idade Triássico a Jurássico inferior, estão incluídas na unidade estratigráfica do Grupo de Silves, que afloram na Bacia Lusitânica no litoral centro, e na Bacia do Algarve no sul. No final do Triássico e início do Jurássico, o território de Portugal estava sobre movimentos tectónicos distensivos relacionados com a fragmentação da Pangeia associados à abertura do Oceano Atlântico. A Bacia Lusitânica, bacia

sedimentar Mesozóica, desenvolveu-se na Margem Ocidental Ibérica e caracteriza-se como uma bacia distensiva. A sua dinâmica tectónica está associada à fragmentação da Pangeia, especificamente à abertura do Atlântico Norte (Kullberg *et al*., 2013). A Bacia do Algarve desenvolveu-se durante o Mesozóico em regime tectónico de estiramento e adelgaçamento litosféricos relacionados com a abertura do Atlântico Central e a formação de crosta oceânica na parte ocidental do Mar de Tétis, entre o Algarve e o Norte de África (Terrinha *et al*., 2006).

Na Bacia Lusitânica o Grupo de Silves é constituída por diversas formações maioritariamente siliciclásticas que mostram fácies sedimentares indicadoras de ambientes continentais, sendo sobrepostas por uma unidade de natureza carbonatada (Formação de Pereiros) marcada na sua base, pela primeira incursão marinha (Camadas de *Isocyprina*) representando uma grande mudança dentro do ambiente sedimentar. A Formação de Pereiros depositou-se em ambientes litorais com forte influência da ação das marés (Palain, 1976; Soares *et al*., 2012; Kullberg *et al*., 2013). Na Bacia do Algarve as formações siliciclásticas do Grupo de Silves estão sobrepostas por rochas vulcânicas máficas pertencentes à PMAC (Martins *et al*., 2008).

Apesar de no Grupo de Silves, em Portugal, a fronteira Triássico-Jurássico baseada na palinostratigrafia ser ainda uma questão em discussão, verificou-se a existência de grandes mudanças na palinoflora nesta importante fronteira (Doubinger *et al*., 1970; Adloff *et al*., 1974; Díez, 2000; Arche and López-Gómez, 2014), corroborando a evidência para a Extinção do Fim do Triássico sobre ecossistemas terrestres. Tal descoberta lança dúvidas sobre as ideias clássicas acerca da dinâmica da Extinção do Final do Triássico e da recuperação dos ecossistemas terrestres no Jurássico Inferior. Apesar dos trabalhos recentes em Portugal (Díez, 2000; Vilas-Boas *et al*., 2021), existem ainda alguns aspetos desafiantes relativos à sequência estratigráfica que permanecem pouco definidos.

Neste trabalho descrevemos os estudos de palinologia e palinofácies do Grupo de Silves em Portugal para o reconhecimento da fronteira Triássico-

Jurássico, a idade dos estratos, as sucessões da flora, as alterações ambientais e a correlação dos estratos na Península Ibérica e Europa.

Os principais objetivos deste estudo de investigação são: (i) estabelecer o quadro palinostratigráfico do Triássico-Jurássico para o Grupo de Silves, documentando biozonas de pólenes e esporos e correlacionar o esquema palinostratigráfico obtido com outros do registo estratigráfico Ibérico e Europeu; ii) identificar e documentar, quer em afloramentos, quer em sondagens, utilizando a palinologia como principal ferramenta, a cronologia da Extinção do Final do Triássico e da Transição do Triássico – Jurássico do Grupo de Silves nas bacias Lusitânica e do Algarve; iii) empregar estudos de palinofácies para reconstruir palinofloras, sucessões de palinofloras e paleoambientes de deposição dentro do registo estratigráfico do Grupo de Silves, a fim de melhor avaliar as alterações paleoclimáticas durante a deposição do Grupo de Silves; iv) documentar palinomorfos de morfologia anormal para avaliar possível poluição ambiental antiga e as suas causas (emissões vulcânicas de SO_2, CO_2, e Hg, aumento da radiação UV-B, entre outros fatores); v) obter um quadro cronostratigráfico credível estabelecido pela palinologia; vi) estabelecer e comparar as mudanças paleoambientais/paleoclimáticas globais do Triássico-Jurássico em Portugal com as mudanças ambientais/climáticas registadas em outros locais do Mundo nesse tempo geológico e vii) contribuir para os conhecimentos paleoambientais e paleogeográficos das bacias Lusitânica e do Algarve, ao longo dos períodos Triássico e Jurássico, durante as primeiras fases de abertura do Oceano Atlântico Norte, com principal base na dispersão de pólenes e esporos.

Esporos e pólenes fazem parte do grupo dos palinomorfos. Palinomorfos são estruturas microscópicas de plantas e animais construídas com substâncias muito resistentes à maioria das formas de degradação além da oxidação, como a esporopolenina, a dinosporina ou compostos relacionados. São abundantes na maioria dos sedimentos e rochas sedimentares e são resistentes a ácidos fortes, bases, acetólise e separação por líquidos densos. Os palinomorfos deixaram um importante registo fóssil nas rochas e são, assim, importantes marcadores biostratigráficos e paleoambientais.

Neste trabalho foram amostradas e estudadas 498 amostras de rochas do Triássico Superior e do Jurássico Inferior das bacias Lusitânica e do Algarve, das quais 65 foram positivas para estudos palinológicos. Análises palinológicas e de palinofácies foram efetuadas nas amostras que foram recolhidas em afloramento e sondagem. As 122 amostras recolhidas na Bacia Lusitânica compreendem o estudo de 12 afloramentos nas regiões de Coimbra e Miranda do Corvo: Parque de Campismo, Alto de São João, Sobral Cid, Castelo de Viegas I, Castelo de Viegas II, Lordemão, IdealMed, Lamas I, Lamas II, Carvalhais, Redonda e Eiras. Na Bacia do Algarve foram recolhidas 254 amostras em 15 afloramentos: Vale de Fuzeiros e Amorosa (São Bartolomeu de Messines), Bengado (São Brás de Alportel), Fonte da Pedra e Autódromo Internacional do Algarve (Portimão), Marco (Santa Catarina Fonte do Bispo), Mina de Sal-Gema (Loulé), Santa Rita e Bodega (Tavira), Praia do Amado (Aljezur), Rocha da Pena (Penina), Barragem do Funcho (Silves), Santa Catarina Fonte do Bispo, Diapiro de Albufeira e Ayamonte (Espanha). Por fim, foram recolhidas um total de 122 amostras das sondagens: Golfinho-1, Santiago do Cacém-3, Santiago do Cacém-42, Santiago do Cacém-61, Campelos-1 e Lula-1.

Com a análise das amostras recolhidas na Bacia Lusitânica foi possível melhorar a datação das formações do Grupo de Silves nesta bacia. As formações que pertencem ao Grupo de Silves na Bacia Lusitânica são da mais antiga para a mais recente, Formação da Conraria, Formação de Penela, Formação de Castelo Viegas e Formação de Pereiros. Com os dados obtidos a partir de uma primeira campanha de campo efetuada nestas quatro formações foi possível propor uma palinozonação informal e restringir idades biostratigráficas para estas formações. A coocorrência de palinomorfos típicos do Noriano e do Retiano, tais como *Classopollis meyerianus, Granuloperculatipollis rudis, Patinasporites densus, Vallasporites ignacii, Duplicisporites granulatus, Paracirculina quadruplicis e Praecirculina granifer* permitiram datar a Formação da Conraria, na base do Grupo de Silves, do Noriano ao Retiano inferior. Da associação palinológica obtida dos afloramentos pertencentes a esta formação foi possível propor a palinozona informal *Classopollis meyerianus-Granuloperculatipollis rudis.* O conteúdo palinológico obtido a partir das amostras recolhidas nos afloramentos pertencentes à Formação de Pereiros permitiram

reconhecer duas palinozonas informais *Ischyosporites variegatus-Kraeuselisporites reissingeri* e *Pinuspollenites minimus.* A palinozona informal *Ischyosporites-variegatus-Kraeuselisporites reissingeri* é associada ao Retiano superior devido à presença de *Classopollis meyerianus, Classopollis torosus* em conjunto com espécies índex desta idade, tais como, *Ischyosporites variegatus, Kraeuselisporites reissingeri* e *Rhaetipollis germanicus.* Esta associação palinológica é facilmente comparável com associações bem documentadas em outros países, tais como, Itália, (Cirilli *et al*., 1994, 2015, 2018; Galli *et al*., 2007; Martini *et al*., 2007), Tunísia, Líbia, Argélia e Marrocos (Adloff *et al*., 1986; Yaroshenko, 2007; Cirilli, 2010) entre outros. A palinozona informal *Pinuspollenites minimus* é definida pela primeira ocorrência de *Pinuspollenites minimus e Perinopollenites elatoides,* acompanhado pelo domínio de *Classopollis meyerianus* e *Classopollis torosus,* datando da base do Hetangiano. Esta palinozona é facilmente correlacionada com zonações palinológicas existentes na Alemanha e Suécia (Van de Schootbrugge *et al*., 2009; Hillebrandt *et al*., 2013; Schobben *et al*., 2019.) Deste modo, tendo por base a associação palinológica obtida nestas duas palinozonas informais é possível datar a Formação de Pereiros como sendo Retiano superior ao Hetangiano inferior. Permitindo concluir que a transição Triássico-Jurássico ocorre na base desta formação, dentro da palinozona informal *Ischyosporites variegatus-Kraeuselisporites reissingeri.* A ausência de dados palinológicos das formações de Penela e Castelo Viegas, devido às litologias não favoráveis aos estudos palinológicos não possibilititaram uma revisão e melhoria na precisão da idade associada a essas formações. No entanto, tendo em conta a posição estratigráfica das mesmas, encaixadas entre a Formação de Conraria (Noriano–?Retiano inferior) e a Formação de Pereiros (Retiano superior–base do Hetangiano) estas formações datariam, indiretamente, do Retiano. Concluindo, as associações palinológicas obtidas na Bacia Lusitânica, nesta primeira campanha, permitiram datar as formações do Grupo de Silves do Noriano ao Hetangiano. É de salientar, a rara presença de pólenes e tétradas com morfologia anormal. Estas características podem estar associadas a episódios de *stress* ambiental relacionados com poluição atmosférica natural por mercúrio de origem vulcânica que geraram mutações nas plantas terrestres no fim do Triássico (Kürschner *et al*., 2013; Lindström *et al*., 2019.) No entanto, estas

anomalias morfológicas, na Bacia Lusitânica, foram identificadas do Noriano ao Retiano inferior e não na transição Triássico-Jurássico, o que pode indicar que neste setor da Pangeia o PMAC se instalou mais cedo, tal como é evidenciando em Marrocos (Panfili *et al*., 2019). Imediatamente acima da base do Hetangiano é possível identificar várias tétradas de *Classopollis* spp. sugerindo um segundo episódio de *stress* ambiental na bacia. Este segundo evento pode estar associado à influência do PMAC do Nordeste da América (Whiteside *et al*., 2007, 2010; Cirilli *et al*., 2009).

A presença de *hiatus* e descontinuidades na sequência estratigráfica e a ausência de fácies favoráveis a estudos palinológicos, fez com que fosse necessária uma segunda campanha para melhorar e tentar preencher essas lacunas. A segunda campanha foi efetuada com o objetivo de identificar e detalhar a transição Triássico-Jurássico e melhorar a datação das formações em que anteriormente não foram obtidos resultados. Apesar de ter sido reforçada a amostragem na Formação de Castelo Viegas, as amostras recolhidas na mesma voltaram a ser estéreis do ponto de vista palinológico, não permitindo melhorar a datação dessa formação. Segundo Palain (1976), a Formação de Pereiros está dividida em três unidades, a parte basal, unidade B2, e as porções média e superior, unidades C1 e C2, respetivamente. Foram recolhidas amostras na parte mais basal da Formação de Pereiros (unidade B2), com o objetivo da identificação do limite entre o Triássico e o Jurássico na Bacia Lusitânica, mas, no entanto, a associação palinológica obtida nas amostras da segunda campanha voltaram a datar a base da Formação de Pereiros (unidade B2) como sendo base do Hetangiano. Esta idade é confirmada pela presença dos esporos *Calamospora tener, Ischyosporites variegatus, Kraeuselisporites reissingeri* e *Porcellispora longdonensis* e os pólenes *Alisporites* sp., *Perinopollenites elatoides* e *Pinuspollenites minimus*. É de salientar a presença de forros de foraminíferos na unidade B2 (Palain, 1976) da Formação de Pereiros documentando nesta unidade o primeiro evento de incursão marinha ocorrido na Bacia Lusitânica. Estes dados permitem interpretar esta unidade como tendo sido depositada num ambiente de estuário e sugerem um pequeno evento de transgressão marinha. A unidade C1 (Palain, 1976) é interpretada como um ambiente de planície costeira dominado por processos de sedimentação fluvial

registando um pequeno evento de regressão marinha. A última unidade da Formação de Pereiros (unidade C2 de Palain, 1976), data do Hetangiano, devido à presença dos pólenes *Perinopollenites elatoides, Pinuspollenites minimus* e o domínio de *Classopollis meyerianus*. Os estudos de palinofácies apontam para uma planície de maré evaporítica sob condições climáticas quentes e áridas.

Na Bacia do Algarve o Grupo de Silves, depositou-se em discordância angular sobre as sequências de tipo *flysch* do Carbonífero da Zona Sul Portuguesa, dobradas e falhadas durante a Orogenia Varisca. O Grupo de Silves representa a fase de sedimentação mais antiga, associada ao início das fases de *rifting* continental da Pangeia. As unidades que constituem o Grupo de Silves na Bacia do Algarve são, da mais antiga para a mais recente: Argilas de São Bartolomeu de Messines, Arenitos de Silves, Complexo Margo-Calcário Evaporítico de Silves e Série Vulcano-Sedimentar. A parte mais basal dos Arenitos de Silves foi amostrada e a sua associação palinológica, que compreendia *Aulisporites astigmosus, Enzonalasporites vigens, Vallasporites ignacii* e *Samaropollenites minimus* permitiu datar a base desta unidade como sendo Carniano inferior. Estes dados permitem interpretar que o início da sedimentação na Bacia do Algarve ocorreu no Triássico Superior (Carniano inferior). A ocorrência conjunta dos taxa *Aulisporites astigmosus, Enzonalasporites vigens, Samaropollenites speciosus* e *Tulesporites briscoensis* (registado pela primeira vez na Ibéria e Europa) indicam uma mistura de microfloras com afinidades da Europa Central e do Norte da América, no Carniano, sendo este dado consistente com a posição paleogeográfica da Península Ibérica durante Triássico Superior.

Os dados obtidos a partir dos estudos das amostras recolhidas nas secções de Amorosa, Praia do Amado, Mina de Sal-Gema de Loulé e Diapiro de Albufeira permitiram melhorar a datação das unidades do Grupo de Silves na Bacia do Algarve, e fazer interpretações paleoambientais das mesmas. Pela primeira vez é possível associar um intervalo de idade ao Grupo de Silves, distribuindo-se desde Carniano inferior ao Hetangiano inferior, incluindo a transição Triássico-Jurássico. Os novos dados desta investigação indicam que o topo da unidade dos Arenitos de Silves data do Carniano superior, a base da unidade Complexo Margo-carbonatado Evaporítico de Silves data do Carniano

superior e a topo desta última unidade data do Retiano superior ao Hetangiano inferior. A presença e rápido aumento de esporos de algas (*Plaesiodictyon mosellanum* spp. *variable, Plaesiodictyon mosellanum* spp. *bullatum, Botryococcus* spp., e *Ovoidites* sp.) na base da unidade Complexo Margo-carbonatado Evaporítico de Silves indicam a transição de sistemas de deposição aluvionares (Arenitos de Silves) para ambientes lacustres inicialmente, que depois mudaram para linhas de costa áridas. O consistente aumento de elementos xerofíticos (por exemplo os pólenes *Alisporites* spp., *Classopollis* spp., *Cerebropollenites* spp. e *Perinopollenites* spp.) indicam uma mudança para condições mais áridas e quentes para o topo do Grupo de Silves, sendo consistente com litofácies depositadas em ambiente de *sabkha* (evaporitos). É, pela primeira vez, descrita a transição Triássico-Jurássico na Bacia do Algarve no topo do Complexo Margo-Carbonatado na Mina de Sal-Gema de Loulé. A transição anterior ocorre numa camada de argilitos, com ca. 1 m de espessura, intercalada com os evaporitos, e deverá corresponder a um curto intervalo de tempo de interrupção do ambiente evaporítico.

Com este trabalho propomos para o Grupo de Silves, na Bacia Lusitânica, uma idade com base em palinomorfos do Noriano – Hetangiano inferior, e na Bacia do Algarve uma idade com base em palinomorfos do Carniano inferior ao Hetangiano inferior, com a identificação, pela primeira vez da transição Triássico-Jurássico em Portugal.

Os novos esquemas litostratigráficos do Grupo de Silves para as bacias Lusitânica e do Algarve, em conjunto com as interpretações paleoambientais obtidos com este trabalho, são uma contribuição significativa para o contexto do Triássico Superior e Jurássico Inferior em Portugal, especialmente para a biostratigrafia.

Palavras-Chave: Palinologia, Triássico, Jurássico, Bacia Lusitânica, Bacia do Algarve, Transição Triássico-Jurássico.

Contents

List of Figures

List of Plates

List of Tables

List of acronyms and abbreviations

AB – Algarve Basin

AF – Algibre Fault

AOM – Amorphous Organic Matter

ca. – *circa* (=about)

CAMP – Central Atlantic Magmatic Province

e.g. – *exempli gratia* (=for exemple)

FA – First Appearance

FAD – First Appearance Datum

FO – First Occurrence

GSSP – Global boundary Stratotype Section and Point

HCl – Hydrochloric acid

HF – Hydrofluoric acid

i.e. – *id est* (=that is)

LA – Last Appearance

LAD – Last Appearance Datum

LB – Lusitanian Basin

LO – Last Occurrence

m – meters

Ma – mega annum

PTFAF – Porto-Tomar-Ferreira do Alentejo Fault

SMSQF – São Marcos da Serra-Quarteira Fault

TJB – Triassic - Jurassic Boundary

CHAPTER I

General Introduction

Chapter I cover:

Praia do Amado section, Aljezur, Late Triassic, Algarve Basin

Chapter I. General Introduction

1. Structure of the thesis

The present Ph.D. thesis is based on four scientific papers. Two works are published and available online in indexed journals. The third article was accepted for publish, and the fourth one was already submitted to indexed journals. Those papers are listed and numbered as below:

Paper 1

Vilas-Boas, M., Pereira, Z., Cirilli, S., Duarte, L. V., Fernandes, P. 2021. New data on the palynology of the Triassic–Jurassic boundary of the Silves Group, Lusitanian Basin, Portugal. Review of Palaeobotany and Palynology, 290, 104426. https://doi.org/10.1016/j.revpalbo.2021.104426. Quartile 2.

Paper 2

Vilas-Boas, M., Pereira, Z., Cirilli, S., Duarte, L.V., Sêco, S.L.R., Fernandes, P. Palynology and palynofacies studies in the lowermost Jurassic of the Lusitanian Basin (Pereiros Formation of the Silves Group), Portugal: evidence of the first transgressive episode. Accepted to Acta Paleobotanica. Quartile 2.

Paper 3

Vilas-Boas, M., Paterson, N. W., Pereira, Z., Fernandes, P., & Cirilli, S. (2022). The age of the first pulse of continental rifting associated with the breakup of Pangea in Southwest Iberia: new palynological evidence. Journal of Iberian Geology, 48(2), 181-190. https://doi.org/10.1007/s41513-022-00189-0. Quartile 2.

Paper 4

Vilas-Boas, M., Pereira, Z., Cirilli, S. and Fernandes, P. New Insights on the Upper Triassic Silves Group in Algarve Basin, Portugal: Palynological, paleophytogeography and paleoclimatology advances. Submitted to Geobios. Quartile 2.

In Chapter I, besides the thesis structure, some significant themes that aid comprehension of the theme studied and discussed in this Ph.D. work are briefly introduced, such as the motivation that drove us to undertake this project and the main objectives. This chapter also includes a comprehensive introduction to basic palynomorph elements, sampling field trips, and laboratory and office procedures.

Chapter II is particularly dedicated to new palynological data from the material collected in the Lusitanian Basin. These local data are compared with other sections from the Triassic – Jurassic boundary and discussed in the European context. This chapter is based on the work presented in the paper 1. In paper 1 the Silves Group's composite Upper Triassic to Lower Jurassic succession is presented, and the results obtained from nine sections of the Lusitanian Basin are discussed and correlated.

Chapter III, based on paper 2, reports new information about the palynostratigraphy and paleoenvironmental interpretations of the Lower Jurassic in the Lusitanian Basin. These data were obtained from palynological and palynofacies studies. The biostratigraphical information of Chapter II is also integrated here (but not pictured) and quoted as “Vilas-Boas *et al*., (2021)”, corresponding to paper 1.

The lower part of the Upper Triassic was sampled in the Algarve Basin, and the palynostratigraphy, mainly based on sporomorphs, is presented in Chapter IV. The presence of certain species of sporomorphs allowed making correlations with the palynoflora of Central Europe and North America and to collect more information about the paleogeographic position of the Iberian Peninsula in the Late Triassic. This data is based on the paper 3.

In Chapter V, the palynological data recovered from four sections along the Algarve Basin allowed the reconstruction of the whole succession of the Silves Group. The correlation between palynomorphs and their palynological affinities allowed some paleoclimatic and paleoenvironmental inferences. Paleophytogeographic implications were also analysed based on the microflora.

Organic maturation studies were conducted in some samples from the Lusitanian Basin. The obtained results and respective interpretations are presented in chapter VI.

The most significant conclusions of this Ph.D. study are summarised in Chapter VII. The value of this effort to scientific background and geological applications in the Lusitanian and Algarve basins is also appraised here. In this chapter, some ideas for future palynological studies in these basins and Silves Group are presented. Two appendices are presented at the end. Appendix 1 presents the list of all the taxa recovered from all the sections studied in this Ph.D. work. In Appendix 2 plates are presented to illustrate selected palynomorphs from the Upper Triassic to Lower Jurassic from the Lusitanian and Algarve basins.

2. State of Art and Scientific Problem

The Triassic-Jurassic time interval represents a critical phase in the Earth's history, marked by tectonic and global changes: the Pangea begins to break-up, large amounts of evaporites accumulated over enormous areas (e.g., Iberia, North Africa; Buratti and Cirilli, 2007), the Upper Triassic Climate is one of the hottest in Earth's history, with red beds deposition and no ice in the high paleolatitudes (Hochuli and Vigran, 2010). This time interval is associated with one of the most severe biotic crises on Earth, the End Triassic Extinction, which caused major floral and fauna turnovers on land, and major extinctions in the marine realm (Whiteside *et al*., 2007; Bonis *et al*., 2010; Lindström, 2016; Lindström *et al*., 2017a, 2017b). The End Triassic Event is marked by rapid and abrupt changes in the palaeoenvironments and palaeoecossystems and a taxonomic severity of about 40-73% loss in diversity, being considered the third most severe crisis (Lindström *et al*., 2017b).

Several causes have been proposed: the effects of the CAMP, with the rise in CO_2 and SO_2 causing a severe greenhouse effect and a generalised global warming (Marzoli *et al*., 1999, 2008). Although, it remains to be resolved if the eruptions occurred before (Marzoli *et al*., 1999, 2008). or after the Triassic-Jurassic Boundary (Whiteside *et al*., 2007). Palynological studies have shown

that CAMP volcanism started before the TJB and, thus, corroborating the hypothesis of these eruptions possibly having an influence on the biotic crisis of this limit (Marzoli *et al*., 2008; Cirilli *et al*., 2009; Cirilli, 2010).

The Silves Group represents the Triassic-Jurassic in Portugal and is present in the Lusitanian and Algarve basins.

The Lusitanian Basin (Fig. I.1) is a sedimentary basin formed in the Western Iberian Margin during the Mesozoic. Its genesis and history are linked to the various Pangea rifting events that resulted in the opening of the North Atlantic Ocean from the Middle?-Upper Triassic to the uppermost part of the Lower Cretaceous. Changes in Mesozoic sedimentary facies and thicknesses have allowed the Lusitanian Basin to be divided into three distinct sub-basins separated by large regional faults (Kullberg *et al*., 2013). The first is the Septentrional sector, which is limited to the south by the Nazaré Fault. The Nazaré Fault to the north and the Arrife Baixo-Vale Inferior Tejo fault system to the south define the Central sector. Finally, through the Torres Vedras-Montejunto fault, the Meridional sector develops to the south. The Lusitanian Basin successions extend offshore as well, as evidenced by seismic studies and numerous exploration wells. Four sequential rifting periods occurred before the creation of the first oceanic crust in the Aptian. The Lusitanian Basin strata represents these four rifting stages, resulting in four main sedimentary cycles of Triassic-Sinemurian age, Pliensbachian-Oxfordian age, Kimmeridgian-early Berriasian age, and late Berriasian-late Aptian age. The first cycle chronicles the transition from alluvial to lacustrine (evaporites) to shallow marine carbonate habitats. The second cycle is entirely made up of marine carbonates. The third cycle documents the transition from marine carbonates to deltaic and alluvial habitats, whereas the fourth cycle documents a mixture of shallow marine carbonates and clastic littoral-lacustrine environments. These sedimentary cycles are defined by disconformities or angular unconformities caused by tectonics and/or variations in sea level (Kullberg *et al*., 2013).

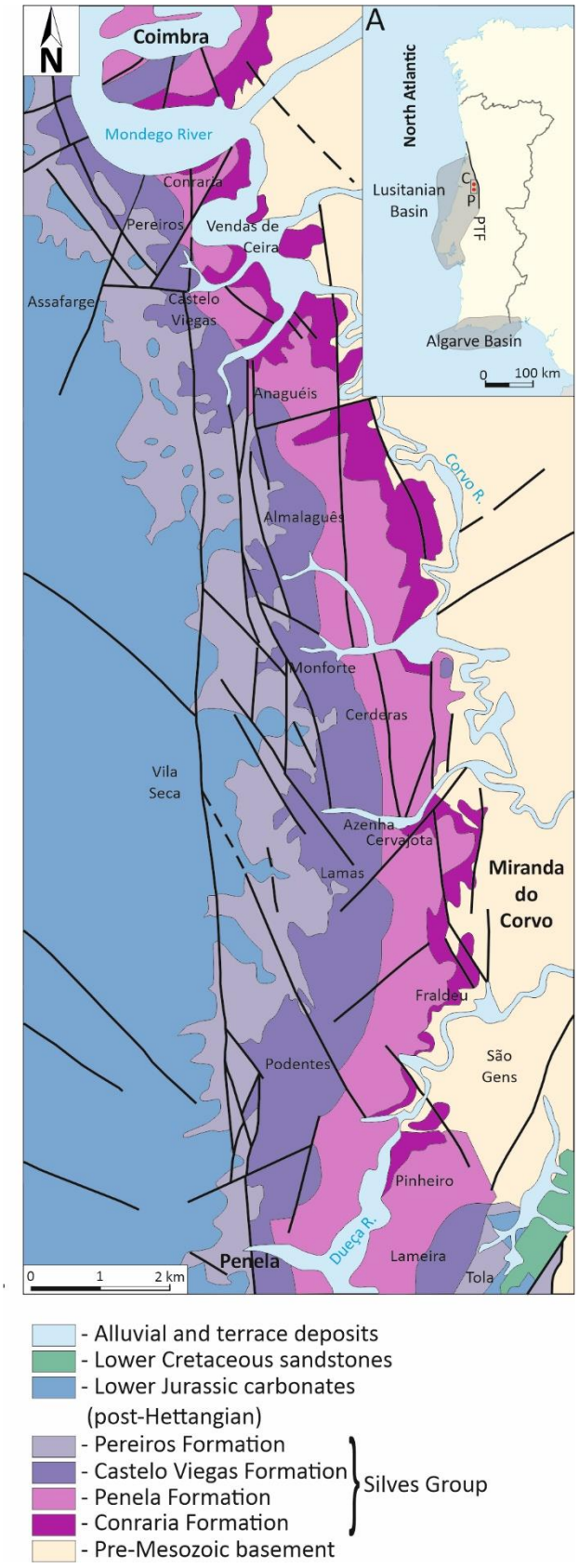

Figure I.1. Map of the studied area in the Lusitanian Basin (based on Soares *et al.*, 2012). **A.** Map of Portugal with the Lusitanian and Algarve basins signed. The square in the Lusitanian Basin represents the area studied in this research. C – Coimbra. P – Penela. PTF – Porto-Tomar Fault.

According to Fig. I.2, which shows the terminological evolution of the lithostratigraphy of the Triassic – extreme base of the Jurassic of the Lusitanian Basin, the base sediments are particularly materialised by conglomeratic deposits (term A1 of Palain, 1976) and their top by a complex unit of fine siliciclastic, evaporitic, and dolomitic sediments (term C2 of Palain, 1976). The lower contact of the Silves Group is made through an angular unconformity on the Hercynian base (essentially on the Black Series; however, north of Coimbra, it is based, locally, on the Permian) (Palain, 1976; Soares *et al*., 2005), which is made up of the Conraria, Penela, Castelo Viegas and Pereiros formations, where sediments associated with river and lagoon environments predominate (Soares *et al*., 2012). Superiorly, the Silves Group is limited by the Coimbra Formation, a unit recently formalised in the easternmost sector of the basin (Dimuccio *et al*., 2016).

The type-section of this succession, known informally as “Grés de Silves”, was initially described by Paul Choffat in the Coimbra region, next to the south bank of the Mondego River, from Conraria to the chapel of Santo Amaro (Choffat, 1903). It was later redefined along the slopes of E.N. 110, from Vendas de Ceira to Pereiros (Palain, 1976; Soares *et al*., 2012).

<table>
<tr><td></td><td colspan="8">LUSITANIAN BASIN</td></tr>
<tr><td></td><td>Choffat
(1880-1903)</td><td>Carvalho
(1950)</td><td>Soares et al.
(1985)</td><td>Palain
(1976)</td><td>Rocha et al.
(1987)</td><td>Soares et al.
(2012)</td><td colspan="2">Vilas-Boas et al.
(2021, 2023)</td></tr>
<tr><td rowspan="6">Silves Group</td><td colspan="3" rowspan="3">Pereiros Beds
(108-129 m) (50-60 m)</td><td>C2</td><td>Claystones and dolomitic sands</td><td rowspan="3">Pereiros Formation</td><td>C2</td><td rowspan="3">Pereiros Formation</td></tr>
<tr><td>C1
(10 m)</td><td>Sandstones with Clathropteris meniscoides</td><td>C1</td></tr>
<tr><td>B2
(6 m)</td><td>Dolomitic sands with Isocyprina and Promathildia</td><td>B2</td></tr>
<tr><td>«Grés à nuance claire»
(115-129 m)</td><td>Castelo Viegas Beds
(200 m)</td><td>Castelo Viegas Beds
(170-190 m)</td><td>B1
(210 m)</td><td>Castelo Viegas Beds</td><td>Castelo Viegas Formation
Penela Formation</td><td>B1</td><td>Castelo Viegas Formation
Penela Formation</td></tr>
<tr><td rowspan="2">«Grés à rouge brique»
(213-269 m)</td><td rowspan="2">Conraria Beds
(420 m)</td><td rowspan="2">Conraria Beds
(≤ 50 m)</td><td>A2
(80 m)</td><td>Sandstones with Voltzia ribeiroi</td><td rowspan="2">Conraria Formation</td><td>A2</td><td rowspan="2">Conraria Formation</td></tr>
<tr><td>A1
(100-140 m)</td><td>Conraria Sandstones</td><td>A1</td></tr>
</table>

Figure I.2. Lithostratigraphic organisation of the Silves Group in the Lusitanian Basin (adapted from Kullberg *et al*., 2013).

The most recent lithostratigraphic organisation (Soares *et al*., 2012; Fig. I.2) subdivides the Silves Group into four formations: Conraria Formation, Penela Formation, Castelo Viegas Formation and Pereiros Formation.

The **Conraria Formation** (Soares *et al*., 2012) includes the terms A1 of Palain (1976, 1979), composed of conglomerates and reddish sandstones, also called "Conraria Sandstones" (Rocha *et al*., 1987) and, uppermost, the term A2 from Palain (1976, 1979), composed of sandstones and lutites of red and/or grey colour with the presence of *Voltzia ribeiroi* (Figs. I.2). From a paleoenvironmental point of view, this unit is associated with an alluvial plain that supported areas of saline flooding, with preferential subsidence; short periods of heavy precipitation and an arid climate were typical (Palain, 1976; Soares *et al*., 2012).

Previously recognised in Soares *et al*. (2007) as the Castelo Viegas Formation, corresponding to the term B1 of Palain (1976, 1979), was recently subdivided into two formations (Soares *et al*., 2012) (Figs. I.2): at the base, the Penela Formation which corresponds to the lower part of the B1 term of Palain (1976, 1979) and, in the upper part, the Castelo Viegas Formation. The **Penela Formation** is predominantly reddish sandy-conglomeratic. The dominant facies in the **Castelo Viegas Formation** are coarse arkoses, sometimes in layers measuring 4 to 5 meters thick, separated by centimetre-long lutitic levels (Palain, 1976).

In discontinuity over the Castelo Viegas follows the **Pereiros Formation** (Figs. I.2) (Soares *et al*., 2012) which corresponds, at the base, to the term B2 by Palain (1976, 1979) (Azerêdo *et al*., 2003), composed of thin, crystalline, and siliciclastic dolomites, interbedded with lutites, in centimetre thick layers, also counting on the peculiar occurrence of fossils of bivalves (*Isocyprina*) and gastropods (*Promathildia*). This unit is followed by the term C1 by Palain (1976, 1979), corresponding to layers of coarse to very coarse, whitish, or brownish sandstones, with rare fossils of *Clathropteris meniscoides* (Kullberg *et al*., 2013). The Pereiros Formation ends through its thickest and most complex subunit from a lithological point of view, the term C2 by Palain (1976, 1979) (Azerêdo *et al*., 2003) (Figs. I.2), materialised by red and grey lutites and finely sandy bodies, thin dolomites, dolomitic marls and, very locally, gypsum levels (Sêco *et al*., 2015).

The upper part of this unit takes on a more dolomitic character, a feature that dominates the overlying unit, the **Coimbra Formation** and which constitutes the first truly carbonated unit in the Lusitanian Basin evolution process (see, for example, Azerêdo *et al*., 2003, 2014; Dimuccio *et al*., 2014, 2016; Duarte *et al*., 2014).

The Algarve Basin (Fig. I.3) is a Meso-Cenozoic basin that unconformably overlies the South Portuguese Zone, which is characterised by deep-marine Pennsylvanian strata that were deformed and metamorphosed during the Variscan Orogeny (Palain, 1976; Terrinha *et al*., 2013). Onshore, this basin crops out from Cap São Vicente to the Portuguese-Spanish border. The Mesozoic strata accumulated on a passive margin created during several extensional stages from the Late Triassic to the Middle Cretaceous are associated with the North Atlantic Ocean's opening (Manuppella *et al*., 1988). The Algarve Basin sedimentation began in the Late Triassic period with the deposition of continental red beds and evaporites that unconformably overlie folded and faulted Carboniferous strata (Palain, 1976).

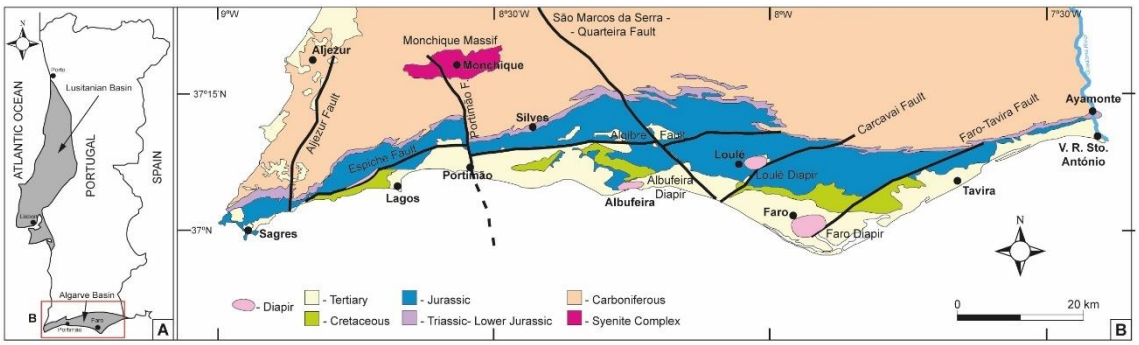

Figure I.3. Map of the Algarve Basin. **A.** Map of Portugal with the locations of the Lusitanian and Algarve basins. **B.** Simplified geological map of Algarve Basin.

At the base of the red bed sequence are sandstones and conglomerates (Silves Sandstones), overlain by variegated mudstones interbedded with siltstones and dolomites. To the south of the E-W trending Algibre Fault, there are thick evaporitic deposits on top of these strata, whereas evaporites are essentially absent to the north of this significant feature. Overlapping these layers are volcanic rocks associated with the Central Atlantic Magmatic Province (CAMP) (Verati *et al*., 2007; Martins *et al*., 2008). The Lower Jurassic Algarve CAMP magmatism was dated 198.1±1.6 to 198.4± 2.8 Ma using the 40Ar/39Ar technique (Verati *et al*., 2007). Subaerial lava flows, peperites, pyroclastic deposits, and contemporaneous resedimented volcanic material constitute the structure (Martins *et al*., 2008). Some sedimentary layers are interbedded with effusive and explosive volcanic products, indicating that volcanism and sedimentation occurred concurrently (Martins *et al*., 2008). The CAMP marks the end of the Algarve Basin's first episode of rifting. Following this significant magmatic outburst, marine carbonate sedimentation spread throughout the Algarve Basin from the Sinemurian to the Tithonian (199-145 Ma). During this epoch, lateral facies alterations in the limestone facies across the basin allowed its division into Western (Sagres), Budens-Lagoa, and Eastern (Faro) (Manuppella *et al*., 1988). These minor sub-basins are divided by strong north-south faults most likely active during deposition. In the Jurassic marine carbonates of the Algarve Basin, three main sedimentary cycles are recognised, separated by regional unconformities related to either global sea level changes or regional tectonic events (Mouterde, 1971; Manupella *et al*., 1988; Terrinha *et al*., 2002). Extensional tectonism is linked to four rifting phases, which are linked to four mega-sedimentary cycles: three in the Jurassic (Lower, Medium, and Upper) and one in the Lower Cretaceous (Manuppella *et al*., 1988). Shallow water limestones, occasionally with coral and sponge bioherms, pelagic limestones, marls, bioherms, and dolomites are the principal carbonate lithologies found in the Algarve Basin (e.g. Manuppella *et al*., 1988; Oliveira, 1992).

The Algarve Basin Triassic deposits developed from continental, primarily river, to shallow marine sedimentation settings. As previously stated, this includes evaporite depocenters and synsedimentary volcanic flows, the temporal bounds of which are difficult to determine. These units document some aspects that are

unique to the Algarve Mesozoic basin, such as: i) the first deformation events of Mesozoic crustal extension, ii) the only episode of volcanism that occurred on this continental margin, iii) the transition of sedimentation conditions from continental to coastal and marine, and iv) the unique existence of a long and lasting period (±20 Ma) of environmental and sedimentation conditions that were uniform throughout the Algarve Basin (Terrinha, 1998; Terrinha *et al*., 2013).

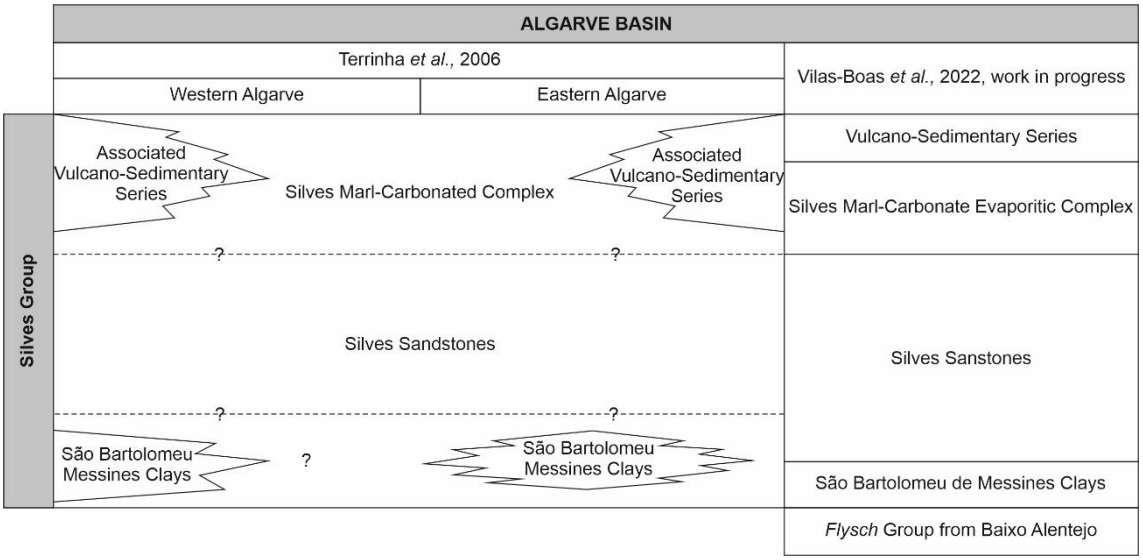

Figure I.4. Lithostratigraphic organisation of the Silves Group in the Algarve Basin (adapted from Terrinha *et al*., 2006).

The lithostratigraphic organisation of the Silves Group in the Algarve Basin (Terrinha *et al*., 2006; Fig. I.4) is subdivided into four units: São Bartolomeu de Messines Clays, Silves Sandstones, Silves Marl-Carbonate Evaporitic Complex and Vulcano-Sedimentary Series.

Silves Sandstones [Lower Triassic (?) - Keuper] (Rocha, 1976). This unit corresponds to the lower part of the «Grés de Silves» sensus Choffat (1887) and the AA and AB1 units of Palain (1976) and is attributed to the Upper Triassic (Keuper) because of the presence of *Euestheria* sp.; the presence of poorly preserved Stegocephalus bones suggests a Lower Triassic age for the pelites at the base, in S. Bartolomeu de Messines, individualised under the name **São Bartolomeu de Messines Clays** in the Geological Lithostratigraphic Chart of

Portugal (Oliveira *et al*., 1992). The Silves Sandstones unit is composed of sandstone-conglomeratic deposits and red pelites at the base, with thin intercalations of siltstones and dolomites seen in the Carrapateira and Silves-S. Bartolomeu de Messines regions (Palain, 1979), and red sandstones in the top section. Pelite and greywacke clasts from the Portuguese South Zone and schists and gneisses from the Ossa-Morena Zone make up the clasts of the conglomerates. The sandstones exhibit sedimentary structures such as load casts, cross-stratification, channel figures, and ripple marks (Terrinha *et al*., 2006).

Silves Marl-Carbonate Evaporitic Complex [Upper Triassic-Hettangian] (Rocha, 1976). Thick pelitic, marly, limestone-dolomitic and bicolour marls sequence corresponding to the upper portion of the «Grés de Silves» sensus P. Choffat and the Palain (1976) units AB2, AB3. The pelites outcrop continuously from one side of the basin to the other, whilst the dolomitic limestones (= AB3) correspond to lenticular layers with distinct morphology. This unit comprises a significant thickness of evaporite rocks south of the Sagres-Algoz-Tavira line; they are currently being explored in the Loulé Diapir (Terrinha *et al*., 2006).

The **Volcano-Sedimentary Series** [Upper Triassic-Hettangian] (Rocha, 1976). This volcanism is of tholeiitic affinity and is the first of three magmatic episodes described by Martins (1991) for the Mesozoic Basin of Portugal. It consists of an alternation of tuffites, cinerites, pyroclasts, and flows intercalated with sediments contemporaneous with the extension associated with the opening of the Central Atlantic during the Lower Jurassic (Terrinha *et al*., 2006).

Palynological and palynofacies studies of the Silves Group in Portugal are important in the recognition of the Triassic-Jurassic Boundary, the age of the strata, flora successions, environmental changes, and correlation of the strata across Iberia and South Europe (Doubinger *et al*., 1970; Adloff *et al*., 1974; Díez, 2000; Arche and López-Gómez, 2014; Vilas-Boas *et al*., 2021, 2022).

In Portugal, the Triassic-Jurassic Boundary based on palynostratigraphy is still a matter of debate, and it was noted that major changes in palynofloras

occurred across this important boundary [Doubinger *et al*., 1970; Adloff *et al*., 1974; Díez, 2000; Arche and López-Gómez, 2014; Vilas-Boas *et al*., 2021, 2022), corroborating the evidence for the End of Triassic Extinction on terrestrial ecosystems, though this need to be investigated in detail. Such a finding, thus, casts doubt on the classic ideas on the dynamics of the End of Triassic Extinction and Early Jurassic recovery for terrestrial ecosystems and is one of the main focuses of this research proposal. There are still some challenging aspects related to Silves Group stratigraphy that remain poorly constrained. Among these are: the detailed age of the End of Triassic Extinction event, the CAMP influence(s) on the ecosystems, the sedimentary environments and climatic conditions present during the deposition around the Triassic-Jurassic Boundary.

Thus, the outcome of this research proposal will help not only to increase the geological knowledge of the Silves Group in Portugal and correlations within Iberia, but more importantly, it will unlock its stratigraphic record and contribute to the debate of the dramatic global changes that occurred during the Triassic-Jurassic time interval.

3. Objectives

The primary goal of this study project was to expand stratigraphic, palaeoclimatic, palaeoenvironmental, and geodynamic understanding of the Silves Group during the Triassic-Jurassic interval and make it available to the scientific and non-scientific groups. The information gap associated with these well-preserved successions may have hampered comprehension of the worldwide changes that occurred during this critical period of time. This idea ensures the resolution of several unresolved scientific concerns. To achieve the overall goal, the project concentrated on the following specific goals:

i. Establish the Triassic-Jurassic palynostratigraphic framework for the Silves Group by documenting pollen and spore biozones and correlating the palynostratigraphic scheme obtained with others from Iberia and European stratigraphic records;

ii. Try to identify and document, either in outcrops or in the sub-surface, using palynology as the main tool, the timeline for the End of Triassic Extinction and the Triassic-Jurassic Boundary in the Silves Group basins (Lusitanian and Algarve basins);

iii. Using palynofacies studies to reconstruct palynofloras, palynofloras successions and paleoenvironments of deposition within the Silves Group stratigraphic record to better assess palaeoclimatic changes of the Silves Group basins studied. Another point of interest will be documenting abnormal palynomorphs morphology in order to evaluate possible ancient environmental pollution and its causes (volcanic SO_2 and CO_2 emissions; Hg poisoning, increased UV-B radiation, etc.);

iv. Assessing the thermal history of the Silves Group basins by means of vitrinite reflectance in order to quantify the effects of thermal diagenesis in the sedimentary successions;

v. Using geochemical analyses (organic C-isotopes, whole-rock geochemistry) to establish correlations with biostratigraphic data and try to identify in the sediments chemical proxies for ancient environmental changes by detecting critical elements (Hg, etc.);

vi. A reliable chronostratigraphic framework and timeline established by palynology is crucial, particularly in sedimentary basin analysis. Therefore, the other type of study proposed (organic maturation) will rely on the accuracy of this time frame;

vii. Establishing and comparing Triassic-Jurassic transition environmental/palaeoclimatic global changes with today's environmental/climatic changes.

4. Sampling and Field Campaigns

To achieve the goals of this project, fieldwork was carried out. Twelve sections were selected in the Lusitanian Basin, fifteen in the Algarve Basin, and six boreholes. The sections with the most representative lithostratigraphy of the Upper Triassic and Lower Jurassic in each basin. In each section, the lithologies

more suitable for palynological studies (mudrocks) were selected and sampled, and if it was the case, based on previous biostratigraphical studies. These sampling field trips took place in the Lusitanian and Algarve basins, and the sampling of the boreholes curated at LNEG in Lisbon, during the four years of this Ph.D. project. All studied sections, lithology, chronostratigraphy, and lithostratigraphic units, are described in depth in Chapters II, III, IV and V.

In the Lusitanian Basin, the sampled sections from the Upper Triassic were: Alto de São João (Fig. I.5), Castelo Viegas I (Fig. I.6), IdealMed, Parque de Campismo (Fig. I.7) and Sobral Cid (Fig. I.8). The sampled sections associated with the Lower Jurassic were Carvalhais, Lamas I (Fig. I.9) and Lamas II (Fig. I.10). Some sections that were sampled had present both Upper Triassic and Lower Jurassic rocks units, as the case of Castelo Viegas II (Fig. I.11), Lordemão, Eiras (Fig. I.12), and Redonda (Fig. I.13).

In the Algarve Basin, due to the lithostratigraphy of the basin most of the sampled sections are from the Upper Triassic, such as Amado's Beach (Figs. I.14 and I.15), Amorosa, Ayamonte (Fig. I.16), Barragem do Funcho, Bengado (Fig. I.17), Bodega, Fonte da Pedra, International Racetrack of Algarve (Fig. I.18), Marco, Rocha da Pena, Santa Catarina da Fonte do Bispo, Santa Rita and Vale Fuzeiros (Fig. I.19). The Loulé Rock Salt Mine (Fig. I.20) section represent both Upper Triassic and Lower Jurassic and the Albufeira's Diapir (Fig. I.21) the Lower Jurassic.

The sampled boreholes, Campelos-1, Golfinho-1, Lula-1, Santiago do Cacém-3, Santiago do Cacém-42, and Santiago do Cacém-61, were selected since, in the reports, one or both aimed study ages was present in the wells. In total, 498 samples were collected (Tables I.1, I.2 and I.3).

Figure I.5. Alto de São João section; Conraria Formation, Lusitanian Basin: **A.** panoramic view of the outcrop; **B.** detailed photograph from sample 1, productive sample; **C.** detailed photograph from sample 2, productive samples; **D.** detailed photograph from sample 3, barren sample.

Figure I.6. Castelo Viegas I section, Castelo Viegas Formation, Lusitanian Basin: **A.** panoramic view of the outcrop; **B.** detailed photograph from sample 1, barren sample; **C.** detailed photograph from sample 2, barren sample.

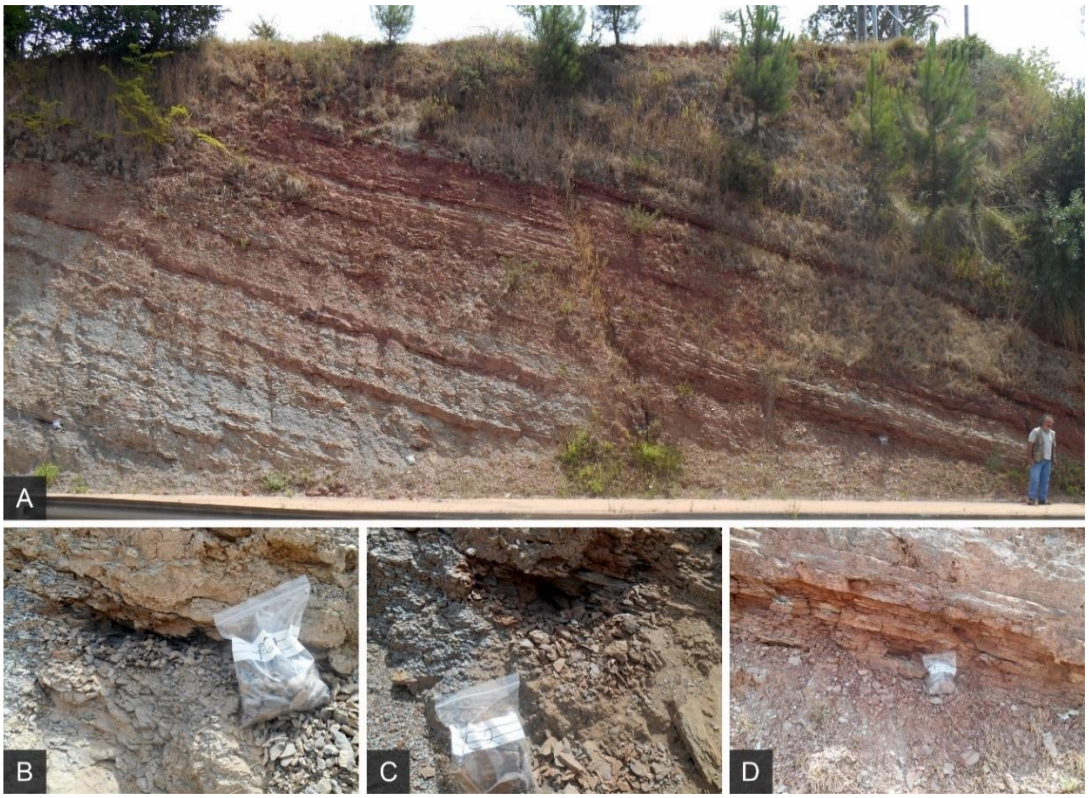

Figure I.7. Parque de Campismo section, Conraria Formation, Lusitanian Basin: **A.** panoramic view of the outcrop; **B.** detailed photograph from sample 1, productive sample; **C.** detailed photograph from sample 2, productive sample; **D.** detailed photograph from sample 3, barren sample.

Figure I.8. Sobral Cid section, Conraria Formation, Lusitanian Basin: **A, B.** panoramic view of the outcrop; **C.** detailed photograph from sample 2, productive sample; **D.** detailed photograph from sample 3, productive sample; **E.** detailed photograph from sample 5, barren sample.

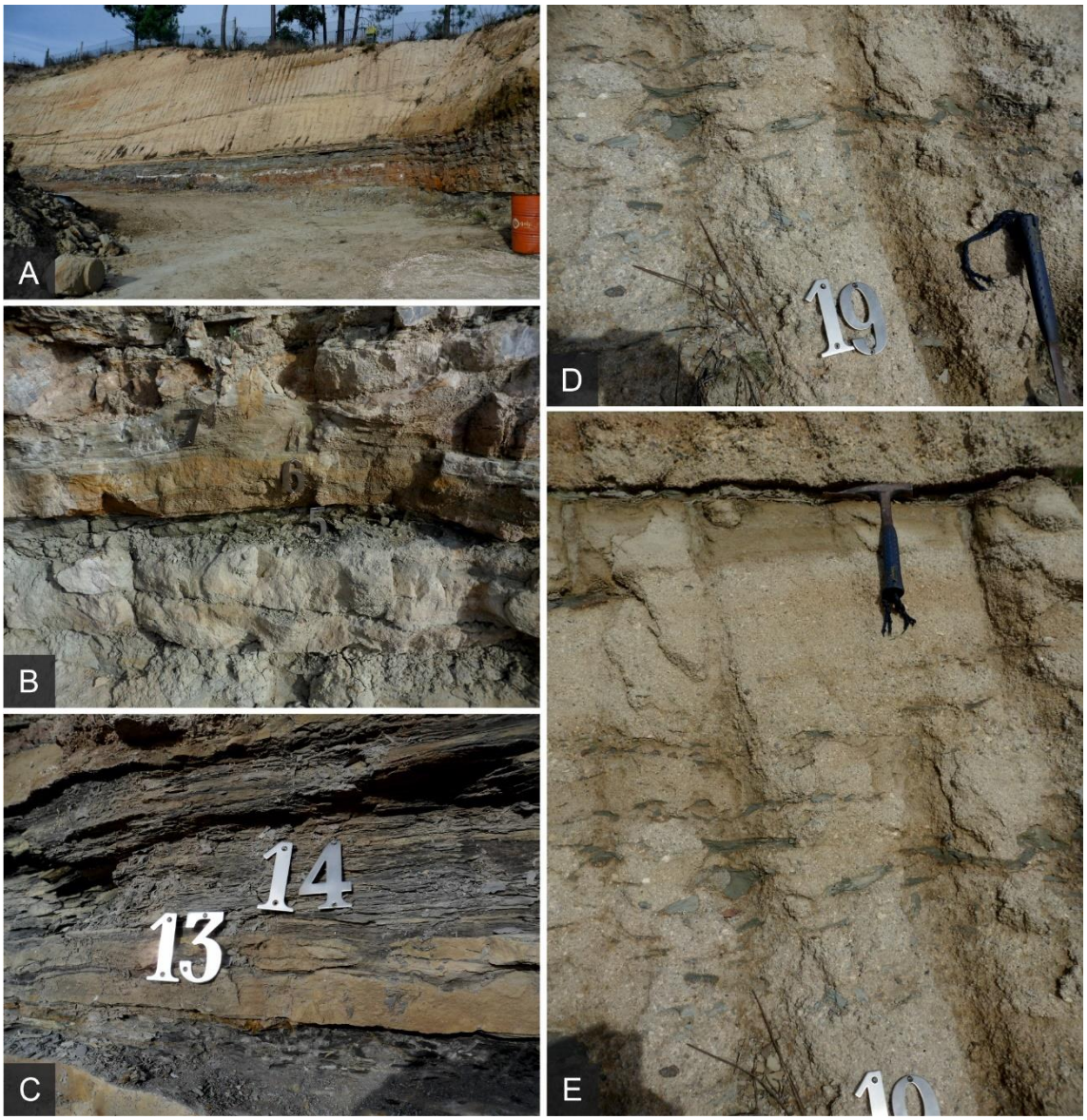

Figure I.9. Lamas I section, Pereiros Formation, Lusitanian Basin: **A.** panoramic view of the outcrop; **B.** detailed photograph from samples 5, 6 and 7, samples 7 is the first productive sample from this section; **C.** detailed photograph from samples 13 and 14, both samples were productive and containing foraminiferal linings; **D, E.** detailed photograph from sample 19, barren sample, to note the details on the sedimentary structures such as erosive channel surfaces and the channelized deposits.

Figure I.10. Lamas II section, Pereiros Formation, Lusitanian Basin: **A.** panoramic view of the outcrop with the location of samples 4, 5, 6, 7 and 8, all productive except for the sample 7; **B.** detailed photograph from sample 11, productive sample; **C.** detailed photograph from sample 12, productive sample.

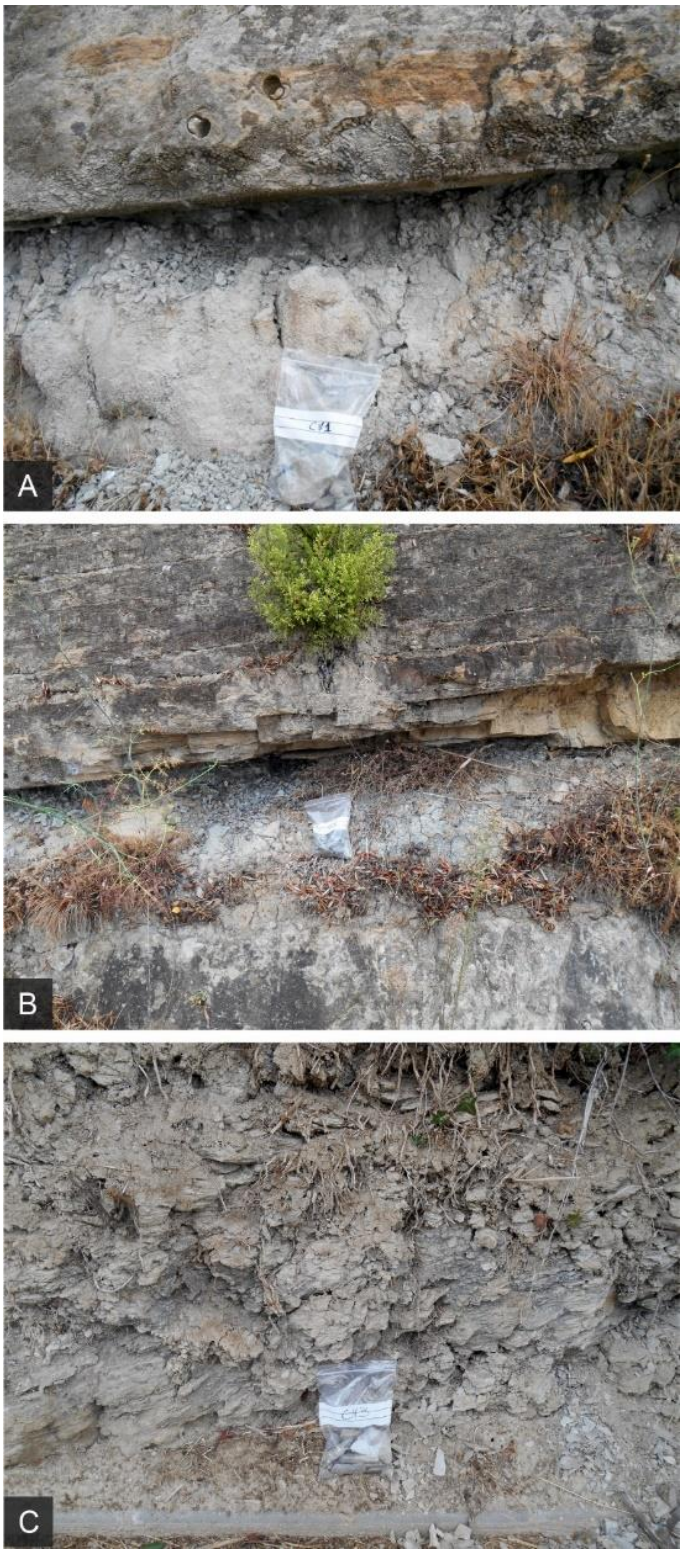

Figure I.11. Castelo Viegas II section, Castelo Viegas (sample 1 and 2) and Pereiros (sample 3) formations, Lusitanian Basin: **A.** detailed photograph from sample 1, barren sample; **B.** detailed photograph from sample 2, barren sample; **C.** detailed photograph from sample 3, productive sample, belongs to the basal gray mudstone beds of the base of unit C2 of Pereiros Formation.

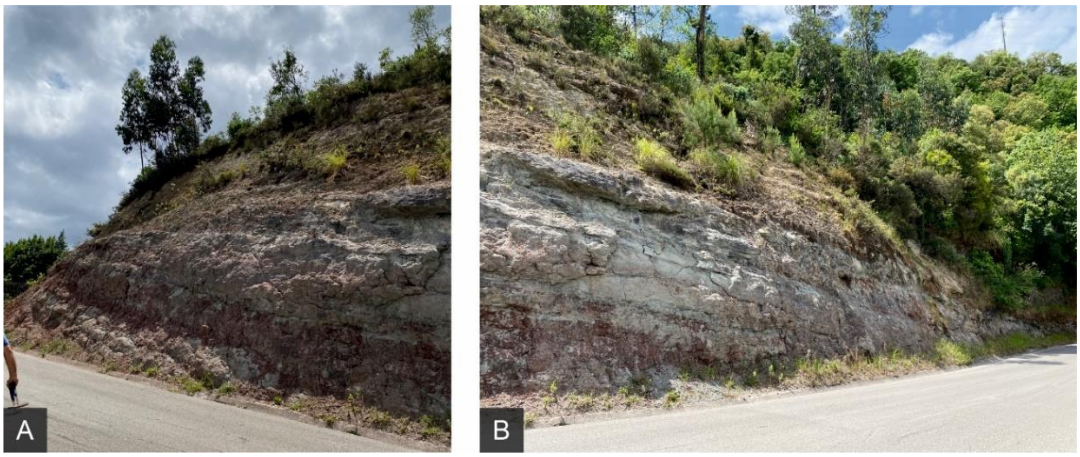

Figure I.12. Eiras section, Castelo Viegas Formation, Lusitanian Basin. **A, B.** panoramic view of the outcrop, all the samples collected were barren. Contact between the units B1 and B2 of Palain, (1976).

Figure I.13. Redonda section, Castelo Viegas and Pereiros formations, Lusitanian Basin: representing the units B1 and B2 of Palain, (1976). **A.** panoramic view of the outcrop with the location of the samples 4 and 5, barren samples, Castelo Viegas Formation; **B.** panoramic view of the outcrop with the location of the sample 6, barren sample, Castelo Viegas Formations; **C.** detailed photograph from the sample 6; **D.** detailed photograph from the sample 8, barren sample, Pereiros Formation.

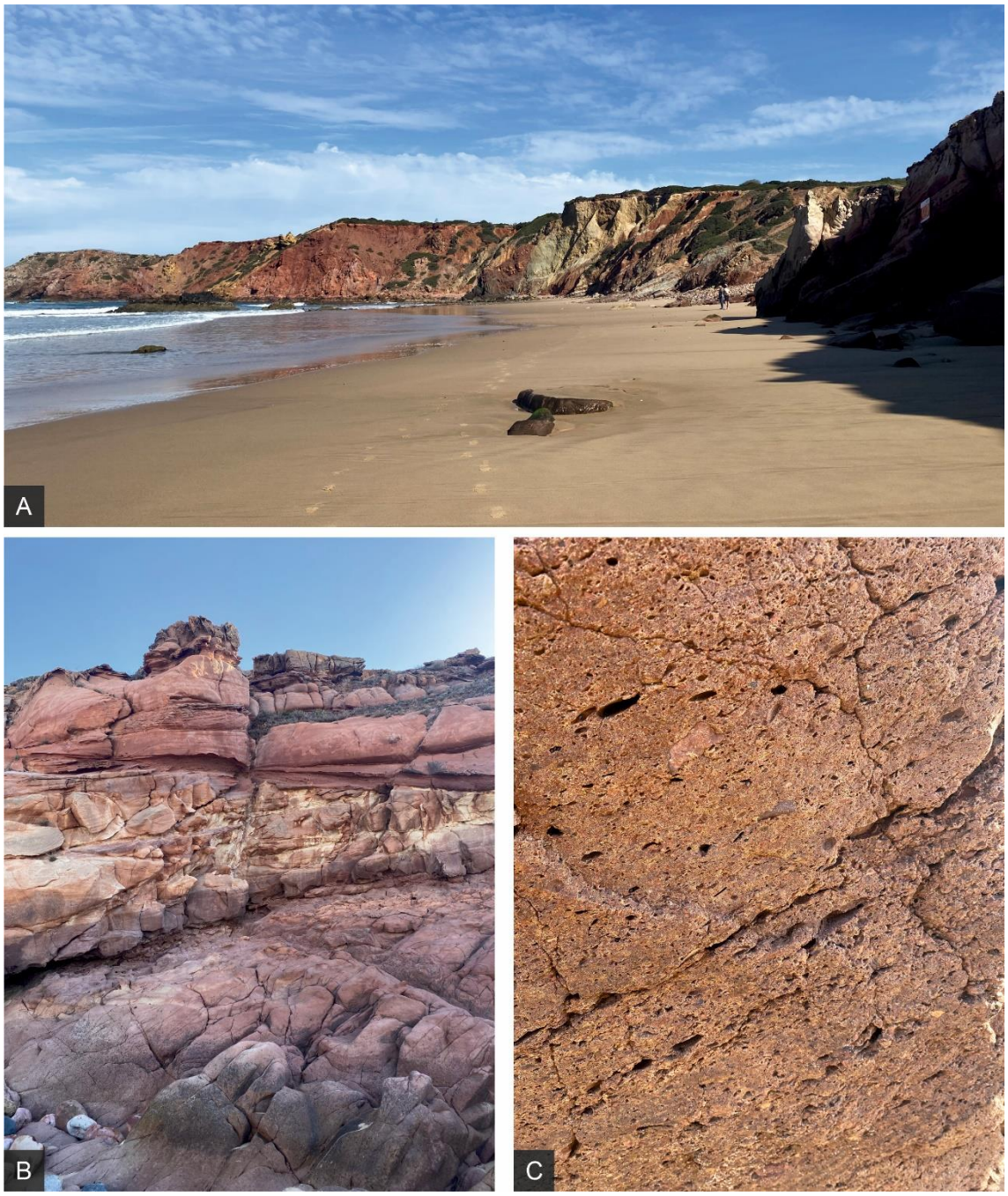

Figure I.14. Amado's Beach section, Silves Marl-Complex Evaporitic Complex, Algarve Basin: **A.** panoramic view of the outcrop, the base of the unit is on the right of the picture and on the left is the contact by fault between the Silves Group and the Vulcano-Sedimentary Series; **B.** detailed photograph of the base of the outcrop, no samples collect due to no favorable facies to palynological studies; **C.** details from of the base of the outcrop.

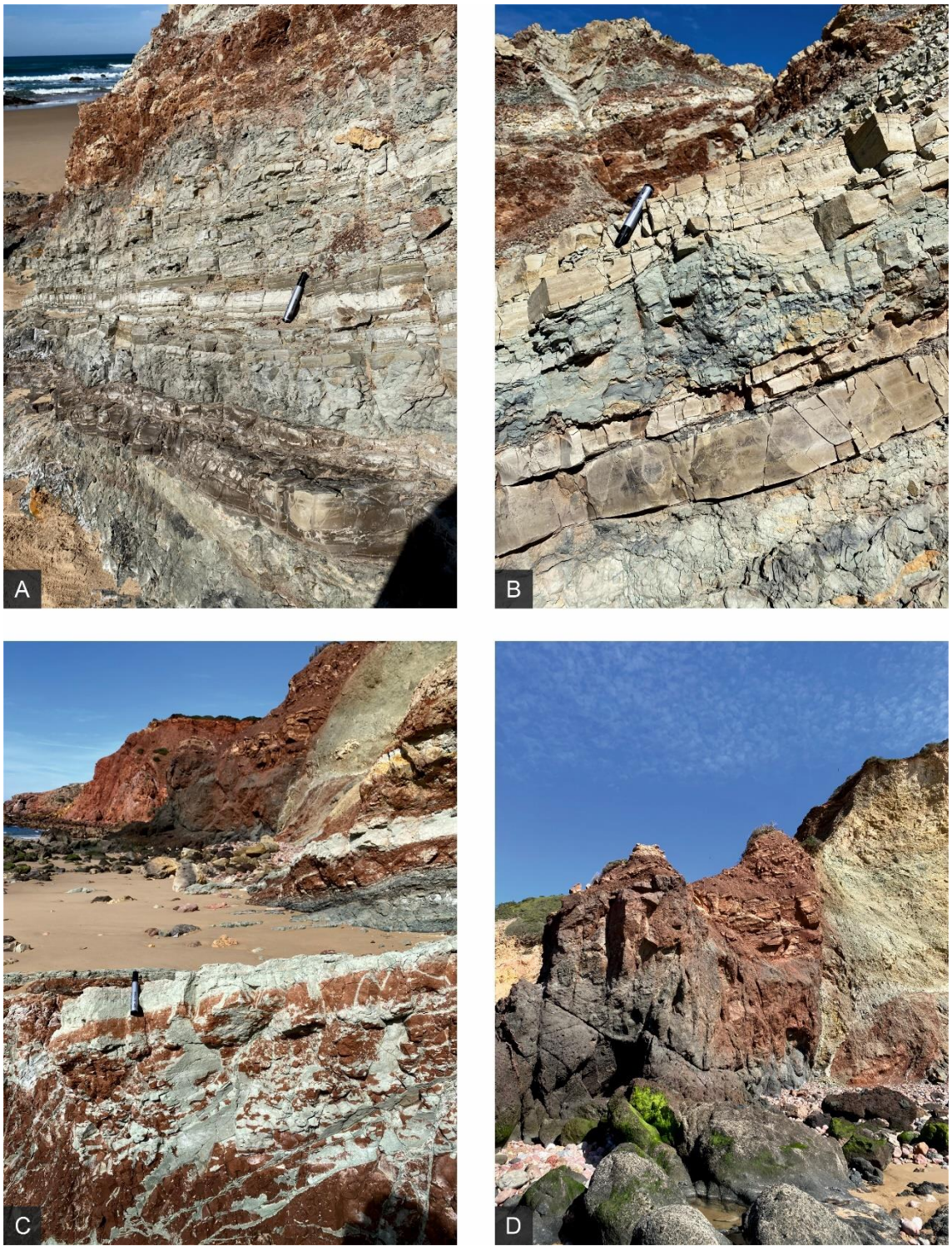

Figure I.15. Amado's Beach section Silves Marl-Complex Evaporitic Complex, Algarve Basin: **A, B.** detailed photograph representing a part of the outcrop with more organic matter, the first beds from the outcrop were the accumulation of organic matter is more evident; **C.** photograph of the middle part of the outcrop with the samples 15 and 16 present, productive samples; **D.** upper part of the outcrop represented the faulted contact between the Volcano-Sedimentary Series and the Silves Group.

Figure I.16. Ayamonte section, Silves Marl-Complex Evaporitic Complex, Algarve Basin in Spain: **A.** panoramic view of the outcrop; **B.** detailed photograph of the samples 6 and 7, barren samples; **C.** detailed photograph of the samples 2 and 3, barren samples.

Figure I.17. Bengado section, Silves Sandstones, Algarve Basin: **A.** photograph from the lower part of the outcrop, to note the facies not favorable to palynological studies making it difficult to collect samples; **B.** detailed photograph from the middle part of the outcrop, one of the few parts of the section where it was possible to collect a sample, even though the sample was barren.

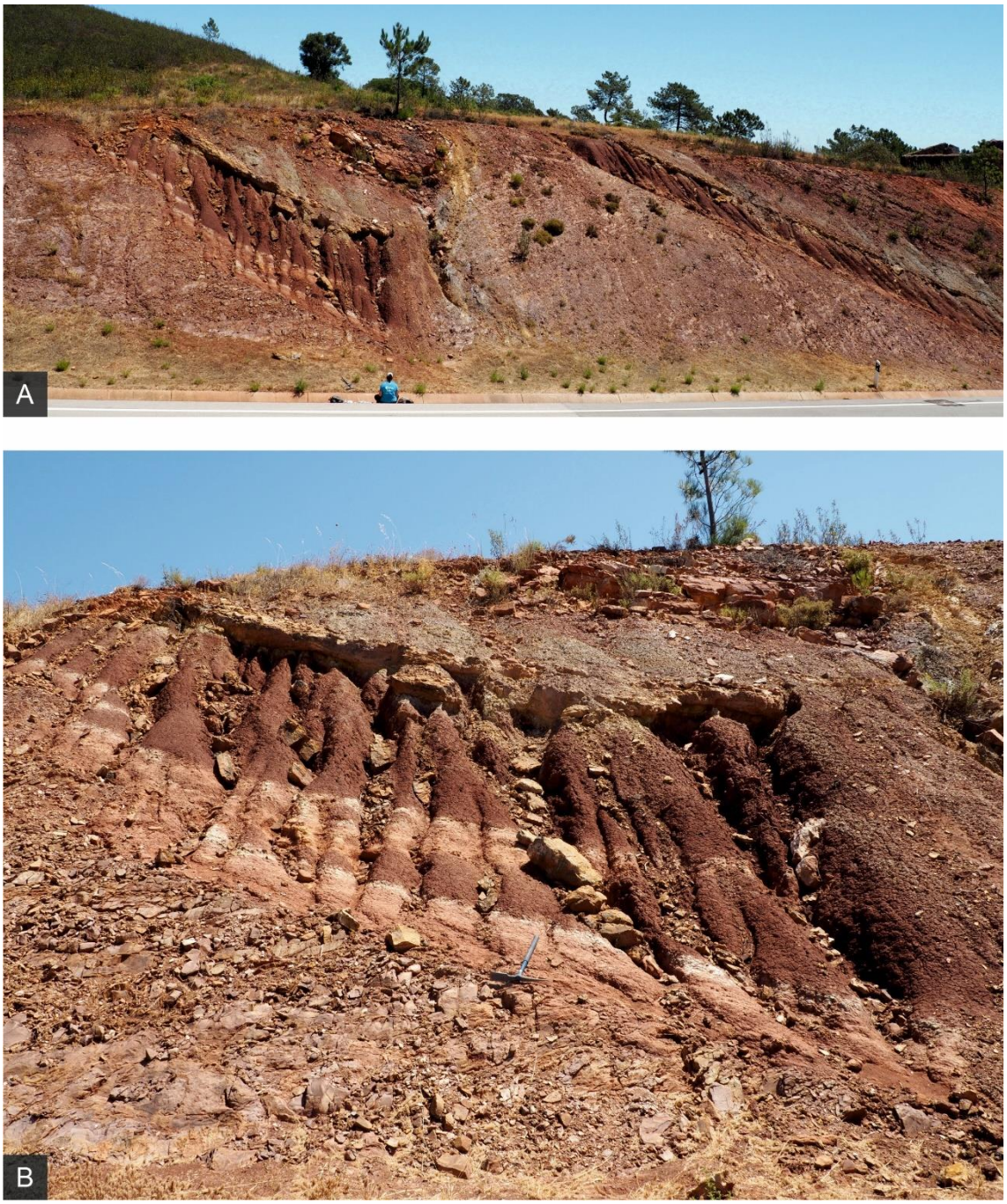

Figure I.18. International Racetrack of Algarve section, Silves Sandstones, Algarve Basin: **A.** panoramic view of the outcrop with the Variscan unconformity; **B.** detailed photograph of the outcrop presenting a closer look of the Variscan unconformity, the grey material above the unconformity was the bed sampled to palynological studies yielding productive samples.

Figure I.19. Vale Fuzeiros section, Silves Sandstones, Algarve Basin: **A.** panoramic view of the outcrop, the sections ages from left to right, in the left is represented the lower part of Silves Sandstones unit and at the right the Silves Marl-Carbonate Evaporitic Complex. In the photograph in not possible to see, but at the end of the section on the right the contact between the Silves Marl-Carbonate Evaporitic Complex and the Volcano-Sedimentary Series is made. This section is probably the most representative section of the Silves Group in the Algarve Basin, however all the samples collected become barren; **B.** detailed photograph of the base of outcrop were the collecting of the samples started; **C, D.** photographs of some details from the samples recovered at the base of the outcrop showing bioturbation.

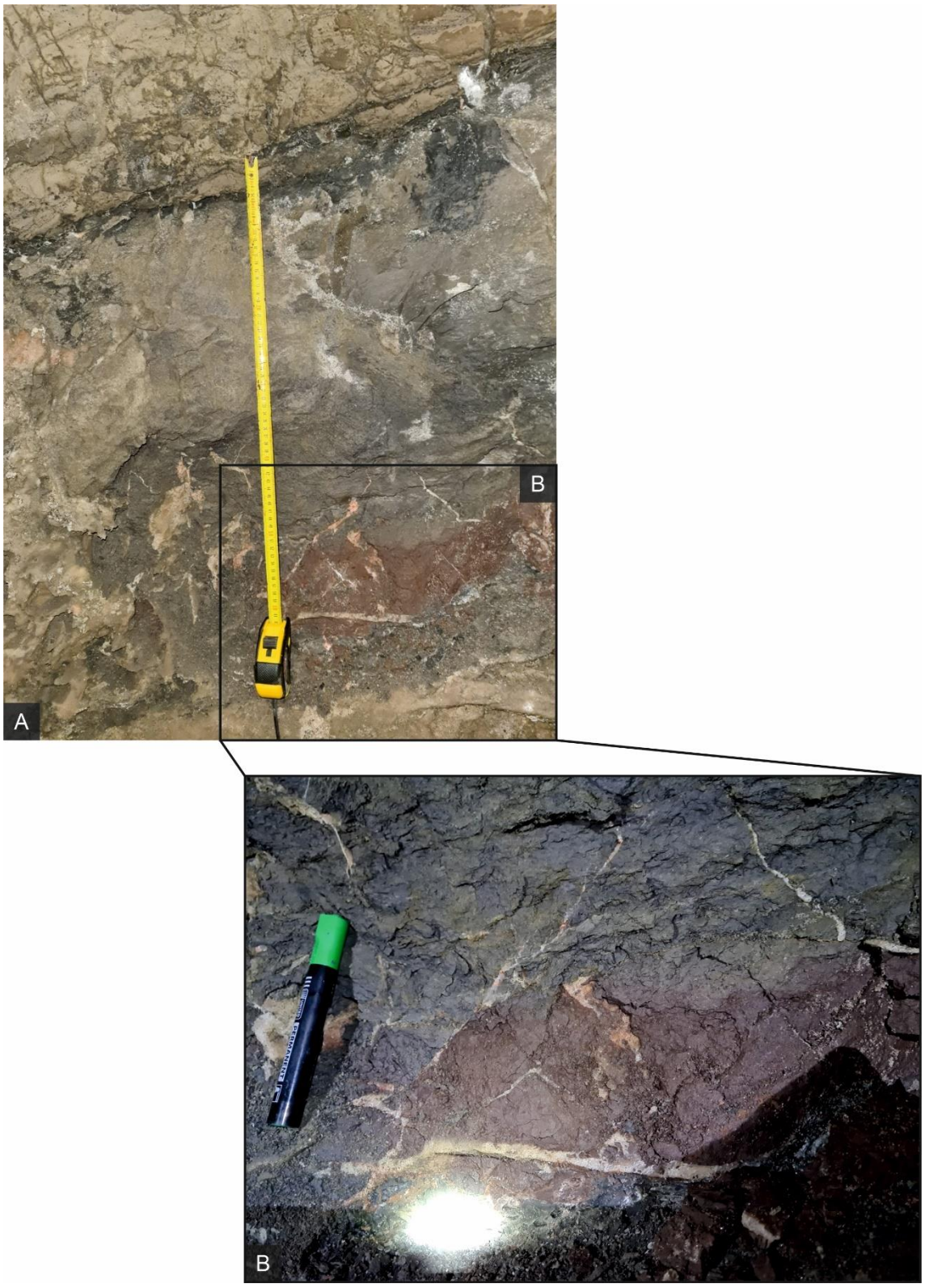

Figure I.20. Loulé Rock Salt Mine section, Silves Marl-Carbonate Evaporitic Complex, Algarve Basin: **A.** photograph of the ca. 1 m thick sampled mudstone bed intercalated with the massive halite beds, productive samples; **B.** detailed photograph of red material found at the base of the bed.

Figure I.21. Albufeira's Diapir section, Silves Marl-Carbonate Evaporitic Complex, Algarve Basin: **A.** panoramic view of the outcrop within the diapir controlled by fault with difficult to recognize any bedding; **B, C.** detailed photograph the sampled material mainly anhydrite and gypsum intercalated with very thin lenses of grey mudstone, productive samples were recovered.

5. Field and Laboratory Work

The organic residues were extracted using standard palynological preparation procedures (Wood *et al*., 1996; Riding and Warny, 2008). Four distinct phases are recognised in the laboratory procedure applied (Wood *et al*., 1996; Riding & Warny, 2008): physical fractional process, demineralisation, concentration of organic residue, mounting and study of samples.

i. **Physical fractional process -** This procedure begins with the removal of areas of the rock that show signs of weathering or alteration. After the initial cleaning, with the aid of a hammer, 150 to 250 g of sample was disaggregated, which were placed in wide-mouthed Teflon® bottles, duly identified.

ii. **Demineralisation -** This phase of sample treatment corresponds to the most complex phase, which includes the application of several strong acids in different concentrations to completely eliminate all mineral fractions existing in the sample. The samples were subjected to treatment with hydrochloric acid (HCl), concentrated at 37%, for approximately 48 hours. This step aims to eliminate all carbonates that the sample could contain. After this initial process, the residue was diluted and decanted until neutralised. Next, the residue is treated with hydrofluoric acid (HF) (48% concentration) for six to ten days in a water bath. To increase this attack's efficiency and eliminate all silicates, the residue goes through several decantations and acid renewals, being stirred periodically (twice a day). When the complete disaggregation of the sample was observed, it was neutralised by several decantations with distilled water and filtered using a 15 µm filter. After this first attack component with HCl and HF, the residue may still contain secondary minerals (insoluble fluorides and sulphides) derived from the first treatment. To resolve this situation, the residue was treated with hot HCl, maintaining the boiling for around 5 minutes to eliminate the mineral fraction. As in previous processes, the

resulting sample is diluted, washed, and filtered (15 µm filter) and subsequently observed under a microscope.

iii. **Concentration of organic residue -** In some samples, the organic residue resulting from the demineralisation process was in small quantities, and the mineral fraction was considerable, resisting even after repeating the chemical treatment. In those cases, another method was used to concentrate the residue. Concentrating the organic residue consisted of panning, using a watch glass filled with water. The organic matter due to its lower density remains in suspension and can be removed with a pipette; this process was repeated several times in order to remove as much organic matter as possible. Another method could be using heavy liquids (density of 2) to separate the mineral fraction and concentrate the organic matter. The recovered residue was stored in small bottles with water duly identified.

iv. **Mounting and study of the samples -** After being stored in plastic bottles, a few drops of dispersant (hydroxyethylcellulose) are added to the residue resulting from the previous steps to facilitate particle dispersion when mounting into coverslips. At this stage, the solution is homogenised by manual stirring and, with a pipette, the palynological sample is distributed over glass coverslips. To speed up the procedure and avoid contamination of the current material, the cover slips were dried in an oven at a constant temperature. After drying, the cover slips were assembled into glass slides, duly identified, using a mounting medium (acrylic resin – Entelan®). The resin drying time was around twenty-four hours, after which the slides were ready for observation. Two and three slides were observed for each sample, identifying and recording each palynomorph on each slide and counting at least 250 palynomorphs per sample. However, when the samples were very poor, as many specimens as possible were counted among the total of slides prepared. Each specimen was referenced according to the coordinates of the cross-movement stage of the microscope, where its observation and identification were carried out.

The laboratory procedure was done in the palynology laboratories of CIMA, University of the Algarve, and LNEG (Portuguese Geological Survey), São Mamede Infesta, Portugal. The unused sample material, aqueous residues, microscope slides and figured specimens are curated in the collections of CIMA-UAlg. The qualitative palynomorphs fluorescence study (Chapter VI) was carried out at the University of the Algarve with the aid of an Olympus BX 51 microscope fitted with a metal halide lamp fluorescence unit XCite Series 120Q and a violet and Blue 12 filter block that yields a wavelength band of 390 and 490 nm. In total, 498 samples from the Upper Triassic and Lower Jurassic from field sections and boreholes of the Lusitanian and Algarve basins were investigated in this project (Tables I.1, I.2 and I.3).

Table I.1. Number of samples collected by section and location in the Lusitanian Basin.

	Locality	Studied Section	Nº Collected Samples
LUSITANIAN BASIN	Coimbra	Alto de São João	3
	Coimbra	Carvalhais	2
	Coimbra	Castelo Viegas I	3
	Coimbra	Castelo Viegas II	3
	Coimbra	Eiras	2
	Coimbra	IdealMed	2
	Miranda do Corvo	Lamas I	25
	Miranda do Corvo	Lamas II	12
	Coimbra	Lordemão	51
	Coimbra	Parque de Campismo	3
	Coimbra	Redonda	11
	Coimbra	Sobral Cid	5
	TOTAL		**122**

Table I.2. Number of samples collected by borehole.

	Borehole	Nº Collected Samples
BOREHOLES	Campelos-1	18
	Golfinho-1	27
	Lula-1	17
	Santiago do Cacém-3	21
	Santiago do Cacém-42	19
	Santiago do Cacém-61	20
	TOTAL	**122**

Table I.3. Number of samples collected by section and location in the Algarve Basin.

	Locality	Studied Section	Nº Collected Samples
ALGARVE BASIN	Albufeira	Albufeira's Diapir	4
	Aljezur	Amado's Beach	20
	São Bartolomeu de Messines	Amorosa	17
	Ayamonte, Spain	Ayamonte	9
	Silves	Barragem do Funcho	4
	São Brás de Alportel	Bengado	9
	Tavira	Bodega	3
	Portimão	Fonte da Pedra	1
	Portimão	International Racetrack of Algarve	24
	Loulé	Loulé Rock Salt Mine	33
	Santa Catarina Fonte do Bispo	Marco	6
	Penina	Rocha da Pena	15
	Santa Catarina Fonte do Bispo	Santa Catarina Fonte do Bispo	6
	Tavira	Santa Rita	15
	São Bartolomeu de Messines	Vale Fuzeiros	88
	TOTAL		**254**

6. Spores and Pollen: general aspects

The term Palynology was created by Hyde and Williams in 1944 and designates the study of fossil and current pollen and spores, deriving from the Greek *palunein* (παλυνειν) (Traverse, 2007) and the Latin *pollen*, which means to pulverize and thin powder. This scientific area goes beyond pollen and spores and encompasses interest in acritarchs, dinoflagellates, algae, chitinozoans, scolecodonts (mouthparts of annelid-type worms), microforaminifera linings, as well as fungi (Jansonius and Mcgregor, 1996). These microorganisms and organic wall structures are collectively called palynomorphs. Palynomorphs have dimensions that vary, on average, between 5 and 500 µm.

Palynomorphs have very varied characteristics, such as their organic walls, which can be composed of sporopollenin, chitin or pseudochitin, with sporopollenin being one of the most chemically inert organic compounds known in nature. It is this fact that allows its extraction by chemical methods. Due to the characteristics of its walls, laboratory preparation for palynological observation involves using acids, namely HCl, HF and, sometimes, nitric acid (HNO_3) (Wood *et al*., 1996).

This type of research, which focuses on studying fossil microorganisms, also allows the analysis of the environmental context of the sedimentation basins, where the palynomorphs and all other sediments were deposited. One of the most economically relevant applications is associated with the study of petroleum potential (palynofacies analysis) and as an important tool in the prospecting and research of hydrocarbons (coal, oil, natural gas) (Robbins, 1996) or even in mineral deposits (such as, for example, example, the Iberian Pyrite Belt; see Pereira *et al*., 2008)

From a stratigraphic point of view, it provides data on depositional environments, allowing inferences regarding paleoclimate, paleotemperature, paleogeography, and environmental parameters such as humidity, depth, and salinity. It is also possible to obtain stratigraphic information by determining the relative age of the sediments (biostratigraphy), allowing the dating of sedimentary rocks using biozonations.

During this research, the focus palynomorphs were the spores and pollen.

6.1. Spores

Spores are produced in the life cycles of lower plants, called cryptogams (plants without a macroscopic reproductive system), which include algae, fungi, some bacteria, bryophytes, and pteridophytes. Spores main function is to protect protoplasmic contents during the process of dispersion and germination of a new plant.

Bryophytes are organised in an intermediate group between green algae and vascular plants. This class of plants comprises liverworts (*Hepaticae*) and mosses (*Musci*), and the difference between these two classes is related to the development of the sporophyte (more developed in mosses) (Playford and Dettmann, 1996). The class of Pteridophytes comprises all seedless vascular plants, such as ferns (*Pterophyta*) and the groups *Psilophyta, Lycopodophyta* and *Sphenophyta*.

The structure of spores is very varied, consisting of several layers, with only the exine (outer layer) having fossilisation capabilities due to its chemical composition, sporopollenin (Playford and Dettmann, 1996; Pereira, 1997). To identify spores, characteristics such as shape, symmetry, polarity, structure, and ornamentation of the exine are essential (Playford and Dettmann, 1996; Pereira, 1997; Armstrong and Brasier, 2005). These palynomorphs are resistant structures; therefore, this characteristic means they are prone to be preserved in the fossil record (Playford and Dettmann, 1996; Armstrong and Brasier, 2005; Loboziak *et al*., 2005).

Trilete spores are less than 150 µm in size (Playford and Dettmann, 1996; Armstrong and Brasier, 2005). Its tetrad mode of association is one of this group's most distinctive structural characteristics. This bond is engraved by a scar (the trilete cleft), which indicates that three surfaces were formed resulting from the contact of this cell with three other cells due to the process of meiosis during cell division, promoting this cellular arrangement, a radial symmetry (Playford and Dettmann, 1996; Pereira, 1997; Wellman and Gray, 2000; Armstrong and Brasier, 2005). The variation for monolete spores is associated with the process of meiosis, which causes them to have a different spatial arrangement, as the cleft

formed is monolete, the result of each unit having only been linked to two more cells (monolete cleft). Monolete spores thus have bilateral symmetry.

It is sometimes difficult to establish a biological affinity with the plants that produce them in fossil spores due to their dispersed nature. Consequently, its systematic classification is based on the analysis of morphology, such as, for example, the equatorial contour in proximal view the structure and ornamentation of the exine, among others (Playford and Dettmann, 1996).

6.2. Pollen

Pollen grains are produced in the life cycle of seed plants, associated with angiospermic and gymnospermic plants. These are increasingly common in palynological associations from Permian (Upper Paleozoic) continental deposits.

Gymnosperms are land plants with a visible reproductive structure and no fruit surrounding the seeds. In plants of the Angiosperm class, the seed is surrounded by the fruit. The pollen grains morphology and fine wall structure are characteristics used in their description, sometimes allowing a comparison with current pollen.

The diversity of floral morphology demonstrated by flowering plants to adapt to adverse and widely varying conditions to achieve successful pollination is impressive. It was necessary to evolve and develop mechanisms that would ensure the transport of pollen from the anthers to the stigmas by insects (entomophilic pollination), bats (chiropterophilic pollination), birds (ornithophilic pollination), reptiles (saurophilic pollination), or small non-flying mammals. (therophily pollination) (Jarzen and Nichols, 1996). Pollination by wind (anemophily) is of great importance for paleopalynological studies because large amounts of pollen from anemophilic plants constitute the largest contribution of material transported by rivers, lakes or lagoon sediments (Jarzen and Nichols, 1996). This process is extremely random, as pollen carried by the wind may or may not reach a stigma of the same species. The distance an anemophilic pollen travels from the parent plant varies among species, depending on the magnitude

and direction of wind currents, plant weight, and density of plant cover. Pollen grains that reach the water have a greater potential for transport and eventually to be incorporated into sediments and, ultimately, fossilised. These are the most interesting pollen for Palynology. Pollen produced by plants growing near ponds or small lakes can be directly incorporated into water body sediments (Jarzen and Nichols, 1996).

The preservation of pollen depends on several factors, the main one being the amount of sporopollenin in the exine, as this characteristic is essential for fossilisation. Some plants produce pollen, limited in sporopollenin and are unlikely to be well represented in the fossil record.

The structures and surface modifications of seed plant pollen grains are more diverse than flowers. Gymnosperm pollen shares typical characteristics, such as the opening structure and the surface ornamentation. These pollen ranges from small, simple, spherical and openness, such as the modern genera *Cupressus* and *Juniperus*, to large, disaccated and ornate, such as the modern genera *Abis* and *Pinus*. They also include distinct polyplicate forms such as the modern genus *Ephedra*. There are families characterized by pollen without opening, such as *Araucariaceae*, *Cephalotaxaceae*, *Cupressaceae*, *Taxaceae* and *Taxodiaceae*, and some genera of the *Pinaceae* family (Jarzen and Nichols, 1996). The pollen of various gymnosperms are typically, but not necessarily, saccate; the grains have one, two or, rarely, three air sacs attached to the central body.

The degree of morphological variation in angiosperms is high. When the pollen grains are mature, they are released from the anthers individually (monads), in pairs (dyads), in groups of four (tetrads) or in multiples of four (polyids). Individual pollen may have no opening, have one or more pores (monoporate, diporate, triporate or periporate), may have slit-like openings or colpos (monosulcate, tricolpate, etc.) or a combination of pores and colps (tricolporate, syncolporate, etc.) (Jarzen and Nichols, 1996). Surface characteristics and their combinations are not always easy to define, which makes the identification and classification of pollen grains more complex.

The pollen grain wall comprises two layers: a resistant outer layer (exine) and a cellulosic inner layer (intine), which immediately surrounds the protoplasm. If fertilisation does not occur, the protoplasm and intine quickly disappear, leaving only the resistant layer (exine), which can be fossilised (Jarzen and Nichols, 1996). This fossilised exine may present various ornamentations.

Variations in pollen characteristics (size, number of openings or even shape) within what is considered “normal” for certain species are not uncommon in current plants and can, therefore, be expected in pollen from the fossil record.

There are distinct morphological differences between pollen, both from angiosperms and gymnosperms. Characteristics can group these differences, and we have saccate pollen, striated saccades, polyplicates, circumpollen, monosulcates and no openings (Jarzen and Nichols, 1996).

Saccades

They are characterised by one or two, rarely three, air sacs attached to the central body and are also the easiest to identify. Saccades are the most common pollen among gymnosperms and some extinct conifers. Late Triassic and Jurassic continental palynomorph associations are dominated by monosaccate and bisaccate gymnosperm pollen (Jarzen and Nichols, 1996).

Striated saccades

Some gymnosperms in the Early Triassic produced striated or teniate bisaccate pollen, a notable pattern on the proximal surface, and are common in rocks of this age (Jarzen and Nichols, 1996).

Polyplicates

The Permian and Triassic bisaccate pollen discussed above contains two common gymnosperm pollen morphologies: the sacs and the grooves or ribs on the body. Some current gymnosperms have non-saccade, striated, or polyplicate, pollen (Jarzen and Nichols, 1996).

Circumpolles

This pollen morphology was common in the Middle Triassic to mid-Cretaceous and numerically dominates Late Triassic to Late Cretaceous assemblages. The pollen contains a circumpolar, subequatorial groove (also called rimula) that divides the spheroidal pollen into unequal hemispheres. Each grain is characterised by a distal pseudopore and a proximal triangular area (Jarzen and Nichols, 1996). They are commonly found in tetrads, with the genus *Classopollis* being one of the best examples.

Monosulcate and without opening

The morphology of monosulcates evolves from quite simple to a degree of greater complexity (for example, *Eucommiidites*). The simplest monosulcates are the most common in the fossil record. Some simple pollen without openings in the fossil record may be from gymnosperms (Jarzen and Nichols, 1996).

CHAPTER II

New data on the palynology of the Triassic-Jurassic of the Lusitanian Basin

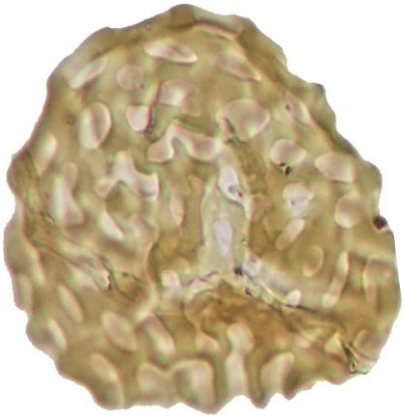

Chapter II cover:

Ischyosporites variegatus, Pereiros Formation, lower Hettangian, Lower Jurassic, sample LAG27b, Lusitanian Basin

Chapter II. New data on the palynology of the Triassic-Jurassic of the Lusitanian Basin

Adapted from the paper 1:

Vilas-Boas, M., Pereira, Z., Cirilli, S., Duarte, L. V., and Fernandes, P., 2021. New data on the palynology of the Triassic–Jurassic boundary of the Silves Group, Lusitanian Basin, Portugal. Review of Palaeobotany and Palynology, 290, 104426. https://doi.org/10.1016/j.revpalbo.2021.104426

Abstract

New evidence is presented on the Triassic–Jurassic boundary in the northern Lusitanian Basin, Portugal, based on miospore assemblages from the Silves Group's composite Upper Triassic to Lower Jurassic succession. The latter comprises, from base to top, the Conraria, Penela, Castelo Viegas and the Pereiros formations. Three informal palynological zones have been documented and compared with coeval palynozones from West and South Europe providing new biostratigraphic data to detail the age of the lower and upper formations of the Silves Group and to review previous age attribution.

A Norian, possibly earliest Rhaetian age, is documented for the Conraria Formation on the basis of a palynological assemblage referable to the *Classopollis meyerianus* - *Granuloperculatipollis rudis* (CG) zone. The Penela and Castelo Viegas formations did not allow a palynostratigraphic revision, due to the not promising lithology for palynological studies. The Pereiros Formation is dated on the basis of microflora assemblages referable, from bottom to top, the *Ischyosporites variegatus* - *Kraeuselisporites reissingeri* (IK) zone of late Rhaetian - earliest Hettangian age and *Pinuspollenites minimus* (Pm) zone of Hettangian age. The unconformity between the underlying Castelo Viegas Formation and the overlying Pereiros Formation did not allow to define the lower

boundary of the IK palynozone. The Triassic-Jurassic boundary lies in the lower part of Pereiros Formation within the IK zone. The microflora assemblages from the Lusitanian Basin show close affinity to those of eastern N America and western Tethys areas.

Keywords: Spores, Pollen, Palynostratigraphy, Triassic-Jurassic boundary (TJB), Lusitanian Basin, Portugal

1. Introduction

One of the initial objectives of this study was to identify in the Silves Group succession (see Soares *et al*., 2012) the Triassic-Jurassic boundary (TJB, 201.4 Ma; Gradstein and Ogg, 2020) since it represents one of the most severe biotic crises of the Phanerozoic (Raup and Sepkoski, 1982; Sepkoski, 1996; Tanner *et al*., 2004). The end-Triassic extinction caused a faunal turnover (Whiteside *et al*., 2007; Van de Schootbrugge *et al*., 2009; Lindström *et al*., 2017a, 2017b), particularly among marine invertebrates (Guex *et al*., 2004; Van de Schootbrugge *et al*., 2008), but the impact on terrestrial floras is debatable (Tanner *et al*., 2004; Cirilli *et al*., 2009; Cirilli, 2010; Lucas *et al*., 2011). Recent studies of European plant macro- and microfloral databases suggest that no major extinction occurred across the TJB (Barbacka *et al*., 2017). Nevertheless, high-resolution studies (Lindström, 2016; Lindström *et al*., 2017a, 2017b, 2021) indicate a major change in the palynoflora composition, varying from a stable pre-extinction, followed by an extinction phase (with great turnover-rates and taxonomic losses), as well as, a recovery phase, and ending in a stable post-extinction phase (the Hettangian radiation). These phases are interpreted as a reaction to the end-Triassic environmental changes (Lindström, 2016; Lindström *et al*., 2017a, 2017b). Additionally, the TJB extinction phase is characterised by high relative abundances of spores, an event (or feature) that can be traced worldwide, and it is marked by a major regression (Hallam and Wignall, 1999; Hesselbo *et al*. 2004; Hillebrandt *et al*., 2013; Lindström *et al*., 2017a, 2017b). The pre-extinction and recovery phases are coincident with a prominent transgression in Western

Europe and Tethys regions (Hallam and Wignall, 1999; Lindström *et al*., 2017a, 2017b).

The increased tectonic activity and sea-level fluctuations at the TJB, particularly in the extinction phase, caused sedimentary hiatuses in many Western European basins (Lindström *et al*., 2017a, 2017b; Schneebeli-Hermann *et al*., 2018). However, each basin displays similar basin-fill evolutions, with a continental sand-prone lower unit, followed upwards by a mud-prone unit deposited in lacustrine and marginal marine environments (Frizon de Lamotte *et al*., 2015).

In southern Portugal, North Africa and Eastern North American regions, the end-Triassic is marked by the magmatic activity of the Large Igneous Province of the Central Atlantic Magmatic Province (CAMP). In Portugal, the CAMP influence is marked by the Messejana Dike (intrusive CAMP, age 200 Ma according to Wilson and Giraud, 1998), and the Volcano-Sedimentary Complex of the Algarve Basin (Verati *et al*., 2007; Martins *et al*., 2008). Except for the southernmost part, there is no direct evidence of CAMP-related rocks in the Lusitanian Basin (West Portugal; Azerêdo *et al*., 2003; Kullberg *et al*., 2013). The CAMP magmatism contributed to global environmental and climatic changes, increasing the effects of the end-Triassic extinction phase (Nomade *et al*., 2007; Cirilli *et al*., 2009; Deenen *et al*., 2010; Capriolo *et al*., 2020). The flora of this age may have been affected by the effects of CAMP volcanism, with acid rain and acidification of freshwater, and global warming due to the greenhouse effect (Hesselbo *et al*., 2002; Guex *et al*., 2004; Marzoli *et al*., 2004; Tanner *et al*., 2004, 2007; Schaltegger *et al*., 2008; Van de Schootbrugge *et al*., 2008, 2009; Cirilli *et al*., 2009, 2018; Lindström, 2016; Davies *et al*., 2017; Lindström *et al*., 2019; Panfili *et al*., 2019).

This work studied the palynological content of thirty-nine samples recovered in several composite sections, representing the Upper Triassic and Lower Jurassic deposits of the Silves Group in the Lusitanian Basin (Fig. II.1 and II.2).

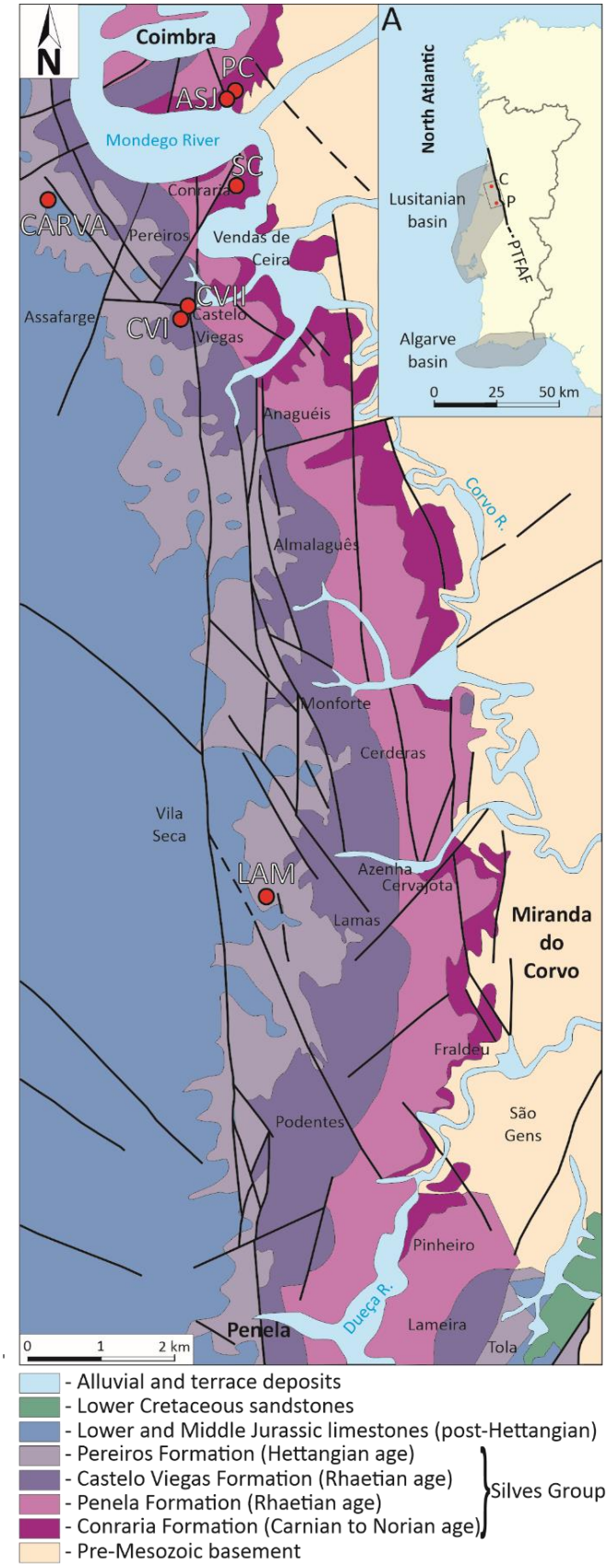

Figure. II.1. Map of the studied area with location of studied sections (based on Soares *et al*., 2012). Section abbreviations are defined in Table II.1.

The palinostratigraphic studies carried out previously in the Silves Group in the Lusitanian Basin, in the Upper Triassic interval - extreme base of the Jurassic, are quite limited. The first investigation was carried out by Doubinger *et al*. (1970). This study was later continued by Adloff *et al*. (1974), where the detailed microflora of the Silves Group in the northern region of the Tagus River (from Anadia to Tomar) was analyzed, based on the sedimentology and alostratigraphy work that was being developed by Palain, with the classic definition in megasequences A, B, and C (Palain, 1976, 1979).

The main goal of this study was to assign relative ages to the different stratigraphic units of the Silves Group, including the recognition of the TJB. Moreover, palynological correlations were established with basins in the same palaeogeographic domain and palaeoclimatic belt during the Late Triassic and Early Jurassic.

2. Geological Setting

The Triassic and Jurassic deposits in the Western Iberia margin are included in the Silves Group and have been recognised as the lowermost Mesozoic in the Lusitanian and Algarve basins (e.g., Palain, 1976; Soares *et al*., 2012; Kullberg *et al*., 2013). Mainly composed of siliciclastic rocks, the Silves Group overlaps Precambrian metamorphic and Carboniferous rocks, being particularly well represented in the Coimbra-Penela region, which corresponds to the studied area in this work (Fig. II.1).

Over the past century, several works have been published regarding the Silves Group in the Lusitanian Basin (e.g., Carvalho, 1950; Palain, 1976, 1979). More recently, during the work and publication of the Geological Map of Portugal, Coimbra-Lousã-19-D 1/50000 scale, Soares *et al*. (2007, 2012) proposed the redefinition of the Silves Group lithostratigraphy, which involves four formations, from base to top (Fig. II.2).

The Conraria Formation is marked by an angular unconformity (D1) at the base and is composed of red conglomerates and sandstones at the base (A1 of Palain, 1976, 1979), followed upwards by red and/or grey sandstones and

mudstones with plant fossils of *Voltzia ribeiroi* (A2 of Palain, 1976, 1979). This unit is interpreted as alluvial plain deposits with sustained areas of saline waterlogging, marked by an arid climate with intermittent and short periods of heavy precipitation (Palain, 1976; Soares *et al*., 2012). In the Coimbra region, this unit has a thickness of about 150 m (Soares *et al*., 2012). The macroelements of the palaeoflora (e.g., *Voltzia ribeiroi, Clathropteris,* and *Otozamites*), found in strata included in the Conraria Formation, are typical of a Rhaetian age (Teixeira, 1942; Carvalho, 1950).

The Penela Formation (basal part of B1 of Palain, 1976, 1979) has an erosional basal contact marked by the D2a disconformity, across the Conraria Formation, and consists of red and brown sandy conglomerates with a thickness of about 90 to 120 m in the Coimbra - Penela region (Soares *et al*., 2012). The upper part of this unit, the Melhorado Beds (Soares *et al*., 2012), comprises brown/red sandy mudstone beds interpreted as overbank deposits, with conspicuous calcite and dolomite diagenetic nodules. This formation is interpreted as deposited in a meandering river system (Soares *et al*., 2012).

The Castelo Viegas Formation (upper part of B1 of Palain, 1976, 1979), conformably overlays the Penela Formation (B1 of Palain, 1976) and consists of coarse-grained arkoses, sometimes as 4 to 5 meters thick intervals, intercalated with centimetric thick mudstone beds. The unit's base is marked by an angular unconformity (D2b), with a significant regional expression. The total thickness in the studied area is about 110 m (Soares *et al*., 2012). Compared with the last unit, the Pereiros Formation marks a very important change of facies, materialised by an important discontinuity (D3a *in* Soares *et al*., 2012). This unconformity may correspond to a period of non-deposition and partial erosion of the uppermost beds of the Castelo Viegas Formation. The basal part of the Pereiros Formation (B2 of Palain, 1976, 1979) is a lacustrine sequence composed of fine crystalline dolostones with siliciclastic intercalations, alternated with centimetric thick layers of mudstones, with some rich levels of bivalves (*Isocyprina*) and gastropods (*Promathildia*) (*Isocyprina* Beds). With around 10 m thick, this mix of carbonate-siliciclastic lower part of the Pereiros Formation is followed by coarse to very coarser brownish sandstone layers (C1 of Palain, 1976, 1979), with rare fossils of the fern *Clathropteris meniscoides* (Kullberg *et*

al., 2013) (*Clathropteris* Beds). The upper part of the Pereiros Formation is composed of a third unit (C2 of Palain, 1976, 1979), dominated by sandy mudstones, with red and grey colours, alternating with fine-grained dolostones, dolomitic marls and, very locally, thin gypsum levels (Azerêdo *et al*., 2003; Sêco *et al*., 2015). At the top of the Pereiros Formation, another important facies change is observed (disconformity D3c), occurring a thick succession of dolostones that belongs to the Coimbra Formation (Azerêdo *et al*., 2003, 2014; Dimuccio *et al*., 2014, 2016; Duarte *et al*., 2014; Gómez *et al*., 2019). The invertebrate and plant macrofossils identified in the Pereiros Formation indicate a Hettangian age (Teixeira, 1942).

3. Studied Sections: stratigraphy and general descriptions

The Silves Group was studied in the Coimbra - Penela region, which is regarded as the type area for this unit (Soares *et al*., 2012) (Fig. II.1). Several composite sections spanning the previously described lithostratigraphic units were sampled and analysed. Locations of the several sections are presented in Fig. II.1, and the stratigraphic position of each section is shown in Fig. II.2 and Table II.1.

The Conraria Formation was sampled in three different sections: Sobral Cid (SC), Camping Site (PC), and Alto de S. João (ASJ). The Sobral Cid outcrop is located on the N110 road and consists of alternating sandstones and red mudstones. This section corresponds to the Conraria Formation type-section of Soares *et al*. (2012) and is equivalent to the lower part of unit A2 of Palain (1976). At the Sobral Cid outcrop, five samples were collected, and from these, only two samples yielded sporomorphs (Fig. II.2, Table II.1). The Camping Site outcrop is located near Coimbra's Camping site, along the N17 road. The sequence sampled comprises intercalations of red/grey sandstone (Miranda *et al*., 2010). Three samples were collected at this locality, but only two were positive for palynology (Table II.1). The Alto de S. João section, is located at the Quinta da Portela street and corresponds to the uppermost part of the Conraria Formation (top of the unit A2 of Palain, 1976), is composed of alternating red and grey mudstones with reddish sandstones. Here three samples were collected, but only two yielded sporomorphs (Fig. II.2).

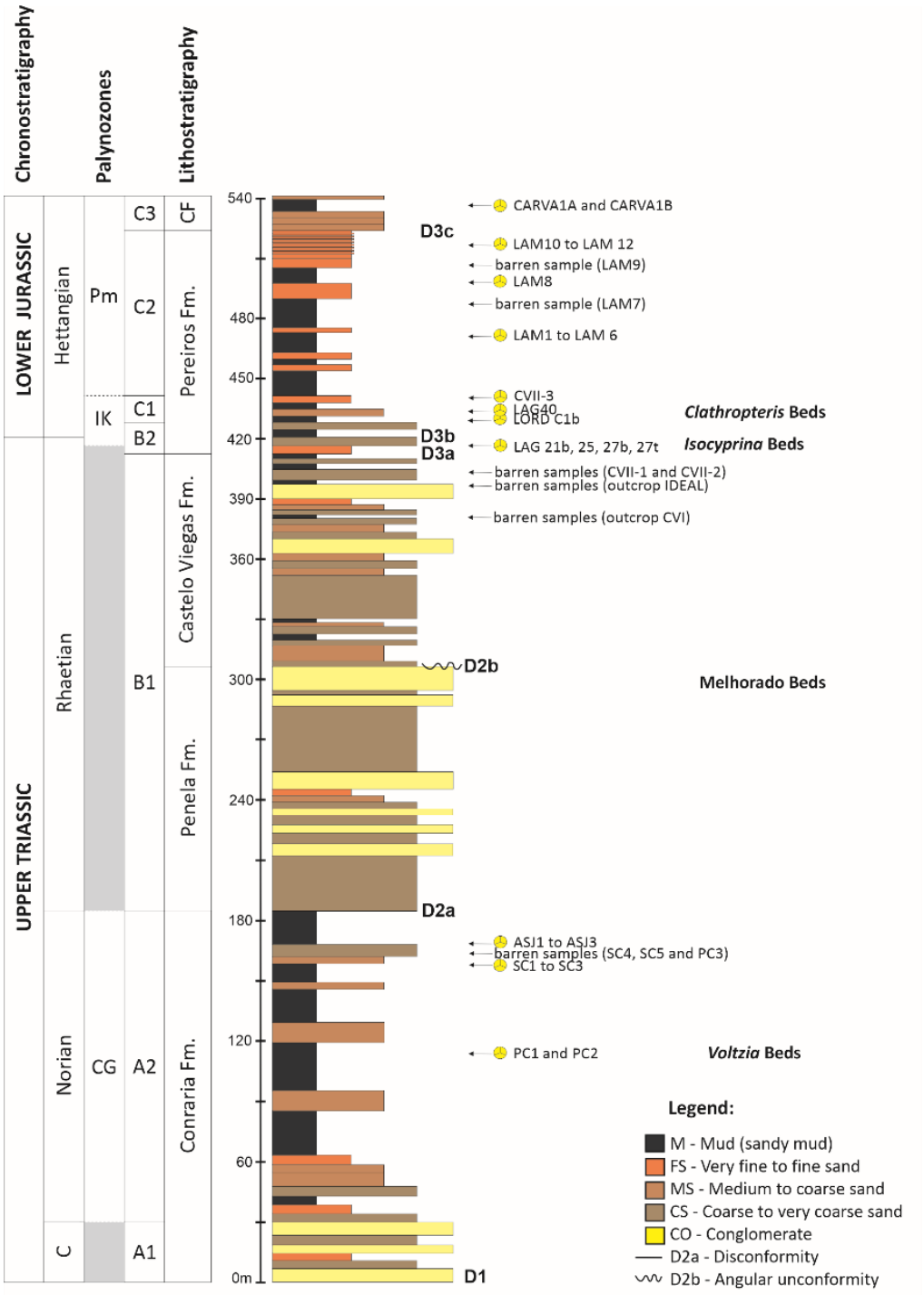

Figure. II.2. Stratigraphic log, with location of studied productive samples and sections (adapted from Soares *et al.*, 2012), C. Carnian. CF - Coimbra Formation. Section abbreviations are defined in Table II.1.

Table II.1. List of studied samples.

Formation		Sample	Section	Geographic Coordinates	Sporomorphs
Coimbra Fm.	**C3**	CARVA 1B	Carvalhais	N40º10'21.59''; W8º26'8.67''	productive
		CARVA 1A			productive
Pereiros Formation	**C2**	LAM 12	Lamas	N40º5'6.42''; W8º23'10.30"	productive
		LAM 11			productive
		LAM 10			productive
		LAM 9			barren
		LAM 8			productive
		LAM 7			barren
		LAM 6			productive
		LAM 5			productive
		LAM 4			productive
		LAM 3			productive
		LAM 2			productive
		LAM 1			productive
		CVII-3	Castelo Viegas II	N40º9'47.63''; W8º24'28.99''	productive
	C1	LAG 40	Lordemão	N40º13'57.48"; W8º24'52.44"	productive
		LORD C1b			productive
	B2	LAG 27t			productive
		LAG 27b			productive
		LAG 25			productive
		LAG 21b			productive
Castelo Viegas Formation	**B1**	CVII-2	Castelo Viegas II	N40º9'47.63''; W8º24'28.99''	barren
		CVII-1			barren
		IDEALB1TT	IdealMed	N40º13'30.55''; W8º25'24.97"	barren
		IDEALB1			barren
		CVI-2	Castelo Viegas I	N40º9'48.58''; W8º24'26.61''	barren
		CVI-1			barren
		CVI-0			barren
Conraria Formation	**A2**	ASJ3	Alto de São João	N40º11'23.57''; W8º24'6.14''	barren
		ASJ2			productive
		ASJ1			productive
		PC3	Parque de Campismo	N40º11'25.78''; W8º23'59.21''	barren
		SC5	Sobral Cid	N40º10'27.20''; W8º23'59.91''	barren
		SC4			barren
		SC3			productive
		SC2			productive
		SC1			productive
		PC2	Parque de Campismo	N40º11'25.78''; W8º23'59.21''	productive
		PC1			productive

No samples were collected from the Penela Formation, due to the absence of lithologies favorable for palynology.

In the Castelo Viegas Formation, two stratigraphic sections were sampled, corresponding to Outcrop Castelo Viegas I (CVI) and Outcrop Castelo Viegas II (CVII), both located in Castelo Viegas road N110. The outcrop CVI correlates to the unit B1 of Palain (1976), and the three samples collected (Table II.1) were

barren for palynology. From the three samples collected in outcrop CVII, two samples did not yield sporomorphs, and the productive sample belongs to the basal grey mudstone beds of the base of unit C2 of Pereiros Formation (Table II.1). The Castelo Viegas Formation is a sequence dominated by coarse-grained sandstones, with some mudstone intercalations, deposited in a paleonviroment evolving from fluvial to transitional (Palain, 1976; Soares *et al.,* 2012). The muddy lithologies were sampled but proved to be barren of palynomorphs, probably because strongly oxidized during sedimentary transport and depositional processes mostly occurred in continental and coastal environments.

The Pereiros Formation was sampled in the Idealmed (IDEAL) and Lordemão (LAG and LORD) sections (Coimbra region), and in the Lamas (LAM) section located at Miranda do Corvo region (Table II.1, Fig. II.1). The Idealmed section is located in Coimbra city (near the Idealmed Hospital) and straddles the boundary between the Castelo Viegas and Pereiros formations. The sequence observed consists of coarse-grained and thick arkose beds, alternated with centimetric to decimetric mudstone beds. At this location, the two collected samples were barren (Table II.1, Fig. II.2). From the Lordemão section, also located in Coimbra city, all five collected samples yielded sporomorphs (Table II.1, Fig. II.2). The samples from this section were collected from the lowermost beds of the Pereiros Formation (unit B2 de Palain, 1976), consisting of thinly dolomitic mudstones. The younger beds exposed in the latter outcrop, are coarse to very coarse-grained white/brown sandstones with thin to very thin mudstone beds. The sample collected from this part of the sequence (Table II.1, Fig. II.2) yielded sporomorphs. The Lamas section is located in the Miranda do Corvo region and is the reference section of unit C2 of the Pereiros Formation. The sequence at this outcrop consists of variegated sandy mudstones intercalated with thinly bedded dolomitic marls and dolostones. Twelve samples were collected from this section, ten yielded sporomorphs, and two were barren (Table II.1, Fig. II.2). The last section studied, the Carvalhais (CARVA) section, marks the contact between the Pereiros and Coimbra formations. The lowermost beds of the Coimbra Formation consist of intercalation of thinly to medium-bedded grey marls and dolostones. From this outcrop, two samples were collected from the

first marly beds of the Coimbra Formation, and both yielded sporomorphs (Table II.1, Fig. II.2).

4. Materials and Methods

Standard palynological laboratory procedures were employed in the extraction (treatments with hydrochloric and hydrofluoric acids) and concentration of the organic matter, following the methodologies described by Wood *et al.* (1996) and Riding and Warny (2008). Twenty-six palynological samples studied (of thirty-nine) were productive, yielding moderate to well-preserved sporomorphs. The residues were sieved using a 20 µm mesh sieve, and the final concentrated sporomorphs were stained using safranine. Semi-quantitative abundance was determined by counting 250 specimens per slide. Two or three slides were scanned for rare taxa, which were recorded as present outside the count.

The slides were examined with transmitted light using a BX40 Olympus microscope equipped with an Olympus C5050 digital camera facility. All samples, residues and slides are currently curated in the collection of the Geological Survey of Portugal, LNEG, S. Mamede Infesta, Porto, Portugal.

5. Previous palynology studies in the Silves Group in the Lusitanian Basin

Previous palynostratigraphic studies in the Silves Group are scarce. A preliminary account of the palynology was presented by Doubinger *et al*. (1970) and Adloff *et al*. (1974), where the microflora of the Silves Group outcrops from the eastern part of the Lusitanian Basin (from Anadia to Tomar, Fig. II.1), were investigated. More recently, based practically on the same outcrops, Díez (2000) conducted a new palynological study. The palynological assemblages and conclusions obtained from these studies can be summarised as follows: i) the Conraria Formation yielded palynomorphs assigned to the early-middle Carnian, which includes *Circulina meyerianus (=Classopollis meyerianus)*, *Duplicisporites granulatus*, *D. mancus*, *Microcachrydites doubingeri*, *M. fastidioides*,

Monosulcites minimus, *Ovalipollis cultus*, *Paracirculina scurrilis* and *P. maljawinae* (Doubinger *et al.*, 1970; Adloff *et al.*, 1974); ii) the palynological assemblages of the Penela and Castelo Viegas formations containing *Araucaria germanicus*, *Circulina granulata*, *C. meyerianus (= Classopollis meyerianus), D. granulatus*, *Ischyosporites mesofoveasolidus*, *Kraeuselisporites altmarkensis (= K. reissingeri), Paracirculina tenebrosa*, *Patinasporites iustus* and *Todisporites major* have been assigned to middle Carnian to late Norian age (Adloff *et al.,* 1974; Díez, 2000; Arche and López-Gómez, 2014); and iii) the Pereiros Formation has been dated as Hettangian-Sinemurian on the basis of an assemblage comprising the taxa *Classopollis classoides*, *Cycadopites granulatus*, *C. deterius*, *Inaperturopollenites dubius* and *K. altmarkensis* (Adloff *et al*., 1974). However, more recently, the common presence of the taxa *K. altmarkensis* in the Pereiros Formation, led Díez (2000) and Arche and López-Gómez (2014) to refine its age, reinterpreted as late Norian to early Rhaetian.

6. Palynology results

In this studied succession, the sporomorph associations are described and documented in Fig. II.3. The quantitative and qualitative distribution of sporomorph associations are presented based on the relative abundance of prominent taxa and its first occurrence (FO) and last occurrence (LO) of selected stratigraphic important taxa (Fig. II.3). Selected specimens are illustrated in Plates II.I to II.V and a species list is presented in the Suplementary Appendix.

In this study, three palynoassociations are recognised. In stratigraphic order, oldest to youngest, they are:

Palynoassociation 1 - The microflora composing this association comes from the Conraria Formation (between 90 m to 182 m, Fig. II.2) and includes about 4 species of spores and 18 of pollen of moderate to well-preserved taxa. The association is characterised by the co-occurrence of *Classopollis meyerianus*, *Granuloperculatipollis rudis*, *Patinasporites densus,* and *Vallasporites ignacii*,

from the base up to the top of the assemblage zone. Other taxa always present are *Duplicisporites granulatus, Paracirculina quadruplicis*, *Praecirculina granifer* associated with *Convolutispora* sp., *Camarozonosporites* sp., *Kyrtomisporis* sp. and rare to common *Playfordiaspora* sp.. Additional components also include the pollen grains *Enzonalasporites vigens*, *Microcachrydites fastidioides*, *M. doubingeri*, *Ovalipollis ovalis*, *Samaropollenites speciosus*, *Triadispora staplini, Alisporites* sp., *Cycadopites* sp., *Ellipsovelatisporites* sp., *Monosulcites* sp. and *Triadispora* sp..

Palynoassociation 2 - The first productive samples characterizing this association come from the lower part of the Pereiros Formation (from 421 m to 428 m, Fig. II.2) which overlies, from bottom to top, the Penela Formation and the Castelo Viegas Formation. These two latter formations, which in total are about 230 m in average thickness (between 180 m to 410 m, Fig. II.2) are barren in palynomorphs and include an unconformity. Therefore, no palynological data are available to trace a continuity between the palynoassociation 1 and 2. The latter combines about 12 species of spores and 10 of pollen, from moderate to well-preserved. It is characterised by the First Occurrence (FO) of *Classopollis torosus*, *Kraeuselisporites reissingeri*, *Ischyosporites variegatus* with some trilete fern spores such as *Carnisporites* sp., *Deltoidospora* sp., *Dictyophyllidites mortonii, Dictyophyllidites* sp., *Todisporites major, Todisporites* sp. and *Trachysporites* sp.. Rare specimen of *Rhaetipollis germanicus* were recorded in two samples. Common to abundant specimens of *Araucariacites* sp. and *Classopollis meyerianus* and rare to common *Cyathidites* sp., *Cycadopites* sp., *Ellipsovelatisporites* sp. *Eucommiidites* sp., *Inaperturopollenites* sp., *Monosulcites* sp., and *Ovalipollis ovalis*, are also present. *Dictyophyllidites mortonii* makes its LO at the bottom of this zone (Fig. II.3).

Palynoassociation 3 - This association comes from the upper part of the Pereiros Formation (from 428 m to 540 m, Fig. II.2) and includes the units C1, C2 and C3. It combines about 14 species of spores and 14 of pollen, which range from

moderate to well-preserved. A group of important taxa have their FO in this association, as *Perinopollenites elatoides*, *Pinuspollenites minimus* and *Porcellispora longdonensis.* Other spores as *Calamospora tener*, *Apiculatisporis* sp., *Cingulatisporites* sp., *Leptolepidites* sp., *Polypodiisporites* sp., and *Chasmatosporites* sp. make also their FO. Pollen grains of *Classopollis meyerianus* and *C. torosus* are common to abundant up to the top of this interval in association with *Ovalipollis ovalis, Alisporites* sp. and *Araucariacites* sp.. *Kraeuselisporites reissingeri,* although rare, is continuously present along the whole zone.

7. Age discussion and correlation with key Eastern North America, Northwest Europe and Tethys basins

Three informal palynological zones are proposed for the Silves Group in the Lusitanian Basin, based mainly on the common abundance of characteristic species and in the FO (First Ocurrence) and LO (Last Ocurrence) of selected taxa (Figs. II.3 and II.4).

7.1 *Classopollis meyerianus - Granuloperculatipollis rudis* (CG) palynozone

It ranges from Norian to lowermost Rhaetian, for the co-occurrence of typical Norian and Rhaetian sporomorphs, such as *C. meyerianus and G. rudis* with *Patinasporites densus, Vallasporites ignacii, Duplicisporites granulatus, Paracirculina quadruplicis*, *Praecirculina granifer* ranging from Carnian up to Norian, rarely to lowermost Rhaetian. In particular, *G. rudis,* in the Northwest European domain, has the FO in late Carnian times, persisting until the middle Rhaetian (Batten and Koppelhus, 1996; Roghi, 2004; Buratti and Cirilli, 2007; Cirilli, 2010). As documented by literature, the European miospore assemblage zones show a transitional nature in the composition of Norian palynomorph assemblages, characterised by the progressive disappearances of Carnian taxa and the first occurrence of species that become dominant during the Rhaetian

(Morbey, 1975; Schuurman, 1977; Cirilli *et al*., 2005; Krystyn and Kürschner, 2005; Warrington *et al*., 2008; Cirilli, 2010; de Jersey and McKellar, 2013; Cirilli *et al*., 2015, 2018). The disappearance of the vesicate forms (e.g., *V. ignacii* and *P. densus*) took place during the late Norian and, occasionally, at the lowermost part of Rhaetian palynozones in numerous continental and marine sections (e.g., Morbey, 1978; Schuurman, 1979; Litwin *et al*., 1991; Krystyn *et al*., 2007a, 2007b; Kürschner *et al*., 2007; Cirilli *et al*., 2009; Cirilli, 2010; Irmis *et al*., 2015; Lindström *et al*., 2016). In addition, *Samaropollenites speciosus*, one of the main European taxa of the Onslow microflora, has been considered to decline in the late Norian (Cirilli and Eshet, 1991; Cirilli, 2010). In particular, the LO of *P. densus* has been commonly recorded and well documented in marine sedimentary successions, before the end of Rhaetian (Cirilli, 2010 and references therein; Kürschner and Herngreen, 2010).

In the CAMP successions of Morocco, the co-occurrence of *P. densus*, with younger taxa (i.e., *Tsugaepollenites pseudomassulae, Perinopollenites elatoides*) and dominant *Classopollis* group suggested an age slightly older than late Rhaetian (Marzoli *et al*., 2004; 2008; Cirilli, 2010; Lindström *et al*., 2016; Panfili *et al*., 2019), also constrained by a set of geochemical (i.e., carbon isotope and mercury shifts) and geochronological data (Blackburn *et al*., 2013; Dal Corso *et al*., 2014; Davies *et al*., 2017; Lindström *et al*., 2017a, 2017b). Similar assemblages were also recorded in the continental volcanic-sedimentary successions from Eastern North American CAMP, such as in the Fundy Basin, Nova Scotia (Fowell and Traverse, 1995; Cirilli *et al*., 2009) and Newark basins (Whiteside *et al*., 2007, 2010 and references therein).

7.2. *Ischyosporites variegatus - Kraeuselisporites reissingeri* (IK) palynozone

It can be overall assigned to the late Rhaetian age, given the presence of *Classopollis* (*C. meyerianus* and minor *C. torosus*) in association with other index species such as *I. variegatus*, *K. reissingeri,* and *Rhaetipollis germanicus*. Similar assemblages are well documented in several Italian areas from the Southern Alps

to Apennines and Sicily (Cirilli *et al*., 1994, 2015, 2018; Galli *et al*., 2007; Martini *et al*, 2007), in some southern Mediterranean areas such as Tunisia, Libya, Algeria, Morocco (Adloff *et al*., 1986; Yaroshenko, 2007; Cirilli, 2010) and other key areas (Morbey, 1975; Schuurman, 1977; Barrón *et al*., 2006; Kürschner *et al*., 2007; Warrington *et al*., 2008; Ruhl *et al*., 2009; Cirilli, 2010; de Jersey and McKellar, 2013; Hillebrandt *et al*., 2013; Lindström, 2016; Lindström *et al*., 2017a, 2017b). The palynological assemblages from northern Spain (Asturias) and France, although showing some common elements (e.g., dominance of *Classopollis* spp.), differ in the presence of rare *Ricciisporites tuberculatus* (Barrón *et al*., 2006; Gómez *et al*., 2007) which has not been recorded in the studied area. The absence or rarity of *R. tuberculatus* has been related to ecological and/or climatological preferences (Kürschner *et al*., 2014), since this taxon is reported in assemblages from Austria (Bonis *et al*., 2009; Bonis and Kürschner, 2012) and the UK (Bonis *et al*., 2010), is the second most abundant pollen type (> 20 %), next to *Classopollis* genus (Kürschner *et al*., 2014). Kürschner *et al*. (2014) referred that, when pollen types occur together, they alternate in abundance, so when *Classopollis* spp. are common, *R. tuberculatus* is rare. Nevertheless, other authors indicate that this pollen species has a latitudinal preference occurring commonly between the 30˚N to 60˚N latitude (Lindström, 2016; Kürschner *et al*., 2014). All these factors may justify the absence of *R. tuberculatus* in the southernmost sub-tropical to tropical regions, such as the location of the Lusitanian Basin in the Late Triassic - Early Jurassic times (Stampfli *et al*., 2001; Ruiz-Martínez *et al*., 2012; Berra and Angiolini, 2014; Scotese and Schettino, 2017). *Rhaetipollis germanicus* is also a valuable biostratigraphical marker to characterise the Rhaetian stage (e.g., "*Rhaetipollis germanicus* assemblage Zone" of Orbell, 1973) as documented in several palynological studies in the Rhaetian reference sections of the Boreal and European realms (Lund, 1977; Schuurman, 1977, 1979; Visscher *et al*., 1980; Koppelhus and Batten, 2002; Warrington, 2002; Barrón *et al*. 2006; Yaroshenko, 2007; Cirilli, 2010; Lindström, 2016; Juncal *et al*., 2020).

The FAD of *R. germanicus* is uncertain due to the lack of independently dated Norian–Rhaetian successions (Cirilli, 2010; Kürschner and Herngreen, 2010). In Svalbard, the limit for a Norian first appearance of this taxon was based

on ammonoid-dated Norian palynomorph assemblages (Smith, 1982), although more recently, Paterson and Mangerud (2015) did not record *R. germanicus* in the same strata. In the Barents Sea, this taxon is already present in Norian deposits (Hochuli *et al*. 1989). In the German Keuper, its first occurrence has been recorded in the lower Rhaetian (Lund, 1977, 2003; Schulz and Heunisch, 2005), although a late Norian occurrence in central and northwestern Europe has been not excluded by Kürschner and Herngreen (2010). In the Cantabrian Mountains (N Spain), an early-middle Norian age has been suggested for a palynological assemblage containing *R. germanicus, Camerosporites secatus,* and *Classopollis* spp. (Juncal *et al*., 2020). Although still uncertain, data from Austria should suggest its lowest occurrence in the middle Rhaetian (Krystyn *et al*., 2007a, 2007b). The LAD of *R. germanicus* has been dated as late Rhaetian (Orbell, 1973; Achilles, 1981; Brenner, 1986) as shown in Austria, where the "*Rhaetipollis germanicus* Assemblage Zone" ranges into the upper part of the pre-planorbis beds (Morbey 1975; Kürschner *et al*. 2007). Phase III of Schuurman (1979), regarded as transitional between phase II (Norian) and phase IV (late Rhaetian) registers the rapid decrease and disappearance of *R. germanicus*. In Northern Europe (North Sea basin, East Greenland, and Scania), the LAD of *R. germanicus* has been dated as 'middle Rhaetian' (Lund, 1977; Pedersen and Lund, 1980; Guy-Ohlson, 1981). In several European reference sections, including the GSSP Kuhjoch section (Hillebrandt *et al*., 2013), *R. germanicus*, seems to disappear in the latest Rhaetian just before the acme of *K. reissingeri* (Barrón *et al*., 2006; Kürschner *et al*., 2007; Galli *et al*., 2007; Cirilli, 2010; Kürschner and Herngreen, 2010; Lindström, 2016; Lindström *et al*., 2017a, 2017b, 2021). In the St. Audrey's Bay section (UK), *R. germanicus* is present from the basal SAB1 to the uppermost SAB2 zones and disappears before the end of the Rhaetian (Hounslow *et al*., 2004; Bonis *et al*., 2010).

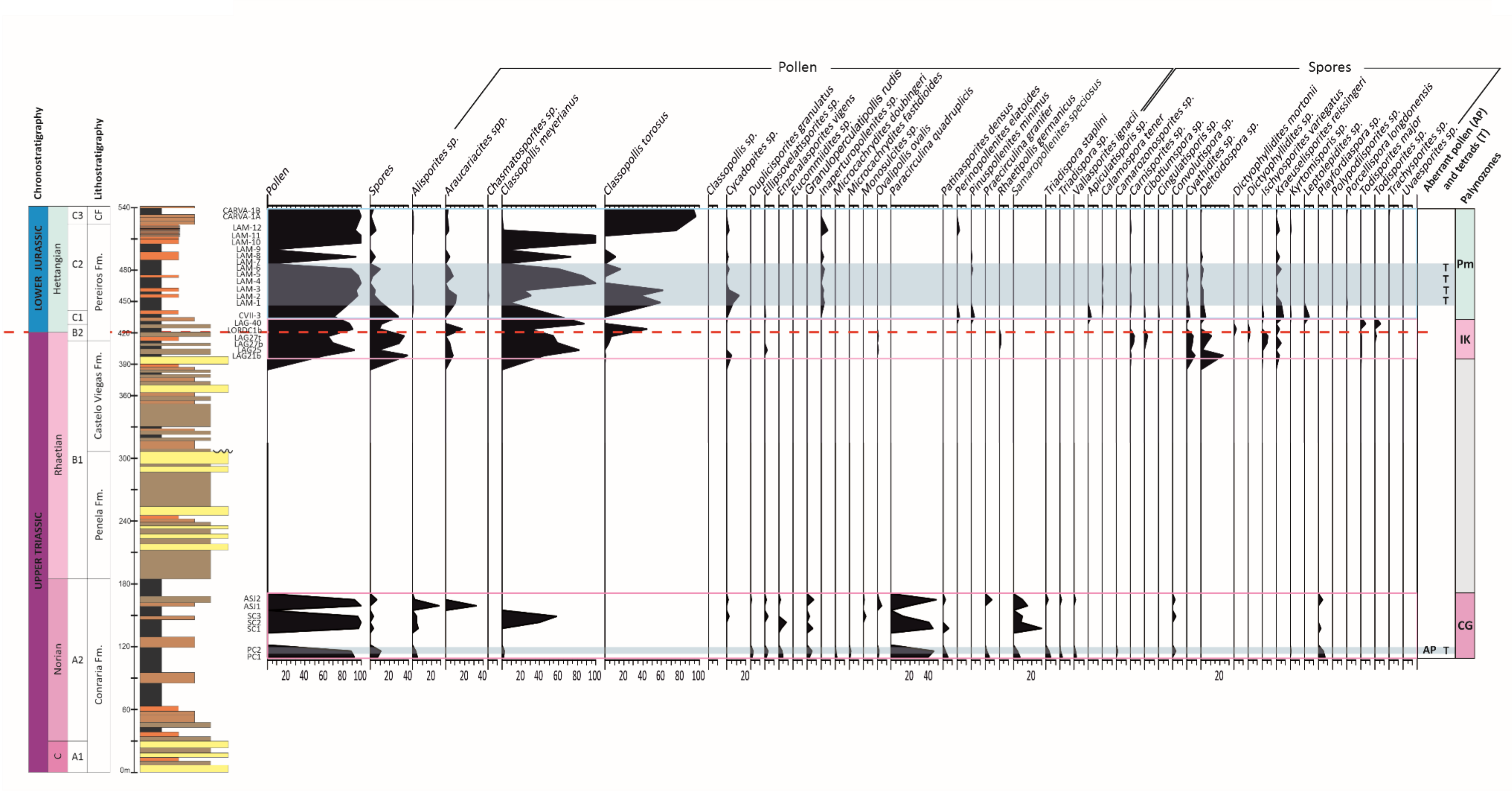

Figure II.3. Composite range chart of the sporomorph taxa found in the Silves Group, Lusitanian Basin and palynozones. Gray bands represent barren palynological intervals. C = Carnian. CG = *Classopollis meyerianus-Granuloperculatipollis rudis* palynozone. IK= *Ischyosporites variegatus-Kraeuselisporites reissingeri* palynozone. Pm = *Pinuspollenites minimus* palynozone.

The first occurrences of *I. variegatus* and *K. reissingeri,* associated with abundant to common *Classopollis* spp. and rare *R. germanicus,* which disappears at the top of this zone, led to tentatively referred this association to the topmost of the RPo Zone, possibly lowermost TH zone, as defined in the base Hettangian GSSP at Kuhjoch (Karwendel Mountains, Austria), therefore below the TJB (Hillebrandt *et al*., 2013). The lower boundary of *Ischyosporites variegatus - Kraeuselisporites reissingeri* (IK) palynozone in the Lusitanian Basin cannot be exactly placed, due to lack of data along a thick portion of the succession. Consequently, by correlating these assemblages with the GSSP at Kuhjoch, the RL and possibly the lowermost part of the RPo zones are missing in the Lusitanian Basin (Fig. II.4). This could be due to the lack of palynological data from approximately 230 m thick interval spanning the Pereiros and the Castelo Viegas formations, and/or the presence of a significant hiatus at the D2b unconformity (Figs. II.2 and II.3). The upper part of *Ischyosporites variegatus - Kraeuselisporites reissingeri* (IK) zone is marked by the disappearance of *R. germanicus,* associated with abundant to common *Classopollis* spp. in addition to *I. variegatus* and *K. reissingeri*. It could represent the transitional zone bracketing the TJB, approximately corresponding to the TH zone (Hillebrandt *et al*., 2013).

7.3. *Pinuspollenites minimus* (Pm) palynozone

It is defined on the FO of *P. minimus* and *Perinopollenites elatoides* accompanied by the dominance of *Classopollis meyerianus* and *C. torosus* and could be dated as early Hettangian (uppermost TH to basal TPi zones in Hillebrandt *et al*., 2013). Van de Schootbrugge *et al*. (2009) and Schobben *et al*. (2019) record, respectively from Germany, Sweden drilling cores and from Bonenburg (Central European Basin) a floral change characterised by a progressive decrease of Rhaetian pollens, including *Rhaetipollis germanicus*, until they disappear and are replaced in the earliest Hettangian by assemblages dominated by *Classopollis* spp., *P. elatoides, P. minimus* and bisaccates (e.g. *Alisporites* spp.) accompanied by acme of *Kraeuselisporites reissingeri*. In the GSSP Kuhjoch section, the *Trachysporites-Pinuspollenites* Zone (TPi Zone),

Jurassic in age, is identified by a marked increase in abundance of *P. minimus*, which is already present in low abundance in the underlying TH zone, abundant *Ricciisporites tuberculatus* and *K. reissingeri* associated with *Classopollis* spp. and *Trachysporites fuscus* (Hillebrandt *et al*., 2013).

However, the low abundance of the index taxa (e.g., *P. minimus*, *K. reissingeri*), and the FO of *Porcellispora longdonensis* that in other reference sections of the European domain occurs in the underlying TH zone, preclude unequivocal assignment to the Hettangian. *Cerebropollenites thiergartii*, the key marker taxon of Hettangian age is absent from the studied sections in the Lusitanian Basin sequence. In Spain, the first occurrence of *P. longdonensis* was recorded in the Hettangian (upper part of the *K. reissingeri* Zone), together with *P. minimus* and *Cerebropollenites thiergartii* (Barrón *et al*., 2002, 2006). Other occurrences of *P. longdonensis* in Hettangian in southern Europe are in the Vicentinian Alps in Italy (Clement-Westerhof *et al*., 1974), as well in northern Germany (Schulz and Heunisch, 2005).

7.4. Summary of palynozones

Based on the above-described palynozones, the studied formations can be dated as follow:

The Conraria Formation, especially the unit A2 of Palain (1976), can be dated as Norian up to earliest Rhaetian age based on the palynological assemblage referred to the *Classopollis meyerianus - Granuloperculatipollis rudis* (CG) palynozone (Figs. II.3 and II.4). Previous age attribution from literature (Díez, 2000) indicated a lower to middle Carnian age for the lower part of the Conraria Formation. The palynomorph assemblage described by this author, is similar to the CG palynozone of this study, with seven pollen taxa identified (e.g., *C. meyerianus*, *Duplicisporites granulatus*, *Microcachrydites doubingeri*, *M. fastidioides* and the genera *Ovalipollis* and *Paracirculina*). However, *G. rudis* is absent, indicating that the recovered assemblage could correspond to the lower part of the Conraria Formation.

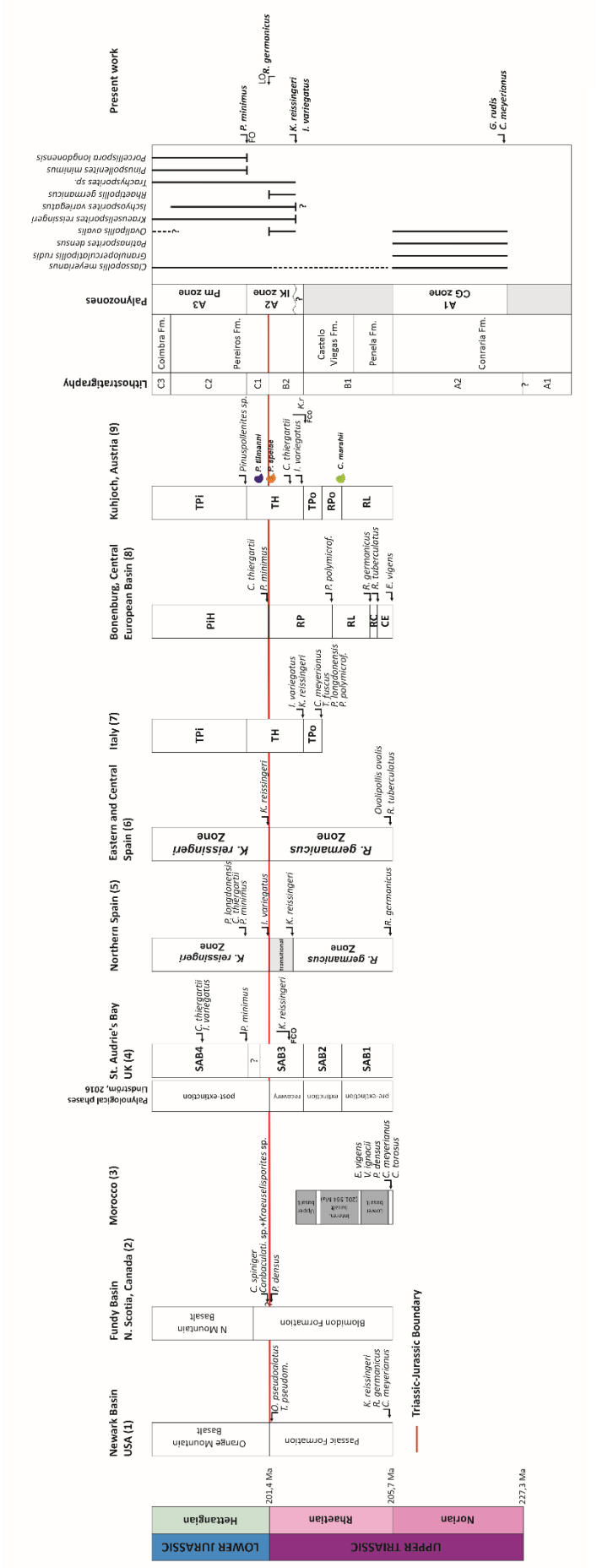

Figure II.4. Palynostratigraphic correlations across the Triassic–Jurassic transition for the Western Europe and Tethys basins. Palynoflora phases, absolute ages, and ammonoid information follows Lindström *et al.* (2017a). T. pseudom. (*Tsugaepollenites pseudomassulae*); Conbaculati. (*Conbaculatisporites* sp.); P. polymicrof. (*Polypodiisporites polymicroforatus*); K.r (*Kraeuselisporites reissingeri*). 1. Newark Basin, USA (Fowell and Traverse, 1995; Whiteside *et al.*, 2007, 2010). 2. Fundy Basin, Nova Scotia, Canada (Cirilli *et al.*, 2009); 3. St. Audrie's Bay, UK (Bonis *et al.*, 2010); 4. Northern Spain (Barrón *et al.*, 2006); 5. Eastern and central Spain (Gómez *et al.*, 2007); 6. Morocco (Panfili *et al.*, 2019); 7. Italy (Galli *et al.*, 2007; Cirilli *et al.*, 2015, 2018); 8. Bonenburg, Central European Basin (Schobben *et al.*, 2019; Gravendyck *et al.*, 2020); 9. Kuhjoch, Austria (Kürschner *et al.*, 2007; Bonis *et al.*, 2009; Hillebrandt *et al.*, 2013). Timescale according to Gradstein and Ogg (2020).

The overlying Penela and Castelo Viegas formations did not provide any new palynological data due to the not promising lithologies for palynological studies. Previous age attribution of Díez (2000) dated the B unit of Palain (1976), which includes the Penela, Castelo Viegas (unit B1), and the base of Pereiros (unit B2) formations, as middle Carnian to Norian age. Based on the new palynological data presented in this paper, deriving from the underlying and overlying formations makes uncertain the previous age attribution.

An overall Rhaetian to Hettangian age could be indicated for the Pereiros Formation.

The lower part of the formation (unit B2), can be dated as Rhaetian up to the TJB on the basis of the *Ischyosporites variegatus* - *Kraeuselisporites reissingeri* (IK) palynozone, and the mid-upper part (C1 and C2 units of Palain, 1976) assigned to the early Hettangian based on the *Pinuspollenites minimus* (Pm) palynozone (Figs. II.3 and II.4).

The lowermost part of the Pereiros is marked by an important unconformity that seems to truncate the siliciclastic beds at the top of the Castelo Viegas Formation. This unconformity surface has been regarded as the Triassic-Jurassic regional mapping boundary (Soares *et al*., 2007, 2012). Nevertheless, the palynological data points to the recognition of the TJB within the B2 unit, at the base of Pereiros Formation.

Therefore, the results of the present study provide a revised age interpretation with respect to Adloff *et al*. (1974) suggesting a Hettangian – Sinemurian age for the Pereiros Formation and to Díez (2000) and Arche and López-Gomez (2014) indicating an early Norian to Rhaetian for the mid part of Pereiros Formation (unit C1 of Palain, 1976).

The basal part of the Coimbra Formation (unit C3 of Palain, 1976) lies within the *Pinuspollenites minimus* zone as documented by the palynological association of the two samples collected and therefore assigned to the early Hettangian, at least for this portion. Further detailed studies are needed to ascertain the age of the Coimbra Formation, and to confirm if the Pereiros and Coimbra formations boundary corresponds to the Hettangian - Sinemurian

transition, as it has been documented in the literature (e.g., Azerêdo *et al*., 2003; Soares *et al*., 2007; Kullberg *et al*., 2013).

In conclusion, the palynological associations of the Silves Group from the middle part of the Conraria Formation to the lowermost beds of the Coimbra Formation can be assigned to an interval ranging from Norian to Hettangian times. However, the presence of hiatuses and disconformities in the stratigraphic sequence, and the lack of suitable lithologies for palynology, precludes a continuous palynostratigraphic record and some missing data to constrain the early and middle Rhaetian time interval.

Besides these questions, the detailed quantitative study of palynofloral assemblages by identifying three informal assemblage zones allows a good palynostratigraphic framework for the Silves Group in the Lusitanian Basin (Fig. II.3).

7.5. Summary of the correlation with key Eastern North America, Northwest Europe, and Tethys basins

The palynological assemblages from the Lusitanian Basin across the Triassic-Jurassic transition show some affinity with coeval assemblages from Eastern North America (Newark Basin in Eastern USA, Fundy Basin in Eastern Canada), Western Europe, and Tethys basins (i.e., UK, Italy, Central European Basin, Austria, Spain, and Morocco) (Fig. II.4). The Late Triassic- early Jurassic paleogeographic reconstructions of Iberian put it in a middle position between Eastern N America, Western Europe, and the Tethyan basins. These would have been reasonably close to Iberia and occupied a similar palaeolatitude.

Plate II.I. Selected palynomorphs from the CG palynoze from Conraria Formation. **1-3, 5-11**: Outcrop Parque de Campismo section; **4**: Outcrop Alto de São João section. All the specimens are housed in the collections of LNEG (Portuguese Geological Survey), S. Mamede de Infesta, Porto, Portugal. Species name is followed by the sample and slide number, and microscope coordinates. Scale bar in the plate.

1. *Paracirculina quadruplicis* Scheuring 1970; sample PC1, slide 7, MC 1333-208.
2. *Paracirculina quadruplicis* Scheuring 1970; sample PC1, slide 7, MC 1460-201.
3. *Samaropollenites speciosus* Goubin 1965; sample PC2, slide 9, MC 1542-181.
4. *Granuloperculatipollis rudis* Venkatachala & Góczán emend. Morbey 1975; sample ASJ2, slide 1, MC 1449-250.
5. *Enzonalasporites vigens* Leschik emend. Scheuring 1970; sample PC2, slide 9, MC 1475-213.
6. *Patinasporites densus* Leschik emend. Scheuring 1970; sample PC1, slide 7, MC 1149-50.
7. *Playfordiaspora* sp.; sample PC1, slide 7, MC 1467-140.
8. *Microcachrydites doubingeri* Klaus 1964; sample PC1, slide 7, MC 1130-115.
9. *Triadispora staplini* (Jansonius) Klaus 1964; sample PC2, slide 9, MC 1405-38.
10. *Microcachrydites fastidioides* (Jansonius) Klaus 1964; sample PC2, slide 9, MC 1475-213.
11. *Praecirculina granifer* (Leschik) Klaus 1960; sample PC1, slide 7, MC 1490-168.

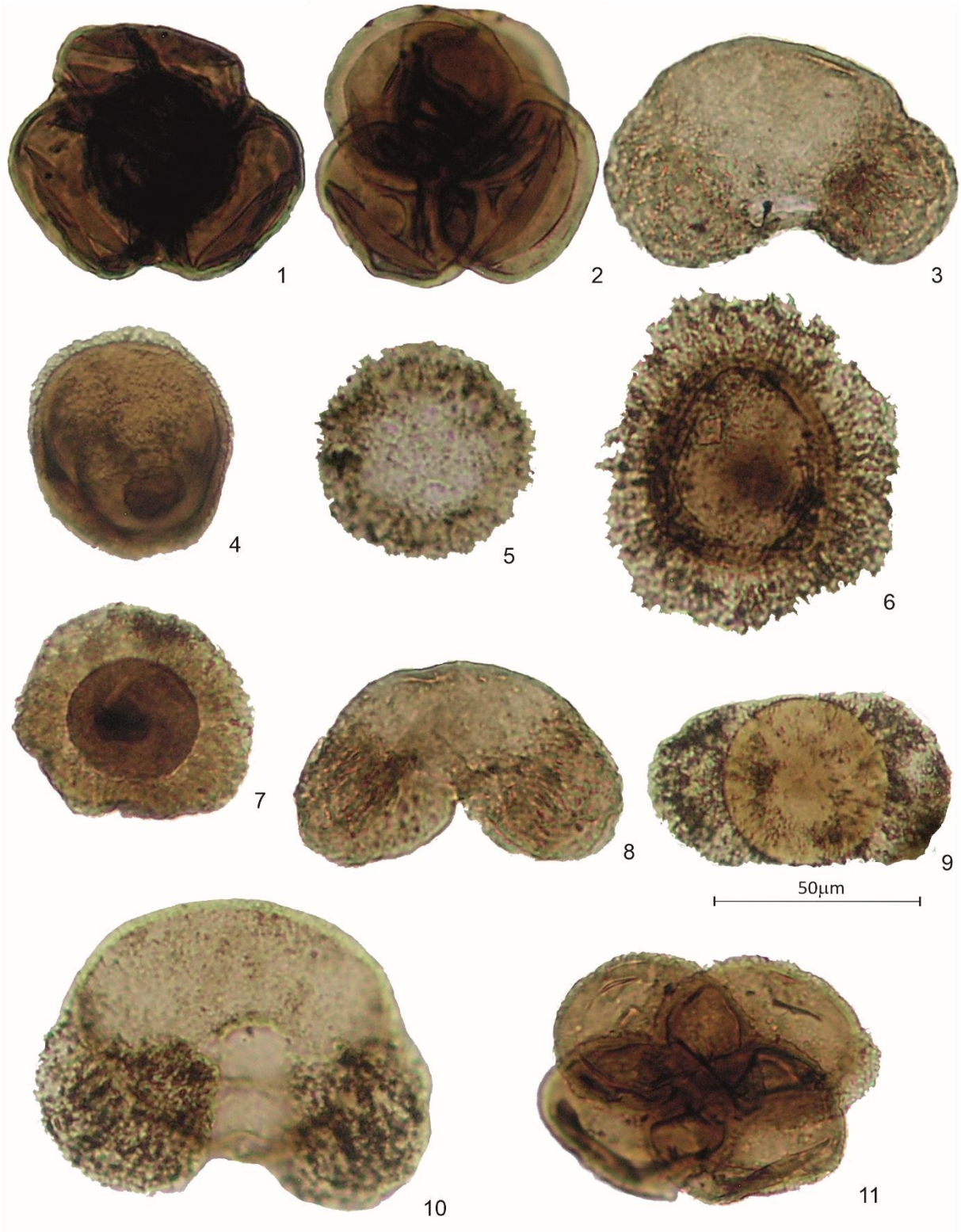

Plate II.I. (caption in the previous page)

Plate II.II. 1-3: Selected palynomorphs from the Conraria Formation at the Outcrop Parque de Campismo section (CG palynozone). **4-8**: Selected palynomorphs from the Pereiros Formation at the Outcrop Lordemão section (IK palynozone). **9**: Selected palynomorph from the Pereiros Formation at the Outcrop Lamas section (Pm palynozone). All the specimens are housed in the collections of LNEG (Portuguese Geological Survey), S. Mamede de Infesta, Porto, Portugal. Species name is followed by the sample and slide number, and microscope coordinates. Scale bar in the plate.

1. *Vallasporites ignacii* Leschik 1955; sample PC1, slide 7, MC 1078-98.
2. *Duplicisporites granulatus* Leschik 1955 emend. Scheuring 1970; sample PC2, slide 9, MC 1261-250.
3. *Alisporites* sp.; sample PC2, slide 9, MC 1478-20.
4. *Ischyosporites variegatus* (Couper) Schulz 1967; sample LAG 27b, slide 7, MC 1339-156.
5. *Dictyophyllidites mortonii* (Jersey) Playford & Dettmann 1965; sample LAG 27b, slide 7, MC 1329-141.
6. *Cibotiumspora* sp.; sample LAG 27b, slide 7, MC 1330-60.
7. *Rhaetipollis germanicus* Schulz 1967; sample LAG 27b, slide 4, MC 1255-128.
8. *Rhaetipollis germanicus* Schulz 1967; sample LAG 27t, slide 7, MC 1395-142.
9. *Classopollis meyerianus* (Klaus) de Jersey 1973; sample LAM 6, slide 1, MC 1520-100.

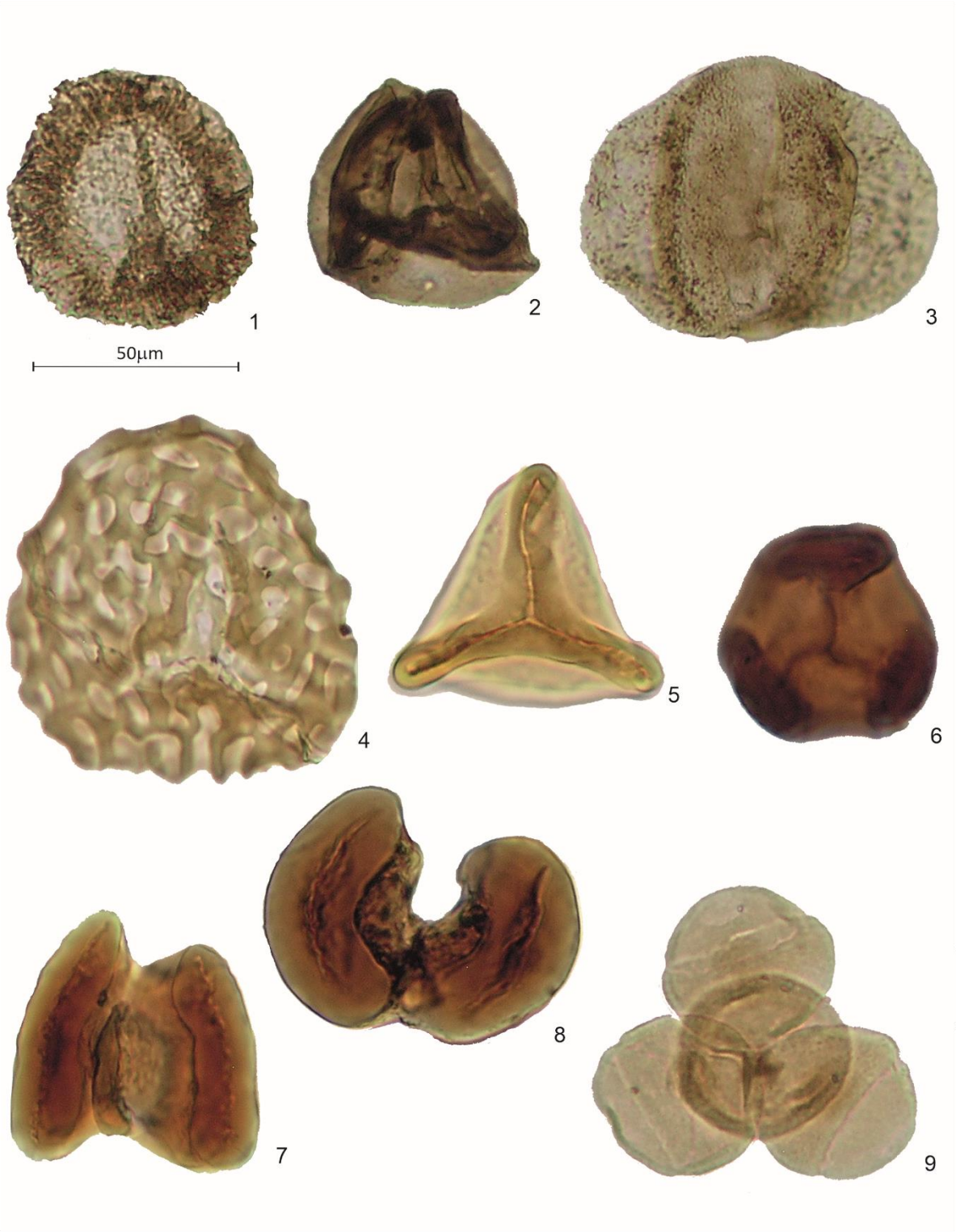

Plate II.II. (caption in the previous page)

Plate II.III. Selected palynomorphs from the Pereiros Formation at the Outcrop Lamas section (Pm palynozone). All the specimens are housed in the collections of LNEG (Portuguese Geological Survey), S. Mamede de Infesta, Porto, Portugal. Species name is followed by the sample and slide number, and microscope coordinates. Scale bar in the plate.

1. *Cycadopites* sp.; sample LAM 2, slide 5, MC 1340-215.
2. *Cycadopites* sp.; sample LAM 1, slide 2, MC 1415-105.
3. *Classopollis torosus* Reissinger 1950; sample LAM 12, slide 3, MC 1370-215.
4. *Classopollis torosus* Reissinger 1950; sample LAM 12, slide 4, MC 1432-172 see the proximal tetrad scar.
5. *Araucariacites* sp.; sample LAM 1, slide 2, MC 1464-60.
6. *Cyathidites* sp.; sample LAM 1, slide 3, MC 1415-215.
7. *Kraeuselisporites reissingeri* (Harris, 1957) Morbey, 1975; sample LAM 1, slide 2, MC 1323-55.
8. *Kraeuselisporites reissingeri* (Harris, 1957) Morbey, 1975; sample LAM 6, slide 1, MC 1470-130.
9. *Kraeuselisporites reissingeri* (Harris, 1957) Morbey, 1975; sample LAM 12, slide 1, MC 1190-210.

Plate II.III. (caption in the previous page)

Plate II.IV. 1, 2, 5-8: Selected palynomorphs from the Pereiros Formation at the Outcrop Lamas section (Pm palynozone). **3, 4:** Selected palynomorphs from the Pereiros Formation at the Outcrop Castelo Viegas II section (Pm palynozone). **9:** Selected palynomorph from the Coimbra Formation at the Outcrop Carvalhais section (Pm palynozone). All the specimens are housed in the collections of LNEG (Portuguese Geological Survey), S. Mamede de Infesta, Porto, Portugal. Species name is followed by the sample and slide number, and microscope coordinates. Scale bar in the plate.

1. *Deltoidospora* sp.; sample LAM 5, slide 1, MC 1300-55.
2. *Carnisporites* sp.; sample LAM 12, slide 3, MC 1380-75.
3. *Ischyosporites variegatus* (Couper) Schulz 1967; sample CVII-3, slide 2, MC 1243-143.
4. *Leptolepidites* sp.; sample CVII-3, slide 2, MC 1557-193.
5. *Pinuspollenites minimus* (Couper) Kemp 1970; sample LAM 8, slide 4, MC 1175-162.
6. *Perinopollenites elatoides* Couper 1958; sample LAM 12; slide 1, MC 1129-161.
7. *Perinopollenites elatoides* Couper 1958; sample LAM 12, slide 4, MC 1420-80.
8. *Polypodiisporites* sp.; sample LAM 1, slide 3, MC 1070-175.
9. *Porcellispora longdonensis* (Clarcke) Scheuring emend. Morbey 1975; sample CARVA 1B, slide 7, MC 1300-170.

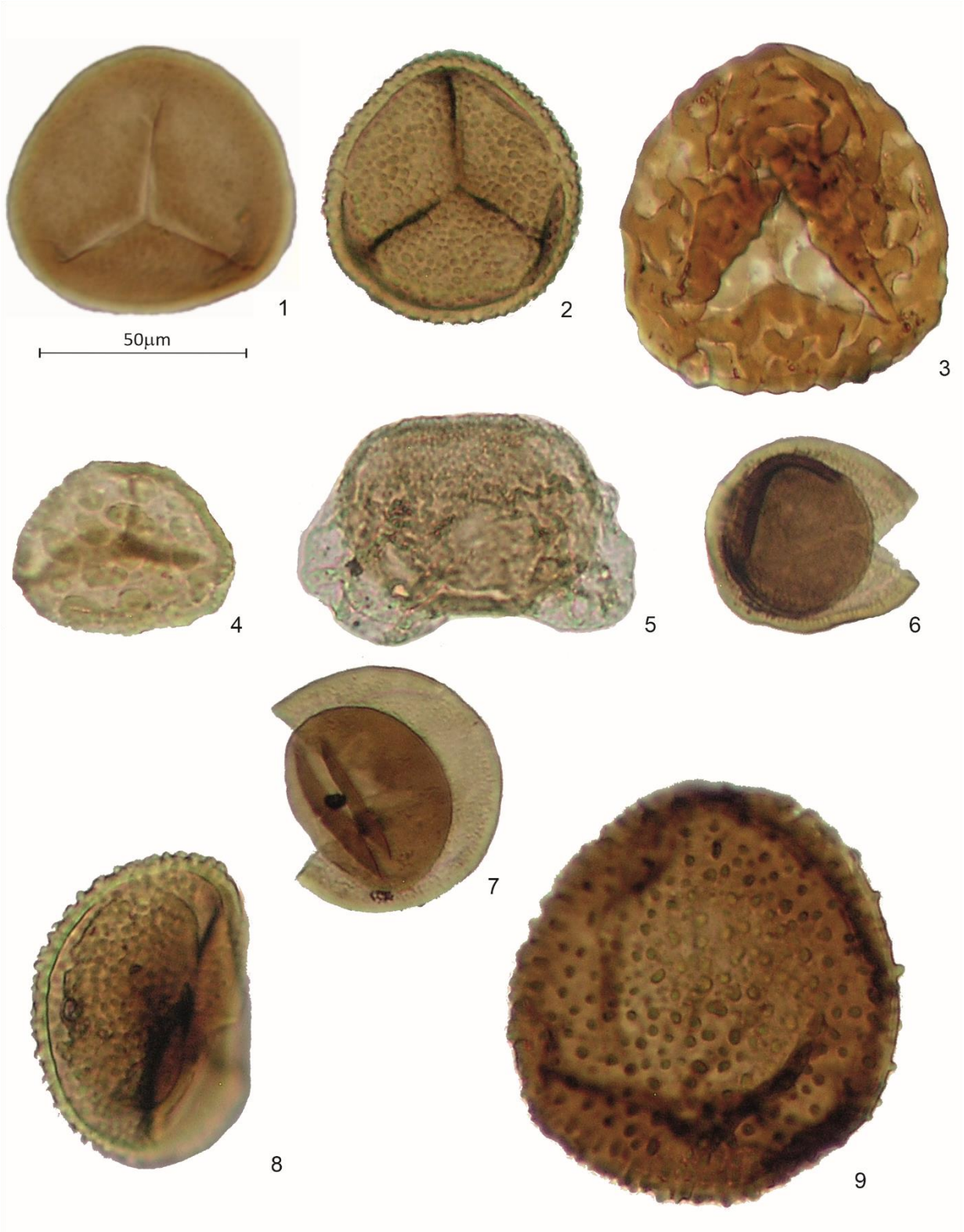

Plate II.IV. (caption in the previous page)

Plate II.V: 1-3, 9: Selected palynomorphs from the Conraria Formation at the Outcrop Parque de Campismo section (CG palynozone). **4-8:** Selected palynomorphs from the Pereiros Formation at the Outcrop Lamas section (Pm palynozone). All the specimens are housed in the collections of LNEG (Portuguese Geological Survey), S. Mamede de Infesta, Porto, Portugal. Species name is followed by the sample and slide number, and microscope coordinates. Scale bar in the plate.

1. Abnormal pollen; sample PC2, slide 9, MC 1340-242.
2. Abnormal pollen; sample PC2, slide 9, MC 1470-190.
3. Abnormal pollen; sample PC2, slide 9, MC 1362-140.
4. *Classopollis torosus* Reissinger 1950; sample LAM 1, slide 8, MC 1400-75. *Cluster* with two abnormal *Classopollis* pollen.
5. *Classopollis torosus* Reissinger 1950; sample LAM 2, slide 1, MC 1310-70. Tetrad with one abnormal *Classopollis* pollen.
6. *Classopollis torosus* Reissinger 1950; sample LAM 1, slide 2, MC 1405-105. Tetrad with two abnormal *Classopollis* pollen.
7. *Classopollis meyerianus* (Klaus) de Jersey 1973; sample LAM 2, slide 1, MC 1375-135. Tetrad with two abnormal *Classopollis* pollen.
8. *Classopollis torosus* Reissinger 1950; sample LAM 1, slide 3, MC 1460-200. *Cluster.*
9. *Paracirculina quadruplicis* Scheuring 1970; sample PC2, slide 9, MC 1411-160. Tetrad with one abnormal *Paracirculina* pollen.

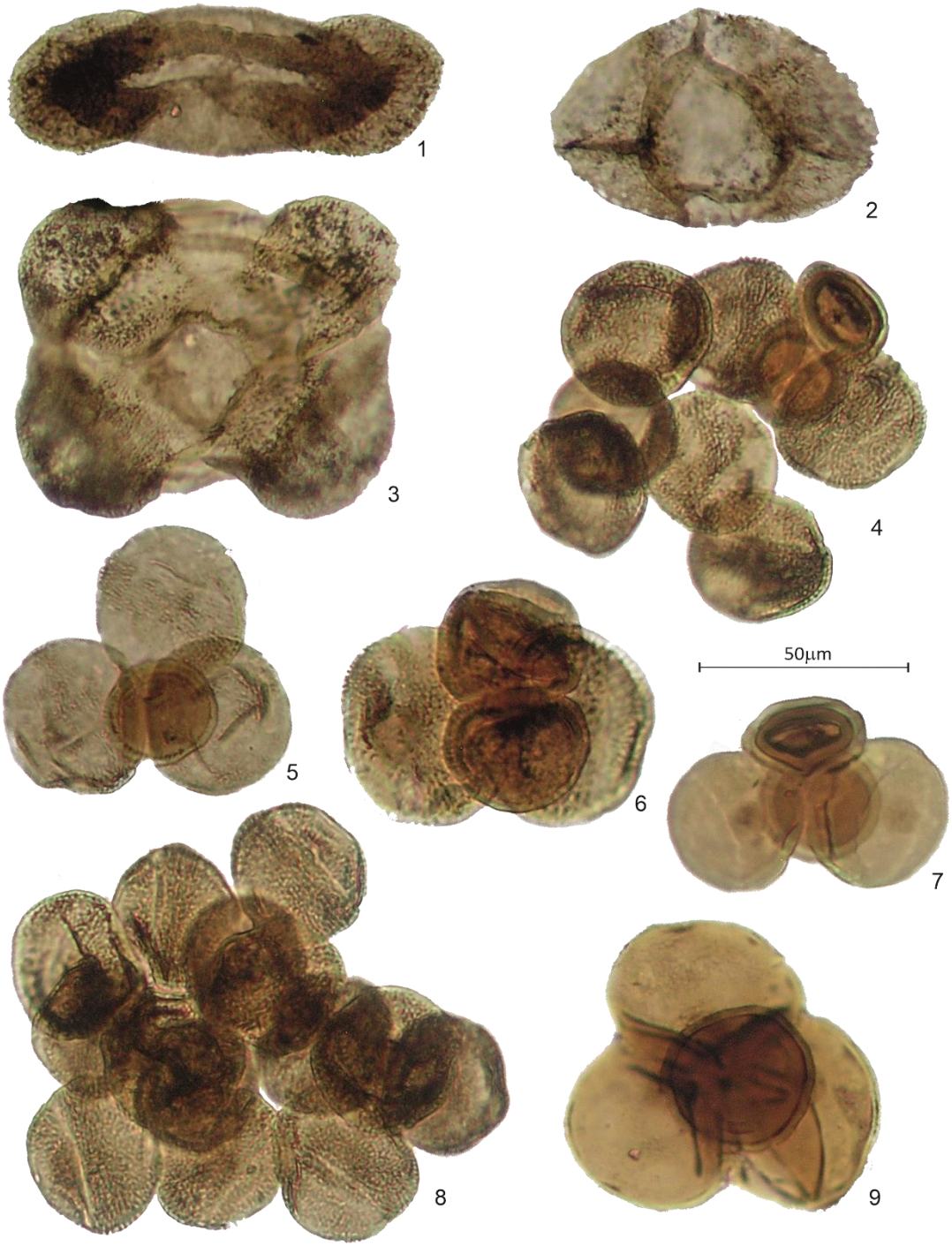

Plate II.V. (caption in the previous page)

The affinity could be due to general homogenous climatic conditions established during that time characterised by global warming and increasing rainfall and runoff (Bonis *et al*., 2010; Michalik *et al*., 2010; Berra, 2012; Haas *et al*., 2012; Cirilli *et al*., 2018). This climate change's causes have been related to intense monsoonal activity (Parrish, 1993; Sellwood and Valdes, 2007; Bonis and Kürschner, 2012) and to the onset of the CAMP. This latter is generally believed to have strongly influenced the climate with the release of gases (mainly CO_2 and SO_2) into the ocean–atmosphere system, by degassing of basalt flows (Marzoli *et al*., 2004; Cirilli *et al*., 2009; Van De Schootbrugge *et al*., 2009; Bonis *et al*., 2010; Schoene *et al*., 2010; Ruhl *et al*., 2011; Schaller *et al*., 2011; Lindström *et al*., 2012, 2017a, 2017b, 2021; Davies *et al*., 2017; Cirilli *et al*., 2018). The increasing atmospheric CO_2 concentrations created up to 3–4°C in global warming that probably controlled the vegetation type and distribution. Sedimentary-volcanic successions related to CAMP are known in the Algarve Basin, and, although the CAMP basalts were not recorded in the central and northern Lusitanian Basin, the effects of CAMP degassing could have also affected this area.

8. Conclusion

The Upper Triassic to Lower Jurassic Silves Group of the Lusitanian Basin, Portugal, was investigated for palynology. A combined stratigraphic succession of the Silves Group formed by nine outcrops, and involving the Conraria, Penela, Castelo Viegas and Pereiros formations, were sampled for this study. The palynological assemblages yielded from these outcrops, allowed the establishment of an informal palynozonation and provide new biostratigraphic constraints for the age attribution of the lower and upper formations of the Silves Group.

Accordingly, the main results of this study are:

- The presence of a palynological assemblage referable to the *Classopollis meyerianus - Granuloperculatipollis rudis* (CG) palynozone allowed to date as

Norian, possibly earliest Rhaetian, the Conraria Formation at the base of the Silves Group;

- The palynological content of the Pereiros Formation, allowed the recognition of two informal palynozones: *Ischyosporites variegatus* - *Kraeuselisporites reissingeri* (IK) and *Pinuspollenites minimus* (Pm) palynozones, to date the formation as upper Rhaetian to early Hettangian. Therefore, the TJB should lie in the lower Pereiros Formation, within the *Ischyosporites variegatus* - *Kraeuselisporites reissingeri* (IK) palynozone;

- The lack of palynological data from the Penela and Castelo Viegas formations due to unsuitable lithologies for this type of biostratigraphic studies did not allow a palynostratigraphic revision and a precise age attribution. However, due to their stratigraphic position sandwiched between the underlying Conraria Formation (Norian-earliest Rhaetian?) and the overlying Pereiros Formation (uppermost Rhaetian to Hettangian age), they would be indirectly dated as Rhaetian;

The presence of an important hiatus between the underlying Castelo Viegas and the overlying Pereiros formations (D3a *in* Soares *et al*., 2012) did not allow recognition of the lower boundary of the IK palynozone;

The microflora assemblages from the Lusitanian Basin recorded along the Late Triassic to Early Jurassic times might shed new light on future palaeogeographic and palaeoclimatic reconstructions of this sector of the Tethys realm. The affinity of these assemblages with those of the Eastern North America, Western Europe, and Tethys basins should suggest general homogenous climate conditions (warm and humid) caused by both intense monsoonal activity and the onset of the CAMP as documented in several Tethyan areas. Although basalt intercalations are absent in the investigated Triassic - Lower Jurassic successions of the Lusitanian Basin, they are known in the volcano-sedimentary successions time equivalent (southernmost part of the basin and in the Algarve Basin) in Portugal, not excluding the effects of CAMP greenhouse degassing also regionally as it is well known in a global scale.

CHAPTER III

Evidence of the first transgressive episode in the Lusitanian Basin

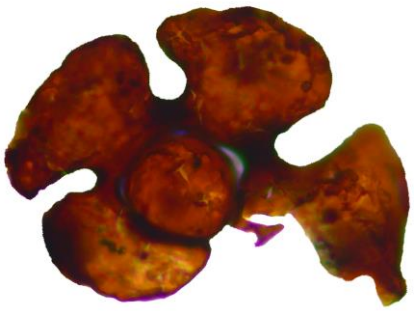

Chapter III cover:

Foraminiferal lining, Pereiros Formation, lower Hettangian, Lower Jurassic, sample LAMAS10/11, Lusitanian Basin

Chapter III. Evidence of the first transgressive episode in the Lusitanian Basin

Adapted from the paper 2:

Vilas-Boas, M., Pereira, Z., Cirilli, S., Duarte, L.V., Sêco, S.L.R. and Fernandes, P., 2023. Palynology and palynofacies studies in the lowermost Jurassic of the Lusitanian Basin (Pereiros Formation of the Silves Group), Portugal: evidence of the first transgressive episode. *Accepted to Acta Paleobotanica.*

Abstract

The Silves Group of the Lusitanian Basin in Portugal represents the initial infill of the continental rifting basins that formed during the breakup of northern Pangaea regions. Evaporites, especially halite, mark the passage from continental to marine settings and the beginning of the deposition on passive margin basins. This work presents the palynostratigraphic and palynofacies analysis results of two partial sections from the Pereiros Formation at the top of the Silves Group. The two sections are composed of sandstones, mudstones, and dolostones interpreted as deposited in fluvial and lacustrine settings without apparent marine influence. The palynological content is diverse and well-preserved, dating both sections of the early Hettangian age (Lower Jurassic), indicated by the presence of spores *Ischyosporites variegatus, Kraeuselisporites reissingeri, Porcellispora longdonensis* and the pollen grains *Perinopollenites elatoides* and *Pinuspollenites minimus*. The palynological content of one of the sections (Lamas I) is noticeable by microforaminifera linings, suggesting evidence for a hitherto marine incursion at this age in the Silves Group stratigraphy. The beds that yielded the microforaminifera linings are interpreted as having been deposited in an estuarine-type setting, created by the first and short-lived marine transgressive event in the Lusitanian Basin during the early Hettangian.

Keywords: Microforaminifera linings, Rift Basin, Marine Transgression, Estuary, Hettangian, Tethys Realm

1. Introduction

The Pangea breakup caused the early stages of the North Atlantic opening. In the western Iberian sector, the Lusitanian Basin (LB) begins to develop, flanked to the east by reliefs left over from the late phases of the Variscan orogeny (see, for example, Wilson, 1975, 1988; Hiscott *et al*., 1990; Kullberg *et al*., 2013).

The basin infill of the Mesozoic in Portugal has been identified as the base unit of the Silves Group that is primarily siliciclastic, composed of coarse-grained pebbly arkoses to feldspar litharenites (Palain, 1976; Soares *et al*., 2007, 2012). The main continuous outcrop area of this group in the LB is approximately 3 to 4 km wide and 35 km long from Coimbra to Penela (Fig. III.1). The Silves Group comprehends four formations, from the oldest to the most recent: the Conraria, Penela, Castelo Viegas and Pereiros formations (Soares *et al*., 2012) (Fig. III.2). There have only been a few palynostratigraphic studies performed in the Silves Group of the LB. Doubinger *et al*. (1970) carried out the initial investigation that was later carried out by Adloff *et al*. (1974), who used Palain's sedimentology and allostratigraphy work applying the traditional definition in megasequences A, B, and C (Palain, 1976, 1979). Recent palynological data from these formations allowed better age detailing, dating the Conraria Formation as Norian (late Triassic) and the Pereiros Formation as Hettangian (early Jurassic; Vilas-Boas *et al*., 2021). The first marine record (*Isocyprina* Beds; B2 term of Palain) caused a significant alteration in the sedimentary record of the Pereiros Formation, with the uppermost part that refers to transitional intertidal settings (Soares *et al*., 2012).

The Triassic-Jurassic Boundary (TJB) (201,4±0,2 My; Gradstein, Ogg, 2020) corresponds to one of the most severe biotic crises of the Phanerozoic (Raup, Sepkoski, 1982; Sepkoski, 1996; Tanner *et al*., 2004), supported by high-resolution studies that demonstrate a significant change in the palynoflora during this time (Lindström, 2016; Lindström *et al*., 2017a, 2017b, 2021). However, some

recent palynological and macrofloristic studies also demonstrate that Europe has no indications of a significant extinction occurring across the TJB (Barbacka *et al*., 2017). An important marker of the end-Triassic in some places like Portugal, North Africa and Eastern North America is the magmatic activity of the Large Igneous Province of the Central Atlantic Magmatic Province (CAMP). The CAMP in Portugal is evidenced by the Messejana Dike (Wilson, Giraud, 1998) and the Volcano-Sedimentary Complex in the Algarve Basin (Verati *et al*., 2007; Martins *et al*., 2008). There is no direct evidence of the CAMP in the LB, except for the southernmost part of the basin (Azerêdo *et al*., 2003; Kullberg *et al*., 2013). Nevertheless, the secondary effects of the volcanism, such as acid rain and the acidification of freshwater and global warming due to the greenhouse effect, are factors that contributed to the climatic changes and may have had an impact on the flora of this age (Hesselbo *et al*., 2002; Guex *et al*., 2004; Marzoli *et al*., 2004; Tanner *et al*., 2004, 2007; Nomade *et al*., 2007; Schaltegger *et al*., 2008; Van de Schootbrugge *et al*., 2008, 2009; Cirilli *et al*., 2009, 2015, 2018; Deenen *et al*., 2010; Lindström, 2016; Davies *et al*., 2017; Lindström *et al*., 2019; Panfili *et al*., 2019; Capriolo *et al*., 2020). Furthermore, the increase in tectonic activity and changes in sea level at the TJB are also related to numerous sedimentary hiatuses in the Western European basins (Lindström *et al*., 2017a, 2017b; Schneebeli-Hermann *et al*., 2018).

In the present research, palynostratigraphic and palynofacies analyses were made from two sections from the Silves Group of the LB in the Coimbra region (Fig. III.1). This study aims to document the base of the Hettangian on the Lusitanian Basin, comment on its biostratigraphical and palaeoenvironmental significance based on palynostratigraphy and palynofacies analyses, with emphasis on sea-level changes as documented by the palynological and sedimentary records. This data complements palynological research conducted previously in the same region (specifically the LAM section in Vilas-Boas *et al*., 2021).

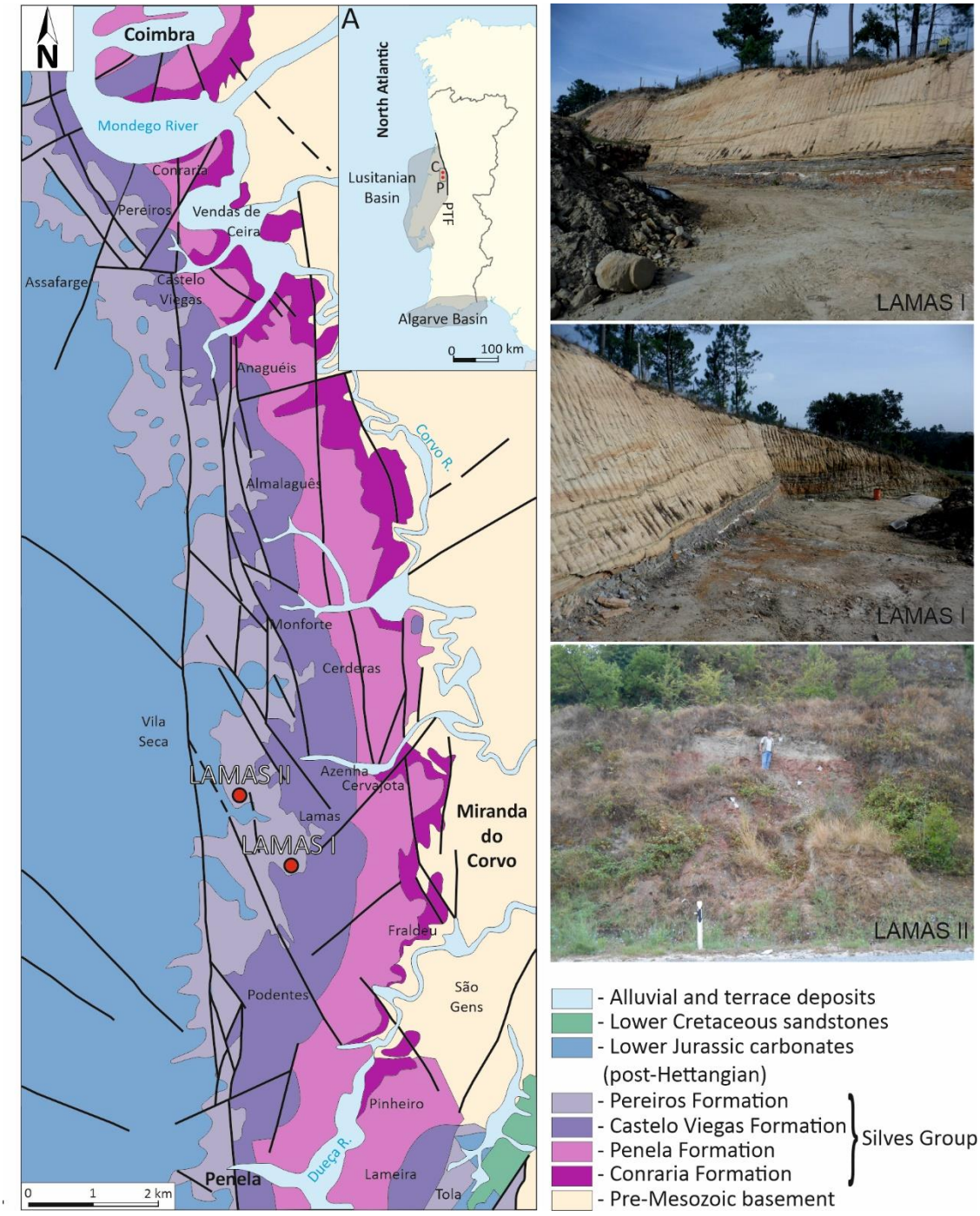

Figure III.1. Map of the studied area with the location of studied sections (based on Soares *et al*., 2012). A – Map of Portugal with the rectangle highlighting the type-area of the Silves Group in the Lusitanian Basin. C – Coimbra. P – Penela. PTF – Porto-Tomar Fault. Corvo R. – Corvo River. Dueça R. – Dueça River.

2. Geological Setting

The Triassic and Lower Jurassic sedimentary units in the western part of the Iberian Peninsula belong to the Silves Group and is considered the lower Mesozoic from the Lusitanian and Algarve (e.g., Palain, 1976; Soares *et al*., 2012; Kullberg *et al*., 2013, and others). The Silves Group mainly consists of siliciclastic rocks. It is moderately well exposed in the Coimbra-Penela region, which is the focus of this work (Fig. III.1). Several authors investigated the Silves Group in the LB (e.g., Carvalho, 1950; Palain, 1976, 1979). More recently, Soares *et al*. (2007, 2012) revised their stratigraphy and proposed a new lithostratigraphic chart: the Conraria, Penela, Castelo Viegas and Pereiros formations (Fig. III.2). The Conraria Formation rests unconformably over late Precambrian or Carboniferous and is composed of ferruginous conglomerates and sandstones, attaining a maximum thickness of ca.150 m in the Coimbra region. This formation is interpreted as alluvial plain deposits formed under an arid climate with intermittent short durations of intense precipitation (Palain, 1976; Soares *et al*., 2012). Plant fossils of *Voltzia ribeiroi*, *Clathropteris,* and *Otozamites* are typical of a Rhaetian age (Teixeira, 1942; Carvalho, 1950). However, recent palynological studies allowed the dating of the Conraria Formation as Norian, reaching possibly the early Rhaetian age (Vilas-Boas *et al*., 2021) (Fig. III.2).

The Penela Formation consists of red and brownish sandy conglomerates with a 90–120 m thickness in the Coimbra–Penela region (Soares *et al*., 2012). This unit is interpreted as deposited in a complex braided to meandering river system (Soares *et al*., 2012). The upper part of this unit, the Melhorado Beds (Soares *et al*., 2012), comprises brown/red sandy lutitic beds interpreted as overbank deposits with conspicuous calcite and dolomite nodules.

The Castelo Viegas Formation, about 110 m thick, consists of 4–5 m thick intervals of coarse-grained arkoses intercalated with centimetric thick lutitic. The unit was deposited in a coastal environment with arid paleoclimatic conditions (Palain, 1976; Soares *et al*., 2012).

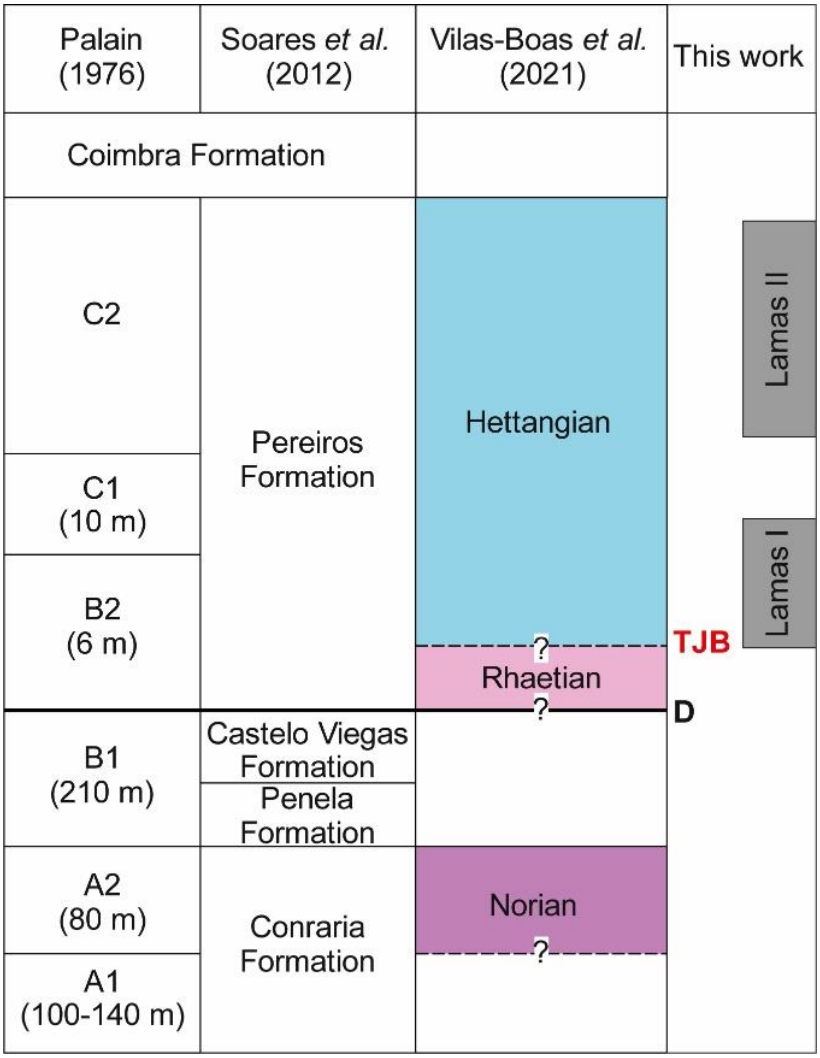

Figure III.2. Chronostratigraphic table of the Silves Group. D – Discontinuity. TJB – Triassic-Jurassic Boundary.

Lastly, the Pereiros Formation marks a significant facies change; the basal part of the Pereiros Formation (B2 of Palain, 1976, 1979) is composed of fine crystalline dolostones with siliciclastics, alternating with millimetric to centimetric-thick mudstones, sometimes with pavements of bivalves (*Isocyprina*) and, very locally, of gastropods (*Promathildia*) (the *Isocyprina* Beds). This mixed carbonate-siliciclastic unit is about 6 m thick. It is followed upwards by a lenticular unit of coarse to very coarse brownish sandstones with rare plant fossils of the fern *Clathropteris meniscoides,* (the *Clathropteris* Beds, or unit C2 of Palain, 1976; see also Soares *et al*., 1993) (Teixeira, 1942; Kullberg *et al*., 2013). The upper

part of the Pereiros Formation consists of reddish and greyish sandy lutites with fine-grained dolomites and dolomitic marls with patchy gypsum lenses; this is the thickest and most lithological complex subunit of the Pereiros Formation (Azerêdo *et al*., 2003; Sêco *et al*., 2015). This unit was deposited in an evaporitic environment of shallow lagoons, changing to lagoonal settings delimited by sandy barrier islands, and culminated at the top with laminated dolostones (Curtis *et al*., 1963; Shinn, 1983; Mazzullo, 2000; Soares *et al*., 2012). The Coimbra Formation overlaps the Pereiros Formation (Dimuccio *et al*., 2014, 2016; Gomez *et al*., 2019; Duarte *et al*., 2022). The invertebrate fauna and plant fossils in the Pereiros Formation indicate a Hettangian age (Teixeira, 1942). However, recent palynological studies date the entire Pereiros Formation as late Rhaetian to early Hettangian (Vilas-Boas *et al*., 2021).

3. Materials and Methods

3.1 Studied Sections: stratigraphy and general descriptions

The Pereiros Formation was sampled in the Lamas I (coordinates: 40º4’44.35’’N; 8º22’48.30’’W) and Lamas II (coordinates: 40º5’6.42’’N; 8º23’10.30’’W) (LAMAS and LAM, respectively) sections located at Lamas, Miranda do Corvo region (Figs. III.1 and III.3).

From the Lamas I section, 19 samples were collected, 15 yielded sporomorphs, and four were barren (Fig. III.5, Table III.1). The samples from this section were collected from the lowermost part of the Pereiros Formation (unit B2 of Palain, 1976), consisting of shallow marine carbonate-siliciclastic intervals.

The Lamas II section is the reference section of unit C2 of the Pereiros Formation; from the 12 samples collected, 10 yielded sporomorphs, and two were barren (Fig. III.5; Table III.1). The lower part of this section consists of argillaceous sandstones sometimes intercalated with meter-thick sandy dolostones, and the upper part consists of dolomitic marls and dolostones. The top of this section marks the contact between the Pereiros and Coimbra formations. The lowermost

part of the Coimbra Formation comprises thinly (centimetre-scale) intercalations of bedded grey marls and metric-scale dolostones.

3.2. Palynostratigraphic and palynofacies techniques

Thirty-one lutitic samples were collected from two sections in the Coimbra region (see Figs. III.1, III.2 and III.3 for the locations of the sections sampled). Palynostratigraphic and palynofacies analyses were carried out in all collected samples. The samples were processed at the Portuguese Geological Survey (LNEG) and Centre for Marine and Environmental Research, the University of Algarve (CIMA-UAlg using standard palynological laboratory procedures in the extraction (treated with hydrochloric and hydrofluoric acids) of the organic residue following the methodologies described by Wood *et al*. (1996) and Riding and Warny (2008). The organic residues were not oxidised. The organic residues were sieved using a 15 µm sieve and then mounted on microscope slides using Entelan®, a commercial resin-based mounting medium. The slides were used in palynostratigraphic and palynofacies studies.

The slides for the palynostratigraphic study were analysed using a Leica DM750 microscope equipped with a Leica ICC50W camera. In the 25 palynological productive samples, semi-quantitative abundance was determined by counting 350 specimens per slide whenever possible. The slides were also scanned for rare taxa, which were recorded as present outside the count (see Table III.1, signed with an X). The counts per sample and taxa are listed in Table III.1. The quantitative data was discussed as follows: rare (0-10%), common (11-50%), and abundant (>51%). Stratigraphical relevant taxa are presented on Plates III.I and III.II.

A quantitative approach was used for all 31 samples studied in palynofacies analyses. Three hundred fifty organic particles were counted in each slide using Olympus BX51 equipped with an Olympus XC-50 digital camera. An adapted scheme from Tyson (1993, 1995) was used for palynofacies interpretation. Absolute and relative counts for all samples are presented in Table III.3. Table III.2 illustrates the different palynofacies groups identified in this study.

Representative palynofacies are shown in Plate III.III. All samples, residues, and slides are curated at the University of Algarve and the Palynological Collection of LNEG, Portugal. All palynostratigraphic and palynofacies results are plotted in Fig. III.4 and III.5 using Tilia 3.0.1 software (Grimm, 1991).

The paleoenvironmental interpretation is based on the relative abundances of specific palynomorph groups and palynofacies integrated with lithofacies.

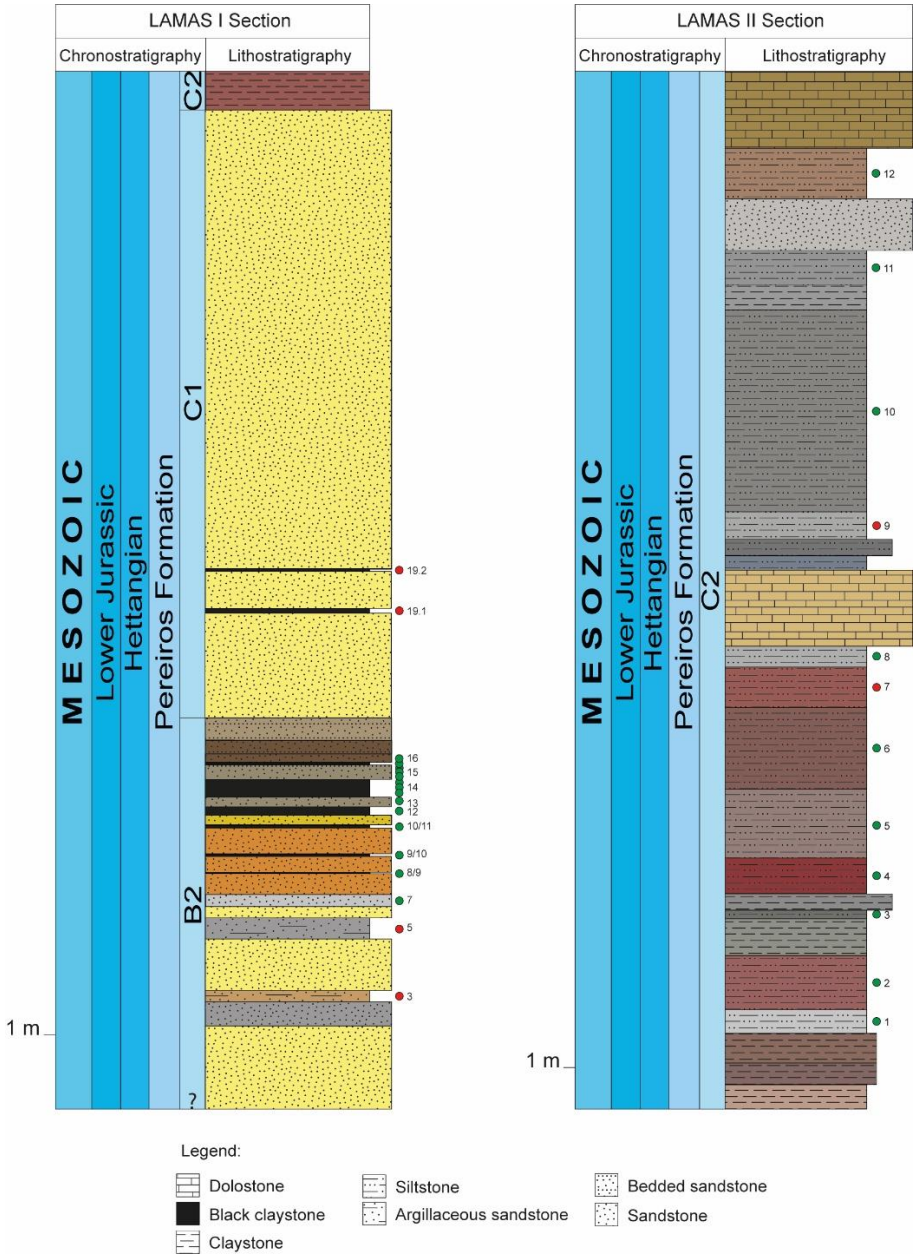

Figure III.3. Stratigraphic Log of Lamas I on the left and Lamas II on the right. Dots in the logs mark the location of the studied samples. Green dots point out productive samples for palynological studies, and red dots point out barren samples for palynological studies.

Table III.1. Dataset (%) for terrestrial palynomorphs (spores and pollen grains) and marine palynomorphs (foraminifera linings). Relative abundance. X – Registered outside the count. SP/F Ratio – Sporomorphs (spores + pollen grains)/Foraminiferal lining.

	Pereiros Formation																							
	Lower Jurassic - Hettangian																							
Outcrops	LAMAS I															LAMAS II								
Samples	LAMAS 7	LAMAS 8/9	LAMAS 9/10	LAMAS 10/11	LAMAS 12	LAMAS 13	LAMAS 14BASE	LAMAS 14INT	LAMAS 14TOPO	LAMAS 15a)BASE	LAMAS 15b)BASE	LAMAS 15INT	LAMAS 15 TOPO	LAMAS 15/16	LAMAS 16	LAM 1	LAM 2	LAM 3	LAM 4	LAM 5	LAM 6	LAM 8	LAM 10	LAM 11	LAM 12
SPORES																								
Apiculatisporis sp.		0,8		0,3																				
Calamospora tener		0,8		0,3	X		X	1,2	0,4	0,4	0,4	0,4	0,4			0,4		0,4		0,4	0,4				
Carnisporites sp.									1,2			3,6	1,6		X	0,4	0,8				0,4				0,4
Carnisporites spiniger		5,2	7,5		16	10,4	13,6	12,4	15,2	14,3	17,2	6	6,8	13,2	7,6										
Cibotiumspora sp.		0,8	0,4	0,9	0,4	X	X	1,2	0,4	0,4		X	X		1,6										
Converrucosisporites sp.								0,4																	
Convolutispora sp.									X	0,4	X	0,4	1,6		0,4										
Cyathidites sp.		12	7,9	10	6,8	4	2	2,8	4,8	5,6	5,2	4,8	5,2	5,2	9,6	1,6		0,8		1,2	0,8				
Deltoidospora halli								0,4																	
Deltoidospora sp.		18,8	27,7	9,1	5,6	9,2	10,4	13,6	16,8	18,3	13,2	15,1	16,8	18	19,2	2	2	2		1,2	2,8	1,2			
Dictyophillidites mortonii						0,4				0,4	0,8	X		1,2	3,2										
Dictyophillidites sp.								1,6	2	2,8	3,6	2	2,4	0,8	4,8										
Foveosporites foveoreticulatus							0,8																		
Foveosporites sp.		0,8						2,4						1,2											
Ischyosporites sp.												1,6	X		0,8										
Ischyosporites variegatus				1,1	X	0,8	X	0,8	0,4	0,4	1,2			2								0,4			0,4
Kraeuselisporites reissingeri	100	19,6	38,3	15,4	28	26,8	23,6	29,2	24,8	27,5	18,8	21,9	25,6	28,4	20	5,2	0,4	2			5,6	3,2			3,6
Kraeuselisporites sp.				1,1	0,8																				
Kyrtomisporis sp.		0,8		0,9	0,4	0,8	2			0,8							0,4					0,4			1,2
Leiotriletes directus					14																				
Leptolepidites sp.														X	2,4										
Polypodiisporites sp.		0,4														0,4	0,4								0,4
Porcellispora longdonensis						0,4			X					X		1,2					0,4				
Retitriletes austraclavatidites									0,4																
Todisporites sp.				11,1						2	1,6	1,2	2,4												
Trachysporites fuscus														0,4											
Trachysporites sp.		0,4												0,4	8,4										
Uvaesporites sp.				0,3																					
Sum Spores	100	60,4	81,8	50,5	72	52,8	52,4	66	66,4	73,3	63,6	55,4	62,8	70,8	78	11,2	4	5,2	0	2,8	10,4	5,2	0	0	6
POLLEN																									
Alisporites sp.						0,4										0,4	0,4	0,4							0,4
Araucariacites sp.																10,4	11,6	4		7,6	4,4	4,8			3,6
Chasmatosporites sp.																	0,8								
Classopollis abnormal							X	X	0,4				3,2	1,6	X	X	X			X	X				
Classopollis meyerianus		33,6	7,9	31,4	23,6	37,2	45,2	30,8	32,4	26,3	33,6	43,8	32,8	23,2	16,8	7,6	31,2	23,2	100	86,4	60,4	73,2	100	100	1,6
Classopollis sp.		2,4	0,4	2		3,2									0,4										
Classopollis torosus			7,5	11,4	3,2	2										58,8	36,4	61,2		0,8	16,8	11,2			75,6
Cycadopites sp.					X		0,8	1,2								7,2	12,8	2,8			2,4	1,6			2,4
Inaperturopollenites sp.																3,6	2,4	3,2		2,4	3,6	2,8			7,6
Paracirculina sp.				4																					
Perinopollenites elatoides				0,6	1,2	1,6		X		0,4	0,4	0,4		0,8		0,4	0,4				0,4	0,4			2,8
Pinuspollenites minimus		2,8	1,6		X	1,6	1,6	1,2	0,4		2	0,4	0,4	3,6	4	0,4					1,6	0,8			
Sum Pollen	0	38,8	17,4	49,4	28	46	47,6	33,2	33,2	26,7	36	44,6	36,4	29,2	21,2	88,8	96	94,8	100	97,2	89,6	94,8	100	100	94
Foraminiferal lining		0,8	0,8			1,2	X	0,8	0,4		0,4		0,8		0,8										
SP/F Ratio		0,992	0,992			0,988		0,992	0,996		0,996		0,992		0,992										

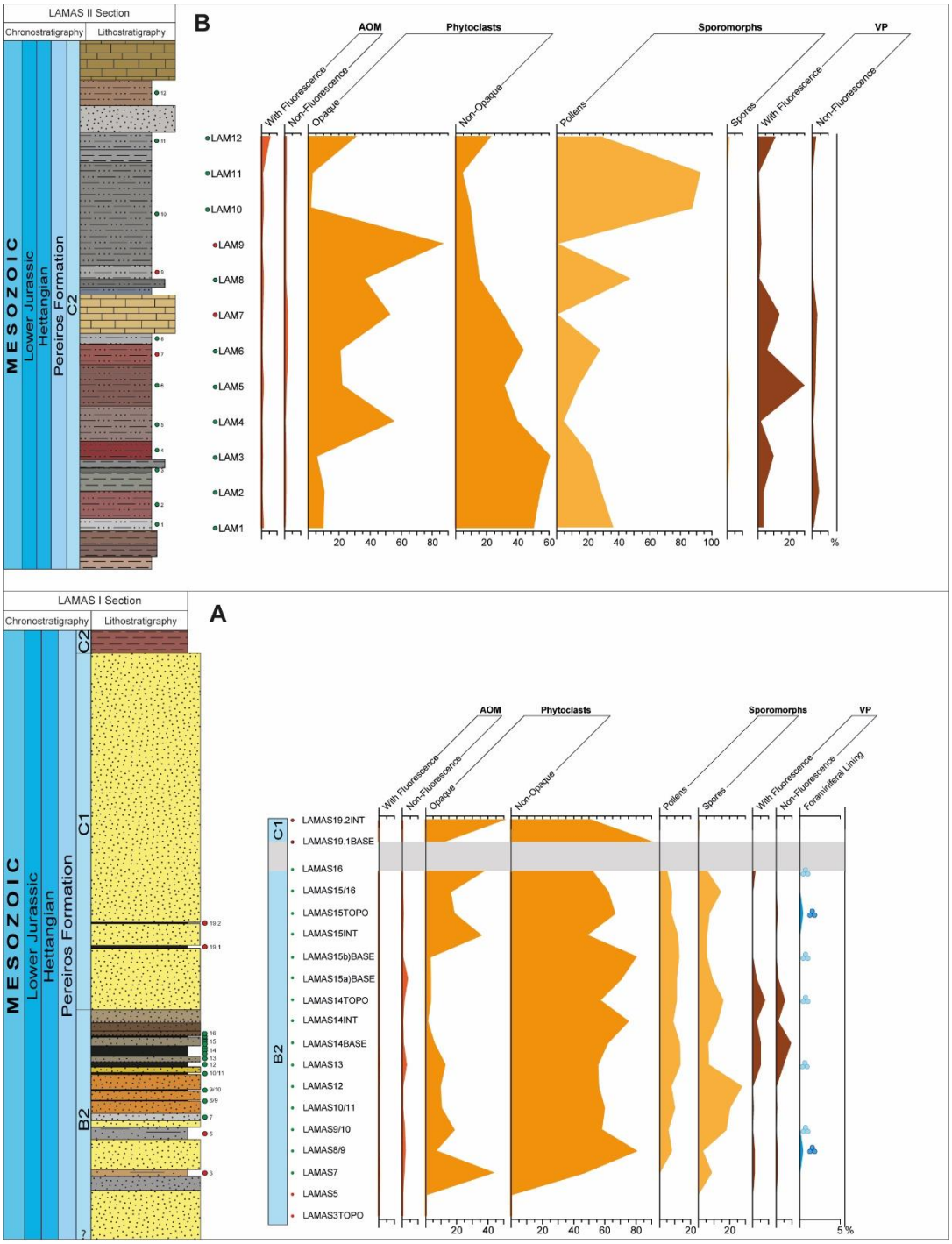

Figure III.4. Palynofacies analysis along the sections. A – Range chart of Lamas I outcrop. The blue symbol marks the samples that contain microforaminifera linings; B – Range chart of Lamas II. AOM – Amorphous organic matter. VP – Vegetal particles. Green dots point out productive samples for palynological studies, and red dots point out barren samples for palynological studies. The symbols of the foraminifera linings in dark blue represent the samples in which these particles were part of the counts. The symbols in light blue represent the samples that contain foraminifera; however, they did not appear in the analysis of palynofacies. The logs are not to scale.

4. Results

4.1. Palynofacies

The studied sections allowed the retrieval of 29 productive palynofacies samples representing the three units from the Pereiros Formation, B2, C1 and C2 (Palain, 1976, 1979) (Tables III.2 and III.3; Plate III.III).

Table III.2. Description of palynofacies groups used in this study (based on Tyson, 1993, 1995).

Palynomorphs	**Spores**	The cell that certain plants (such as Filicopsids, Sphenophytes, Lycophytes, and Bryophytes) produce and use to reproduce. Consisting of monolete, trilete and alete spores.	
	Pollen	The cell that Gymnosperms and Higher Seed Ferns use to reproduce.	
	Foraminiferal lining	The preserved internal organic remains of Microforaminifera. The presence of foraminiferal linings indicates marine influence.	
Phytoclasts	Organic material derived from the ligno-cellulosic tissues of terrestrial macrophytes.	**Non-opaque**	Ligno-cellulosic tissue that under the microscopy light are non-opaque or translucent.
		Opaque	Ligno-cellulosic tissue that have no visible structure and appear to be homogeneous. Under the light of the microscopy appears completely black (opaque).
		Vegetal Particles	Tissue of probable plant origin.
Amorphous Organic Matter		Includes phytoplankton- or bacterially derived amorphous organic matter and amorphous products of the diagenesis of macrophyte tissues that under the light of the microscope appears structureless. The preservation of AOM indicates dysoxic or anoxic conditions.	

Unit B2

Seventeen samples were collected from this unit, and fifteen were productive for palynofacies analyses. The phytoclast group is dominant in all the 15 samples (average 76.1 %; Table III.3). The non-opaque subgroup is the most representative of the phytoclast group with an average abundance of 61.5 %, achieving the lower percentage of 46.3 % at ca. 2.8 m (LAMAS 7) and the highest percentage value of 79.7 % at ca. 3.2 m (LAMAS 8/9) (Table III.3; Fig. III.4). The

relative abundance of opaque phytoclasts is 14.5 % and reaches a peak of 42.3 % at ca. 2.8 m (LAMAS 7) and a minimum of 1 % at ca. 4.5 m (LAMAS 14 INT) (Table III.3; Fig. III.4; Plate III.III). The percentage of the terrestrial palynomorphs (spores and pollen) is consistent over all the outcrops, with the spores dominating the pollen with an average percentage of 9.6 % and 7.8 %, respectively. The foraminifera linings are recorded at ca. 3.2 m and 4.5 m (LAMAS 15TOPO), with a relative abundance of 0.3 % in both samples; however, they are present in most of the samples from this unit. A relative abundance of 0.7 % of amorphous organic matter (AOM) is identified; the subgroup with fluorescence is only recognised at ca. 2.8 and 4.2 m (LAMAS 13) with a value of 0.3 %, and the subgroup with no fluorescence ranges from 0.3 % at ca. 4.5 m to 3.3 % to ca. 4.6 m (LAMAS 15a) BASE). In addition, a relative abundance of the vegetal particle group, ranging from 0.3 % at ca. 3.9 m (LAMAS 10/11) to 7.7 % at ca. 4.5 m (LAMAS 14TOPO) with fluorescence and ranging from 0.3 % at 3.9 m to 9.3 % ca. 4.5 m (LAMAS 14BASE) is identified (Table III.3; Plate III.III).

Unit C1

From unit C1, two samples were collected. Both were productive for palynofacies analyses, although only phytoclasts were present (Table III.3). The non-opaque subgroup is the most representative of the phytoclast group with an average abundance of 70.5 %, achieving the lower percentage of 51.3 % at ca. 7.3 m (LAMAS 19.2INT) and the highest percentage value of 89.7 % at ca. 6.8 m (LAMAS 19.1BASE) (Table III.3; Fig. III.4). The relative abundance of opaque phytoclasts is 29.5 % and reaches a peak of 48.7 % at 6.8 m and a minimum of 10.3 % at ca. 7.3 m (Table III.3; Fig. III.4). The samples were barren for vegetal particles, AOM and palynomorphs (e.g., spores, pollen grains, foraminifera linings).

Table III.3. Quantitative analysis, percentage data presented per sample and group for the palynofacies analyses. AOM – Amorphous organic matter.

Pereiros Formation

Outcrop			Palynomorphs				Phytoclasts			Vegetal Particles			AOM			
LAMAS I	**Samples**		Spores	Pollen	Foraminiferal lining	Total	Opaque	Non-opaque	Total	With Fluorescence	No Fluorescence	Total	With Fluorescence	No Fluorescence	Total	Total
	LAMAS 19.2INT	Count	0	0	0	**0**	146	154	**300**	0	0	**0**	0	0	**0**	**300**
		%	0	0	0	**0**	48,7	51,3	**100**	0	0	**0**	0	0	**0**	**100**
	LAMAS 19.1BASE	Count	0	0	0	**0**	31	269	**300**	0	0	**0**	0	0	**0**	**300**
		%	0	0	0	**0**	10,3	89,7	**100**	0	0	**0**	0	0	**0**	**100**
	LAMAS 16	Count	16	15	0	**31**	113	157	**270**	4	0	**4**	0	0	**0**	**305**
		%	5,2	4,9	0	**10,1**	37	51,5	**88,5**	1,3	0	**1,3**	0	0	**0**	**100**
	LAMAS 15/16	Count	43	24	0	**67**	47	186	**233**	0	0	**0**	0	0	**0**	**300**
		%	14,3	8	0	**22,3**	15,7	62	**77,7**	0	0	**0**	0	0	**0**	**100**
	LAMAS 15TOPO	Count	22	24	1	**47**	57	208	**265**	0	2	**2**	0	1	**1**	**315**
		%	7	7,6	0,3	**14,9**	18,1	66	**84,1**	0	0,6	**0,6**	0	0,3	**0,3**	**100**
	LAMAS 15INT	Count	19	41	0	**60**	121	165	**286**	0	0	**0**	0	0	**0**	**346**
		%	5,5	11,8	0	**17,3**	35	47,7	**82,7**	0	0	**0**	0	0	**0**	**100**
	LAMAS 15b)BASE	Count	16	38	0	**54**	8	241	**249**	0	0	**0**	0	0	**0**	**303**
		%	5,3	12,5	0	**17,8**	2,6	79,5	**82,1**	0	0	**0**	0	0	**0**	**100**
	LAMAS 15a)BASE	Count	27	33	0	**60**	9	211	**220**	7	3	**10**	0	10	**10**	**300**
		%	9	11	0	**20**	3	70,3	**73,3**	2,3	1	**3,3**	0	3,3	**3,3**	**100**
	LAMAS 14TOPO	Count	47	33	0	**80**	9	169	**178**	23	16	**39**	0	3	**3**	**300**
		%	15,7	11	0	**26,7**	3	56,3	**59,3**	7,7	5,3	**13**	0	1	**1**	**100**
	LAMAS 14INT	Count	37	26	0	**63**	3	224	**227**	6	4	**10**	0	0	**0**	**300**
		%	12,3	8,7	0	**21**	1	74,7	**75,7**	2	1,3	**3,3**	0	0	**0**	**100**
	LAMAS 14BASE	Count	18	39	0	**57**	16	184	**200**	14	28	**42**	0	1	**1**	**300**
		%	6	13	0	**19**	5,3	61,3	**66,6**	4,7	9,3	**14**	0	0,3	**0,3**	**100**
	LAMAS 13	Count	20	40	0	**60**	37	166	**203**	15	14	**29**	1	7	**8**	**300**
		%	6,7	13,3	0	**20**	12,3	55,3	**67,6**	5	4,7	**9,7**	0,3	2,3	**2,6**	**100**
	LAMAS 12	Count	83	23	0	**106**	27	167	**194**	0	0	**0**	0	0	**0**	**300**
		%	27,7	7,7	0	**35,4**	9	55,7	**64,7**	0	0	**0**	0	0	**0**	**100**
	LAMAS 10/11	Count	65	31	0	**96**	32	190	**222**	1	1	**2**	0	0	**0**	**320**
		%	20,3	9,7	0	**30**	10	59,4	**69,4**	0,3	0,3	**0,6**	0	0	**0**	**100**
	LAMAS 9/10	Count	56	18	0	**74**	57	183	**240**	0	0	**0**	0	4	**4**	**318**
		%	17,6	5,7	0	**23,3**	17,9	57,5	**75,4**	0	0	**0**	0	1,3	**1,3**	**100**
	LAMAS 8/9	Count	8	24	1	**33**	18	239	**257**	3	2	**5**	0	5	**5**	**300**
		%	2,7	8	0,3	**11**	6	79,7	**85,7**	1	0,7	**1,7**	0	1,7	**1,7**	**100**
	LAMAS 7	Count	25	0	0	**25**	127	139	**266**	3	2	**5**	1	3	**4**	**300**
		%	8,3	0	0	**8,3**	42,3	46,3	**88,6**	1	0,7	**1,7**	0,3	1	**1,3**	**100**
Outcrop	**Samples**															
LAMAS II	LAM 12	Count	3	88	0	**91**	90	66	**156**	33	6	**39**	15	2	**17**	**303**
		%	1	29	0	**30**	29,7	21,8	**51,5**	10,9	2	**12,9**	5	0,7	**5,7**	**100**
	LAM 11	Count	0	277	0	**277**	7	12	**19**	1	0	**1**	1	2	**3**	**300**
		%	0	92,3	0	**92,3**	2,3	4	**6,3**	0,3	0	**0,3**	0,3	0,7	**1**	**100**
	LAM 10	Count	0	279	0	**279**	4	29	**33**	3	1	**4**	3	1	**4**	**320**
		%	0	87,2	0	**87,2**	1,3	9,1	**10,4**	0,9	0,3	**1,2**	0,9	0,3	**1,2**	**100**
	LAM 9	Count	0	0	0	**0**	257	36	**293**	6	0	**6**	0	1	**1**	**300**
		%	0	0	0	**0**	85,7	12	**97,7**	2	0	**2**	0	0,3	**0,3**	**100**
	LAM 8	Count	1	142	0	**143**	106	45	**151**	2	1	**3**	2	1	**3**	**300**
		%	0,3	47,3	0	**47,6**	35,3	15	**50,3**	0,7	0,3	**1**	0,7	0,3	**1**	**100**
	LAM 7	Count	0	0	0	**0**	156	89	**245**	41	9	**50**	1	4	**5**	**300**
		%	0	0	0	**0**	52	29,7	**81,7**	13,7	3	**16,7**	0,3	1,3	**1,6**	**100**
	LAM 6	Count	0	83	0	**83**	61	129	**190**	17	6	**23**	0	4	**4**	**300**
		%	0	27,7	0	**27,7**	20,3	43	**63,3**	5,7	2	**7,7**	0	1,3	**1,3**	**100**
	LAM 5	Count	3	43	0	**46**	64	93	**157**	89	5	**94**	3	2	**5**	**302**
		%	1	14,2	0	**15,2**	21,2	30,8	**52**	29,5	1,7	**31,2**	1	0,7	**1,7**	**100**
	LAM 4	Count	1	13	0	**14**	165	119	**284**	4	1	**5**	0	0	**0**	**303**
		%	0,3	4,3	0	**4,6**	54,5	39,3	**93,8**	1,3	0,3	**1,6**	0	0	**0**	**100**
	LAM 3	Count	4	65	0	**69**	15	180	**195**	29	5	**34**	1	1	**2**	**300**
		%	1,3	21,7	0	**23**	5	60	**65**	9,7	1,7	**11,4**	0,3	0,3	**0,6**	**100**
	LAM 2	Count	0	87	0	**87**	30	166	**196**	10	12	**22**	0	1	**1**	**306**
		%	0	28,4	0	**28,4**	9,8	54,2	**64**	3,3	3,9	**7,2**	0	0,3	**0,3**	**100**
	LAM 1	Count	0	109	0	**109**	28	149	**177**	10	2	**12**	2	0	**2**	**300**
		%	0	36,3	0	**36,3**	9,3	49,7	**59**	3,3	0,7	**4**	0,7	0	**0,7**	**100**

Unit C2

In this unit, all the twelve samples analysed were productive. The phytoclast group is dominant in all the samples (average 57.9 %; Table III.3; Fig. III.4) except for ca. 16.2 m (LAM 10) and ca. 19.9 m (LAM 11). The non-opaque subgroup is the most representative of the phytoclast group with an average abundance of 30.7 %, achieving the lower percentage of 4 % at ca. 19.9 m and the highest percentage of 60 % at ca. 4.8 m (LAM 3) (Table III.3). The relative abundance of opaque phytoclasts is 27.2 %, reaching a peak of 85.7 % at ca. 13.5 m (LAM 9) and a minimum of 1.3 % at ca. 16.2 m (Table III.3). The pollen subgroup dominates the group of the sporomorphs, in all samples, with an average percentage of 32.4 % to an average percentage of 0.3 % for the spore

subgroup. A relative abundance of the AOM is identified, the subset fluorescent varies from a value of 0.3 % at ca. 4.8, 10 (LAM 7), and 19.9 m to a value of 5 % at ca. 22 m (LAM 12) and the subgroup with no fluorescence ranges from 0.3 % at ca. 2.9 (LAM 2), 4.8, 10.5 (LAM 8; Plate III.III), 13.5 and 16.2 m to 1.3 % at ca. 8.5 (LAM 6) and 10 m.

In addition, a relative abundance of the vegetal particle group has been recorded, ranging from 0.3 % at ca. 19.9 m to 29.5 % at ca. 6.8 m (LAM 5) with an average percentage of 6.8 % for the fluorescent subgroup and ranging from 0.3 % at ca. 5.5 (LAM 4), 10.5 and 16.2 m to 3.9 % at ca. 2.9 m with an average of 1.3 % for the non-fluorescent subgroup (Table III.3).

4.2. Palynological assemblages

Unit B2

Unit B2 presents moderate to well-preserved 21 species of spores and 6 pollen grains (Table III.1, Fig. III.5, Plates III.I and III.II). This unit is characterised by the presence *of Kraeuselisporites reissingeri* and *Ischyosporites variegatus*, together with some other spores such as common to abundant *Carnisporites spiniger*, *Cyathidites* sp., *Deltoidospora* sp., and rare *Calamospora tener, Dictyophyllidites mortonii*, *Dictyophyllidites* sp., *Porcellispora longdonensis, Todisporites* sp., *Trachysporites fuscus* and *Trachysporites* sp.. *Dictyophyllidites mortonii* makes its last occurrence (LO) in the sample LAMAS16, ca. 4.8 m in the section. Complete the association common to abundant pollen grains *Classopollis meyerianus* with rare to common *Classopollis torosus* and rare *Alisporites* sp., *Cycadopites* sp., *Perinopollenites elatoides, Pinuspollenites minimus.* In this unit, well to moderate preserved foraminifera linings are notable in 9 samples collected (Table III.1).

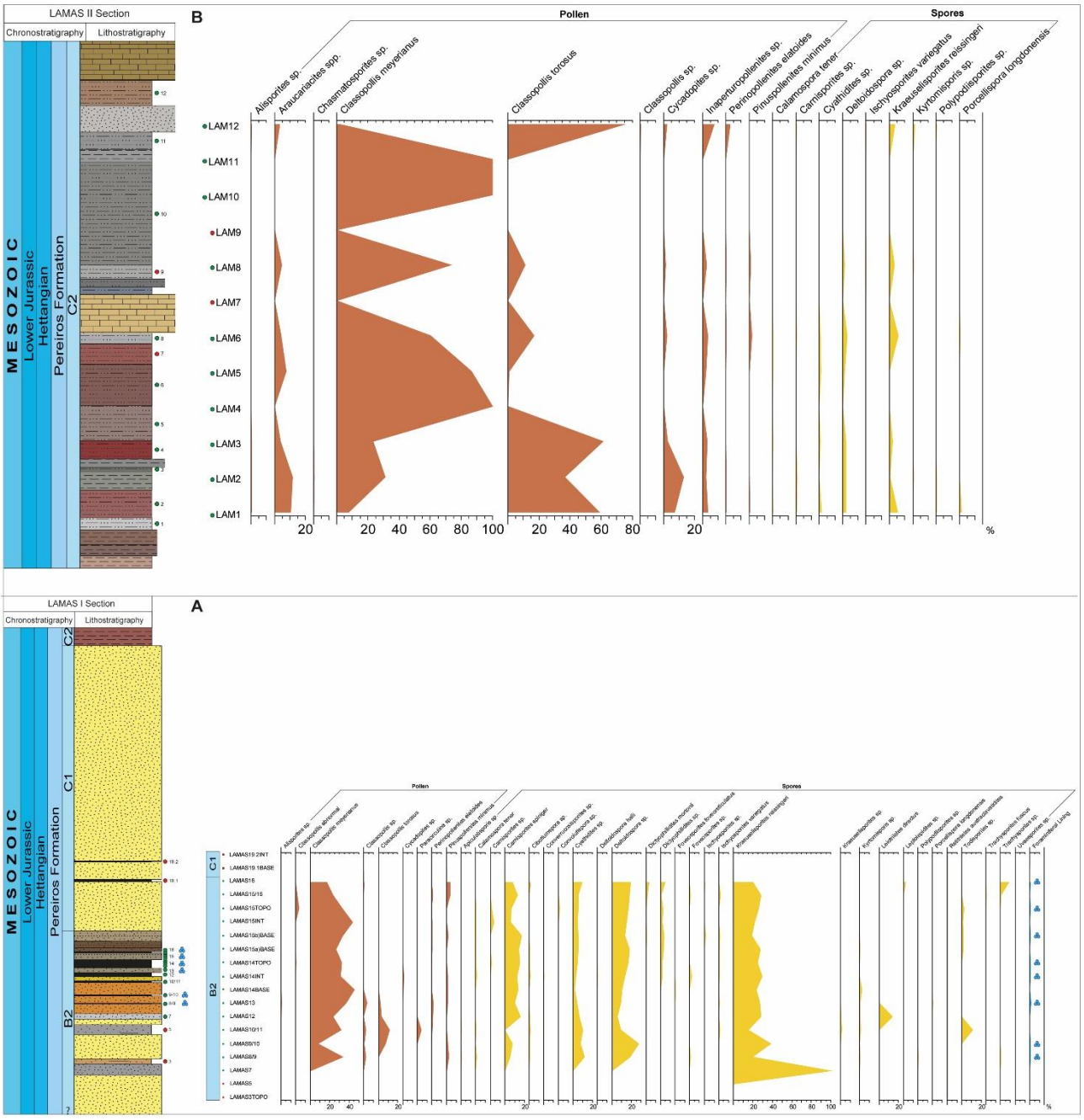

Figure III.5. Composite range chart of the sporomorph taxa found in the studied sections. A – Range chart of Lamas I outcrop, the blue symbol marks the samples that contain foraminifera linings; B – Range chart of Lamas II. Green dots point out productive samples for palynological studies, and red dots point out barren samples for palynological studies. The logs are not to scale.

Unit C2

The palynological assemblage recovered in unit C2 includes well-preserved spores (nine species) and pollen grains (eight species) (Table III.1, Fig. III.5, Plates III.I and III.II). The spores include *Calamospora tener, Ischyosporites variegatus,* and *Kraeuselisporites reissingeri.* Complete the association of the spores *Carnisporites* sp., *Cyathidites* sp., *Deltoidospora* sp., *Kyrtomisporis* sp., *Polypodiisporites* sp., and *Porcellispora longdonensis. Classopollis meyerianus* and *Classopollis torosus* are common to abundant and rare to common *Alisporites* sp., *Araucariacites* sp., *Cycadopites* sp., *Inaperturopollenites* sp., *Perinopollenites elatoides,* and *Pinuspollenites minimus* are also present.

5. Discussion

5.1. Age of the Pereiros Formation

Palynostratigraphic studies previously carried out in the Triassic-Jurassic Silves Group are relatively limited. The first investigations were carried out by Doubinger *et al*. (1970), and continued by Adloff *et al*. (1974), based on the sedimentology and allostratigraphy work of Palain, who divided the Silves Group into three megasequences A, B, and C (Palain, 1976, 1979). Díez (2000) studied the same associations and concluded that the Conraria Formation [Megasequence A from Palain (1976)] dates from the lower to middle Carnian and includes the taxa *Classopollis meyerianus, Duplicisporites granulatus, D. mancus, Microcachrydites doubingeri, M. fastidioides, Monosulcites minimus, Ovalipollis cultus, Paracirculina scurrilis* and *P. maljawkinae*. The Penela and Castelo Viegas formations [Megasequence B from Palain (1976)] show palynological associations (Adloff *et al*., 1974) that include *Araucariacites germanicus, Classopollis granulatus, C. meyerianus, Duplicisporites granulatus, Ischyosporites mesofoveasolidus, Kraeuselisporites reissingeri, Paracirculina tenebros*a and *Todisporites major,* suggesting an age from middle Carnian to latest Norian (Díez, 2000; Arche, López-Gómez, 2014). The Pereiros Formation [Megasequence C, Term C1 from Palain (1976)] presents an association

comprising taxa as *Classopollis classoides, Cycadopites granulatus, C. deterius, Inaperturopollenites dubius* and *Kraeuselisporites reissingeri*, among others, and was considered of Hettangian to Sinemurian age since Adloff *et al*. (1974). Based on the common presence of the taxa *Kraeuselisporites reissingeri*, Díez (2000) and Arche and López-Gómez (2014) propose a Norian to lower Rhaetian age for the C1 term.

However, type-sections of the Silves Group have recently been investigated, suggesting different ages for these formations (Vilas-Boas *et al*., 2021). Based on palynostratigraphic studies, Vilas Boas *et al*. (2021) date the Conraria Formation as Norian, possibly early Rhaetian, and the Pereiros Formation as late Rhaetian to early Hettangian, suggesting that the TJB should lie in the lowermost Pereiros Formation.

Therefore, an early Hettangian age could be indicated for the unit B2 studied in this work. In the previous study, the lower portion of the Pereiros Formation (unit B2 of Palain, 1976; Lamas I) was dated as Rhaetian up to the TJB based on the informal palynozone *Ischyosporites variegatus - Kraeuselisporites reissingeri* (IK), while the mid-upper portion (units C1 and C2 of Palain, 1976; Lamas II) was dated as early Hettangian based on the informal palynozone *Pinuspollenites minimus* (Pm) (Vilas-Boas *et al*., 2021). An important discontinuity in the lowermost portion of the Pereiros Formation truncates the siliciclastic beds at the top of the Castelo Viegas Formation (Fig. III.2), which has been regarded as the regional mapping boundary between the Triassic and Jurassic (Soares *et al*., 2007, 2012). However, the palynological evidence supports a position of the TJB within unit B2 at the base of the Pereiros Formation (Vilas-Boas *et al*., 2021). In this new study, the presence of *Carnisporites spiniger* in the unit B2 is noteworthy. This spore is very common through most of the samples in this unit, ranging from the Anisian (Middle Triassic), where this spore has its first occurrence, being consistent throughout all of the Upper Triassic (Vigran *et al*., 2014; Paterson and Mangerud, 2020).

Based on the presence of *Pinuspollenites minimus, Perinopollenites elatoides,* and the dominance of *Classopollis meyerianus,* these sections date from the Hettangian, being the base of unit B2 from the base of the Hettangian.

However, the presence of *P. longdonensis* can also reinforce a Hettangian age. The first occurrence of *P. longdonensis* in the Hettangian (upper part of the *K. reissingeri* Zone) was documented in Spain, where this taxon occurs with *Pinuspollenites minimus* and *Cerebropollenites thiergartii* (Barrón *et al*., 2002, 2006). Other locations in southern Europe where *P. longdonensis* was found in the Hettangian age include northern Germany (Schulz, Heunisch, 2005) and the Vicentinian Alps in Italy (Clement-Westerhof *et al*., 1974). The presence of *Paracirculina* sp., a typical Upper Triassic species, and the fact that there is an acme of lycopodiophyte spores (e.g., *Kraeuselisporites reissingeri*) in the Lamas I section when compared to Lamas II section place the first in a lower position, the base of the Hettangian, agreeing with the stratigraphic interpretation (Cirilli, 2010).

The presence of foraminifera linings in the Lamas I section is noteworthy, even though it does not contribute information to the age discussion.

Several Hettangian key taxa are missing in the studied sections. *Cerebropollenites thiergartii*, the critical marker taxon of the Hettangian age, is not present in the studied sections in the Lusitanian Basin (Vilas-Boas *et al*., 2021). The presence of *C. thiergartii* marks the base of the Jurassic but is very rare and hard to recognize (Lindström *et al*., 2017b). However, it may not be a reliable taxon because its FO seems not to be synchronous, varying between localities (Heunisch *et al*., 2010; Cirilli *et al*., 2015, 2018; Lindström *et al*., 2016, 2017b; Panfili *et al*., 2019). The regression-transgression 'couplet' may influence the FO of *C. thiergartii* (Lindström *et al*., 2017b).

Several authors discussed this issue; for example, Van de Schootbrugge *et al*. (2009) and Schobben *et al*. (2019) reported from the Central European Basin (Germany, Sweden, and Bonenburg) a floral transition characterised by a gradual decline in Rhaetian pollen grains, including *Rhaetipollis germanicus*, until they extinguished, being replaced in the early Hettangian, by assemblages containing abundant *Classopollis* spp., *Perinopollenites elatoides, Pinuspollenites minimus* and bissacates (e.g. *Alisporites* spp.) accompanied by the *Kraeuselisporites reissingeri* acme.

In the GSSP Kuhjoch section for the TJB, the *Trachysporites-Pinuspollenites* Zone (TPi Zone) assigned to the Hettangian age is distinguished by a marked increase in the abundance of *P. minimus*, which was previously present in low abundance in the underlying TH zone, as well as by the abundance of *Ricciisporites tuberculatus* and *K. reissingeri* together with *Classopollis* spp. and *Trachysporites* spp. (Hillebrandt *et al*., 2013).

5.2. Depositional setting

There are few sedimentological studies carried out in the Silves Group. Thus, the depositional interpretations are based on the classic works of sedimentology and allostratigraphy by Palain (1976, 1979) based on the description of megasequences, complemented by Soares *et al*. (2012). The two studied sections form a composite succession ca. 40 m thick [which includes the units B2, C1, and C2 of Palain (1976, 1979)], enabling us to envisage the probable depositional environments during the early Jurassic times based on studies of palynology and palynofacies compared with lithofacies.

5.3. Palynofacies data

Unit B2

The phytoclast group dominates this unit, and the percentage between opaque and non-opaque phytoclasts are related, as one increases when the other decreases. The moderate percentage of spores and pollen grains does not vary much throughout the unit, with spores dominating pollen grains. The constant presence of foraminifera linings indicates marine water influence. The overall ratio of high continental organic debris (e.g., phytoclast vegetable particles, sporomorphs) on marine elements points to a coastal environment. It also fits with lithofacies, mainly consisting of coarse to medium-grained plane-bedded sandstones alternate with carbonate (mostly dolostone).

The low percentage of AOM throughout the entire unit indicates well-oxygenated conditions, as expected along a coastal environment, but the presence of three intervals of dark mudstone-siltstones characterized by a relatively higher content of non-fluorescent AOM, which can be related to the presence of coastal swamps and ponds. In such conditions, the stagnant waters could preserve the AOM, trapped within fine-grained sediments, by strong oxidation processes.

Unit C1

The palynofacies elements of this lithofacies are strongly oxidized and characterized by phytoclasts. This siliciclastic unit, composed chiefly of mature arkosic sandstones, shows sedimentary structures such as erosive channel surfaces, cross-bedded sandstones, hummocky, and herringbone structures. The river flow strongly influences the depositional setting, as documented by the frequency of channelized deposits. On the other side, the proximity to the marine environment is testified by the presence of the herringbone structures indicating bi-directional flows such as tidal currents. For unit B2 the depositional setting records a regression of the coastal line. The high energy, high oxygenated conditions and the temporarily prolonged subaerial exposures could be responsible for the organic matter's strong oxidation.

Unit C2

In most parts of unit C2, the phytoclast group remains the most representative group as in the other units, joined to a very marked presence of pollen grains which could indicate a depositional environment close to the parent flora. Compared with lithofacies, the palynofacies features confirm the previous attribution to a lagoonal–tidal flat setting with mixed siliciclastic-carbonate and evaporite deposits (Soares *et al*., 2012). The warm-arid conditions are supported by the presence, in the recorded palynological assemblage, of abundant *Classopollis meyerianus* and *Classopollis torosus* together with common

Deltoidospora sp., that have a preference for drier and warmer conditions, with xerophytic microflora as *Alisporites* sp., *Pinuspollenites minimus,* and *Porcellispora longdonensis*.

Although the marine influence is expected on a tidal flat, foraminifera linings are absent. It could be explained by the presence of hypersaline waters that prevent the settling of foraminifera. The decrease of phytoclasts and the increase of sporomorphs (mostly pollen grains) and vegetal particles in the uppermost portion of unit C2 suggest more proximity of the depositional environment to the parent flora.

Compared with lithofacies, the palynofacies variations across the composite section point to a depositional environment ranging from coastal to tidal flat in response to short-lived, marine transgression-regression events. Furthermore, the palynological assemblages and lithofacies indicate a shift towards a warm-arid climate in the upper Hettangian (unit C2).

The facies transition between units B1 and B2 has been interpreted as the first mainly flooding event in the LB based on the molluscs fauna of *Promathildia* and *Isocyprina* in unit B2 (e.g., Soares *et al*., 1993; Azerêdo *et al*., 2003). The evidence of the first marine transgressive episode in unit B2 is further supported by abundant foraminifera linings recorded within the grey to blackish lutites at the lower part of the sequence.

The short-lived marine transgression phase recorded in B2 could be tentatively related to tectonics rather than only eustatic sea-level fluctuations (Hallam, 1981; Haq *et al*., 1988; Rasmussen *et al*., 1998).

Hence, we suggest that the tectonism associated with the first rifting phases of the Lusitanian Basin created areas of low topography with embayments that sea waters could more easily inundate. These embayments may have been similar to estuaries where the lower energy conditions in the central basin promote the deposition of fine-grained sediments. Estuarine depositional systems are associated with brackish waters, which explains the presence of foraminifera linings as also recorded in modern estuarine settings in the Iberian Peninsula (Leorri, Cearreta, 2009; Schönfeld, Mendes, 2022). A high

percentage of continental-derived OM (e.g., phytoclasts, pollen grains, and spores, vegetal particles) were transported and deposited by rivers into an estuarine-type sedimentary environment.

The lower Jurassic transgressive phase followed that recognised in Europe and Canadian Artic (Embry, Suneby, 1994; Hallam, 1997; Aurell *et al*., 2003; Gomes, Goy, 2005). According to Hallam *et al*. (2004), a similar pattern of successive sea-level fall and rise can also be observed in Europe's north and south Triassic-Jurassic sequences; however, like the LB, the upper Rhaetian is missing in southern Sweden and NW Poland, due to the presence of an unconformity at the base of the Jurassic strata (Hallam *et al*., 2004).

Unit C1 could be interpreted as deposited during a successive rapid sea-level fall, followed by a new episode of transgression under more arid climate conditions with the deposition of unit C2. According to Soares *et al*. (2012), this unit records sedimentary processes in an evaporitic tidal flat environment that pass upwards to lacustrine facies, delimited by shoals or sandy bars of laminated “dolomitic” sediments (Soares *et al*., 2012). The equivalent lateral saline units from the Dagorda Formation can explain the early dolomitization processes affecting unit C2 (Soares *et al*., 2012). It is worth noting in this unit the sporadic occurrence of *Isocyprina*, which testifies to an environment, locally, not so different from that of unit B2 (Azerêdo *et al*., 2003).

Plate III.I. Selected spores from Lamas I and Lamas II sections. The species name is followed by the outcrop, sample, slide number, and microscope coordinates.

1. *Calamospora tener* (Leschik) Mädler 1964, Outcrop Lamas I; sample LAMAS 14INT; slide 1 (1202-205).
2. *Calamospora tener* (Leschik) Mädler 1964, Outcrop Lamas II; sample LAM 1; slide 2 (1130-115).
3. *Carnisporites spiniger* (Leschile) Morbey 1975, Outcrop Lamas I, sample LAMAS 8/9; slide 1 (1309-105).
4. *Carnisporites* sp., Outcrop Lamas II; sample LAM 1; slide 8 (1440-205).
5. *Cibotiumspora* sp., Outcrop Lamas I; sample LAMAS 10/11; slide 1 (1281-209).
6. *Deltoidospora* sp., Outcrop Lamas II, sample LAM 5; slide1 (1355-125).
7. *Ischyosporites variegatus* (Couper) Schulz 1967, Outcrop Lamas II, sample LAM 12; slide 3 (1305-205).
8. *Kraeuselisporites reissingeri* Leschik emend. Jansonius 1962, Outcrop Lamas I; sample LAMAS 13; slide 1 (1240-60).
9. *Kraeuselisporites reissingeri* Leschik emend. Jansonius 1962, Outcrop Lamas II; sample LAM 12; slide 1 (1387-175).
10. *Kyrtomisporis* sp., Outcrop Lamas II; sample LAM 12; slide 1 (1395-71).
11. *Convolutispora* sp., Outcrop Lamas I; sample LAMAS 12; slide 1 (1205-161).
12. *Porcellispora longdonensis* (Clarke) Scheuring emend. Morbey 1975, Outcrop Lamas II; sample LAM 1; slide 8 (1200-125).

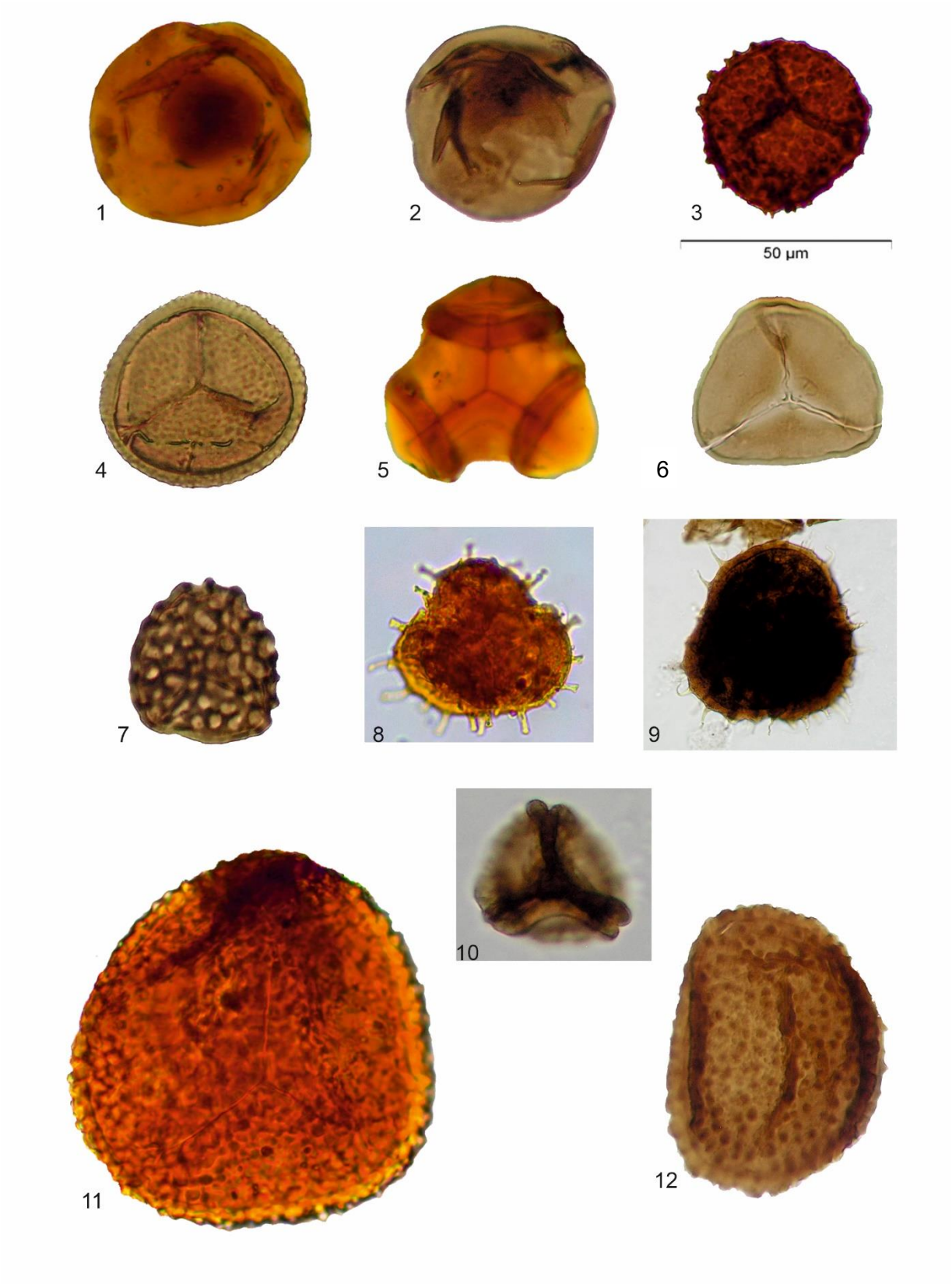

Plate III.I. (caption in the previous page)

Plate III.II. Selected pollen and foraminifera lining from Lamas I and Lamas II sections. The species name is followed by the outcrop, sample, slide number, and microscope coordinates.

1. *Araucariacites* sp., Outcrop Lamas II; sample LAM 1; slide 2 (1145-184).
2. *Classopollis meyerianus* (Klaus) Venkatachala & Góczán 1964, Outcrop Lamas II; sample LAM 2; slide 5 (1340-25).
3. *Cycadopites* sp., Outcrop Lamas II; sample LAM 2; slide 1 (1225-95).
4. *Classopollis torosus* (Reissinger) Klaus emend. Cornet & Traverse 1975, Outcrop Lamas II; sample LAM 1; slide 2 (1430-150).
5. *Pinuspollenites minimus* (Couper) Kemp 1970, Outcrop Lamas II; sample LAM 6; slide 2 (1415-268).
6. *Perinopollenites elatoides* Couper 1958, Outcrop Lamas II; sample LAM 12; slide-4 (1055-117).
7. *Classopollis meyerianus* with abnormal pollen of *Classopollis* (Klaus) Venkatachala & Góczán 1964, Outcrop Lamas I, sample LAMAS 14INT; slide 1 (1212-205).
8. Foraminiferal lining, Outcrop Lamas I, sample LAMAS 13; slide 1 (1250-150).
9. Foraminiferal lining, Outcrop Lamas I, sample LAMAS 8/9; slide 1 (1381-112).
10. Foraminiferal lining, Outcrop Lamas I, sample LAMAS 10/11; slide 1 (1203-90).
11. Foraminiferal lining, Outcrop Lamas I, sample LAMAS 13; slide 1 (1385-110).
12. Foraminiferal lining, Outcrop Lamas I, sample LAMAS 10/11; slide 1 (1201-171).

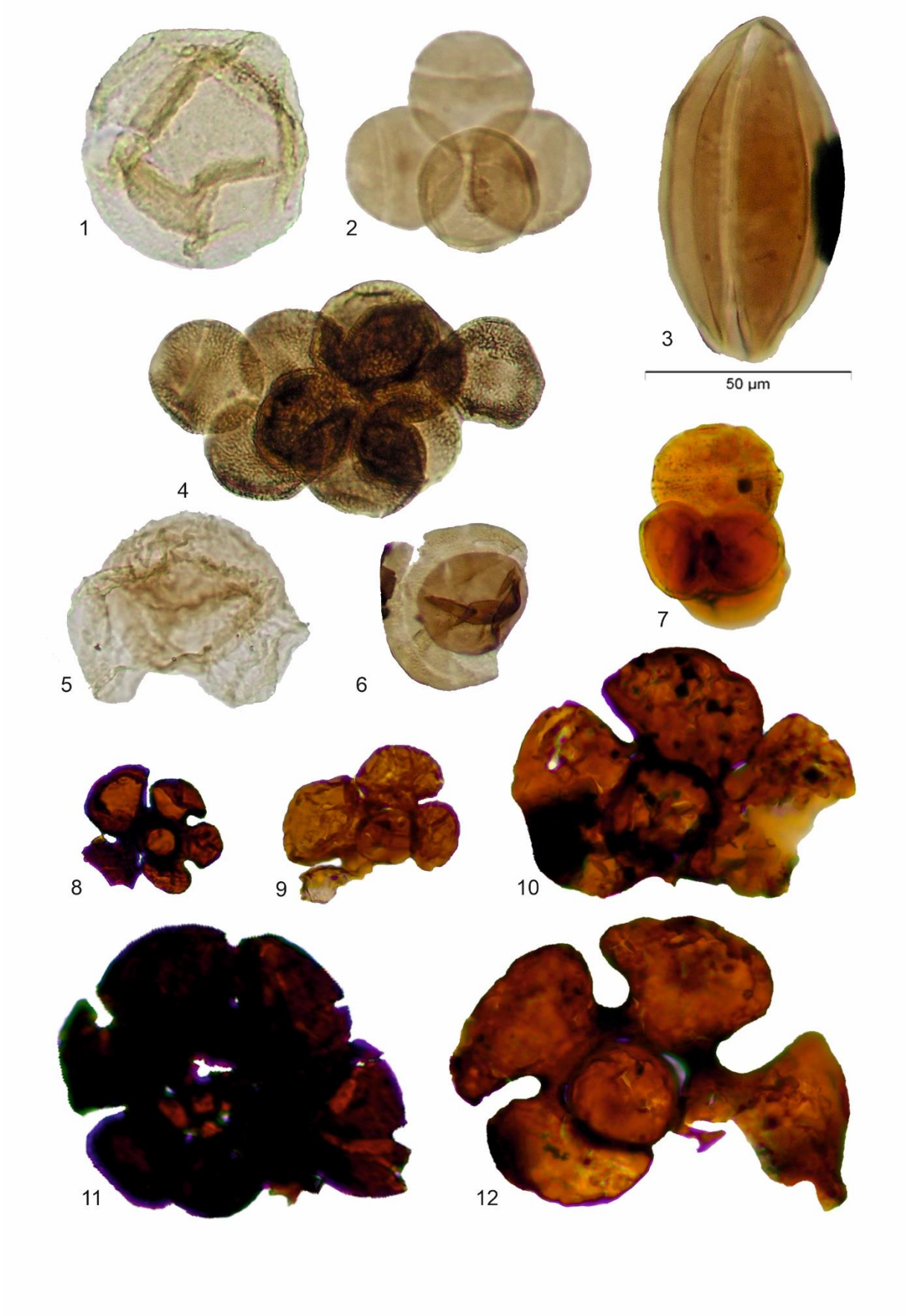

Plate III.II. (caption in the previous page)

Plate III.III. Selected palynofacies assemblages from the outcrops Lamas I and Lamas II.

1. Dominance of phytoclasts opaque and non-opaque and spores from the Lamas I outcrop, sample LAMAS 12;
2. Presence of foraminiferal lining from the Lamas I outcrop, sample LAMAS 13;
3. Dominance of non-opaque phytoclasts from the Lamas I outcrop, sample LAMAS 14BASE;
4. Dominance of phytoclasts opaque and non-opaque and spores from the Lamas I outcrop, sample LAMAS 14INT;
5. Presence of more common *Classopollis* spp. pollen grains in tetrads from the Lamas II outcrop, sample LAM 8;
6. Dominance of pollen grains and opaque phytoclasts from the Lamas II outcrop, sample LAM 12.

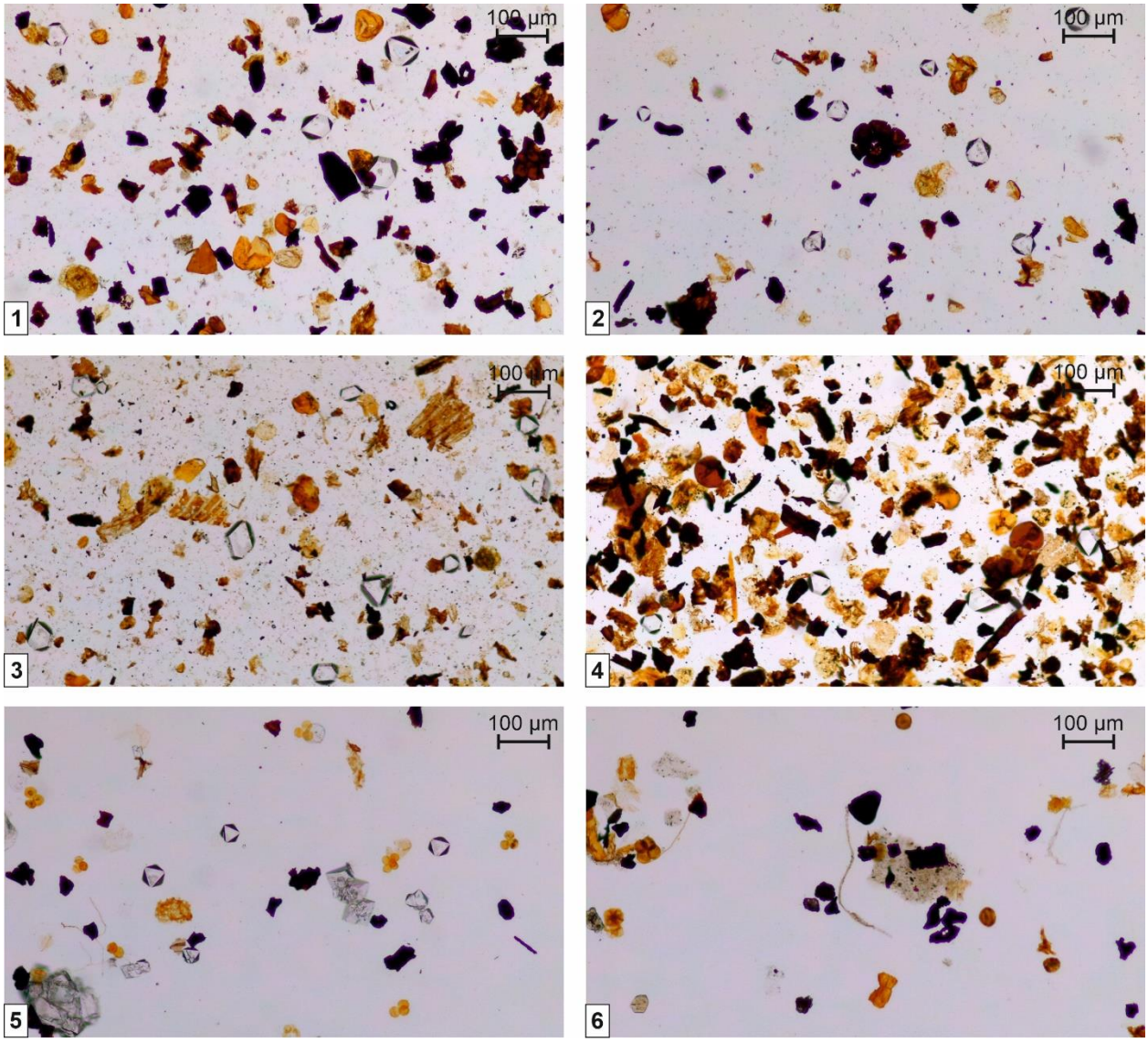

Plate III.III. (caption in the previous page)

6. Conclusions

The palynological data allow us to conclude that the two studied sections belong to the Pereiros Formation and are of early Hettangian age, Early Jurassic. This age is confirmed by the presence of the spores *Calamospora tener*, *Ischyosporites variegatus, Kraeuselisporites reissingeri* and *Porcellispora longdonensis,* and the pollen grains *Alisporites sp., Perinopollenites elatoides* and *Pinuspollenites minimus* in both sections.

After analysing the data obtained from the palynology and palynofacies studies, we can conclude that:

- In **unit B2**, *Carnisporites spiniger, Kraeuselisporites reissingeri,* and *Ischyosporites variegatus* spores and pollen grains *Pinuspollenites minimus, Perinopollenites elatoides,* and the dominance of *Classopollis meyerianu*s allow dating this unit from the base of the Hettangian. The presence of foraminiferal linings documents, in this unit, the first event of marine flooding occurred in the Lusitanian Basin. The data allow the interpretation of this unit as an estuarine-type environment, suggesting a short-lived marine transgression event;

- **Unit C1** is interpreted as a river-dominated coastal environment with episodes of tidal current influence and records a short regression episode;

- **Unit C2**, the presence of *Kraeuselisporites reissingeri* and *Ischyosporites variegatus* and pollen grains *Perinopollenites elatoides, Pinuspollenites minimus* and the dominance of *Classopollis meyerianus* indicate a Hettangian age for this unit. Palynofacies, dominated by pollen grains and phytoclasts, and lithofacies point to an evaporitic tidal flat under warm-arid climate conditions.

Therefore, we can conclude that marine-marginal depositional settings dominated the Lusitanian Basin during the Hettangian and were interrupted by river-dominated episodes related to the short-lived regressive phase.

The microflora assemblages from the Lusitanian Basin recorded along the Early Jurassic times might shed new light on future palaeogeographical and paleoclimatic reconstructions of this sector of the Tethys realm. Nevertheless, more studies are needed to enhance further this information.

CHAPTER IV

The beginning of the sedimentation in the Algarve Basin

Chapter IV cover:

Autódromo outcrop, Portimão, Upper Triassic, Algarve Basin

Chapter IV. The beginning of the sedimentation in the Algarve Basin

Adapted from the paper 3:

Vilas-Boas, M., Paterson, N. W., Pereira, Z., Fernandes, P., and Cirilli, S., 2022. The age of the first pulse of continental rifting associated with the breakup of Pangea in Southwest Iberia: new palynological evidence. Journal of Iberian Geology, 48(2), 181-190. https://doi.org/10.1007/s41513-022-00189-0

Abstract

In this work, we report the first palynological age for the base strata of the Silves Sandstones of the Silves Group in the Algarve Basin, located in Southern Portugal. The group is the oldest sedimentary unit of the Algarve Basin and was deposited unconformably over late Pennsylvanian turbidites of the Brejeira Formation, which were folded and faulted during the Variscan Orogeny. The Silves Group comprises a detrital red bed succession, representing the earliest phase of sedimentation associated with the initial rifting of Pangaea. Macrofossils are rare, occurring predominantly in the top layers of this group, and do not accurately constrain the age of the entire group's deposition. From an outcrop exposed in the central Algarve, a grey mudstone bed positioned 2.5 m above the Variscan unconformity plane yielded palynomorphs that date the beginning of sedimentation in this basin to the early Carnian age (Late Triassic). The moderately well preserved and low-diversity palynological association comprises *Aulisporites astigmosus*, *Enzonalasporites densus, Ovalipollis pseudoalatus*, *Samaropollenites speciosus*, *Tulesporites briscoensis* and *Vallasporites ignacii*, among others, and is indicative of an early Carnian age.

Keywords: Upper Triassic, Variscan Unconformity, Palynology, Algarve Basin, Portugal

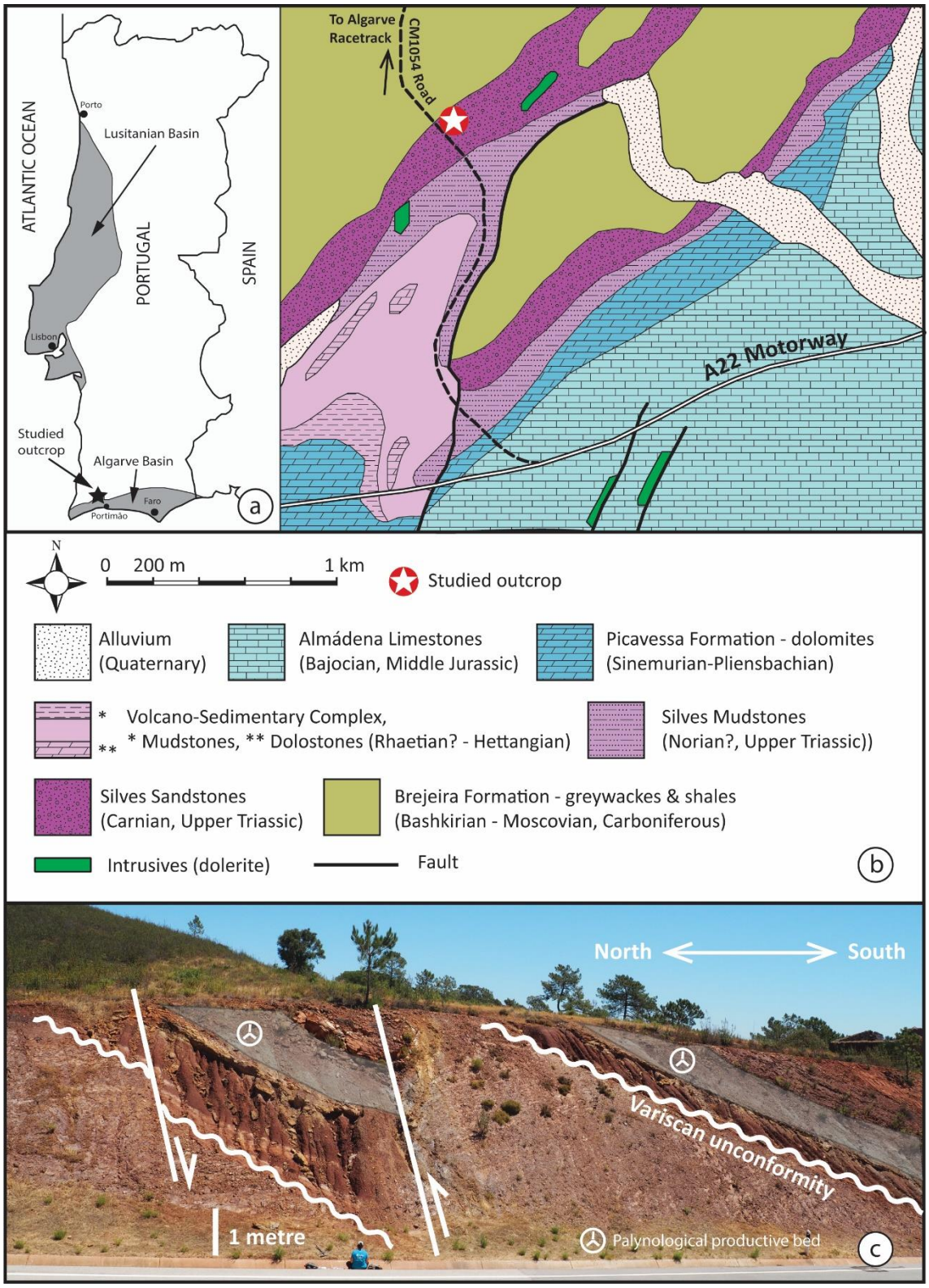

Figure IV.1. Map of the studied area with location of studied sections, a – Map of Portugal with the Lusitanian and Algarve basins represented. The star symbol represents the studied outcrops; b – a detailed geological map of the area where the studied outcrop is located, geological map and inferred ages for formations adapted from Manuppella *et al*., (1992); c – photography of the outcrop, with the Variscan unconformity and the bed that yielded palynomorphs marked.

1. Introduction

The Algarve Basin (Fig. IV.1a), located in the South of Portugal, is one of the Mesozoic sedimentary basins bordering the Iberian Massif. The origin of the Algarve Basin is related to the breakup of Pangaea and the following extensional tectonic episodes that led to the opening of the North and Central Atlantic oceans. Sedimentation in the Algarve Basin started with detrital continental red beds that unconformably overlie deep-marine Pennsylvanian strata, deformed, and metamorphosed during the Variscan Orogeny (Palain, 1976; Terrinha, 2013). Overlying the red beds are variegated mudstones, interbedded with siltstones and dolostones, followed upwards by evaporites representing the first episodes of marine transgression in the Algarve Basin. The evaporites are covered by volcanics associated with the Central Atlantic Magmatic Province (CAMP) (Verati *et al*., 2007). The red sandstones, mudstones, evaporites, and the volcanics comprise the Silves Group (or Grés de Silves Group) and represent the first tectono-sedimentary cycle related to the initial phase of Pangaea continental rifting. The following sedimentary cycles, ranging from Lower Jurassic to Lower Cretaceous, are dominated by carbonate sedimentation on a passive continental margin (Manuppella *et al*., 1988; Fernandes *et al*., 2013; Terrinha, 2013).

The Silves Group is poorly studied from a biostratigraphic point of view, perhaps due to its sparse macrofossil content. In western central Portugal, the Lusitanian Basin (Fig. IV.1a) is another important sedimentary basin related to the breakup of Pangaea. In this basin the Silves Group has been subdivided into four formations, from the oldest to the most recent; the Conraria, Penela, Castelo Viegas and Pereiros formations (Soares *et al*., 2012). These units were previously described by Choffat (1894, 1903) and Palain (1976, 1979), and dated as Carnian–Norian age, through the first palynostratigraphic studies carried out by Doubinger *et al*. (1970) and by Adloff *et al*. (1974). This last study, at the time, did not permit accurate dating of this interval in the Lusitanian Basin, but it did provide the first evidence of Carnian–Norian age palynomorphs in the Silves Group. According to Palain (1976), the base of the Silves Group is of Carnian age. More recently, palynological data from these formations allowed better detailing of the age, thus dating the Conraria Formation and the base of the Silves

Group as Norian, (late Triassic), and the Pereiros Formation at the top of the group, as Hettangian (early Jurassic; Vilas-Boas *et al*., 2021).

In the Algarve Basin, the Silves Group's fossil record is scarce (Palain, 1976) and characterised by the lack of important age-diagnostic index fossils. Thus, the relative ages of the constituent formations are poorly constrained. However, the presence of bivalves of the genus *Euestheria* sp. (Palain, 1976), vertebrate remains of *Phytosauria* (Mateus *et al*., 2014), and a new *Metoposaurus* species (Brusatte *et al*., 2015), all found in beds stratigraphically above the basal red sandstones, strongly suggests a Late Triassic age for this part of the stratigraphic succession of the Silves Group. Regarding the upper part of the Silves Group lithologies, the CAMP volcanism is dated 198.1±0.4 Ma based on the radio-isotopic ages for the basalt flows determined from $^{40}Ar/^{39}Ar$ data. This age attribution is consistent with a palynological assemblage found in mudstones ca. 50 m below the CAMP (Cirilli oral commun. in Verati *et al*., 2007). It is also close to the late Hettangian age assigned to the microfloral assemblage from the evaporites (Fechner,1989). New palynological studies recently confirmed this age determination in the Triassic basins of the Betic Cordillera in southern Spain and the Algarve Basin (Peréz-López *et al*., 2021; Vilas Boas *et al*., 2021a). These data show that new studies are needed to ascertain the age of the Silves Group.

Since the age of the strata of the Silves Group may encompass the record of important changes of Earth's history that occurred during Late Triassic to Early Jurassic times (i.e., the Late Triassic Extinctions), the precise biostratigraphic scheme for the Silves Group is necessary to unlock its stratigraphic record. This work contributes to this last part; we report palynological assemblages from the Silves Group's basal beds.

2. Location and description of the studied outcrop

The studied section is located in the central Algarve, in a road cut of the CM1054 road, near the International Racetrack of Algarve (Fig. IV.1b). The road cut provides good exposures of the Variscan angular unconformity, and a ca. 24

m thick sequence assigned to the Silves Group's lowermost unit, the Silves Sandstones (Figs. IV.1c and IV.2). The lithologies below the unconformity plane consist of folded greywackes and shales belonging to the Brejeira Formation of Bashkirian to upper Moscovian age (Pereira *et al.*, 2008; Fernandes *et al.*, 2019).

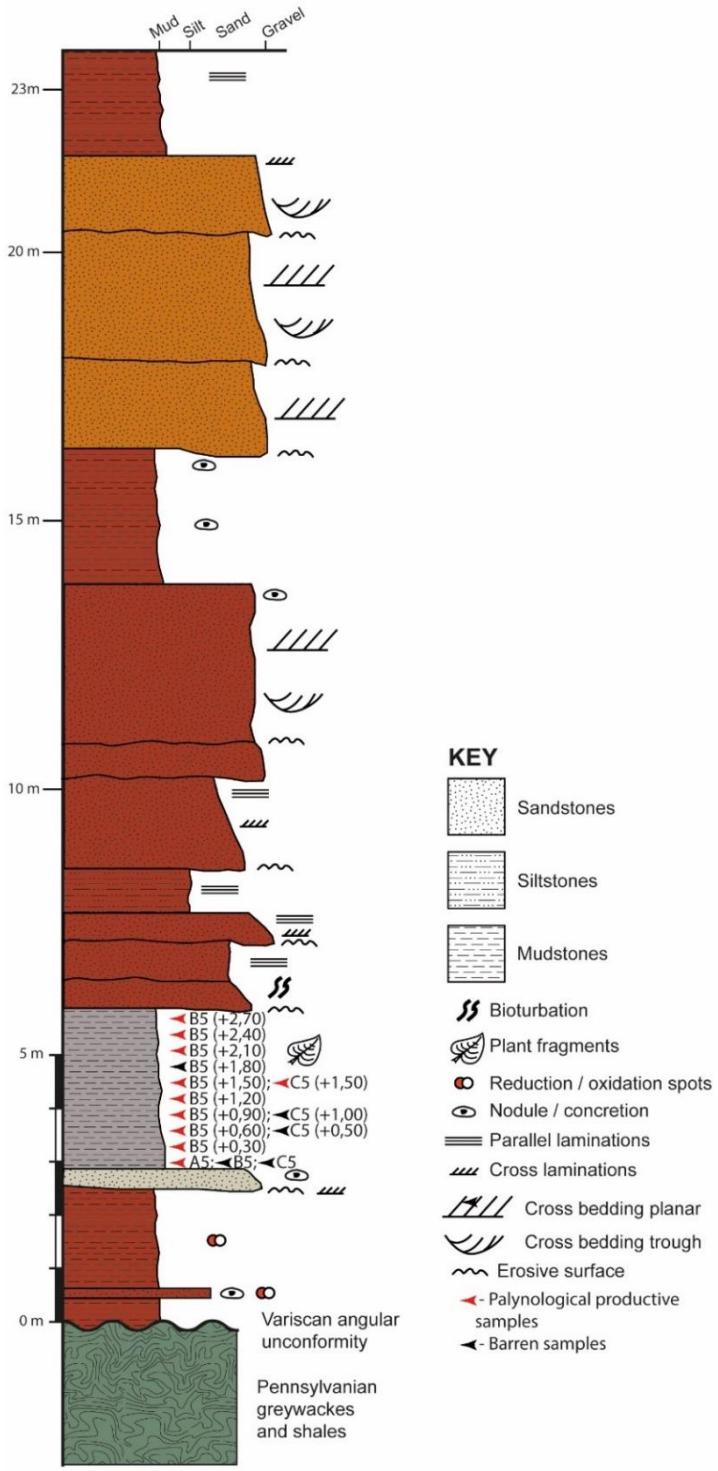

Figure IV.2. Stratigraphic log of the studied outcrop with location of palynological productive samples. The colors represented are in accordance with the colors observed in the section.

Above the unconformity, the Silves Sandstones include a ca. 2.5 m thick succession consisting mainly of red mudstones, interbedded with a 20 cm thick bed of fine- to medium-grained sandstone showing reduction spots. Above the basal beds is a 25 cm thick coarse to medium-grained sandstone showing current ripples, cross-lamination, and diagenetic calcite nodules. This unit is followed upwards by a 3 m thick bed of grey mudstones with common small plant impressions and parallel lamination. Towards the top of this bed, the colour of the mudstones changes from grey to red. The sedimentary features observed in this latter bed suggest deposition in either a shallow lake or the fill of an abandoned river channel, where fine-grained sediments gradually accumulate by successive river floods. All of the palynological productive samples were collected from this latter bed. Above the grey mudstones, and until the end of the road cut exposure, the succession is dominated by fine-grained red sandstone beds. The sandstone beds contain a range of massive bedding, normal graded bedding, tabular and trough cross-bedding, and diagenetic concretions. These sedimentary features suggest fluvial channel fill successions. Between 14 to 16 meters above the unconformity plane, the sandstones are interbedded with a red mudstone interval, which may relate to floodplain deposition.

3. Materials and Methods

Twenty-five samples were collected from the Silves Sandstones (lowermost Silves Group) on an outcrop along the studied section in the CM1054 road towards the International Roadtrack of Algarve in Portimão. The outcrop consists of two facing road cuts on the eastern and western sides of the road (Figs. IV.1 and IV.2). The layer was sampled every 30 cm on the western side of the road (positive samples: B5(+0,30), B5(+0,60), B5(+0,90), B5(+1,20), B5(+1,50), B5(2,10), B5(+2,40) and B5(+2,70)) and every 50 cm on the eastern side of the road (positive samples: A5 and C5(+1,50)). In this last road cut, this bed was sampled in both the hanging wall and footwall blocks of a reverse fault (Fig. IV.2). Standard palynological laboratory techniques were used for extraction and concentration of organic matter, with treatments with hydrochloric (HCl) and

hydrofluoric (HF) acids, as described by Wood *et al*. (1996) and Riding and Warny (2008).

The residues were sieved using a 15μm sieve and were mounted on microscope slides using Entelan®, a commercial resin-based mounting medium. The slides were analysed using a Leica ICC50W microscope equipped with a camera. Biostratigraphically significant taxa are illustrated in Plate IV.I. All samples, residues, and slides are held at the University of Algarve and the Palynological Collection of LNEG, Portugal.

4. Palynology

Palynomorph recovery was obtained only in samples collected from a 3 m thick layer, starting at about 2.5 m above the Variscan unconformity plane. The resulting residues contained palynological material that was moderate to well-preserved, which allowed the identification of some age-diagnostic palynomorphs.

Plate IV.I. Selected palynomorphs from the Silves Sandstone, Silves Group, Portimão section. The sample slide number and microscope coordinates follow the species' name.

1. *Calamospora* sp., sample AUTO3, slide B, EF D36|3.
2. *Conbaculatisporites* sp., sample AUTO3, slide A, EF T47|3.
3. *Converrucosisporites* sp., sample AUTOB5(+2,10), EF F22|3.
4. *Deltoidospora* sp., sample AUTOB3, slide B, EF D53|4.
5. *Lycopodiacidites rugulatus* (Couper) Schulz, 1967, sample AUTO3, slide B, EF R31.
6. *Nevesisporites* cf. *vallatus* Jersey & Paten, 1964, sample AUTO3, slide C, EF K36|1.
7. *Verrucosisporites* sp., sample AUTO3, slide C, EF S24.
8. *Alisporites* sp., sample AUTO3, slide B, EF X49|3.
9. *Aulisporites astigmosus* (Leschik, 1956) Klaus 1960, sample AUTO3, slide c, EF J47|2.
10. *Cycadopites* sp., sample AUTO3, slide A, EF O49|2.
11. *Enzonalasporites vigens* Leschik, 1956 emend. Scheuring, 1970, sample AUTO3, slide A, EF D46|2.
12. ?*Klausipollenites* sp., sample AUTO3, slide A, EF P32.
13. *Ovalipollis pseudoalatus* Krutzsch, 1955, sample AUTO3, slide C, EF E51|2.
14. ?*Protodiploxypinus* sp., sample AUTO3, slide A, EF O54.
15. *Samaropollenites speciosus* Goubin, 1965, sample AUTO3, slide A, EF F43|2.
16. *Tulesporites briscoensis* Dunay and Fischer, 1979, sample AUTO3, slide A, EF Q47.
17. *Tulesporites briscoensis* Dunay and Fischer, 1979, sample AUTO3, slide A, EF J42|2.
18. *Vallasporites ignacii* Leschik, 1956 emend. Scheuring, 1970, sample AUTOB5(+0,90), EF K30.
19. *Vallasporites ignacii* Leschik, 1956 emend. Scheuring, 1970, sample AUTOB5(+2,10), EF N31.
20. *Vallasporites ignacii* Leschik, 1956 emend. Scheuring, 1970, sample AUTO3, slide A, EF Y41|2.

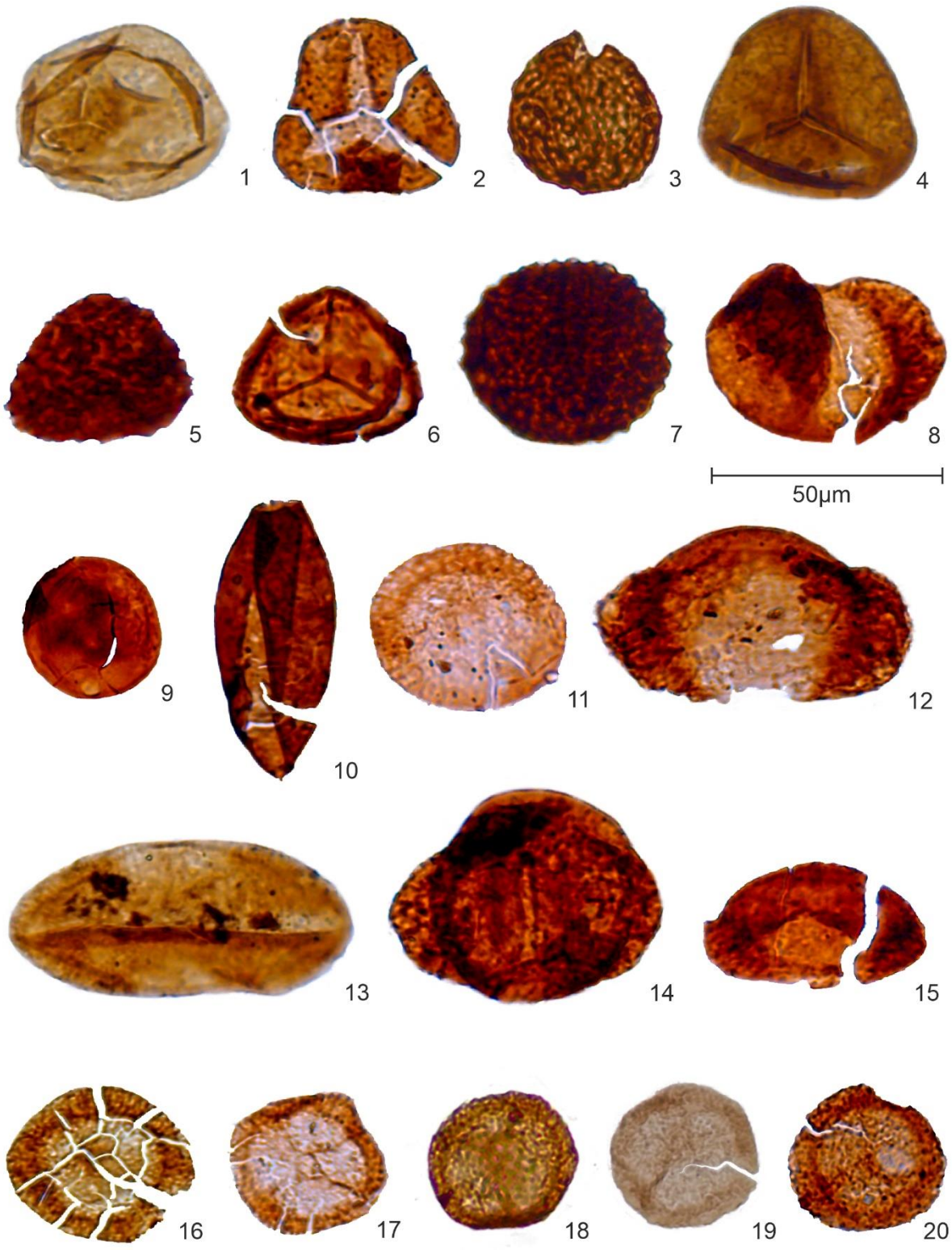

Plate IV.I. (caption in the previous page)

The assemblage is characterised by the common to abundant presence of the pollen taxa *Aulisporites astigmosus* and *Tulesporites briscoensis,* and by the spores *Calamospora* sp., *Conbaculatisporites* sp.*, Converrucosisporites* sp., *Deltoidospora* sp., *Lycopodiacidites rugulatus, Nevesisporites* cf. *vallatus* and *Verrucosisporites* sp.. Other rarer taxa present in the assemblage include the pollen *Alisporites* sp., *Cycadopites* sp., *Enzonalasporites vigens,* ?*Klausipollenites* sp., *Ovalipollis pseudoalatus*, ?*Protodiploxypinus* sp., *Samaropollenites speciosus, Triadispora* sp. and *Vallasporites ignacii*. The recovered palynomorph assemblage is of low taxonomic diversity and is impoverished relative to coeval assemblages from similar palaeolatitudes, e.g.: Cantabrian Mountains, northern Spain (Juncal *et al*., 2020); Catalan Coastal Ranges, northeast Spain (García-Ávila, 2020); Paris Basin, France (Juncal *et al*., 2018); northwest Sicily, Italy (Visscher and Krystyn, 1978; Martini *et al*., 2007; Buratti and Carillat, 2007); Western Dolomites, Italy (Van der Eem, 1983); Julian and Southern Alps, northeast Italy (Roghi, 2004; Mietto *et al*., 2012); Central Atlas of Tunisia and Gulf of Gabes, southern Tunisia (Mehdi *et al*., 2009; Buratti *et al*., 2012); Moroccan High Atlas (Cousminer and Manspeizer, 1976). The reason for the low diversity is presently unclear but may be the result of either ecological or taphonomic controls.

5. Biostratigraphic discussion

The stratigraphic range of some key taxa recorded in the palynological preparations from the Silves Sandstones in the Portimão section sheds new light on the age of this lithostratigraphic unit and provides important age constraints for the opening Algarve Basin. Specifically, the co-occurrence of *Aulisporites astigmosus, Enzonalasporites vigens, Samaropollenites speciosus,* and *Vallasporites ignacii* strongly suggest a Carnian age. In the Germanic Basin and Alpine realm, *Aulisporites astigmosus* first occurs in the Ladinian but reaches an acme in the lower Carnian (Julian) (Kürschner and Herngreen, 2010). At the Carnian GSSP at Prati di Stuores / Stuores Wiesen, *Aulisporite*s cf. *astigmosus*, *Samaropollenites speciosus* and *Vallasporites ignacii* have their first occurrences

in the *canadensis* Subzone and are thus firmly dated as earliest Carnian (early Julian) (Cirilli and Roghi, 1999; Roghi, 2004; Cirilli, 2010; Mietto *et al*., 2012). In the circum-Mediterranean areas, similar Carnian microfloral assemblages were recorded from independently dated strata in Sicily (Visscher and Krystyn, 1978), and in southern Albany (Cirilli and Montanari, 1994), north-western Libya (Muttoni *et al*., 2001), southern Israel (Cirilli and Eshet, 1991) highlighting a microfloristic provincialism referable to the Onslow Microflora (Buratti and Cirilli, 2007). Similarly, in the Boreal Realm, *A. astigmosus* and *V. ignacii* first occur in beds independently dated as early Carnian (Vigran *et al*., 2014; Paterson and Mangerud, 2020). Collectively, the first occurrences of these taxa indicate the basal Silves Sandstones at the Portimão section are no older than early Carnian.

Most of the taxa present in the Silves Sandstones assemblage have relatively long ranges. Nonetheless, an upper age limit is provided by *A. astigmosus*. In the Germanic and Alpine realms, Kürschner and Herngreen (2010, Fig. IV.3) indicate that the last taxon occurrence corresponds with the Julian–Tuvalian boundary. However, ammonoid-calibrated occurrences from the Cave del Predil area of northeast Italy suggest that the taxon, and its acme, range into the lower Tuvalian (Roghi, 2004). These observations, combined with the absence of characteristic Norian taxa in our assemblage, indicate an age no younger than late Carnian.

Our analyses provide the first documentation for *Aulisporites astigmosus* in the Grés de Silves Group. This taxon has not been recorded in the Carnian age Manuel Formation, the Silves Group equivalent stratigraphic unit in Spain (Arche and López-Gómez, 2014).

Also registered for the first time in Europe, with a common to abundant presence, is the pollen species *T. briscoensis*. This taxon has previously only been recorded in North American assemblages. It was first described by Dunay and Fisher (1979) in assemblages from the Dockum Group in the Texas Panhandle region. It was subsequently recorded in the Chinle Formation of Arizona, Colorado, New Mexico, and Utah (Scott, 1982; Baranyi *et al*., 2017), and

from Carnian lacustrine deposits in North Carolina and Virginia (Robbins, 1982). We highlight that *A. astigmosus* is seemingly absent in North American assemblages, which was not reported in the abovementioned studies. However, *S. speciosus* is present in the Carnian Zone I and *E. vigens* in the succeeding Zone II of Litwin *et al*., (1991).

Thus, the co-occurrence of *T. briscoensis* and *A. astigmosus* suggests the existence of a previously undescribed palynoflora, which combines elements typical of the North American and Central Europe Carnian. Other taxa present in our assemblage, such as *E. vigens* and *S. speciosus* are cosmopolitan and are present both in North America and Europe. These data are consistent with the paleogeographic position of the Algarve Basin, Portugal, in the Late Triassic (Palain, 1976; Terrinha *et al*., 2013).

More detailed studies are in progress on the recorded sporomorphs and their palaeobotanical affinities for palaeophytogeographic and climatic reconstructions, which will contribute to a better understanding of the local sedimentary environments.

6. Conclusions

The main results of this study are summarized below:

- The basal part of the Silves Sandstone of the Silves Group in the Algarve Basin yielded a biostratigraphically significant palynological assemblage, including *Aulisporites astigmosus, Enzonalasporites vigens*, *Vallasporites ignacii, and Samaropollenites speciosus* and is referable to the early Carnian;

- The age attribution based on the recorded palynological assemblage represents a significant result as it constrains the beginning of sedimentation within the Algarve Basin to the early Late Triassic;

- The taxon *T. briscoensis* is recorded for the first time in Europe and in Iberia;

- The co-occurrence of taxa such as *A. astigmosus*, *E. vigens*, *S. speciosus* and *T. briscoensis* indicates a mixing of early Carnian palynofloral elements with Central European and North America affinities, which is consistent with the paleogeographic position of the Iberian Peninsula in the Late Triassic;

- The present study contributes to a more complete documentation and illustration of the palynoflora from Iberia.

CHAPTER V

The Triassic-Jurassic boundary in the Algarve Basin

Chapter V cover:

Cerebropollenites macroverrucosus (Thiergart) Schulz, 1967, Silves Marl-Carbonate Evaporitic Complex, lower Hettangian, Lower Jurassic, sample MSG6, Algarve Basin

Chapter V. The Triassic-Jurassic in the Algarve Basin

Adapted from the paper 4:

Vilas-Boas, M., Pereira, Z., Cirilli, S. and Fernandes, P. New Insights on the Upper Triassic Silves Group in Algarve Basin, Portugal: Palynological, paleophytogeography and paleoclimatology advances. *Submitted to Geobios.*

Abstract

This paper presents the results of palynostratigraphic studies conducted in the Silves Group in the Algarve Basin, southern Portugal. From bottom to top, this group comprises the Silves Sandstones, the Silves Marl-Carbonate Evaporitic Complex, and the Volcano-Sedimentary Series. This study aimed to detail the age of the Silves Group in the Algarve Basin, bracketing the Upper Triassic - Lower Jurassic transition, using a palynological approach. Furthermore, the palynological results shed new light on the paleoclimatology and paleophytogeography of the Upper Triassic to Lower Jurassic period in this region of the western Tethys. For this purpose, two hundred fifty samples were collected from 14 main sections. Based on the microfloral content, three palynoassemblages have been recognized that allow to date the Silves Group to a time interval ranging from the lower Carnian to the lower Hettangian. Previous results from a section above the Variscan unconformity, containing *Aulisporites astigmosus, Enzonalasporites densus, Ovalipollis pseudoalatus, Samaropollenites speciosus, Tulesporites briscoensis*, and *Vallasporites ignacii*, among others, enabled to date the base of the Silves Sandstones and the onset of the Mesozoic sedimentary cycle in the Algarve Basin to lower Carnian. In this work, the palynoassemblage 1 recorded at the top of the Silves Sandstones, marked by the presence *of Camerosporites secatus, Enzonalasporites vigens, Granuloperculatipollis rudis, Lagenella martinii, Patinasporites densus,*

Samaropollenites speciosus, and *Vallasporites ignacii* allow to date this part of the unit as upper Carnian. Palynoassemblage 1 also contains the algae *Botryococcus* sp., *Plaesiodictyon mosellanum* ssp. *variable*, *P. mosellanum* ssp. *bullatum, Plaesiodictyon* sp. and *Leiosphaeridia* sp.. Palynoassemblage 2, found at the base of the Silves Marl-Carbonate Evaporitic Complex and consisting of *Alisporites* sp., *Araucariacites australis, Araucariacites* sp., *Classopollis meyerianus, Classopollis torosus, Cycadopites* sp., *Paracirculina quadruplicis* and *Triadispora* sp., indicates an upper Carnian age. Palynoassemblage 3 yielded *Alisporites diaphanus, Araucariacites australis, Cerebropollenites macroverrucosus, Cerebropollenites* sp., *Classopollis meyerianus, Classopollis torosus, Perinopollenites elatoides, Calamospora mesozoica* and *Kraeuselisporites reissingeri* dating the top of the Silves Marl-Carbonate Evaporitic Complex as upper Rhaetian-lower Hettangian. The recorded assemblages show a predominance of warm-climate flora. Based on palynostratigraphy, we can now constrain the age of the Silves Group in the Algarve Basin to the interval lower Carnian - lower Hettangian (Triassic-Jurassic boundary) for the first time. Furthermore, it advances our understanding of the Iberian palynoflora, paleoenvironment, and paleoclimate evolution. The presence of brackish algae at the base of the Silves Marl-Carbonate Evaporitic Complex indicates a marine influence, signifying the transition from a continental fluvial setting (Silves Sandstones) to a coastal environment with swamps, ponds, and lagoons. Quantitative data on the most important recorded sporomorphs and parent plants suggest a shift towards warmer and drier conditions at the top of the group. The Carnian microflora, characterized by the presence of *Enzonalasporites vigens, Patinasporites densus, Samaropollenites speciosus,* and *Vallasporites ignacii* contributes new insights into the of the Onslow Microflora in the Western Tethys.

Keywords: Carnian, Rhaetian, Triassic-Jurassic Boundary, Spores, Pollen, Palynostratigraphy, Paleophytogeography

1. Introduction and Geological Setting

The Algarve Basin (AB), located in the South of Portugal (Fig. V.1), is a Mesozoic sedimentary basin that formed during the breakup of Pangaea and subsequent extensional tectonic events that led to the opening of the North Atlantic Ocean (Terrinha *et al*., 2013). The initial sedimentary infill of the AB consists of continental siliciclastic red beds, volcanics, and evaporites, collectively known as the Silves Group. It unconformably overlies Carboniferous turbidites, which were deformed and underwent low-grade metamorphism during the Variscan Orogeny (Palain, 1976; Terrinha *et al*., 2013).

The Silves Group comprises sedimentary rocks deposited in various environments, ranging from continental, primarily alluvial, to shallow marine evaporitic settings (Terrinha *et al*., 2006). The group comprises three stratigraphic units, arranged from base to top: the Silves Sandstones, the Silves Marl-Carbonate Evaporitic Complex, and the Volcano-Sedimentary Series.

The sedimentary facies, textures, and thickness of the Silves Sandstones vary depending on their position within the AB. In outcrops West of the São Marcos da Serra-Quarteira Fault (SMSQF, Fig. V.1), the Silves Sandstone succession begins at the base with 6 to 10 m thick mudstones and siltstones (São Bartolomeu de Messines Clays, Palain, 1976), which have yielded palynomorphs indicating a lower Carnian age (Vilas-Boas *et al*., 2022). Above the last beds are coarse to fine-grained reddish sandstones displaying cross-stratification and lamination and trough cross-stratification, without any interbedded clay and silt size sediment. Massive strata usually display an erosive basal surface followed by gravel lags as channel-fill deposits. The facies and sedimentary structures suggest deposition in fluvial settings. The absence of significant floodplain deposits suggests deposition by bedload-dominated (braided) river systems. East of the SMSQF, the Silves Sandstones unit shows most of the aforementioned features. However, notable differences exist, such as the absence of mudstones at the base, coarser clastic sediments, and matrix-supported conglomerates interbedded with the sandstones. These differences suggest a more pronounced tectonic control on sedimentation in the eastern part of the SMSQF and a shorter distance to the sediment source regions.

The Silves Marl-Carbonate Evaporitic Complex conformably overlies the Silves Sandstones unit. Similar to the Silves Sandstones, the stratigraphy of this unit is strongly influenced by tectonic controls. Consequently, evaporitic deposits are absent to the north of the west-east trending Algibre Fault (AF; Fig. V.1). South of this fault, evaporites are only found in diapirs that intrude into Jurassic and Lower Cretaceous sedimentary rocks, such as the Loulé and Albufeira diapirs.

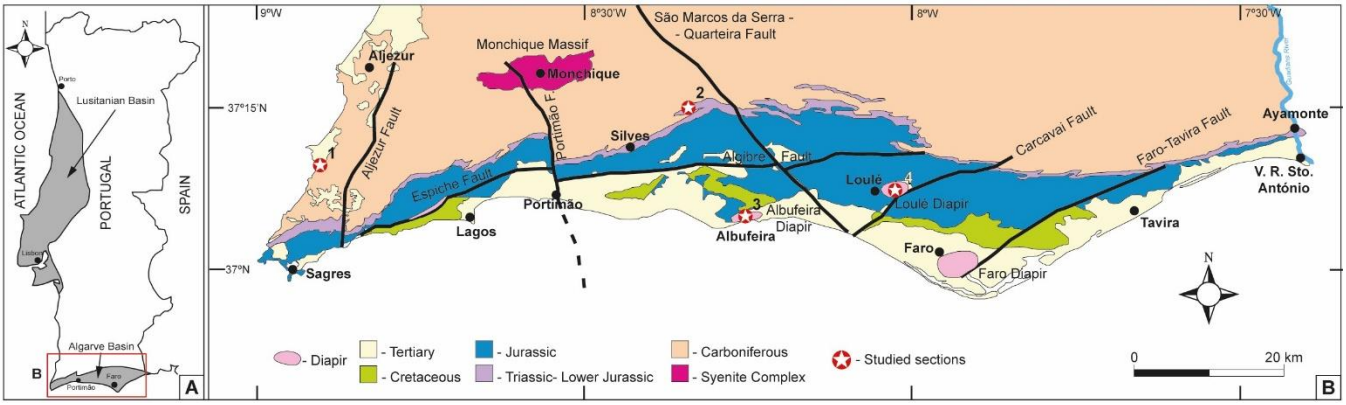

Figure V.1. Map of the studied area with the location of studied sections. A - Map of Portugal with the Lusitanian and Algarve basins represented. The red rectangle represents the area of the studied sections; B - detailed geological map of the Algarve Basin with the studied sections signed by the star symbol. 1 – Amado Beach section, 2 – Amorosa section, 3 – Albufeira Diapir section, 4 – Loulé Rock Salt Mine.

North of the AF, the Silves Marl-Carbonate Evaporitic Complex consists of variegated mudstones interbedded with marls, fine-grained sandstones, and siltstones reaching a maximum thickness of over 100 m. Sedimentary structures observed in this unit include rare wave ripples, current ripples, parallel laminations, desiccation cracks, bioturbation and pedogenic structures. Fossils found within this unit, including bivalves (*Eustheria* sp.) and vertebrate remains of *Phytosauria* (Mateus *et al*., 2014) and *Metoposaurus* (Brusatte *et al*., 2015), indicate an Upper Triassic age for this unit. In the town of Ayamonte, located near the Portuguese-Spanish border, the upper part of this unit is carbonate-rich. It has yielded a relatively rich fauna of bivalves, ostracods, gastropods (Santos *et al*., 2022), and a rare neural arch of a sauropterygian reptile (Reolid *et al*., 2022), These recent palaeontological data further support an Upper Triassic age for this portion of the Silves Marl-Carbonate Evaporitic Complex. The sedimentary

structures and the fossils from this stratigraphic unit suggest deposition in a shallow lacustrine environment frequently affected by desiccation events (ephemeral lakes).

The stratigraphic sequence of the Silves Group is topped by the Volcano-Sedimentary Series, which primarily comprises pyroclasts and a few basalt flows, indicating a prevalence of explosive volcanism over effusive phases. However, a basalt flow located at the uppermost part of this unit was dated using radio-isotopic analysis based on 40Ar/39Ar, and it was assigned an age of 198.1 ± 0.4 Ma (Lower Jurassic). This age was correlated with the Central Atlantic Magmatic Province (CAMP). The assigned age is consistent with a palynological assemblage discovered in mudstones approximately 50 m below the dated basalt flow (Verati *et al*., 2007).

The present research aims to refine the ages of the Upper Triassic - Lower Jurassic stratigraphic record of the Silves Group in the Algarve Basin through palynology. To achieve this goal, 250 samples were collected from 14 stratigraphic sections. Amongst these sections, five yielded samples that were suitable for palynological analysis. These selected sections were further examined to establish a detailed palynostratigraphic age based on the identification of key palynomorph taxa.

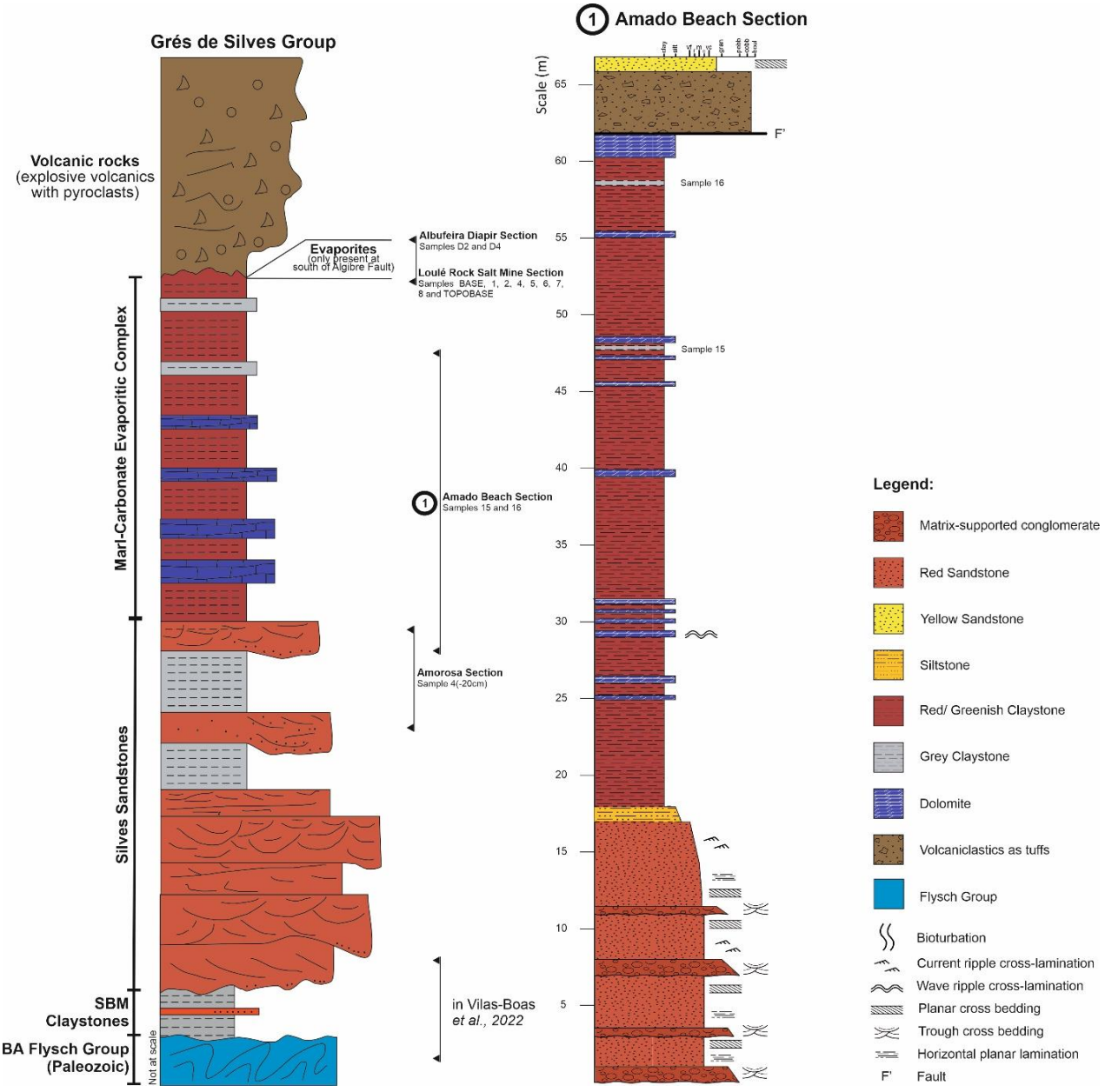

Figure V.2. General stratigraphic log of the Silves Group with location with the location of the studied sections and productive samples of each; 1 – Detailed log of Amado Beach section with the productive samples signed.

2. Materials and Methods

2.1.Studied Sections

2.1.1 Amorosa Section

This section is a roadcut outcrop located South of the village of Amorosa (37°15'38.65"N; 8°19'11.66"W) and exposes the stratigraphic limit between the Silves Sandstone and the Silves Marl-Carbonate Evaporitic Complex (Fig. V.2). The section is ca. 6 m thick, composed at the base of reddish silty mudstones that pass upward abruptly to a 1.2 m thick red sandstone bed (Fig. V.3D). The sandstone bed shows an erosive base, normal grading, cross-bedding and cross-lamination. Overlying the sandstone bed is a ca. 2 m thick of reddish silty mudstones with pedogenic structures, which pass gradually upwards to grey mudstones having thin beds of micrite limestone interbedded (Fig. V.3D). The sample with palynological results (AMOROSA 4(-20cm); Fig. V.2) corresponds to the basal layers of the Silves Marl-Carbonate Evaporitic Complex.

2.1.2 Amado's Beach Section

This section is exposed along the northern seacliffs at Amado Beach near the Carrapateira village (37°10'9.37"N; 8°54'10.72"W; Fig. V.2). The section is ca. 61 m thick and depicts the upper part of the Silves Sandstones and the lower part of the Silves Marl-Carbonate Evaporitic Complex.

The Silves Sandstones are a ca. 17 m thick sequence showing cross-bedding, trough cross-bedding, cross-lamination, normal grading, and basal erosional surfaces, often having matrix-supported conglomerates above. No mudstones or siltstone beds are interbedded with the sandstones, indicating that this sequence relates to amalgamated beds, probably due to the aggradation of channel fill deposits.

A 0.7 m thick bed consisting of fine-grained sandstones and siltstones showing current ripples and cross-laminations, sometimes showing climbing laminae (Fig. V.3C), separates the Silves Sandstones from the ca. 45 m thick

mudstone dominant sequence belonging to the Silves Marl-Carbonate Evaporitic Complex. The mudstones are variegated (reddish to grey). They are interbedded with thin dolomite beds and fine-grained sandstones, occasionally showing wave ripples (Fig. V.3C). Very common are reduction spots and whirls. The grey-to-dark mudstones and the dolomite beds often show parallel laminations. This part of the Amado Beach sequence is intruded by dolerites and contact by a fault with the volcanic rocks (mafic tuffs) of the Volcano-Sedimentary Series.

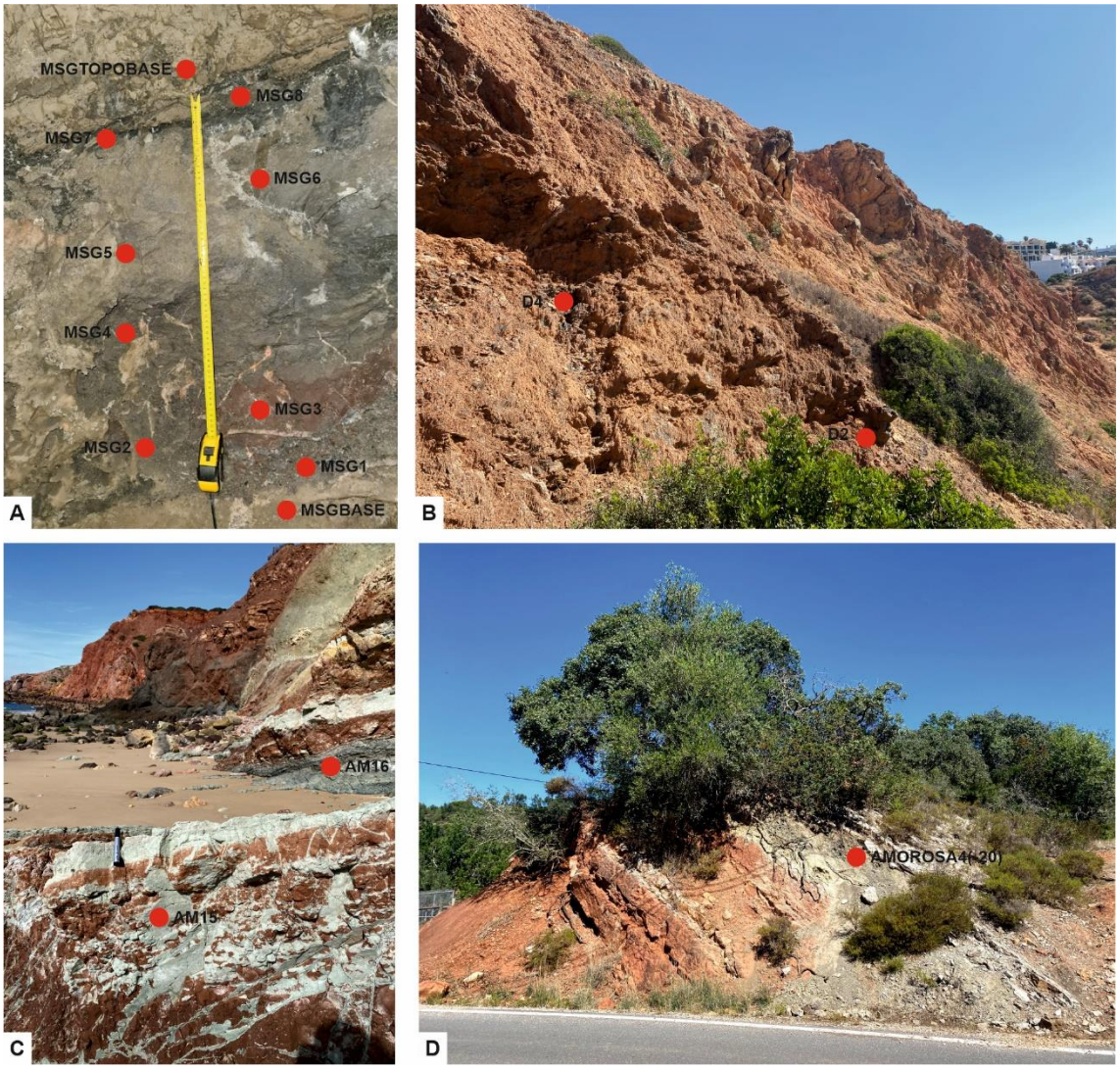

Figure V.3. Field photographs of the studied sections and the location of the productive samples signed by the red dot. **A** – Loulé Rock Salt Mine section; **B** – Albufeira Diapir section; **C** – Amado Beach section; **D** – Amorosa section.

2.1.3 Loulé Rock Salt Mine Section

The underground gallery (N01G01N between N01C0100 and N01C0101, located at 230 m deep), of the Loulé Rock Salt Mine (37°8'5.53"N; 8°0'28.05"W; Fig. V.2) intersects a ca. 1 m thick mudstone bed intercalated with the massive halite beds (Fig. V.3A). The mudstone bed is structureless and shows grey to dark-grey colour. Eight samples were taken from the mudstone bed, and two additional samples were collected from the impure halite at the bottom and top of the mudstone bed.

2.1.4 Albufeira Diapir Section

The Albufeira's Diapir is exposed at the seacliff of Baleeira's Cove, West of the town of Albufeira (37°4'54.18"N; 8°15'45.27"W; Fig. V.2). This diapir is fault-controlled by the East-West trending Baleeira Fault, and bedding is difficult to recognize within the diapir outcrop. The evaporite consists mainly of anhydrite and gypsum intercalated with very thin lenses of grey mudstone (Fig. V.3B). Two samples were taken from the grey mudstones.

2.2. Palynology

Forty-three samples were collected from five sections that yielded productive samples for palynological studies in the Silves Group of the Algarve Basin. Twenty-nine samples were collected from the Silves Sandstones unit along the Amorosa and Amado Beach sections, while fourteen samples were collected from the Silves Marl-Carbonate Evaporitic Complex along the Loulé Rock Salt Mine and Albufeira's Diapir sections. Fourteen of the forty-three samples were productive, showing moderate to well-preserved sporomorphs. In the Amorosa area, three sections were sampled along the M1080 road in the Vale Fuzeiros, close to São Bartolomeu de Messines. From those three sections, ten samples were collected (positive sample: AMOROSA4(-20cm). From Amado Beach, located South of Aljezur, nineteen samples were collected (positive samples: AM15 and AM16). Ten samples were collected in the Loulé Rock Salt

Mine (positive samples: MSGBASE, MSG 1, MSG2, MSG4, MSG5, MSG6, MSG7, MSG8 and MSGTOPOBASE). Four samples were collected from the Diapir in Baleeira Cove, Albufeira (positive samples: D2 and D4).

Standard palynological laboratory techniques were employed for organic matter extraction and concentration, including treatments with hydrochloric (HCl) and hydrofluoric (HF) acids (Wood *et al*., 1996; Riding and Warny, 2008). The residues were sieved through a 15µm sieve and mounted on microscope slides using Entelan®, a commercially available resin-based mounting medium. The slides were examined using a Leica DM750 microscope equipped with a Leica ICC50W camera and a BX40 Olympus equipped with an Olympus CS50 digital camera. Semi-quantitative abundance was determined by counting, when possible, 250 specimens per slide. Additionally, two or three slides were examined for rare taxa outside the count, represented with an X in Table 1. Plates I to III provide illustrations of the biostratigraphically significant taxa. All samples, residues, and slides are stored at the University of Algarve and the Palynological Collection of LNEG, Portugal.

3. Results

3.1. Palynoassemblages

The sporomorph assemblages recorded in the studied successions are described and documented in Fig. V.4. The quantitative and qualitative distribution of sporomorph associations is presented based on the relative abundance of prominent taxa, as well as the first appearance (FA), last appearance (LA), first appearance datum (FAD), last appearance datum (LAD), first occurrence (FO) and last occurrence (LO) of selected stratigraphically important taxa (Fig. V.4 and Table V.1). Selected specimens are illustrated in Plates I to III and a species list is presented in the Supplementary Appendix.

Table V.1. Dataset (%) for terrestrial palynomorphs (spores and pollen grains) and marine palynomorphs (algae). The light grey vertical band represents Albufeira's Diapir section because the stratigraphical position of this section is not certain. Relative abundance. X – Registered outside the count.

Silves Group Units	Silves Sandstones			Silves Marl-Carbonate Evaporitic Complex											
Age of the Section	Upper Triassic - Upper Carnian			Upper Triassic - Rhaetian						Lower Jurassic - Hettangian				? Rhaetian- ? Hettangian	
Sections	Amorosa	Amado's Beach		Loulé Rock Salt Mine										Albufeira's Diapir	
Samples	4(-20cm)	15	16	BASE	1	2	3	4	5	6	7	8	TOPO BASE	D2	D4
POLLEN															
Alisporites diaphanus											X				
Alisporites sp.		3,8	3		0,4										
Araucariacites australis				X						X		X			
Araucariacites sp.				17,5	24,9			10,2	14,3	36,7	18,7	48	36,1	6,4	31,2
Camerosporites secatus		X													
Cerebropollenites macroverrucosus										0,4					
Cerebropollenites sp.										0,4	0,4	0,4			
Classopollis malformed										X	X			21,6	6,8
Classopollis meyerianus				61,4	67,5			44,9	64,3	26,7	46	31,6	41	22,4	13,2
Classopollis sp.				7	0,4	0,6		18,4		2,4	0,4			8	1,2
Classopollis torosus										29,9	31,5	17,2	22,3	32,4	24,8
Cycadopites sp.				5,3						0,8	0,4	0,8			
Ellipsovelatisporites sp.	2,5		0,4												
Enzonalasporites vigens		X	9												
Ephedripites sp.												X			
Granuloperculatipollis rudis			0,4												
Lagenella martinii			X												
Microcachrydiites doubingeri			2,2												
Microcachrydiites fastidioides			1,9												
Microcachrydiites sp.		3,4	1,5												
Paracirculina malformed	17,3														
Paracirculina quadruplicis	50,6	8,3	25,5	3,5											
Paracirculina sp.	4,9	0,4	4,9												
Patinasporites densus	X	0,7	7,5												
Perinopollenites elatoides										2,4	2,6				
Samaropollenites speciosus	2,5	2,6	38,9												
Triadispora sp.	12,3	X	1,9					2							
Vallasporites ignacii	1,2	X	0,4												
Sum Pollen	91,3	19,2	97,5	94,7	93,2	0,6	0	75,5	78,6	99,7	100	98	99,4	90,8	77,2
SPORES															
Anapiculatisporites sp.											X				
Calamospora mesozoica					X					X					
Calamospora sp.		X										0,4			
Carnisporites sp.														6	1,2
Convolutispora sp.	0,6	X													
Deltoidospora sp.											X			0,4	
Deltoidospora toralis											X				
Kraeuselisporites reissingeri	0,6											1,6	0,6		
Kraeuselisporites sp.												X			
Kyrtomisporis sp.										0,4					
Leptolepidites argaenteaeformis											X				
Playfordiaspora sp.	7,4	0,8	2,6		0,4										
Verrucosisporites sp.	X	X													
Sum Spores	8,6	0,8	2,6	0	0,4	0	0	0	0	0,4	0	2	0,6	6,4	1,2
ALGAE															
Algae sp. A		6,4													
Botryococcus sp.		0,8													
Leiosphaeridia sp.		52,1										X		2,8	21,6
Ovoidites sp.		X													
Plaesiodictyon mosellanum ssp. *bullatum*		7,5													
Plaesiodictyon mosellanum ssp. *variable*		12,1													
Plaesiodictyon sp.		1,1													
Reworked algae				5,3	6,4	99,4		24,5	21,4						
Sum Algae		80	0	5,3	6,4	99,4	0	24,5	21,4	0	0	0	0	2,8	21,6
TOTAL SUM	100	100	100	100	100	100	0	100	100	100	100	100	100	100	100

This study recognized three palynoassemblages that, in stratigraphic order, from oldest to youngest, are:

Palynoassemblage 1

The microflora found in this assemblage is derived from the Amorosa and Amado Beach sections of the Silves Sandstones and the Silves Marl-Carbonate Evaporitic Complex units, respectively. It consists of approximately 16 species of moderate to well-preserved taxa of pollen, five species of spores, and seven

species of algae. The distinguishing feature of this assemblage is the concurrent presence of *Enzonalasporites vigens, Granuloperculatipollis rudis, Patinasporites densus, Samaropollenites speciosus* and *Vallasporites ignacii*. Other consistently present taxa include *Paracirculina* sp., *Paracirculina quadruplicis, Playfordiaspora* sp., and *Triadispora* sp.. Additionally, the assemblage includes *Alisporites* sp., *Camerosporites secatus, Ellipsovelatisporites* sp., *Lagenella martinii, Microcachrydiites doubingeri, Microcachrydiites fastidioides, Microcachrydiites* sp., malformed specimens of *Paracirculina* sp. and spores such as *Calamospora* sp., *Convolutispora* sp., *Kraeuselisporites reissingeri*, and V*errucosisporites* sp.. The algal association consists of *Botryococcus* sp., *Leiosphaeridia* sp., *Ovoidites* sp., *Plaesiodictyon mosellanum* ssp. *bullatum*, *Plaesiodictyon mosellanum* ssp. *variable* and *Plaesiodictyon* sp. and of an undetermined species provisionally referred to as Algae sp. A.

Palynoassemblage 2

The samples containing this assemblage came from the lower part of the Loulé Rock Salt Mine section that belongs to the Silves Marl-Carbonate Evaporitic Complex. The assemblage comprises about moderate to well-preserved eight species of pollen, two species of spores, and one species of algae. The notable feature of this assemblage is the FA of *Classopollis meyerianus*, *Classopollis torosus,* and *Classopollis* sp.. Other components include the pollen *Alisporites* sp., *Araucariacites australis, Araucariacites* sp., *Cycadopites* sp., *Paracirculina quadruplicis* and *Triadispora* sp., and the spores *Calamospora mesozoica* and *Playfordiaspora* sp.. Additionally, the palynoassemblage contains some specimens with fungal or algal affinity which appear to be reworked due to their darker color and resemblance to Neo-Proterozoic-age algae (e.g. *Ourasphaira giraldae*).

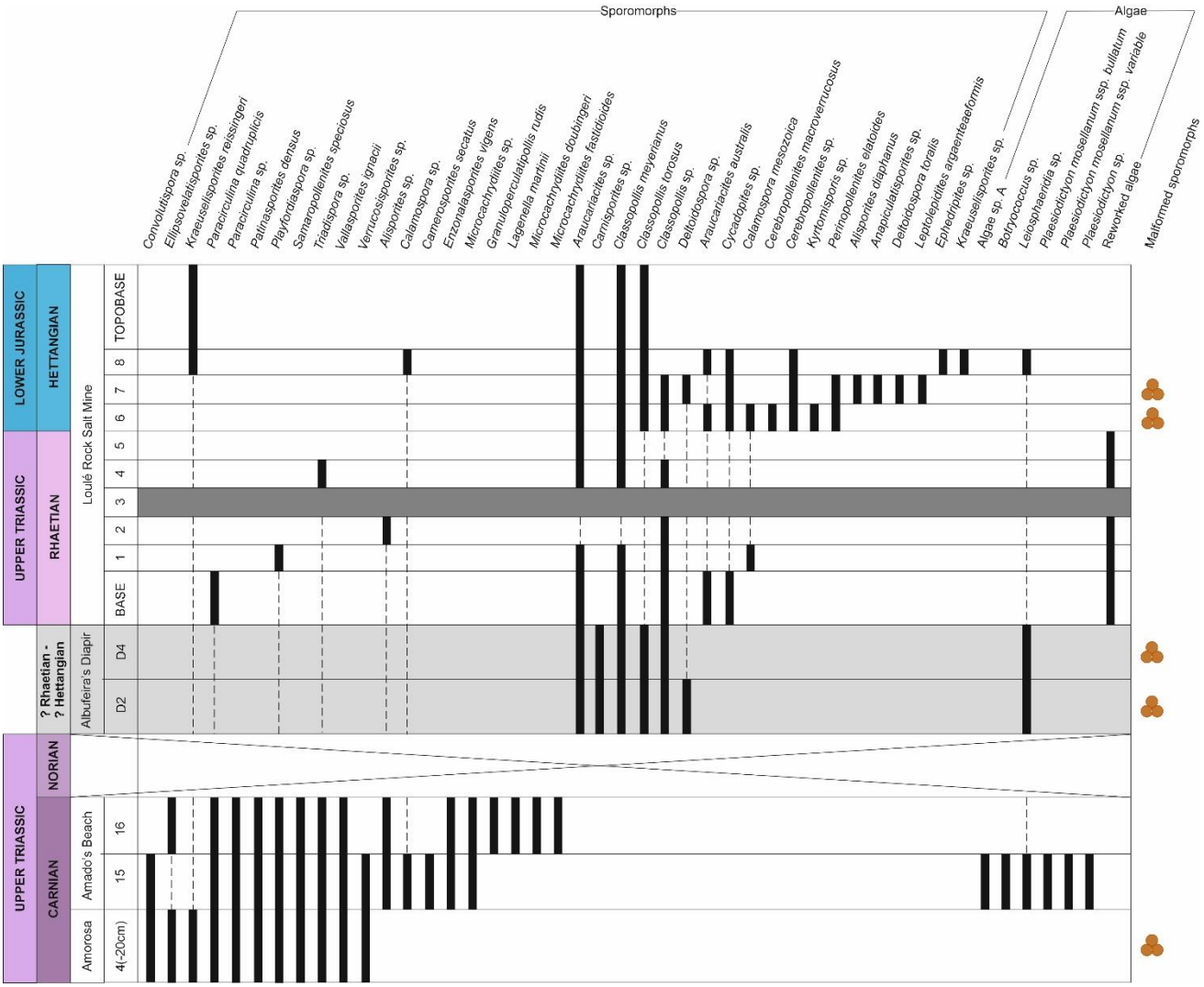

Figure V.4. Composite range chart of the sporomorph and algae found in the Silves Group, Algarve Basin. Dark grey band represent barren palynological sample. Light grey band represent Albufeira's Diapir section, because the stratigraphical position of this section is not certain. The tetrad symbol on the right of the chart signs the samples that have malformed sporomorphs in the palynological content.

Palynoassemblage 3

This assemblage derives from the upper part of the Loulé Rock Salt Mine section included in the Silves Marl-Carbonate Evaporitic Complex. It encompasses approximately twelve species of pollen, nine species of spores, and one species of algae, ranging from moderate to well-preserved. The FA of

Cerebropollenites macroverrucosus, Cerebropollenites sp., and *Perinopollenites elatoides* distinguishes this assemblage. Other components include the pollen *Alisporites diaphanus, Araucariacites australis, Araucariacites* sp., malformed specimens of *Classopollis* sp., *Classopollis meyerianus, Classopollis torosus, Classopollis* sp., *Cycadopites* sp., and *Ephedripites* sp.. Additionally, the spores *Anapiculatisporites* sp., *Calamospora mesozoica, Calamospora* sp., *Deltoidospora toralis, Deltoidospora* sp., *Kraeuselisporites reissingeri, Kraeuselisporites* sp., *Kyrtomisporis* sp. and *Leptolepidites argaenteaeformis* are present. The algae *Leiosphaeridia* sp. is also identified.

The palynoassemblage recovered from the Albufeira's Diapir, consists of six species of pollens, two species of spores, and one species of algae, and the material is moderately well preserved. The assemblage includes the pollen *Araucariacites* sp., malformed specimens of *Classopollis* sp., *Classopollis meyerianus, Classopollis* sp., *Classopollis torosus*, and *Cycadopites* sp. and the spores *Deltoidospora* sp. and *Carnisporites* sp.. The algae *Leiosphaeridia* sp. is also present.

4. Discussion

4.1. Age of Silves Group

By correlating the present results with those from Vilas-Boas *et al*., (2022), we can reconstruct the entire stratigraphic succession of the Silves Group.

The lower part of Silves Sandstones. This part of the Silves Group has been dated as early Carnian based on a palynological assemblage found in a 3m thick layer situated 2.5 m above the Variscan unconformity in the North of Portimão (Vilas-Boas *et al*., 2022). The assemblage includes *Alisporites* sp., *Aulisporites astigmosus, Cycadopites* sp., *Enzonalasporites vigens, Nevesisporites* cf. *vallatus, Ovalipollis pseudoalatus*, ?*Protodiploxypinus* sp., *Samaropollenites speciosus, Triadispora* sp., *Tulesporites briscoensis*, and *Vallasporites ignacii* along with the spores *Calamospora* sp., *Conbaculatisporites* sp., *Converrucosisporites* sp., *Deltoidospora* sp., ?*Klausipollenites* sp., *Lycopodiacidites rugulatus* and *Verrucosisporites* sp.. It is noteworthy the presence of *A. astigmosus* which along with *E. vigens, S. speciosus* and *T. briscoensis*, suggests a mixture of early Carnian palynofloral elements with affinities to Central European and North American domains, consistent with the paleogeographic position of the Iberian Peninsula at that geological period (Palain, 1976; Terrinha *et al*., 2013; Vilas-Boas *et al*., 2022).

Uppermost Silves Sandstones. This portion of the Silves Sandstones was sampled at the Amorosa section. The presence of a significant abundance of Circumpolles, such as *Paracirculina quadruplicis*, along with the monosaccate pollen *Patinasporites densus*, and the bisaccate pollen *Samaropollenites specious* indicates a palynological record of Carnian age (Mehdi *et al*., 2009; Cirilli, 2010; Buratti *et al*., 2012). Furthermore, the presence of *Ellipsovelatisporites* sp., *Triadispora* sp., and *Vallasporites ignacii*, in conjunction with the other palynological findings, enables the dating of the uppermost part of the Silves Sandstones to the upper Carnian (Schuurman, 1977, 1979; Visscher

and Krystyn, 1978; Visscher *et al*., 1980; Visscher and Brugman, 1981; Van der Eem, 1983; Fisher and Dunay, 1984; Blendinger, 1988; Hochuli *et al*., 1989; Cirilli and Eshet 1991; Cirilli and Montanari, 1994; Broglio Loriga *et al*., 1999; Hochuli and Frank, 2000; Warrington, 2002; Roghi, 2004; Mietto *et al*. 2007; Cirilli, 2010).

The lowermost part of the Silves Marl-Carbonate Evaporitic Complex. The basal portion of this unit was studied along the northern cliffs of Amado Beach, Aljezur. The significant presence of *Paracirculina quadruplicis, Paracirculina* sp., *Camerosporites secatus* and *Patinasporites densus*, along with *Ellipsovelatisporites* sp., *Enzonalasporites vigens* and *Triadispora* sp. indicates a general Carnian age as documented in the European domain (phase 1 of Schuurman, 1977, 1979; Dolby and Balme, 1976; Buratti and Cirilli, 2007; Cirilli, 2010; Kürschner and Herngreen, 2010; Mietto *et al*., 2012). In Central and North-Western Europe, the Carnian-Norian boundary is marked by the LAD of *Camerosporites secatus* (Cirilli, 2010; Kürschner and Herngreen, 2010). Furthermore, the presence of *Granuloperculatipollis rudis*, which FO was dated as Tuvalian (Kürschner and Herngreen, 2010; Mietto *et al*., 2012; Kustatscher *et al*., 2018) and of *Lagenella martinii* which LO was referred to the same substage in the European domain (Kürschner and Herngreen, 2010), constrains the age of the lower part of the Silves Marl-Carbonate Evaporitic Complex to the upper Carnian.

Uppermost Silves Marl-Carbonate Evaporitic Complex. The evaporite rocks at the top of this sequence were sampled in the Loulé Rock Salt Mine. The palynological assemblage is dominated by *Araucariacites* sp., *Classopollis meyerianus,* and *Classopollis torosus* and characterized by an increase in *Kraeuselisporites reissingeri.* The FO of *Cerebropollenites macroverrucosus, Cerebropollenites* sp., and *Perinopollenites elatoides* at the top of the sampled bed indicates a Hettangian age for top of this section. The absence of this taxa together with the absence of significant Carnian-early Norian forms (such as *Camerosporites* spp., *Ellipsovelatisporites* spp., *Enzonalasporites* spp., *P. densus, Rhaetipollis germanicus, V. ignacii* along with *G. rudis*) at the base of the

section points to an upper Rhaetian age for the basal part (Morbey, 1975; Schuurman, 1977, 1979; Visscher *et al*., 1980; Fisher and Dunay, 1981; Visscher and Brugman, 1981; Cirilli, 2010). Therefore, this interval encompasses the Triassic-Jurassic boundary, as it occurs in other different in Europe (Clement-Westerhof *et al*., 1974; Morbey, 1975, 1978; Van Erve, 1977; Visscher *et al*., 1980; Fisher and Dunay, 1981; Kürschner *et al*., 2007; Kürschner and Herngreen, 2010). Based on palynological findings, an overall upper Rhaetian to lowermost Hettangian age is indicated for the uppermost part of the Silves Marl-Carbonate Evaporitic Complex represented in the Loulé Rock Salt Mine.

The palynoassemblage of the samples recovered from the Albufeira's Diapir is very poor and dominated by *Classopollis meyerianus, Classopollis torosus, Classopollis* sp., and malformed specimens of *Classopollis* sp. with common *Araucariacites* sp.. The malformed species of *Classopollis* sp., when in tetrads, exhibit one of the four grains of the tetrad that appear much darker and smaller, sometimes with lack of ornamentation compared to the other pollen grains. These abnormalities in the aspect of the pollen grains of *Classopollis* sp. could be indicative of environmental stress related to atmospheric pollution, volcanic mercury (that could be related to the Eastern North America CAMP volcanism), and UVB radiation, generating mutagenesis in the land plants at the end of the Triassic (Visscher, *et al*., 2004; Foster and Afonin, 2005; Whiteside *et al*., 2007, 2010; Cirilli *et al*., 2009; Filipiak and Racki, 2010; Kürschner *et al*., 2013; Hochuli *et al*., 2017; Lindström *et al*., 2019). The lack of typical age-indicative sporomorphs does not allow us to determine this section's age more precisely and better define stratigraphic constraints. However, considering the similarity with the palynoassemblage from the Loulé Rock Salt Mine, both of which represent the evaporitic part of this unit, a possible Rhaetian-Hettangian age could be indicated for the Albufeira's Diapir.

Plate V.I. Selected pollen grains from the Silves Group sections studied in this work. Species name is followed by the outcrop, sample, slide number and England Finder coordinates.

1. *Samaropollenites speciosus* Goubin, 1965, outcrop Amorosa, sample Amorosa4(-20cm), slide 1, EF J42|3.
2. *Samaropollenites speciosus* Goubin, 1965, outcrop Amado's Beach, sample AM15, slide 1, EF Y40|3.
3. *Microcachrydiites* sp., outcrop Amado's Beach, sample AM15, slide 1, EF K33|1.
4. *Alisporites* sp., outcrop Amado's Beach, sample AM15, slide 1, EF R29.
5. *Alisporites diaphanus* (Pautsch, 1958) Lund, 1977, outcrop Rock Salt Mine, sample MSGvd7, slide 1, EF M29|2.
6. *Triadispora* sp., outcrop Amorosa, sample Amorosa4(-20cm), slide 1, EF R28.
7. *Triadispora* sp., outcrop Amorosa, sample Amorosa4(-20cm), slide 1, EF O23|3.
8. *Triadispora* sp., outcrop Amado's Beach, sample AM16, slide 1Z, EF L42.
9. *Enzonalasporites vigens* Leschik, 1956 emend. Scheuring, 1970, outcrop Amado's Beach, sample AM15, slide 1Z, EF O16.
10. *Patinasporites densus* Leschik emend. Scheuring, 1970, outcrop Amado's Beach, sample AM15, slide 2, EF W35.
11. *Patinasporites densus* Leschik emend. Scheuring, 1970, outcrop Amado's Beach, sample AM16, slide 1Z, EF J46.
12. *Patinasporites densus* Leschik emend. Scheuring, 1970, outcrop Amado's Beach, sample AM16, slide 1Z, EF K41|2.
13. *Vallasporites ignacii* Leschik, 1956 emend. Scheuring, 1970, outcrop Amado's Beach, sample AM16, slide 1Z, EF P43|3.
14. *Vallasporites ignacii* Leschik, 1956 emend. Scheuring, 1970, outcrop Amorosa, sample Amorosa4(-20cm), slide 1, EF S30.
15. *Paracirculina quadruplicis* Scheuring, 1970, outcrop Amado's Beach, sample AM15, slide 1, EF N25.
16. *Araucariacites australis* Cookson, 1947, outcrop Rock Salt Mine, sample MSGvdBASE, slide 1, EF O12|2.
17. *Araucariacites* sp., outcrop Amado's Beach, sample AM15, slide 1, EF L15.
18. *Perinopollenites elatoides* Couper, 1958, outcrop Rock Salt Mine, sample MSGvd6, slide 1F, EF D40.
19. *Perinopollenites elatoides* Couper, 1958, outcrop Rock Salt Mine, sample MSGvd7, slide 1F, EF R35.
20. *Perinopollenites elatoides* Couper, 1958, outcrop Rock Salt Mine, sample MSGvd6, slide 1F, EF M38|3.

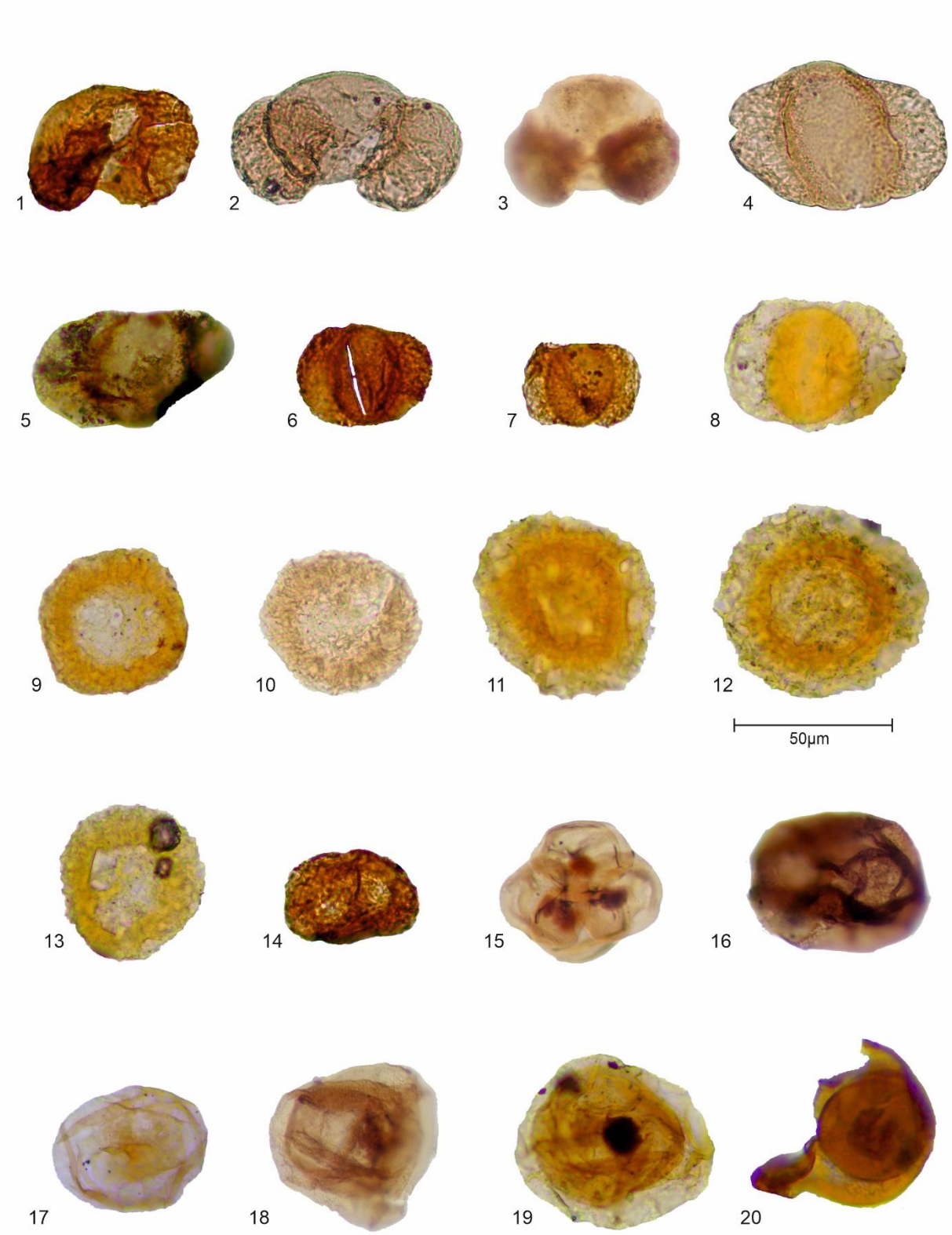

Plate V.I. (caption in the previous page)

Plate V.II. Selected pollen grains (1-10) and spores (11-21) from the Silves Group sections studied in this work. Species name is followed by the outcrop, sample, slide number and England Finder coordinates.

1. *Classopollis meyerianus* (Klaus) de Jersey, 1973, outcrop Rock Salt Mine, sample MSGvd8, slide 1F, EF T12|3.
2. *Classopollis* sp.*,* outcrop Rock Salt Mine, sample MSGvd6, slide 1, EF G34|1.
3. *Classopollis torosus* Reissinger, 1950, outcrop Rock Salt Mine, sample MSGvd6, slide 1F, EF S34|4.
4. *Cycadopites* sp., outcrop Rock Salt Mine, sample MSGvdBASE, slide 1, EF E41.
5. *Ephedripites* sp.*,* outcrop Rock Salt Mine, sample MSGvd8, slide 1F, EF N37|2.
6. *Cerebropollenites* sp.*,* outcrop Rock Salt Mine, sample MSGvd8, slide 1F, EF O29|1.
7. *Cerebropollenites* sp.*,* outcrop Rock Salt Mine, sample MSGvd7, slide 1F, EF C37|2.
8. *Cerebropollenites* sp.*,* outcrop Rock Salt Mine, sample MSGvd6, slide 1F, EF S28.
9. *Cerebropollenites* sp.*,* outcrop Rock Salt Mine, sample MSGvd6, slide 1F, EF S28.
10. *Cerebropollenites macroverrucosus* (Thiergart) Schulz, 1967*.,* outcrop Rock Salt Mine, sample MSGvd6, slide 1F, EF O20|3.
11. *Calamospora mesozoica* Couper, 1958, outcrop Rock Salt Mine, sample MSGvd1, slide 1, EF V35|1.
12. *Calamospora mesozoica* Couper, 1958, outcrop Rock Salt Mine, sample MSGvd5, slide 1F, EF L19.
13. *Calamospora tener* (Leschik 1955) Mädler, 1964, outcrop Rock Salt Mine, sample MSGvd7, slide 1F, EF R23|3.
14. *Playfordiaspora* sp.*,* outcrop Amorosa, sample Amorosa4(-20cm), slide 1, EF F30.
15. *Deltoidospora toralis* (Leschick) Lund, 1977, outcrop Rock Salt Mine, sample MSGvd7, slide 1F, EF T42.
16. *Deltoidospora* sp., outcrop Rock Salt Mine, sample MSGvd7, slide 1F, EF Z39|1.
17. *Leptolepidites argaenteaeformis* (Bolkhovitina) Morbey, 1975, outcrop Rock Salt Mine, sample MSGvd7, slide 1F, EF M27|2.
18. *Anapiculatisporites* sp., outcrop Rock Salt Mine, sample MSGvd7, slide 1F, EF N25.
19. *Carnisporites spiniger* (Leschik) Morbey, 1975, outcrop Albufeira's Diapir, sample D2, slide 3, EF M33.
20. *Kraeuselisporites* sp., outcrop Rock Salt Mine, sample MSGvd8, slide 1, EF S31.
21. *Kyrtomisporis* sp., outcrop Rock Salt Mine, sample MSGvd6, slide 1F, EF M21|3.

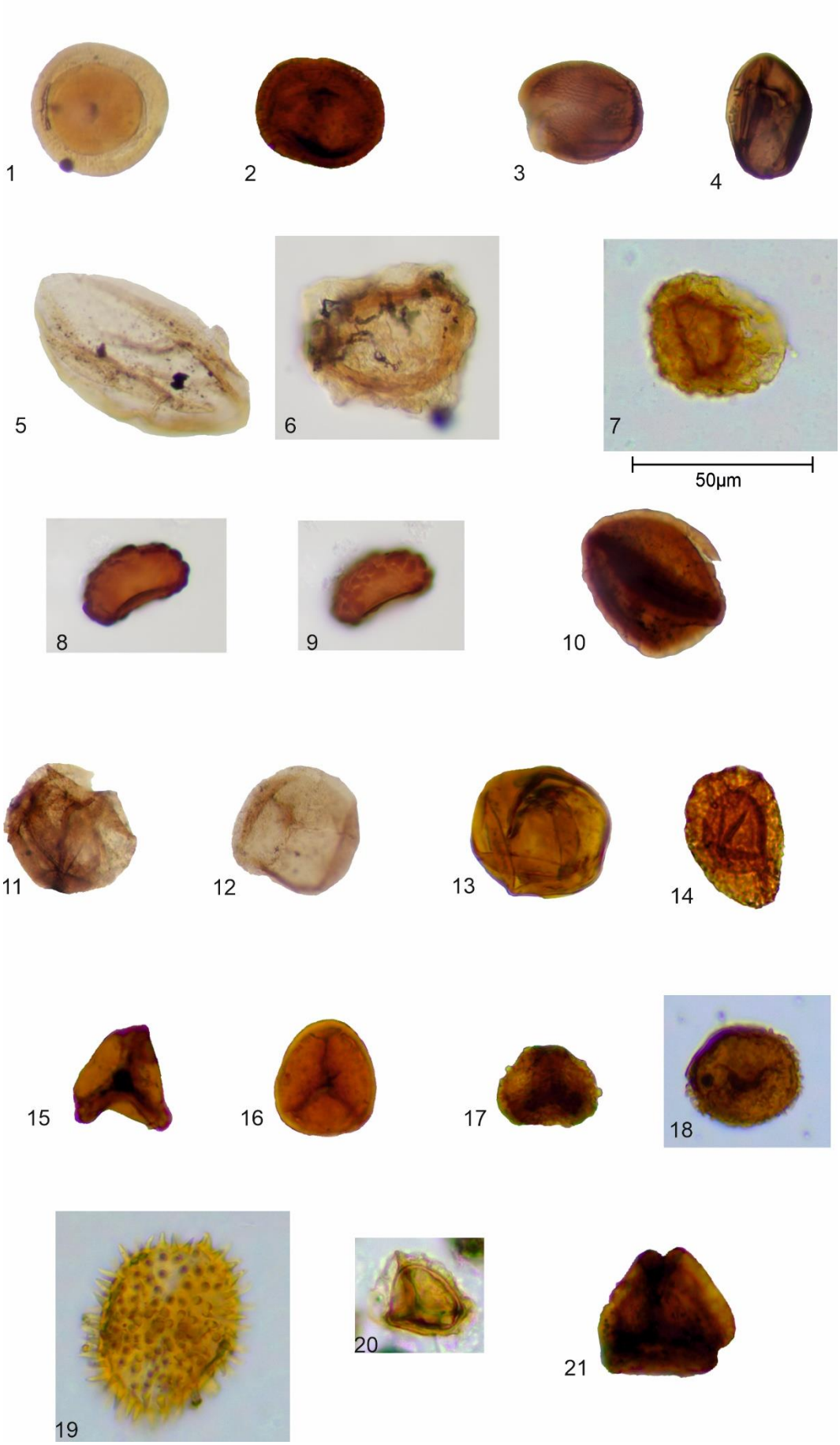

Plate V.II. (caption in the previous page)

Plate V.III. Selected aquatic material from the Silves Group sections studied in this work. Species name is followed by the outcrop, sample, slide number and England Finder coordinates.

1. *Plaesiodictyon mosellanum* ssp. *variable* Willie, 1970, outcrop Amado's Beach, sample AM15, slide 1Z, EF S38|4.
2. *Plaesiodictyon mosellanum* ssp. *variable* Willie, 1970, outcrop Amado's Beach, sample AM15, slide 1, EF N47|3.
3. *Plaesiodictyon mosellanum* ssp. *variable* Willie, 1970, outcrop Amado's Beach, sample AM15, slide 1Z, EF O37|3.
4. *Plaesiodictyon mosellanum* ssp. *variable* Willie, 1970, outcrop Amado's Beach, sample AM15, slide 1Z, EF O34.
5. *Leiosphaeridia* sp., outcrop Amado's Beach, sample AM15, slide 1Z, EF H17|4.
6. *Ovoidites* sp., outcrop Amado's Beach, sample AM15, slide 1Z, EF P27.
7. Algae sp. A, outcrop Amado's Beach, sample AM15, slide 1Z, EF K39|4.
8. Fungal Remains, outcrop Amado's Beach, sample AM15, slide 1Z, EF T38|2.
9. *Botryococcus* sp., outcrop Amado's Beach, sample AM16, slide 1Z, EF K34.
10. ?Scolecodont, outcrop Amado's Beach, sample AM15, slide 1, EF M43.
11. ?Scolecodont, outcrop Amado's Beach, sample AM15, slide 1, EF E32.
12. ?*Ourasphaira giraldae*, outcrop Rock Salt Mine, sample MSG1, slide 1, EF R28|1.
13. ?*Ourasphaira giraldae*, outcrop Rock Salt Mine, sample MSG1, slide 1, EF P21.
14. ?*Ourasphaira giraldae*, outcrop Rock Salt Mine, sample MSG1, slide 1, EF L41|3.

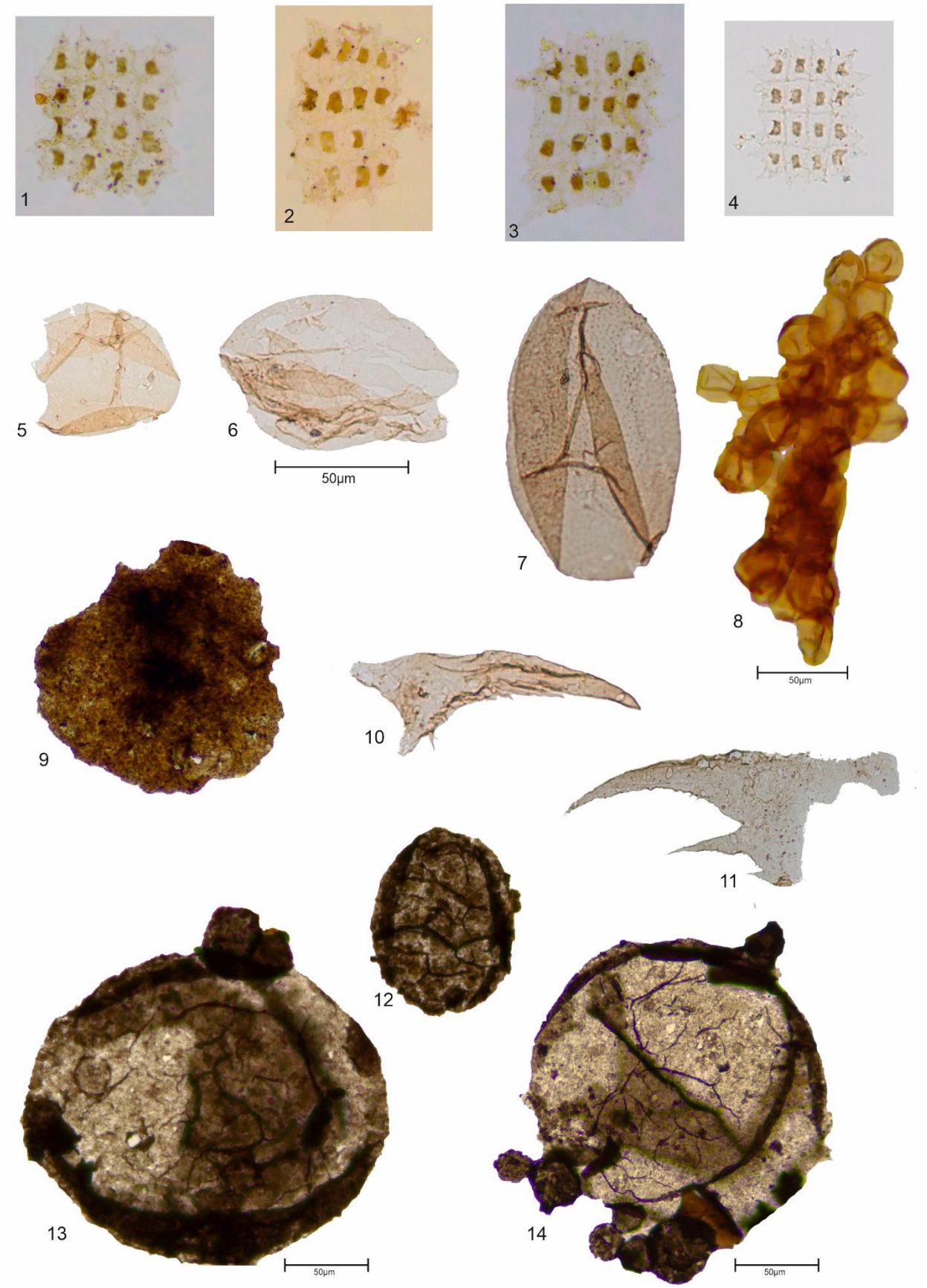

Plate V.III. (caption in the previous page)

Table V.2. List of sporomorphs and algae genera found in the Silves Group, in the Algarve Basin and their probable botanical affinities, and possible ecological remarks.

Pollen genera	Botanical affinity	Ecological Remarks
Alisporites spp.	seed fern, Corystospermales, Peltaspermales	xerophytic, upper canopy, mire, wet lowland/hinterland, inhabit upland seasonally dry habitats
Araucariacites spp.	conifer, Araucariaceae	xerophytic, upper canopy, well drained, coastal
Camerosporites spp.	Cheirolepidiaceae	xerophytic, hinterland
Cerebropollenites spp.	conifer, Taxodiaceae	upper canopy, well drained
Classopollis spp.	conifer, Cheirolepidiaceae	xerophytic, upper canopy, well drained, coastal, lowland, drier, warmer
Cycadopites spp.	gymnosperm, Cycadophyta, Ginkgoales, Peltaspermales	hygrophytic, dry lowland, warmer
Ellipsovelatisporites spp.	conifer	xerophytic, (?)hinterland/upland
Enzolasporites spp.	conifer, Voltziales, Majonicaceae, Glyptolepis	xerophytic, (?)hinterland/upland
Ephedripites spp.	gymnosperm, Gnetales, Ephredraceae	Unknown
Granuloperculatipollis spp.	conifer, Cheirolepidiaceae	upper canopy, well drained
Lagenella spp.	Unknown	hygrophytic, river, lowland
Microcachrydiites spp.	Podocarpaceae	xerophytic, upland, hinterland
Paracirculina spp.	Unknown	Unknown
Patinasporites spp.	conifer, Voltziales, Majonicaceae	xerophytic, (?)dryland, upland, dry lowland
Perinopollenites spp.	conifer, Cupressaceae/Taxodiaceae	hygrophytic, upper canopy, mire, river
Samaropollenites spp.	conifer	Unknown
Triadispora spp.	conifer, Voltziaceae	xerophytic, upland, hinterland
Vallasporites spp.	conifer, Voltziales, Majonicaceae	xerophytic, hinterland, dry lowland, upland
Spore genera	**Botanical affinity**	**Ecological Remarks**
Anapiculatisporites spp.	lycopsids, fern, moss?	hygrophytic, ground cover, mire, coastal, river/lowland, wet lowland
Calamospora spp.	horsetails, Sphenophyta, Equisetopsids	hygrophytic, river, lowland, wetter, warmer, acquire wet habitat in sub-tropical and temperate regions
Carnisporites spp.	lycophyta, Filicales	hygrophytic, river, wet lowland
Convolutispora sp.	Schizaeales	Unknown
Deltoidospora spp.	pteridophyta, fern, Filicales - Dicksoniaceae, Cyatheaceae, Dipteridaceae, Matoniaceae	hygrophytic, understory, mire, drier patches, dry lowland
Kraeuselisporites spp.	Lycopodiophyta; Lycopsida; Lycopodiales	hygrophytic, ground cover, mire, coastal, river
Kyrtomisporis spp.	pteridophyta, fern, Dipteridaceae	hygropghytic, river, (?)dry lowland
Leptolepidites spp.	Filicopsida; Filicales; Pteridaceae	(?)wet lowland
Playfordiaspora spp.	lycopsids	stress tolerant opportunistc plants which grow near water bodies
Verrucosisporites spp.	pteridophyta, Ferns, Marattiales, Filicales especially Osmundaceae	hygrophytic, river, wet lowland, acquire wet habitat in sub-tropical and temperate regions
Algae genera	**Botanical affinity**	**Ecological Remarks**
Botryococcus spp.	chlorococcale green algae, Dictyosphaeriaceae	open water, brackish/freshwater
Leiosphaeridia spp.	Prasinophyceae	marine, swamp, lake/pond
Ovoidites spp.	Zygnemataceae, Spirogyra	shallow, stagnant, oxygen-rich fresh waters, lake margins
Plaesiodictyon mosellanum spp.	chlorococcale green algae	brackish/freshwater

4.2. Palaeoclimatology and paleoenvironmental inferences

A correlation between palynomorphs and the ecological affinity of their parent plants has been attempted, to provide data for palaeoclimatological and palaeoenvironmental reconstructions. In Table V.2, a list of selected Triassic–Jurassic spore-pollen genera, their probable parent plant affinities, and possible ecological and climatological preferences is given (Bonis and Kürschner, 2012; Césari and Colombi, 2016; Paterson *et al*., 2016; Lindström *et al*. 2017; Li *et al*., 2018; Mishra *et al*., 2018; Baranyi *et al*., 2019; Tverdokhlebov *et al*., 2020). Based on the water needs of the different plants and/or their adaptability to dry environments, the sporomorphs were divided into two groups, those related to hygrophytic, plants that preferentially thrive in wet environments, and those pertaining to xerophytic plants adapted for growth under dry conditions (Bonis and Kürschner, 2012; Césari and Colombi, 2016; Paterson *et al*., 2016; Lindström *et al*. 2017; Li *et al*., 2018; Mishra *et al*., 2018; Baranyi *et al*., 2019; Tverdokhlebov *et al*., 2020).

The "Unknown Affinity group" includes species for which there is not enough data available to assign them a botanical affinity.

Table V.3. Dataset (%) for the stratigraphical distribution of the palynological assemblage based on their probable botanical affinities. Light grey bands represent no results. Chrono. – Chronostratigraphy. Litho. – Lithostratigraphy.

Chrono.		Litho.	Sections	Samples	% Hygrophytic	% Xerophytic	% Unknown Affinity	% Algae	% Reworked Algae
Lower Jurassic	Rhaetian-Hettangian	Evaporitic Complex	Albufeira's Diapir	D4	1,2	77,2		21,6	
				D2	6,4	90,8		2,8	
	Hettangian			TOPOBASE	0,6	99,4			
			Salt Mine	8	2,8	96,8	0,4		
				7	3	96,6	0,4		
				6	3,6	95,7	0,8		
Upper Triassic	Rhaetian	Silves Marl-Carbonate	Loulé Rock	5		78,6			21,4
				4		75,5			24,5
				3					
				2		0,6			99,4
				1	0,4	93,2			6,4
				BASE	5,3	85,9	3,5		5,3
	Upper Carnian		Amado Beach	16	2,6	27,8	69,7		
				15	0,8	7,9	11,3	80	
		Silves Sandstones	Amorosa	4(-20cm)	8,6	16	75,3		

Based on a quantitative analysis was established that the xerophytic plants are the most representative of all the sections (Fig. V.5, Table V.3). At the top of the Silves Sandstones, most of the palynological content (around 75%) does not allow us to determine an environmental preference, due to the unknown botanical affinity or ecological characteristics of these plants." (Fig. V.5, Table V.3). However, out the approximately 25% of the palynological material for which we

were able to associate an environmental preference, 16% consists of xerophytic plants (e.g., *Ellipsovelatisporites* sp., *Patinasporites densus, Triadispora* sp., and *Vallasporites ignacii*), while 8,6% consists of hygrophytic plants (e.g., *Convolutispora* sp., *Kraeuselisporites reissingeri, Leptolepidites argaenteaeformis*, and *Verrucosisporites* sp.). At the base of the Silves Marl-Carbonate Evaporitic Complex, there is an increase in xerophytic plants (e.g., *Alisporites* sp., *Camerosporites secatus, Ellipsovelatisporites* sp., *Enzonalasporites ignacii*, *Microcachrydiites* spp., *Patinasporites densus, Triadispora* sp. and *Vallasporites ignacii*), accounting for up to 27,8%, and a decrease in hygrophytic plants (e.g., *Calamospora* sp., *Kraeuselisporites reissingeri, Lagenella martinii* and *Verrucosisporites* sp.,), with a maximum of 2,6% (Fig. V.5, Table V.3). Approaching the top of the Silves Marl-Carbonate Evaporitic Complex, at the Triassic-Jurassic transition, there is a significant increase in xerophytic plants (*Alisporites* sp., *Araucariacites* sp., *Classopollis meyerianus, Classopollis* sp. and *Triadispora* sp.) ranging from 75% to 93%, along with almost no presence of hygrophytic type-plants (*Calamospora mesozoica* and *Playfordiaspora* sp.) at the top of Rhaetian (Fig. V.5, Table V.3). At the base of the Hettangian, the palynological content is dominated by xerophytic plants (*Alisporites diaphanus, Araucariacites australis, Araucariacites* sp., *Classopollis meyerianus, Classopollis torosus*, and *Classopollis* sp.) accounting for 95% to 99% of the assemblage, with the hygrophytics plants (*Cycadopites* sp., *Perinopollenites elatoides, Anapiculatisporites* sp., *Calamospora mesozoica, Deltoidospora toralis, Deltoidospora* sp., *Kraeuselisporites reissingeri* and *Kyrtomisporis* sp.) consistently present but in very low percentages, approximately 2.5% (Fig. V.5, Table V.3). This increase in xerophytic plants towards the top of the section aligns with the sedimentary facies observed at the top of the Silves Group, which consist of sulphate evaporites deposited in a sabkha environment. This is primarily observed through the presence of conifer sporomorphs, such as *Ellipsovelatisporites* sp., *Enzonalasporites vigens, Microcachrydiites* spp., *Patinasporites densus, Triadispora* sp., and *Vallasporites ignacii* and with *Classopollis* group and *Araucariacites* sp. which become prominent upwards in the upper Rhaetian-lower Jurassic strata.

The *Classopollis* group is produced by the *Cheirolepidiaceae*, one of the most prominent and diverse families of Mesozoic conifers. This extinct conifer family, believed to be related to the *Cupressaceae* or *Araucariaceae*, occupied a wide range of ecological niches and displayed diverse growth habits, indicating warm conditions (Abbink, 1998; Buratti and Cirilli, 2007; Kürschner *et al*., 2013; Lindström, 2016). This data suggests a shift towards drier conditions during the upper Triassic to lower Jurassic, which aligns well with the lithofacies of this interval of the Silves Marl-Carbonate Evaporitic Complex, referred to as a coastal sabkha depositional setting. The presence of malformed sporomorphs in the upper Carnian and at the base of Hettangian can provide information about climate conditions in terms of atmospheric pollution, volcanic mercury (associated with CAMP volcanism), and/or UVB radiation (Visscher, *et al*., 2004; Foster and Afonin, 2005; Whiteside *et al*., 2007, 2010; Cirilli *et al*., 2009; Filipiak and Racki, 2010; Kürschner *et al*., 2013; Hochuli *et al*., 2017; Lindström *et al*., 2019).

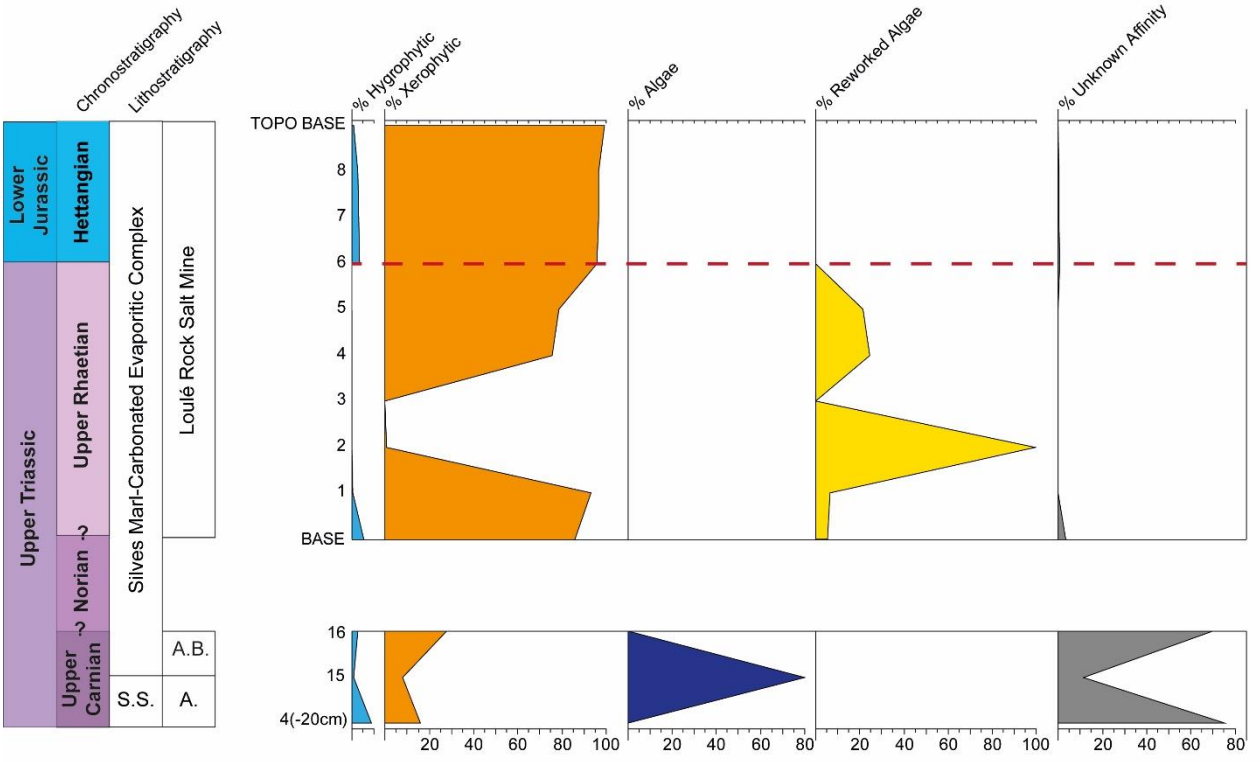

Figure V.5. Stratigraphic distribution of the palynological assemblages based on their probable botanical affinities. S.S. – Silves Sandstones. A.B. – Amado Beach.

The algae group has the lowest representation along the sections, making their first appearance at the base of the Silves Marl-Carbonate Evaporitic Complex, in the upper Carnian, constituting 80% of the palynological assemblage (*Botryococcus* sp., *Leiosphaeridia* sp., *Ovoidites* sp., *Plaesiodictyon mosellanum* ssp. *bullatum*, *Plaesiodictyon mosellanum* ssp. *variable*, *Plaesiodictyon* sp.) (Fig. V.5, Table V.3).

At the top of the Silves Marl-Carbonate Evaporitic Complex, reworked algae from the Neo-Proterozoic become prevalent in the assemblage, from 5% to a maximum of 99%; being the only algae material present at the top of this unit (Fig. V.5, Table V.3). Reworked material is palynological material eroded, transported, and redeposited into sediments of a stratigraphically different age. At the beginning of the Hettangian, the algae disappear. The presence and the rapid increase of freshwater/brackish algae like *Botryococcus* sp., *Leiosphaeridia* sp., *Ovoidites* sp., *Plaesiodictyon mosellanum* ssp. *bullatum* and *Plaesiodictyon mosellanum* ssp. *variable* at the base of the Silves Marl-Carbonate Evaporitic Complex indicates a seawater influence and the establishment of a coastal environment during the upper Carnian. This suggests that during the deposition of the Silves Marl-Carbonate Evaporitic Complex, there was a transition from a continental environment, in the lower Carnian, represented by the underlying siliciclastic red beds of the Silves Sandstones to a coastal-lacustrine environment, in the upper Carnian. During the upper Rhaetian, the presence of reworked Neo-Proterozoic algae (e.g., *Ourasphaira giraldae*) in the Silves Marl-Carbonate Evaporitic Complex, suggests a significant increase in the rate of erosion in the continental area, leading to the transportation of older material into the sedimentary environments. The absence of Norian to lower Rhaetian terranes in the studied area aligns with the hypothesis of a regional relative sea-level fall and a regressive episode, exposing extensive continental areas to erosion.

It is important to note that this interpretation is a working hypothesis and requires further confirmation through additional sedimentological and stratigraphic data.

4.3. Palaeophytogeographic implications

The microfloral assemblage documented in the study area, spanning from the upper Carnian to the Triassic-Jurassic boundary, provides new insights into understanding microfloristic provincialism and palaeophytogeographic implications during this geological period. The palynological assemblage from the upper Carnian of the Silves Group includes taxa such as *Camerosporites secatus, Enzonalasporites vigens, Paracirculina quadruplicis, Paracirculina* sp., *Patinasporites densus, Samaropollenites speciosus* and *Vallasporites ignacii,* which are typical of the Onslow microflora. The occurrence of bisaccate pollens is rare; however, the presence of *Samaropollenites speciosus*, a crucial taxon for palaeofloristic reconstructions, along with other typical southern elements, suggest an Onslow microflora affinity for several localities of the northern hemisphere (Visscher and Krystyn, 1978; Besems, 1982; Fisher and Dunay, 1984; Adloff *et al*., 1985; Cirilli and Eshet, 1991; Litwin *et al*., 1991; Cirilli and Montanari, 1994; Gòczàn and Oravecz-Scheffer, 1996; Broglio Loriga *et al*., 1999; Roghi, 2004; Buratti and Cirilli, 2007; Traverse, 2008; Cirilli, 2010). This microfloral province, comprising a mixture of Gondwana and European taxa, extended across western Europe and northwestern Australia, and it characterized continental margins under warm temperate climate, likely influenced by a monsoonal regime (Dolby and Balme, 1976; Cirilli and Eshet, 1991; Foster *et al*., 1994; Buratti and Cirilli, 2007; Cirilli, 2010; Césari and Colombi, 2013, 2016; Cirilli *et al*., 2015, 2018).

The current microfloral assemblage, in conjunction with that documented in the basal Silves Sandstones of the Silves Group (Vilas-Boas *et al*., 2022), provides further evidence of the extension of the Onslow Microflora into the Western Tethys.

In the uppermost Triassic, the emergence and spread of the *Cheirolepidiaceae* (Circumpolles producers) represent another significant floral event that began during the Norian, triggering a gradual decrease in Upper Triassic microfloral provincialism and subsequently leading to the global dispersal of a more homogenous Lower Jurassic flora (Cirilli, 2010). The occurrence of the *Classopollis* (= Circumpolles) group, among other Gondwanan taxa, in the Upper

Triassic - Lower Jurassic assemblages of Europe is attributed to the migration of the *Cheirolepidiaceae* parent plants from the southern areas of the Tethyan region to higher latitudes in the Late Triassic-Early Jurassic, during a warm climatic phase (Cirilli, 2010; Cirilli *et al*., 2015, 2018). It is likely that the *Cheirolepidiaceae* expanded through coastal migration routes formed by the Carnian-Norian plate rearrangement (Martini *et al*., 1997; 2004; Buratti and Cirilli, 2007; Cirilli, 2010). The presence of this group in the Algarve Basin and the Lusitanian Basin (Vilas-Boas *et al*., 2021, 2022) confirms its global distribution, indicating a gradual decline in microfloral provincialism leading into the Lower Jurassic.

5. Conclusions

The palynological study of the Silves Group in the Algarve Basin leads to the following conclusions:

-For the first time, it is possible to assign an age to the entire stratigraphic succession of the Silves Group, from the lower Carnian to the lower Hettangian (Triassic-Jurassic boundary included) based on palynostratigraphy. Previous research had dated the base of Silves Sandstones as lower Carnian (Vilas-Boas *et al*., 2022). In this study, the upper part of the Silves Sandstones is dated as upper Carnian. The basal part of the Silves Marl-Carbonate Evaporitic Complex is dated as upper Carnian, and the upper part of this unit is dated as upper Rhaetian – lower Hettangian.

- In the upper Carnian, at the base of the Silves Marl-Carbonate Evaporitic Complex, the appearance and rapid increase of algal spores (e.g. *Plaesiodictyon mosellanum* ssp. *variable*, *Plaesiodictyon mosellanum* ssp. *bullatum*, *Botryococcus* spp. and *Ovoidites* sp.), which adapted well to brackish water environment, support the lithological evidence of a transition from a continental fluvial setting (Silves Sandstones) to a coastal environment with swamps, ponds and lagoons (base of Silves Marl-Carbonate Evaporitic Complex);

- The quantitative analysis of xerophytic vs. hygrophytic sporomorph categories, reveals a consistent increase of plants with xerophytic affinities upwards in the Silves Group, indicating a shift toward warmer and drier conditions from the upper Carnian to the lower Hettangian. This trend aligns with lithofacies evidence, which suggests an evolution from a coastal pond/lagoon environment (base of Silves Marl-Carbonate Evaporitic Complex) to a sabkha depositional setting (top of Silves Marl-Carbonate Evaporitic Complex).

- The presence of malformed sporomorphs in the upper Carnian and lower Hettangian could indicate environmental changes, potentially in response to external environmental stressors such as atmospheric pollution, volcanic mercury, and/or UVB radiation.

-The presence of *Ourasphaira giraldae* (reworked Neo-Proterozoic algae) at the top of the Silves Marl-Carbonate Complex (upper Rhaetian) suggests increased erosion during that time, leading to the transport of older material. The absence of Norian and lower Rhaetian terranes in the studied area, supports the hypothesis of a brief regressive episode, that exposed those areas to erosion.

-The lower Carnian to upper Carnian interval in the Silves Group exhibits a microflora that correlates with the Onslow Microflora, distributed along the continental margins of the southwestern Tethys. This correlation provides new insights into the microfloral distribution during this period and offers information about the climate in the Algarve Basin during Carnian.

-In the uppermost Triassic, another significant microfloral event is recorded, marked by the increased diffusion of the *Cheirolepidiaceae* into the Lower Jurassic. This event indicates the migration of the Circumpolles producers to higher latitudes within the context of plate rearrangement.

CHAPTER VI

Organic Maturation

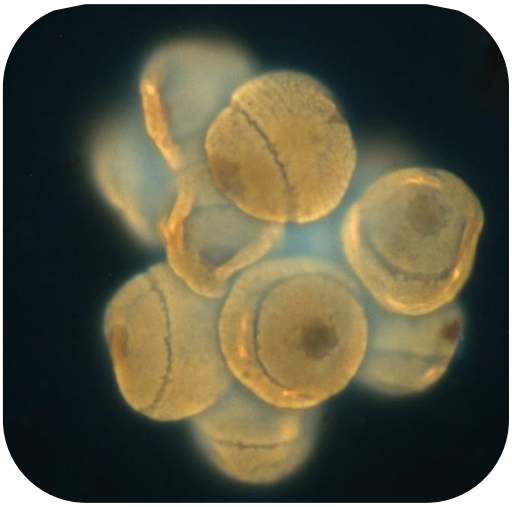

Chapter VI cover:

Cluster of *Classopollis meyerianus* (Klaus) de Jersey with fluorescence, Pereiros Formation, lower Hettangian, Lower Jurassic, sample LAM6, Lusitanian Basin

Chapter VI. Organic Maturation

1. Organic Maturation techniques

Selected samples used in paper two from the Lusitanian Basin entitled "Palynology and palynofacies studies in the lowermost Jurassic of the Lusitanian Basin (Pereiros Formation of the Silves Group), Portugal: evidence of the first transgressive episode", were studied for organic maturation (Chapter III; Table VI.1). Three independent microscope techniques assessed the organic maturation levels: vitrinite reflectance, spore colour, and spore UV fluorescence.

1.1. Vitrinite Reflectance

The organic residues obtained for the palynology and palynofacies studies were also used for vitrinite reflectance. The same microscope slides used in palynology and palynofacies were used for spore colour and spore UV fluorescence. The organic residues used for vitrinite reflectance measurements were mounted and polished on microscope slides using a technique derived from Hillier and Marshall (1988). Since the mounting method used for vitrinite reflectance provides non-oriented vitrinite particles, mean random vitrinite reflectance (%Ro) was the vitrinite reflectance (VR) parameter selected for the maturation assessment of these samples (Fig. VI.1).

For vitrinite identification and measurement, several criteria were considered following the guidelines recommended by the ASTM D7708-14 (2014), ISO 7404-5 (2009), and the International Committee for Coal and Organic Petrology (1998). VR measurements were made at the University of the Algarve using an Olympus BX 51 microscope with a 50x oil-immersion objective lens and a digital camera that captures black-and-white (8-bit) digital photographs images. The graphical program VITRINITE, part of the Mirone Suite (Luis, 2007) that calibrates the scale of 256 grey levels with standards of known reflectivity, was used to evaluate the black-and-white of vitrinite particles (Fernandes *et al*., 2013). The standards employed in this investigation have reflectance values of 0.428%,

0.595%, 0.897%, 1.314%, 1.715%, 3.15%, and 5.37%. At 20°C room temperature, VR was measured in immersion oil with a refractive index of 1.518 and incident light with a wavelength of 546 nm. The arithmetic mean and standard deviation of 100 random reflectance measurements across the slides were computed when possible (Table VI.1). The arithmetic mean was the %Ro for the sample. Paleotemperatures were calculated using Barker's (1988) empirical equation T(°C)=104ln(%Ro)+148, where T(°C) is the highest palaeotemperature that the sedimentary rock was subjected to during burial. Table VI.1 displays the palaeotemperatures determined by this equation.

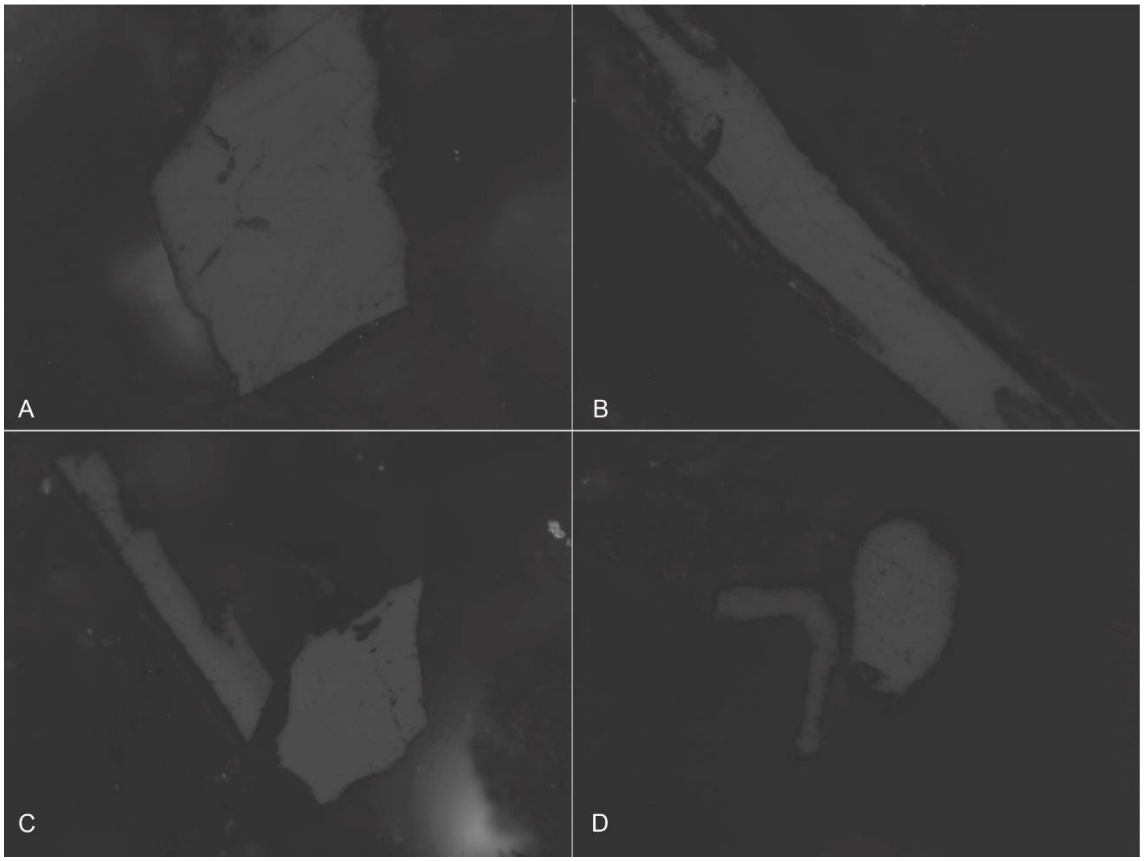

Figure VI.1. Example of vitrinite particles used in the vitrinite reflectance analysis. A – sample LAMAS 10/11 with RO% = 1.04; B – samples LAMAS 14INT with RO% = 0.9; C – sample LAM 3 with RO% = 0.8; D – sample LAM 6 with RO% = 0.8.

1.2. Spore fluorescence and spore colour

A portion of the organic residue extracted from the samples was also mounted on slides to study the spore UV fluorescence and spore colour. Qualitative spore fluorescence and spore colour are two optical parameters of

thermal maturity of organic maturation, helpful in evaluating maturation levels of low-rank rocks until the end of the oil window (1.35–1.5%Ro) (Van Gijzel, 1975, 1979; McPhilemy, 1988; Suárez- Ruiz *et al*., 2012). The correlation of those parameters with the quantitative VR method provides additional support for the thermal maturity of the rocks.

Under UV light, spores' exine fluorescence. The fluorescence colours gradually vary with increasing organic maturation, from shorter to longer wavelengths (redshift), i.e., from blue and green to yellow, orange, and red. Sporinite exhibits the most consistent changes in fluorescence colour spectrum and intensity with rising organic maturation of all the sub-macerals in the liptinite group. It changes colour under fluorescence UV excitation from green to yellow to orange to red as it matures to the top of the oil window; at this point, it stops fluorescing.

The fading effect is a phenomenon that is frequently observed in fluorescent palynomorphs (Van Gijzel, 1979). This effect is observed in fluorescing palynomorphs that underwent photochemical alteration after extended exposure (30 min–2 h or more) to UV light. The fluorescence intensity may rise or decrease throughout this prolonged exposure; if it increases, the fading is considered positive; if it falls, it is negative. In other words, the emitted fluorescence spectrum might shift in two directions: towards higher wavelengths (red band) or shorter wavelengths (green band). The first scenario is referred to as positive fading, and the second as negative fading.

These analyses were undertaken at the University of the Algarve using an Olympus BX51 microscope with a metal halide fluorescence lamp unit, XCite Series 120Q, and a violet and Blue þ12 filter block that generates a 390–490 nm wavelength band. The system was given five minutes to stabilise before examining the sample's fluorescence palynomorphs. Their fluorescence colours were noted after 5 minutes of stimulation on the appropriate spore species. The same spores were exposed for 30 minutes to observe any fading effects. Blue (B), green (G), yellow (Y), dark yellow (DY), orange (O), dark orange (DO), and red (R) were the terms used to denote fluorescent colours.

Palynologists have long advised using the spore exine colour to estimate sedimentary rocks' thermal maturity because they saw that as burial depth increased, the colour of the spores gradually and irreversibly changed from light to dark (Correia, 1971; Staplin, 1982). The Staplin Thermal Alteration Index (TAI) scale's colour indices, which run from 1 to 5, show how the colour of spores changes over time from light yellow to dark yellow, golden brown to brown, and dark brown to black. The Phillips Petroleum Colour Standard version no. 2 (Pearson, 1984), a modification of Staplin's original TAI chart that offers more shades for the same colour index, was used in this work to record spore colours. The dominant and lightest spore colour observed was used to determine the sample's spore colour index, which was then compared to the Phillips Petroleum Colour Standard chart. The sample was then given the index number from this chart. For each sample, the vitrinite reflectance values and the results of the TAI determinations are present (Table VI.1 and Fig. VI.2).

Not all spore species are suitable for TAI determinations, and avoiding spores with thin walls or delicate ornamentation is recommended. Furthermore, spores with thick walls and heavy ornamentation were also avoided. The species best suited for TAI determinations were acamerate, azonate spores with a smooth exine of medium thickness, such as *Cyathidites* spp., which occur throughout the Hettangian sections of the Lusitanian Basin (Vilas-Boas *et al*., 2021). Due to its abundance throughout the Lusitanian Basin's succession, Classopollis spp. pollen grains were used to measure TAI in samples where *Cyathidites* spp spores were absent.

As discussed, spore fluorescence and colour are qualitative indicators of organic maturation. It is less objective than VR since the operator's past experiences affect how they view the fluorescence colours and the colours of the palynomorph walls. There needs to be more widely accepted criteria for organic maturation, like VR, which is another drawback of these two methods. Additionally, it has been reported that the acid treatment (HCl and HF maceration) used to obtain kerogen concentrates modifies the fluorescence spectra of liptinites, pushing it to higher wavelengths (red-shift) when compared to the fluorescence spectra of whole rock samples (Mendonça Filho *et al*., 2010).

Despite these drawbacks, spore fluorescence, colour, and VR are vital for organic maturation assessment, especially for low and medium-rank rocks.

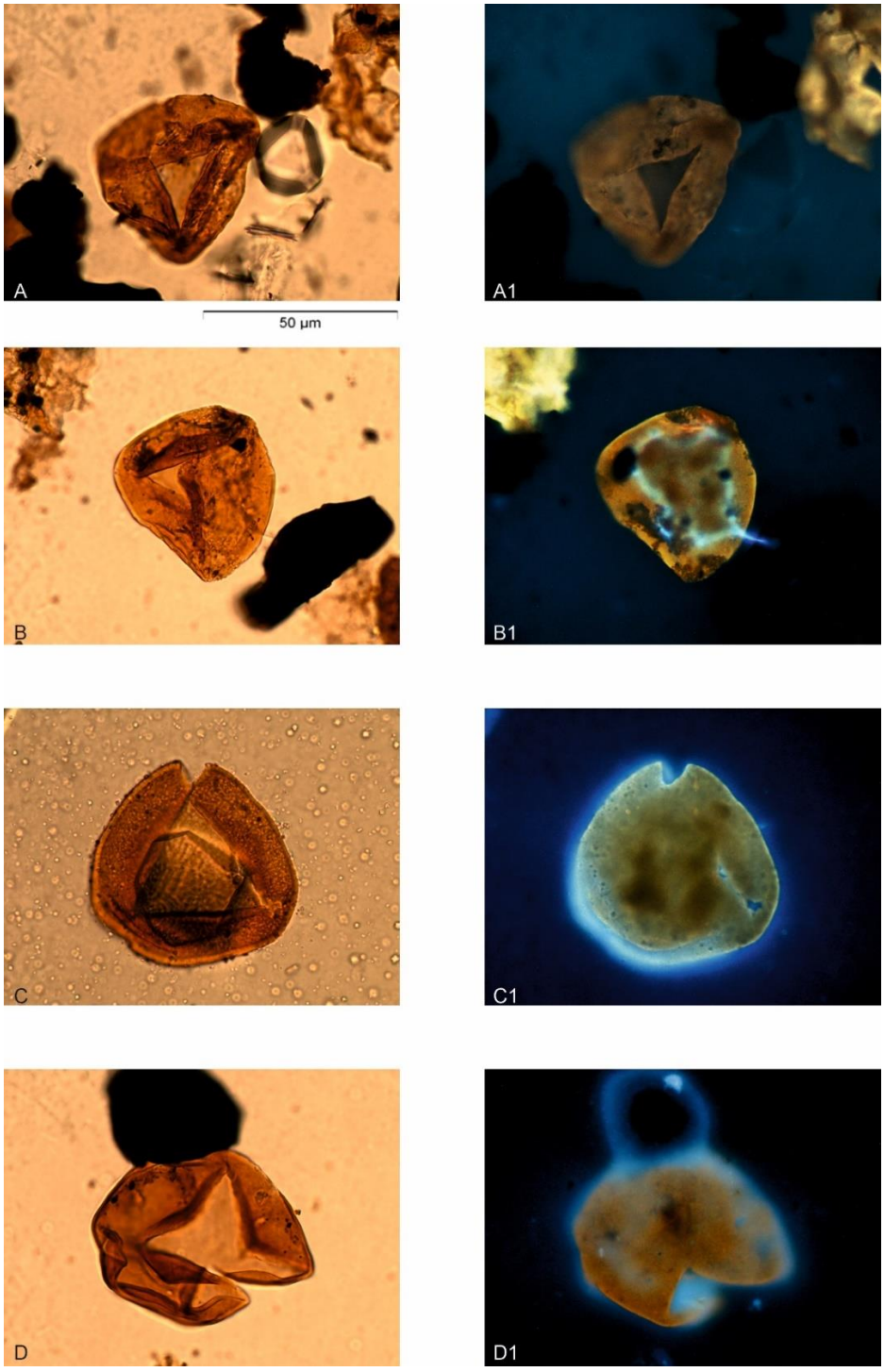

Figure VI.2. Differences observed in transmitted and fluorescent light between the spore *Cyathidites* sp. in the samples studied for organic maturation in the Algarve Basin. **A, A1** – Spore *Cyathidites* sp. in the sample LAMAS 10/11 showing orange fluorescence colour; **B, B1** – Spore *Cyathidites* sp. in the sample LAMAS 14INT showing orange fluorescence colour; **C, C1** - Spore *Cyathidites* sp. in the sample LAM 3 showing dark yellow fluorescence colour; **D, D1** - Spore *Cyathidites* sp. in the sample LAM 3 showing dark yellow fluorescence colour.

2. Results and Discussion on the Organic Maturation

Table VI.1. Organic maturation results and palaeotemperatures (°C) were calculated using the method described by Barker (1988). Ro(%) - vitrinite reflectance values, SD - standard deviation, n – number of vitrinite particles measured, Fluo. - spore fluorescence colours (DY – dark yellow, O - orange), spore colour TAI - Thermal Alteration Index.

	Sample	*Ro(%)*	SD	*n*	Fluo.	TAI	Palaeotemp. (ºC)
LAMAS II	LAM 6	0,82	0,09	45	DY	2+/3-	127,4
	LAM 3	0,9	0,08	51	DY	2/2+	137
LAMAS I	LAMAS 14INT	0,87	0,11	100	O	3+	133,5
	LAMAS 10/11	1,11	0,15	66	O	3+/4-	158,9

The VR values measured an increase with depth in these outcrops, ranging from 0.82 %Ro at the top (Lamas II) to 1.11 %Ro at the bottom (Lamas I) indicating a position in the oil-window (Figs. VI.3 and VI.4; Table VI.1). These values measured for the Lamas I and II outcrops indicate that oil-window peak conditions were attained during the subsidence phase.

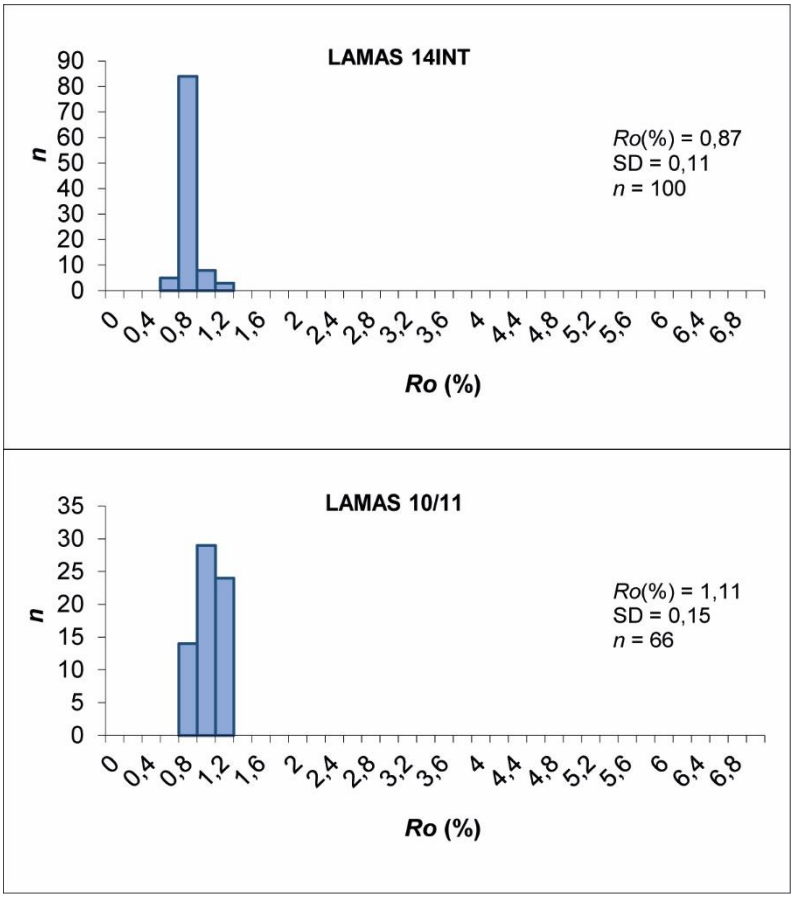

Figure VI.3. Histogram of the vitrinite study of samples from the Lamas I section.

Spore fluorescence and colour were also observed in the samples analysed and generally agreed well with the VR results. Spore fluorescence colours change intensity from dark yellow at the Lamas II to orange at the Lamas I. TAI values also change from 2+/3- to 3+/4- with increasing depth indicating that Lamas II has a thermal maturity at the onset of the oil-window and Lamas I is close to the thermal maturity of dry gas.

Peak burial temperatures between 127 – 159ºC were calculated for the two sections. Assuming an average palaeogeothermal gradient between 30 – 50ºC/km as typical of continental rift basins (Allen and Allen, 2005), a sedimentary succession with a minimum of 2.5 km and a maximum of 5.2 km was necessary to attain the VR measured. This also indicates considerable uplift and denudation after peak burial temperatures were attained for the samples studied. With the limited data, the age of the organic maturation, when peak burial temperatures were reached, and uplift and denudation started, cannot be constrained with confidence.

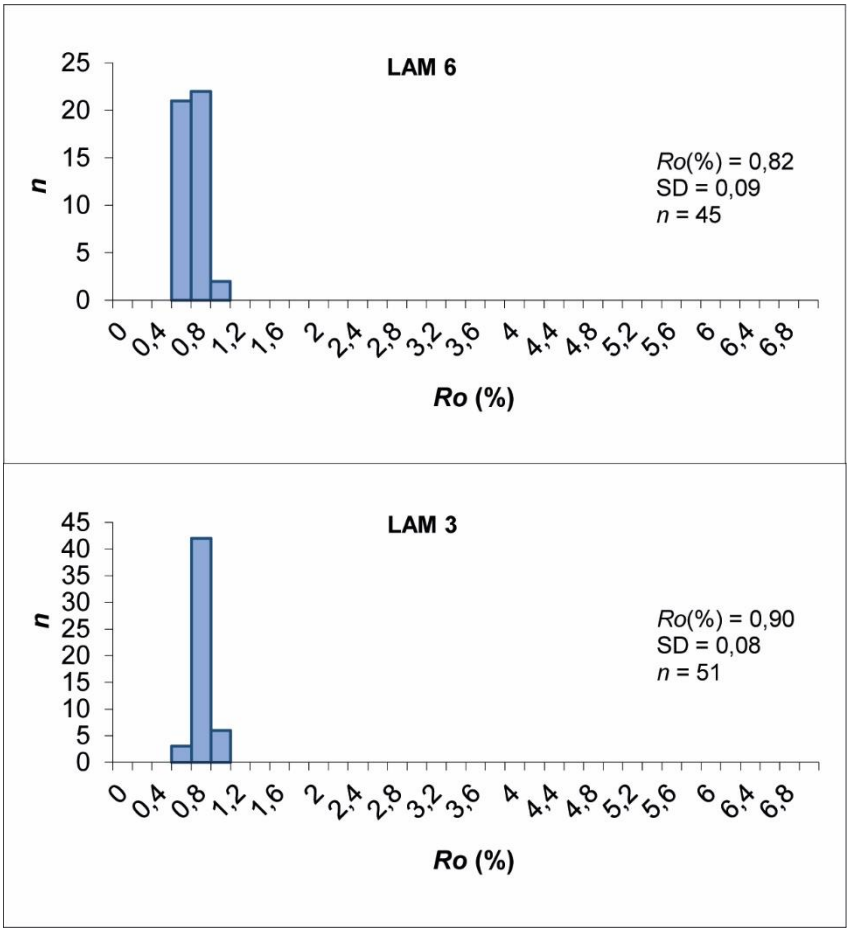

Figure VI.4. Histogram of the vitrinite study of samples from the Lamas II section.

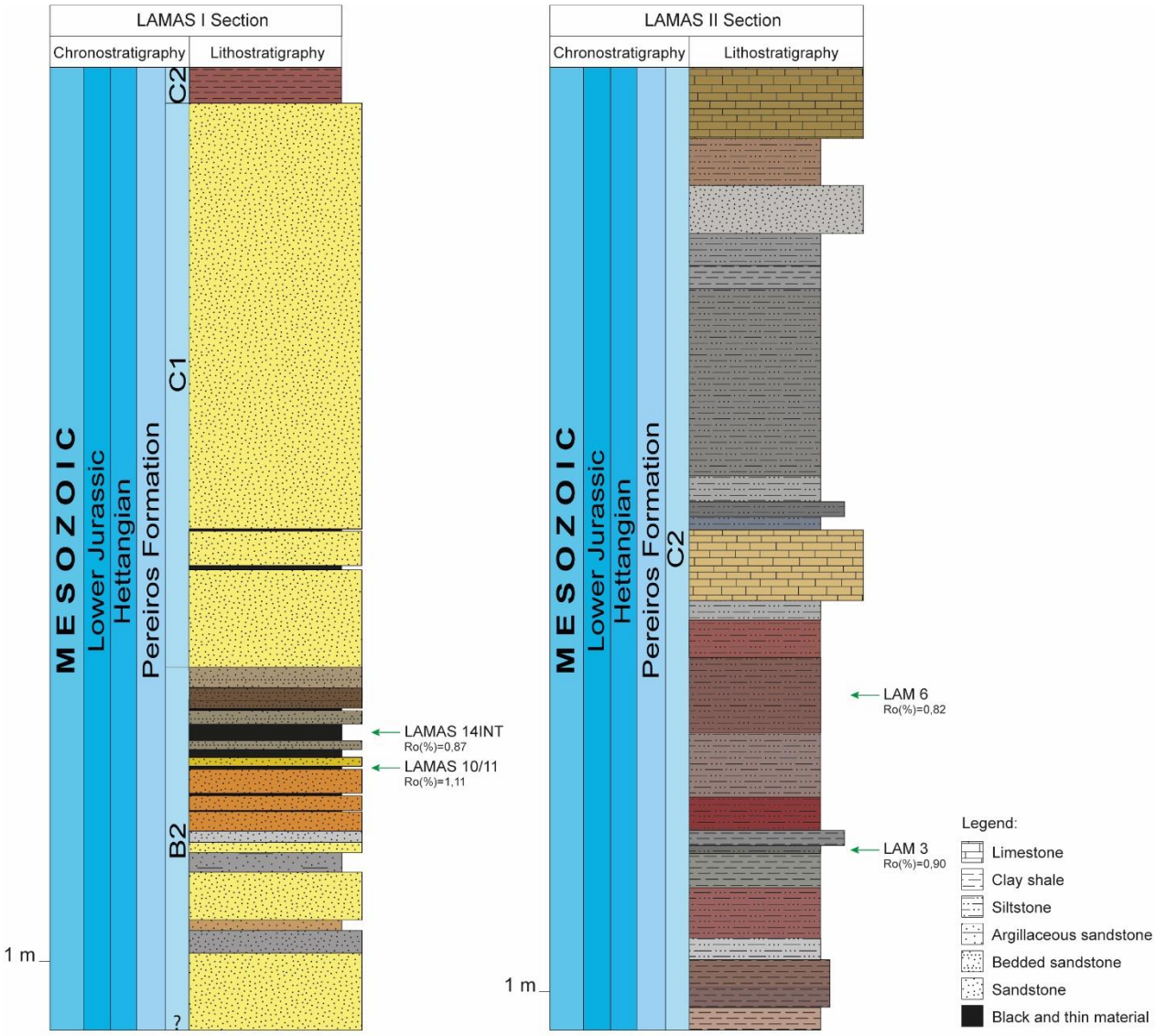

Figure VI.5. Logs from the sections Lamas I and Lamas II with the location of the samples used for the vitrinite studies. Values obtained from the vitrinite studies per sample are presented.

This data allows us to conclude that the maturation increases with increasing depth in the sequence; this is backed up by the palynological age that shows that the LAMAS I section is older than the LAMAS II section (Fig.VI.5).

CHAPTER VII

Final Remarks

Chapter VII. Final Remarks

1. General conclusions

This PhD represents a comprehensive contribution to the stratigraphic palynology of the Triassic-Jurassic in Portugal. In this study, 498 samples were studied in detail, of which 65 proved productive. The Lower Jurassic samples were generally more productive than the Upper Triassic samples. In the Lusitanian Basin, 41 samples were productive, giving a general productivity of about 33,6% (Table VI.1). This lower percentage is related to the high number of barren samples collected near the Triassic-Jurassic boundary. In the Algarve Basin, 24 samples were productive, giving a general productivity of about 9,4% (Table VI.2). This lower percentage is related to the studied facies of the Silves Group in the Algarve Basin, not being so favourable for palynological studies. Unfortunately, all the samples collected from the boreholes were barren (Table VI.3).

Table VII.1. Summary of the number of studied samples in each section of the Lusitanian Basin and their productivity in percentage. The totals are also presented.

	Locality	Studied Section	Nº Collected Samples	Nº Productive Samples	Productivity %
LUSITANIAN BASIN	Coimbra	Alto de São João	3	2	66,7
	Coimbra	Carvalhais	2	2	100
	Coimbra	Castelo Viegas I	3	1	5,9
	Coimbra	Castelo Viegas II	3	0	0
	Coimbra	Eiras	2	0	0
	Coimbra	IdealMed	2	0	0
	Miranda do Corvo	Lamas I	25	15	60
	Miranda do Corvo	Lamas II	12	10	83,3
	Coimbra	Lordemão	51	6	11,8
	Coimbra	Parque de Campismo	3	2	66,7
	Coimbra	Redonda	11	0	0
	Coimbra	Sobral Cid	5	3	60
	TOTAL		**122**	**41**	**33,6**

Table VII.2. Summary of the number of studied samples in each section of the Algarve Basin and their productivity in percentage. The totals are also presented.

	Locality	Studied Section	Nº Collected Samples	Nº Productive Samples	Productivity %
ALGARVE BASIN	Albufeira	Albufeira's Diapir	4	2	50
	Aljezur	Amado's Beach	20	2	10
	São Bartolomeu de Messines	Amorosa	17	1	5,9
	Ayamonte, Spain	Ayamonte	9	0	0
	Silves	Barragem do Funcho	4	0	0
	São Brás de Alportel	Bengado	9	0	0
	Tavira	Bodega	3	0	0
	Portimão	Fonte da Pedra	1	0	0
	Portimão	International Racetrack of Algarve	24	10	41,7
	Loulé	Loulé Rock Salt Mine	33	9	27,3
	Santa Catarina Fonte do Bispo	Marco	6	0	0
	Penina	Rocha da Pena	15	0	0
	Santa Catarina Fonte do Bispo	Santa Catarina Fonte do Bispo	6	0	0
	Tavira	Santa Rita	15	0	0
	São Bartolomeu de Messines	Vale Fuzeiros	88	0	0
	TOTAL		**254**	**24**	**9,4**

Table VII.3. Summary of the number of studied samples in each borehole and their productivity in percentage. The totals are also presented.

	Borehole	Nº Collected Samples	Nº Productive Samples	Productivity %
BOREHOLES	Campelos-1	18	0	0
	Golfinho-1	27	0	0
	Lula-1	17	0	0
	Santiago do Cacém-3	21	0	0
	Santiago do Cacém-42	19	0	0
	Santiago do Cacém-61	20	0	0
	TOTAL	**122**	**0**	**0**

All this research was focused on the Upper Triassic and Triassic-Jurassic boundary in the Lusitanian and Algarve basins.

1.1. Lusitanian Basin

The recovered palynological assemblages provided new age biostratigraphic constraints for the various formations present in the Triassic-Lower Jurassic time interval of the Lusitanian Basin (Chapters II and III). The Conraria Formation, at the base of the Silves Group, is dated as Norian, possibly the earliest Rhaetian (Fig. VI.1). The palynological content recovered from the Pereiros Formation, allowed to date the formation as upper Rhaetian to early Hettangian, pointing the Triassic-Jurassic boundary to the lower part of the Pereiros Formation (Fig. VI.1). The absence of palynological data from the Penela and Castelo Viegas Formations due to unsuitable lithologies for this type of studies did not allow a precise dating. However, due to the stratigraphic position of these formations, they would be indirectly dated as Rhaetian. In conclusion, the Silves Group in the Lusitanian Basin dates from Norian to Hettangian (Fig. VI.1).

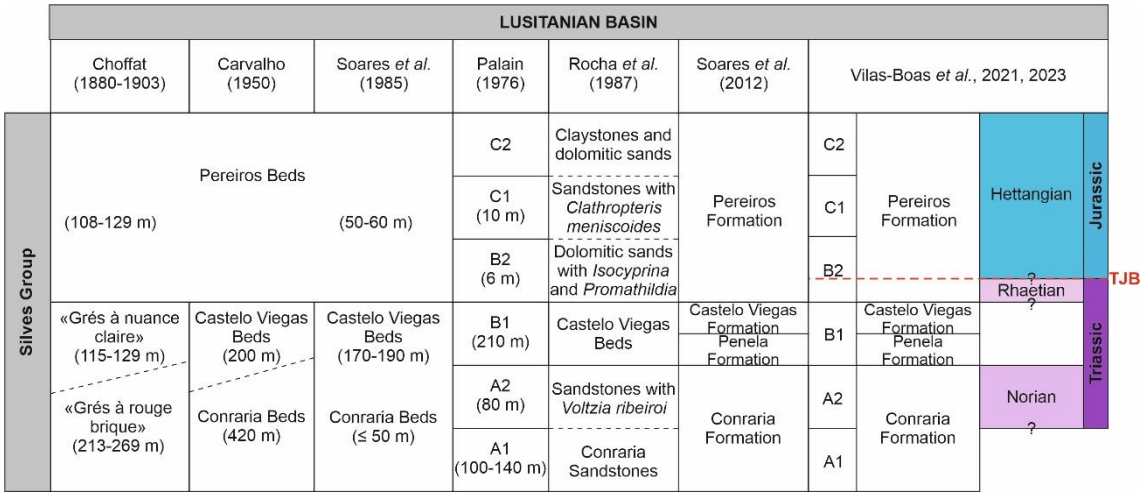

Figure VII.1. Lithostratigraphic organisation of the Silves Group in the Lusitanian Basin with the new age data (adapted from Kullberg *et al*., 2013).

The presence of microforaminiferal linings at the base of Pereiros Formation documents the first marine flooding event that occurred in the Lusitanian Basin, which is dated as lower Hettangian (Fig. VI.2). The paleoenvironmental studies allow to interpret the base of this formation as an

estuarine-type environment, suggesting a short-lived marine transgression event, shifting to a river-dominated coastal environment with episodes of tidal influence recording a short regression episode. The upper part of this formation points to an evaporitic tidal flat under warm-arid climate conditions. In conclusion, during the Hettangian age, the Lusitanian Basin was dominated by marine-marginal depositional settings interrupted by river-dominated episodes related to the short-lived regressive phase.

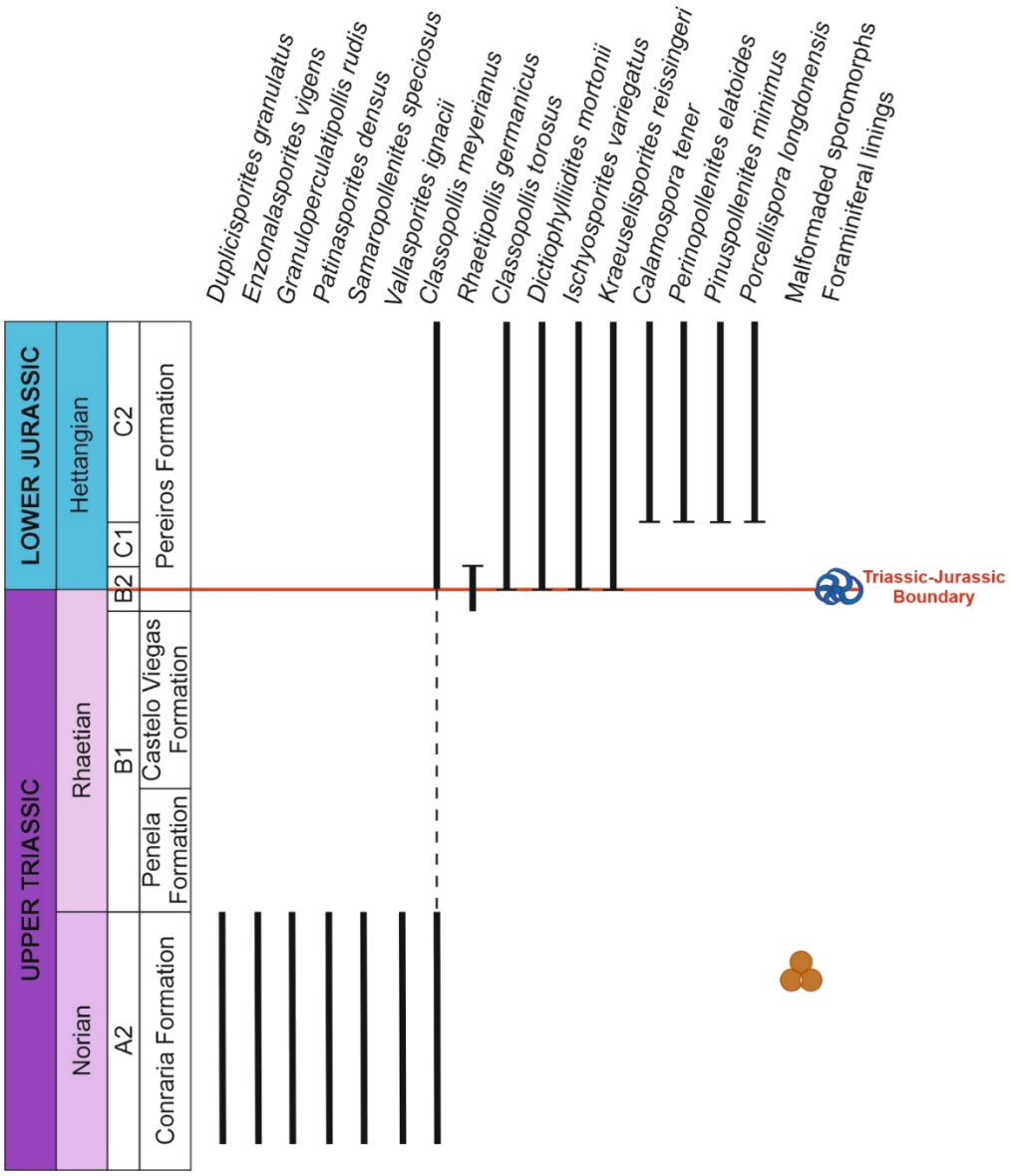

Figure VII.2. Overview of the stratigraphically significant ranges of 10 pollen grains and 5 spores of the Lusitanian Basin. The range limits, with horizontal bars, represent true range bases and tops (i.e., inceptions and apparent extinctions, respectively). The dotted ranges represent inferred occurrences in an interval with no results.

The microflora assemblages from the Lusitanian Basin recorded along the Late Triassic to Early Jurassic times might shed new light on future palaeogeographical and palaeoclimatic reconstructions of this sector of the Tethys realm. The affinity of these assemblages with those of the Eastern North America, Western Europe and Tethys basins should suggest general homogenous climate conditions (warm and humid) caused by both to intense monsoonal activity and the onset of the CAMP as documented in several Tethyan areas.

1.2. Algarve Basin

Even though the palynological associations recovered in the Algarve Basin could have been more productive, the material obtained provided new information of great relevance. The recovered palynological assemblages provided new-age biostratigraphic constraints of the Algarve Basin units (Chapters IV and V). The basal part of the Silves Sandstones (the base of the Silves Group in the Algarve Basin) is dated as lower Carnian and the upper part of this unit is dated upper Carnian age. This constrains the Silves Sandstones from lower Carnian to upper Carnian age (Fig. VI.3). The base of the Silves Marl-Carbonate Evaporitic Complex is dated as upper Carnian age and the upper part, as upper Rhaetian-lower Hettangian age, constraining this unit from the upper Carnian to Rhaetian-lower Hettangian age and identifying the Triassic-Jurassic boundary at the upper part of the Silves Marl-Carbonate Evaporitic Complex (Fig. VI.3). All this data allows to date the Silves Group, in the Algarve Basin, from the lower Carnian to lower Hettangian age based in palynostratigraphic data.

The age assignment based on the documented palynological assemblage is an important result because it limits the start of sedimentation throughout the Algarve Basin to the early Late Triassic.

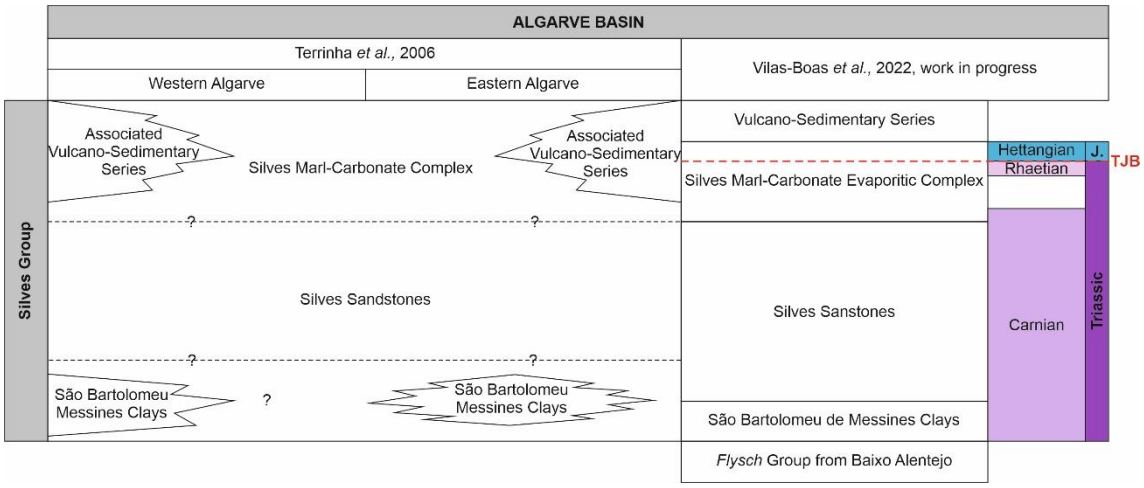

Figure VII.3. Lithostratigraphic scheme of the Silves Group in the Algarve Basin with the new age data (adapted from Terrinha *et al*., 2006). J. – Jurassic.

The arrival and rapid increasing of algal spores in the upper Carnian strata at the base of the Silves Marl-Carbonate Evaporitic Complex, such as *Plaesiodictyon mosellanum* ssp*. variable, Plaesiodictyon mosellanum* ssp*. bullatum, Botryococcus* spp*. and Ovoidites* sp., well adapted to brackish waters environments, supports the lithological evidence of a change from a continental fluvial setting (Silves Sandstones) to a coastal environment comprising swamps, ponds, and lagoons (base of Silves Marl-Carbonate Evaporitic Complex) (Fig. VI.4). The analysis of the sporomorphs with xerophytic and hygrophytic affinity in the Silves Group displays a persistent upward trend of plants with xerophytic affinities, indicating a transition toward warmer and drier conditions from the upper Carnian to the lower Hettangian age. This trend is consistent with the lithofacies evidence, which implies a transition from a coastal pond/lagoon environment (base of Silves Marl-Carbonate Evaporitic Complex) to a *sabkha* depositional setting (top of Silves Marl-Carbonate Evaporitic Complex). The existence of malformed sporomorphs in the upper Carnian and lower Hettangian age may indicate environmentally degraded conditions caused by external environmental stressors such as atmospheric pollution, volcanic mercury, and/or UVB radiation. Also, the hypothesis of a brief regressive episode in the Upper Triassic is supported by the presence of reworked algae from the Neo-Proterozoic (*Ourasphaira giraldae*) and the absence of material from Norian and lower Rhaetian. This data suggests that during that time, there was an increase

in erosion, leading to the transport of older material and exposure of the Norian and lower Rhaetian terranes.

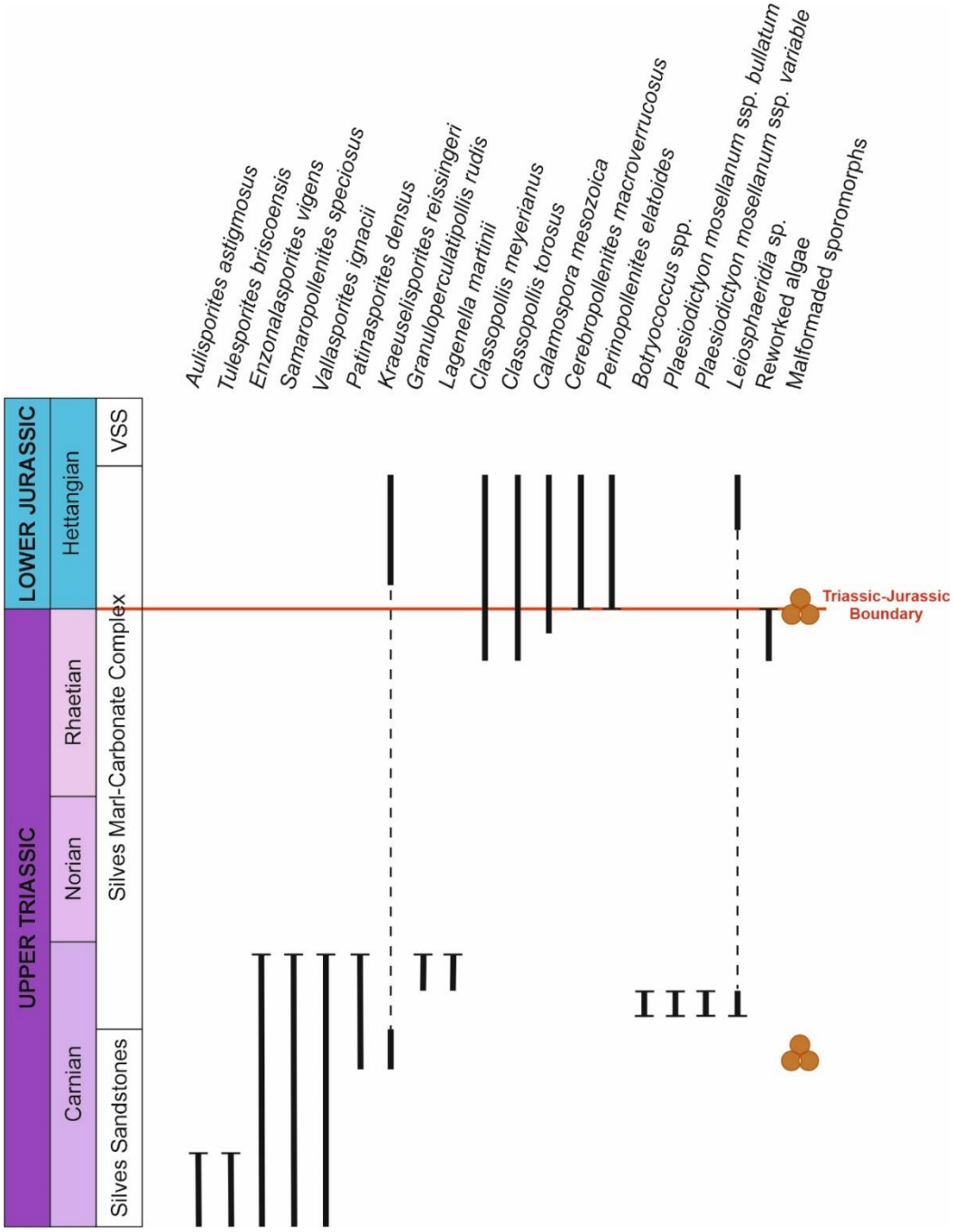

Figure VII.4. Overview of the stratigraphically significant ranges of 12 pollen grains, 2 spores and 5 algae of the Algarve Basin. The extremities of ranges with horizontal bars represent true range bases and tops (i.e., inceptions and apparent extinctions). The dotted ranges represent inferred occurrences in the interval with no results. VSS – Volcano-Sedimentary Series.

The co-occurrence of early Carnian palynofloral elements with Central European and North American affinities reinforces the Iberian Peninsula's paleogeographic position in the Late Triassic. The microflora from the Carnian interval in the Algarve Basin can be correlated with the Onslow Microflora, a mixture of Gondwana and European taxa typically distributed along the southwest of the continental margins of Tethys. This data provides new information about the palaeoclimate during Carnian in the Algarve Basin, indicating that these margins were under a warm temperate climate during this time. The increased diffusion of the *Cheirolepidiaceae* in the lower Jurassic is also recorded in the Algarve Basin, demonstrating the migration of the *Circumpolles* producers to higher latitudes derived from the rearrangement of the tectonic plates.

As a result, most of the initial goals of this PhD project were attained. Portugal's Upper Triassic to Lower Jurassic period is better detailed based on high-resolution palynological studies. The Norian to Hettangian age palynostratigraphic chart of the Lusitanian Basin (Fig. VI.2), as well as the Carnian to Hettangian age palynostratigraphic chart of the Algarve Basin (Fig. VI.4), were correlated with palynological data from other countries and coeval basins. All this data can now be a valuable instrument for palynostratigraphy, palaeoecological and palaeobiological interpretations of Upper Triassic and Lower Jurassic key events. As was expected, the palynomorphs assemblages recorded in this investigation gave new information and a significant contribution to the Lusitanian and Algarve basins background, particularly for biostratigraphy, palaeoenvironmental and paleoclimatic point of view, improving the Upper Triassic - Lower Jurassic age period knowledge.

2. Future Perspectives

For this research, all the outcrops, in both basins, more favorable for obtaining palynological results, were studied. Even though the obtained results were of high importance and very valuable, future investigations can be performed.

In the Lusitanian Basin, the Dagorda Formation may well be sampled for palynological studies, for a possible correlation with the evaporites from the Algarve Basin and the search for a better identification of the Triassic-Jurassic Boundary in the basin.

The Triassic-Jurassic Boundary in the Algarve Basin is well-detailed. However, geochemical studies for the detection of critical elements (e.g., Hg) are a good proxy for future studies to confirm the TJB transition and for interpretation of ancient environmental changes.

In both basins, the vitrinite reflectance can be used to assess the thermal history of the Silves Group basins to estimate the consequences of thermal diagenesis in the sedimentary succession. Another valuable instrument to apply are the geochemical analyses (organic C-isotopes, whole-rock geochemistry) to establish correlations with biostratigraphic data. Another point of interest will be better documenting abnormal palynomorph morphology to evaluate possible ancient environmental pollution and its causes (volcanic SO_2 and CO_2 emissions; Hg poisoning, increased UV-B radiation, etc.).

This data and knowledge may improve the correlation with the Triassic-Jurassic basins from Central Europe, North America and North Africa. The relatively well-preserved palynomorphs and substantial abundances of material are promising evidence of useful data to continue the Lusitanian and Algarve basins palynostratigraphical study.

References

Abbink, O.A. 1998. Palynological investigations in the Jurassic of the North Sea region. *LPP Contribution Series 8*: 192 pp.

Achilles, H. 1981. Die Rhaetische and Liassische Microflora Frankens. *Palaeontographica Abteilung B*, 179, 1-86.

Adloff, M. C., Doubinger, J., Palain, C. 1974. Contribution à la palynologie du Trias et Lias Inférieur du Portugal. "Grès de Silves" du Nord du Tage. *Comunicações Serviços Geológicos Portugal*, 18, p. 91-144.

Adloff, M.C., Doubinger, J., Massa, D., Vachard, D. 1985. Trias de Tripolitaine (Libye). Nouvelles données biostratigraphiques et palynologiques. Première partie. *Revue de l'Institut Français du Pétrole,* 40, 723–753.

Adloff, M.C., Doubinger, J., Massa, D., Vachard, D. 1986. Trias de Tripolitaine (Libye). Nouvelles données biostratigraphiques et palynologiques. *Revue de l'Institut Français du pétrole*. 41, 27-72.

Adloff, M.C., Doubinger, J., Palain, C. 1974. Contribution à la palynologie du Trias et du Lias inférieur du Portugal. «Grés de Silves» du Nord du Tage. *Comunicações Serviços Geológicos Portugal*, LVIII, 91-144.

Allen, P.A., Allen, J.R. 2005. Basin Analysis: Principles and Applications, second ed. *Blackwell Publishing*, Oxford.

Arche, A., López-Gómez, J. 2014. The Carnian Pluvial Event in Western Europe: new data from Iberia and correlation with the Western Neotethys and Eastern North America–NW Africa regions. *Earth-Science Reviews*, 128, 196-231.

Armstrong, H.A., Brasier, M.D. 2005. Microfossils, 2nd edition. *Blackwell Publishing*, Oxford, 1-304.

ASTM D7708-14. 2014. Standard Test Method for Microscopical Determination of the Reflectance of Vitrinite Dispersed in Sedimentary Rocks. *ASTM, International, West Conshohocken*, PA, USA, pp. 10.

Aurell, M., Robles, S., Bádenas, B., Rosales, I., Quesada, S., Meléndez, G., Garcia-Ramos, J.C. 2003. Transgressive–regressive cycles and Jurassic palaeogeography of northeast Iberia. *Sedimentary Geology*, 162(3-4), 239-271.

Azerêdo, A.C., Duarte, L.V., Henriques, M.H., Manuppella, G. 2003. Da dinâmica continental no Triásico aos mares do Jurássico Inferior e Médio. *Cadernos de Geologia de Portugal, Instituto Geológico Mineiro, Portugal*, p. 43.

Azerêdo, A.C., Duarte, L.V., Silva, R.L. 2014. Configuração sequencial em ciclos (2ª ordem) de fácies transgressivas-regressivas do Jurássico Inferior e Médio da Bacia Lusitânica (Portugal). *Comunicações Geológicas*, 101, 1, 383-386.

Baranyi, V., Reichgelt, T., Olsen, P. E., Parkerm W. G., Kürschner, W. M. 2017. Norian vegetation history and related environmental changes: New data from the Chinle Formation, Petrified Forest National Park (Arizona, SW USA). *GSA Bulletin*, 130 (5-6)

Baranyi, V., Rostási, Á., Raucsik, B., Kürschner, W. M. 2019. Palynological and X-ray fluorescence (XRF) data of Carnian (Late Triassic) formations from western Hungary. *Data in brief*, 23, 103858.

Barbacka, M., Pacyna, G., Kocsis, Á.T., Jarzynka, A., Ziaja, J., Bodor, E. 2017. Changes in terrestrial floras at the Triassic-Jurassic Boundary in Europe. *Palaeogeography, Palaeoclimatology, Palaeoecology,* 480, 80–93.

Barker, C.E. 1988. Geothermics of petroleum systems: implications of the stabilisation of kerogen thermal maturation after a geologically brief heating duration at peak temperature. In: Magoon, L.B. (Ed.), Petroleum Systems of the United States, vol. 1870. *United States Geological Survey Bulletin*, pp. 26–29.

Barrón, E., Gómez, J.J., Goy, A. 2002. Los materiales del tránsito Triásico–Jurásico en la región de Villaviciosa (Asturias, España). Caracterización palinológica. *Geogaceta,* 31, 197-200.

Barrón, E., Gómez, J.J., Goy, A., Pieren, A.P. 2006. The Triassic–Jurassic boundary in Asturias (northern Spain): palynological characterisation and facies. *Review of Palaeobotany and Palynology,* 138 (3–4), 187–208.

Batten, D.J., Koppelhus, E.B. 1996. Biostratigraphic significance of uppermost Triassic and Jurassic miospores in Northwest Europe. In: Jansonius, J., Mcgregor, D. C. (Eds), Palynology: principles and applications. *American Association of Stratigraphic Palynologists Foundation,* 2, 795-806.

Berra, F. 2012. Sea-level fall, carbonate production, rainy days: how do they relate? Insight from Triassic carbonate platforms (Western Tethys, Southern Alps, Italy). *Geology,* 40, 271–274.

Berra, F., Angiolini, L. 2014. The evolution of the Tethys region throughout the Phanerozoic: a brief tectonic reconstruction. In: Marlow, L., Kendall, C., Yose, L. (Eds.), Petroleum Systems of the Tethyan Region. *AAPG Memoir,* 106, 1-27.

Besems, R.E. 1982. Aspects of Middle and Late Triassic Palynology. 4. On the Triassic of the External Zone of the Betic Cordilleras in the Province of Jaén Southern Spain (with a note on the presence of Cretaceous palynomorphs in a presumed ‘‘Keuper’’section). *Proceedings of the Koninklijke Nederlandse Akademie, Wetenschappen*, 85, 1-27.

Blackburn, T.J., Olsen, P.E., Bowring, S.A., McLean, N.M., Kent, D.V., Puffer, J., McHone, G., Rasbury, E.T., Et-Touhami, M. 2013. Zircon U-Pb geochronology links the end Triassic extinction with the Central Atlantic Magmatic Province. *Science,* 340, 941-945.

Blendinger, E. 1988. Palynostratigraphy of the late Ladinian and Carnian in the southeastern Dolomites. *Review of Palaeobotany and Palynology*, 53(3-4), 329-348.

Bonis, N.R., Kürschner, W.M. 2012. Vegetation history, diversity patterns, and climate change across the Triassic/Jurassic boundary. *Paleobiology,* 38 (2), 240–264.

Bonis, N.R., Kürschner, W.M., Krystyn, L. 2009. A detailed palynological study of the Triassic– Jurassic transition in key sections of the Eiberg Basin (Northern Calcareous Alps, Austria). *Review of Palaeobotany and Palynology,* 156, 376-400.

Bonis, N.R., Ruhl, M., Kürschner, W.M. 2010. Climate change driven black shale deposition during the end-Triassic in the western Tethys. *Palaeogeography, Palaeoclimatology, Palaeoecology*, 290, 1-4, 151-159.

Brenner, W. 1986. Bemerkungen zur Palynostratigraphie der Rhät-Lias-Grenze im SW-Deutschland. *Neues Jahrbuch für Geologie und Paläontologie-Abhandlungen*, 173, 131–166.

Broglio Loriga, C., Cirilli, S., De Zanche, V., Di Bari, D., Gianolla, P., Laghi, G.F., Lowrie, W., Manfrin, S., Mastandrea, A., Mietto, P., Muttoni, G., Neri, C., Posenato, R., Reichichi, M., Rettori, R., Roghi, G. 1999. The Prati di Stuores/Stuores Wiesen section (Dolomites, Italy): a candidate global stratotype section and point for the base of the Carnian stage. *Rivista Italiana di Paleontologia e Stratigrafia,* 105, 37–78.

Brusatte, S.L., Butler, R.J., Mateus, O., Steyer, J.S. 2015. A new species of Metoposaurus from the Late Triassic of Portugal and comments on the systematics and biogeography of metoposaurid temnospondyls. *Journal of Vertebrate Paleontology*, 35(3), e912988.

Buratti, N., Carrillat, A. 2002. Palynostratigraphy of the Mufara Formation (Middle–Upper Triassic, Sicily). *Rivista Italiana di Paleontologia e Stratigrafia*, 108, 101–117.

Buratti, N., Cirilli, S. 2007. Microfloristic provincialism in the Upper Triassic Circum-Mediterranean area and palaeogeographic implication. *Geobios*, 40(2), 133-142.

Buratti, N., Mehdi, D., Cirilli, S., Kamoun, F., Mzoughi, M. 2012. A Carnian (Julian) microflora from the Djerba Melita 1 borehole (Gulf of Gabes, South-eastern Tunisia). *Micropaleontology*, 377-388.

Capriolo, M., Marzoli, A., Aradi, L.E., Callegaro, S., Dal Corso, J., Newton, R.J., Mills, B.J.W., Wignall, P.B., Bartoli, O., Baker, D.R., Youbi, N., Remusat, L., Spiess, R., Szabó, C. 2020. Deep CO_2 in the end-Triassic Central Atlantic Magmatic Province. *Nature Communications*, 11 (1), 1–11.

Carvalho, G.S. 1950. Considerações sobre a estratigrafia das formações mais antigas da orla meso-cenozóica ocidental de Portugal. *Revista Faculdade Ciências Universidade Coimbra*, 19, 39-48.

César, S.N., Colombi, C.E. 2016. Palynology of the Late Triassic Ischigualasto Formation, Argentina: paleoecological and paleogeographic implications. *Palaeogeography, Palaeoclimatology, Palaeoecology*, 449, 365-384.

César, S.N., Colombi, C.E. 2013. A new Late Triassic phytogeographical scenario in westernmost Gondwana. *Nature Communications*, 4(1), 1889.

Choffat, P. 1887. Recherches sur les terrains secondaires au Sud du Sado. *Comunicações Comissão dos Trabalhos Geológicos de Portugal*, I (II), 222-312.

Choffat, P. 1894. Notice stratigraphique sur les gisements de végétaux fossiles dans le Mésozoique du Portugal. *Memórias Serviços Geológicos de Portugal*, pp. 229-282.

Choffat, P. 1903. L'Infralias et le Sinémurien du Portugal. *Comunicações Serviços Geológicos de Portugal,* 5, pp.49-114.

Cirilli, S. 2010. Upper Triassic–lowermost Jurassic palynology and palynostratigraphy: a review. *Geological Society, London, Special Publications*, 334(1), 285-314.

Cirilli, S., Bucefalo Palliani, R., Pontini, M.R., 1994. Palynostratigraphy and palynofacies of the Late Triassic R. contorta facies in Northern Apennines: II The Monte Cetona Formation. *Revue de Paléobiologie,* 13(2), 319-339.

Cirilli, S., Buratti, N., Gugliotti, L., Frixa, A. 2015. Palynostratigraphy and palynofacies of the Upper Triassic Streppenosa Formation (SE Sicily, Italy) and inference on the main controlling factors in the organic rich shale deposition. *Review of Palaeobotany and Palynology*, 218, 67–79.

Cirilli S., Buratti, N., Senowbari-Daryan, B., Fursich, F.T. 2005. Stratigraphy and palynology of the Upper Triassic Nayband Formation of East-Central Iran. *Rivista Italiana di Paleontologia e Stratigrafia*, 2, 111, 259-270.

Cirilli, S., Eshet, Y.1991. First discovery of Samaropollenites and the Onslow Microflora in the Upper Triassic of Israel, and its phytogeographic implications. *Palaeogeography, Palaeoclimatology, Palaeoecology*, 85(3-4), 207-212.

Cirilli, S., Marzoli, A., Tanner, L., Bertrand, H., Buratti, N., Jourdan, F., Bellieni, G., Kontak, D., Renne, P.R. 2009. Latest Triassic onset of the Central Atlantic magmatic province (CAMP) volcanism in the Fundy basin (Nova Scotia): new stratigraphic constraints. *Earth and Planetary Science Letters,* 286 (3–4), 514–525.

Cirilli, S., Montanari, L. 1994. The Carnian evaporites succession of Bistriça River (southern Albany). *Palaeopelagos*, 4, 107–118.

Cirilli, S., Panfili, G., Buratti, N., Frixa, A. 2018. Paleoenvironmental reconstruction by means of palynofacies and lithofacies analyses: an example from the Upper Triassic subsurface succession of the Hyblean Plateau Petroleum System (SE Sicily, Italy). *Review of Palaeobotany and Palynology,* 253, 70–87.

Clement-Westerhof, J.A., Van Der Eem, J.G.L.A., Van Erve, A.W., Klasen, J.J., Schuurman, W.M.L., Visscher, H. 1974. Aspects of Permian, Triassic and Early Jurassic palynology of western Europe - a research project. *Geologie en Mijnbouw*, 53(6), 329-341.

Correia, M. 1971. Diagenesis of sporopollenin and other comparable organic substances: application to hydrocarbon research. In: Brooks, J., Grant, P.R., Muir, M., van Gijzel, P., Shaw, G. (Eds.), *Sporopollenin. Academic Press, New York*, pp. 569–620.

Cousminer, H.L, Manspeizer, W. 1976. Triassic pollen date Moroccan High Atlas and the incipient rifting of Pangea as middle Carnian. *Science*, 191(4230): 943-945.

Curtis, R., Evans, G., Kinsmann, D.J.J., Shearman D.J. 1963. Association of dolomite and anhydrite in recent sediments of the Persian Gulf. *Nature*, 196, 679-680.

Dal Corso, J., Marzoli, A., Tateo, F., Jenkyns, H.C., Bertrand, H., Youbi, N., Mahmoudi, A., Font, E., Buratti, N., Cirilli, S. 2014. The dawn of CAMP volcanism and its bearing on the end-Triassic carbon cycle disruption. *Journal of the Geological Society,* 171, 153-164.

Davies, J.H.F.L., Marzoli, A., Bertrand, H., Youbi, N., Ernesto, M., Schaltegger, U. 2017. End-Triassic mass extinction started by intrusive CAMP activity. *Nature Communications*, 8, 1–8.

de Jersey, N.J., McKellar, J.L. 2013. The palynology of the Triassic–Jurassic transition in southeastern Queensland, Australia, and correlation with New Zealand. *Palynology*, 37(1), 77-114.

Deenen, M.H., Ruhl, M., Bonis, N.R., Krijgsman, W., Kürschner, W.M., Reitsma, M., Van Bergen, M.J. 2010. A new chronology for the end-Triassic mass extinction. *Earth and Planetary Science Letters,* 291 (1–4), 113–125.

Díez, J.B. 2000. Geologia y Paleobotanica de la facies Buntsandstein en la Rama Aragonesa de la Cordillera Iberica. Implicaciones bioestratigráficas en el Peritethys occidental. Unpublished PhD Thesis, Univ. de Zaragoza/Univ. Pierre et Marie Curie-París-6.

Dimuccio, L.A., Duarte, L.V., Cunha, L. 2014. Facies and stratigraphic controls of the palaeokarst affecting the Lower Jurassic Coimbra Group, Western Central Portugal. In: Rocha, R.B., Pais, J., Kullberg, J.C., Finney, S. (Eds.), Strati 2013. First International Congress on stratigraphy t the cutting edge of Stratigraphy. *Springer Geology*, XLV, pp. 787–791.

Dimuccio, L.A., Duarte, L.V., Cunha, L. 2016. Definição litostratigráfica da sucessão calcodolomítica do Jurássico Inferior da região de Coimbra-Penela (Bacia Lusitânica, Portugal). *Comunicações Geológicas*, 103 (1), 77–96.

Dolby, J.H., Balme, B.E. 1976. Triassic palynology of the Carnarvon Basin, Western Australia. *Review of Palaeobotany and Palynology*, 22, 105– 168.

Doubinger, J., Adloff, M., Palain, C., 1970. Nouvelles précisions stratigraphiques sur la série de base du Mésozoïque portugais. *Comptes Rendus Academie des Sciences Paris*, 270, 1770–1772.

Duarte, L.V., Comas-Rengifo, M.J., Silva, R.L., Paredes, R., Goy, A. 2014. Carbon isotope stratigraphy and ammonite biochronostratigraphy across the Sinemurian-Pliensbachian boundary in the western Iberian margin. *Bulletin of Geosciences*, 89(4), 719-736.

Duarte, L.V., Silva, R.L., Azerêdo, A.C., Comas-Rengifo, M.J., Mendonça Filho, J.G. 2022. Shallow-water carbonates of the Coimbra Formation, Lusitanian Basin (Portugal): contributions to the integrated stratigraphic analysis of the Sinemurian sedimentary successions in the western Iberian Margin. *Comptes Rendus. Géoscience*, 354(S3), 1-18.

Dunay, R. E., Fisher, M. J. 1979. Palynology of the Dockum Group (Upper Triassic), Texas, USA. *Review of Palaeobotany and Palynology*, 28(1), 61-92.

Embry, A.F., Suneby, L.B. 1994. The Triassic-Jurassic boundary in the Sverdrup Basin, *Arctic Canada,* 857-868.

Fechner, G.G. 1989. Eine unterliassische Mikroflora aus dem Salzdiapir bei Loulé (Süd-Portugal). *Berliner Geowissenschaftliche Abhandlungen. Reihe A, Geologie und Paläontologie,* 106, 37–47.

Fernandes, P., Quesada, C., Braid, J., Pereira, Z., Ferreira, P., Jorge R.C.G.S., Matos, J.X., Murphy, J.B., Oliveira, T., Pedro, J. 2019. SW Iberia Variscan Suture Zone: Oceanic Affinity Units. In: The Geology of Iberia: A Geodynamic Approach, Volume 2: The Variscan Cycle. Cecilio Quesada José Tomás Oliveira Editors. *Springer Nature Switzerland AG*, pp. 131-172

Fernandes, P., Rodrigues, B., Borges, M., Matos, V., Clayton, G. 2013. Organic maturation of the Algarve Basin (southern Portugal) and its bearing on thermal history and hydrocarbon exploration. *Marine and Petroleum Geology*, 46, 210-233.

Filipiak, P., Racki, G. 2010. Proliferation of abnormal palynoflora during the end-Devonian biotic crisis. *Geological Quarterly,* 54, 1–14.

Fisher, M.J., Dunay, R.E. 1981. Palynology and the Triassic/Jurassic boundary. *Review of Palaeobotany and Palynology*, 34, 129–135.

Fisher, M.J., Dunay, R.E. 1984. Palynology of the petrified forest member of the Chinle Formation (Upper Triassic), Arizona, USA. *Pollen et spores*, 26(2), 241-284.

Foster, C.B., Afonin, S.A. 2005. Abnormal pollen grains: an outcome of deteriorating atmospheric conditions around the Permian–Triassic boundary. *Journal of the Geological Society, London*, 162, 653–659.

Foster, C.B., Balme, B.E., Helby, R. 1994. First record of Tethyan palynomorphs from the Late Triassic of east Antarctica. *AGSO Journal of Australian Geology and Geophysics*, 15, 239– 246.

Fowell, S.J., Traverse, A. 1995. Late Triassic palynology of the Fundy basin, Nova Scotia and New Brunswick. *Review of Palaeobotany and Palynology,* 86, 211–233.

Frizon de Lamotte, D., Fourdan, B., Leleu, S., Leparmentier, F., de Clarens, P. 2015. Style of rifting and the stages of Pangea breakup. *Tectonics,* 34(5), 1009-1029.

Galli, M., Jadoul, F., Bernasconi, S.M., Cirilli, S., Weissert, H. 2007. Stratigraphy and paleoenvironmental analysis of the Triassic–Jurassic transition in Western southern Alps (Northern Italy). *Palaeogeography, Palaeoclimatology, Palaeoecology,* 244, 52-70.

García-Ávila M., Mercedes-Martín, R., Juncal, M. A., Diez, J. B. 2020. New palynological data in Muschelkalk facies of the Catalan Coastal Ranges (NE of the Iberian Peninsula). *Comptes Rendus. Géoscience*, 352(6-7), pp. 443-454.

Gòczàn, F., Oravecz-Scheffer, A. 1996. Tuvalian sequence of the Balaton Highland and the Zsàmbék Basin: Part II. Characterization of sporomorph and foraminifer assemblages, biostratigraphic, palaeogeographic and geohistoric conclusion. *Acta Geologica Hungarica,* 39, 33–101.

Gómez, J.J., Aguado, R., Azerêdo, A.C., Cortés, J.E., Duarte, L.V., O'Dogherty, L., Bordalo da Rocha, R., Sandoval, J. 2019. The Late Triassic—Middle Jurassic Passive Margin Stage. In: The Geology of Iberia: A Geodynamic Approach. Vol. 3: The Alpine Cycle (Quesada, C. and Oliveira, J.T., Eds.), *Springer*, *Switzerland*, 113—167.

Gómez, J.J., Goy, A., 2005. Late Triassic and Early Jurassic palaeogeographic evolution and depositional cycles of the Western Tethys Iberian platform system (Eastern Spain). *Palaeogeography, Palaeoclimatology, Palaeoecology*, 222(1-2), 77-94.

Gómez, J.J., Goy, A., Barrón, E. 2007. Events around the Triassic–Jurassic boundary in northern and eastern Spain: a review. *Palaeogeography, Palaeoclimatology, Palaeoecology*, 244, 1-4, 89-110.

Gradstein, F.M., Ogg, J.G. 2020. The chronostratigraphic scale. Geologic Time Scale 2020. *Elsevier*, pp. 21–32.

Gravendyck, J., Schobben, M., Bachelier, J.B., Kürschner, W.M. 2020. Macroecological patterns of the terrestrial vegetation history during the end-Triassic biotic crisis in the central European Basin: A palynological study of the Bonenburg section (NW-Germany) and its supra-regional implications. *Global and Planetary Change*, 194, 103286.

Grimm, E.C. 1991. TILIA and TILIAGRAPH. PC Spreadsheet and Graphics Software for Pollen Data. INQUA Working Group on Data Handling Methods.

Guex, J., Bartolini, A., Atudorei, V., Taylor, D. 2004. High-resolution ammonite and carbon isotope stratigraphy across the Triassic–Jurassic boundary at New York Canyon (Nevada). *Earth and Planetary Science Letters,* 225, 29–41.

Guy-Ohlson, D. 1981. Rhaeto-Liassic palynostratigraphy of the Valhall bore No. 1, Scania. *Geologiska Föreningen i Stockholm Förhandlingar,* 103(2), 233–248.

Haas, J., Budai, T., Raucsik, B. 2012. Climatic controls on sedimentary environments in the Triassic of the Transdanubian Range (Western Hungary). *Palaeogeography, Palaeoclimatology, Palaeoecology*, 353-355, 31-44.

Hallam, A. 1981. A revised sea-level curve for the early Jurassic. *Journal of the Geological Society*, 138(6), 735-743.

Hallam, A. 1997. Estimates of the amount and rate of sea-level change across the Rhaetian—Hettangian and Pliensbachian—Toarcian boundaries (latest Triassic to early Jurassic). *Journal of the Geological Society*, 154(5), 773-779.

Hallam, A., Wignall, P.B. 1999. Mass extinctions and sea-level changes. *Earth-Science Reviews,* 48, 4, 217-250.

Hallam, T., Wignall, P., Hesselbo, S.P., Robinson, S.A., Surlyk, F. 2004. Discussion on sea-level change and facies development across potential Triassic–Jurassic boundary horizons, SW Britain. *Journal of the Geological Society*, 161(6), 1053-1056.

Haq, B.U., Hardenbol, J., Vail, P.R. 1988. Mesozoic and Cenozoic chronostratigraphy and cycles of sea-level change. *Society of Economic Paleontologists and Mineralogists Special Publication*, v. 42, p. 71–108.

Hesselbo, S.P., Robinson, S.A., Surlyk, F. 2004. Sea-level changes and facies development across potential Triassic-Jurassic boundary horizons, SW Britain. *Journal of the Geological Society*, 161, 365–379.

Hesselbo, S.P., Robinson, S.A., Surlyk, F., Piasecki, S. 2002. Terrestrial and marine extinction at the Triassic-Jurassic boundary synchronized with major carbon-cycle perturbation: a link to initiation of massive volcanism?. *Geology,* 30 (3), 251–254.

Heunisch, C., Luppold, F.W., Reinhardt, L., Röhling, H.G. 2010. Palynofazies, Bio-und Lithostratigraphie im Grenzbereich Trias/Jura in der Bohrung Mariental 1 (Lappwaldmulde, Ostniedersachsen). *Zeitschrift der Deutschen Gesellschaft für Geowissenschaften,* 161, 51–98.

Hillebrandt, A.V., Krystyn, L., Kürschner, W.M., Bonis, N.R., Ruhl, M., Richoz, S., Schobben, M.A.N., Urlichs, M., Bown, P.R., Kment, K., McRoberts, C.A., Simms, M., Tomãsových, A. 2013. The Global Stratotype Sections and Point (GSSP) for the base of the Jurassic Systemat Kuhjoch (Karwendel Mountains, Northern Calcareous Alps, Tyrol, Austria). *Episodes,* 36, 162–198.

Hillier, S., Marshall, J. 1988. A rapid technique to make thin sections of sedimentary organic matter concentrates. *Journal of Sedimentary Research*, 58, 754–755.

Hiscott, R.N., Wilson, R.C., Gradstein, F.M., Pujalte, V., Garcia-Mondéjar, J., Boudreau, R.R., Wishart, H.A. 1990. Comparative stratigraphy and subsidence history of Mesozoic rift basins of North Atlantic. *AAPG Bulletin*. 74 (1), 60-76.

Hochuli, P.A., Colin, J.P., Vigran, J.O. 1989. Triassic biostratigraphy of the Barents Sea area. In Correlation in Hydrocarbon Exploration: Proceedings of the conference

Correlation in Hydrocarbon Exploration organized by the Norwegian Petroleum Society and held in Bergen, Norway, 3–5 October 1988 (pp. 131-153). *Dordrecht: Springer Netherlands.*

Hochuli, P.A., Frank, S.M. 2000. Palynology (dinoflagellate cysts, spore-pollen) and stratigraphy of the Lower Carnian Raibl Group in the Eastern Swiss Alps. *Eclogae Geologicae Helvetiae,* 93(3), 429-444.

Hochuli, P.A., Schneebeli-Hermann, E., Mangerud, G., Bucher, H. 2017. Evidence for atmospheric pollution across the Permian–Triassic transition. *Geology,* 45, 1123–1126.

Hochuli, P.A., Vigran, J.O. 2010. Climate variations in the Boreal Triassic—inferred from palynological records from the Barents Sea. *Palaeogeography, Palaeoclimatology, Palaeoecology*, 290(1-4), 20-42.

Hounslow, M.H., Posen, P.E. Warrington, G. 2004. Magnetostratigraphy and biostratigraphy of the Upper Triassic and lowermost Jurassic succession, St. Audrie's Bay, UK. *Palaeogeography, Palaeoclimatology, Palaeoecology*, 213, 331-358.

International Committee for Coal and Organic Petrology, 1998. The new vitrinite classification (ICCP System 1994). *Fuel,* 77, 349–358.

Irmis, R.B., Chure, D.J., Engelmann, G.F., Wiersma, J.P., Lindström, S. 2015. The alluvial to eolian transition of the Chinle and Nugget Formations in the southern Uinta Mountains, northeastern Utah. In: Vanden Berg, M.D., Ressetar, R., and Birgenheier, L.P., (Eds), *Geology of Utah's Uinta Basin and Uinta Mountains: Utah Geological Association Publication*, 44, 13-48.

ISO 7404-5, 2009. Methods for the Petrographic Analysis of Coal, Part 5: Methods of Determining Microscopically the Reflectance of Vitrinite. *International Organization for Standardization, Geneva, Switzerland*, pp. 14.

Jansonius, J., Mcgregor, D.C. 1996. Palynology: principles and applications. Vol. 1, Principles. *American Association of Stratigraphic Palynologists Foundation*, 462 p.

Jarzen, D.M., Nichols, D.J. 1996. Chapter 9. Pollen; In: Jansonius, J. & McGregor, D.C. (ed.), Palynology: principles and applications. *American Association of Stratigraphic Palynologists Foundation*, Vol. 1, pp. 261-291.

Juncal, M.A., Bourquin, S., Beccaletto, L., Diez, J. B. 2018. New sedimentological and palynological data from the Permian and Triassic series of the Sancerre-Couy core, Paris Basin, France. *Geobios*, 51, 6, 517-535.

Juncal, M.A., Diez, J.B., De la Horra, R., Barrenechea J.F., Borruel-Abadía V., López-Gómez, J. 2020. State of the art of Triassic palynostratigraphical knowledge of the Cantabrian Mountains (N Spain). *Comptes Rendus. Géoscience*, 352, 6-7, pp. 475-493.

Koppelhus, E.B., Batten, D.J. 2002. Application of a palynomorph zonation to a series of short borehole sections, Lower to Middle Jurassic, Øresund, Denmark. In. Jansonius, J., Mcgregor, D.C. (Eds), Palynology: Principles and Applications. Vol 2. *American Association of Stratigraphical Palynologists Foundation*, pp. 779-793.

Krystyn, L., Bouquerel, H., Kürschner, W.M., Richoz, S., Gallet, Y. 2007a. Proposal for a candidate GSSP for the base of the Rhaetian stage. *New Mexico Museum of Natural History and Science Bulletin*, vol. 41 (2007), pp. 189-199.

Krystyn, L., Kürschner, W.M. 2005. Biotic events around the Norian–Rhaetian boundary from a Tethyan perspective. *Albertiana,* 32, 17-20.

Krystyn, L., Richoz, S., Gallet, Y., Bouquerel, H., Kürschner, W.M., Spötl, C. 2007b. Updated bio- and magnetostratigraphy from Steinbergkogel (Austria), candidate GSSP for the base of the Rhaetian stage*. Albertiana,* 36, 164–174.

Kullberg, J.C., Rocha, R.B., Soares, A.F., Rey, J., Terrinha, P., Azerêdo, A.C., Callapez, P., Duarte, L.V., Kullberg, M.C., Martins, L., Miranda, R., Alves, C., Mata, J., Madeira, J., Mateus, O., Moreira, M., Nogueira, C.R. 2013. A Bacia Lusitaniana: estratigrafia paleogeografia e tectónica. In: Dias, R., Araújo, A., Terrinha, P., Kullberg, J.C. (Eds.), Geologia de Portugal. Vol. II. *Livraria Escolar Editora*, pp. 195–347.

Kürschner, W.M., Herngreen, G.W. 2010. Triassic palynology of central and northwestern Europe: a review of palynofloral diversity patterns and biostratigraphic subdivisions. *The Geological Society of London Special Publications*, 334, 1, 263-283.

Kürschner, W.M., Batenburg, S.J., Mander, L. 2013. Aberrant Classopollis pollen reveals evidence for unreduced (2n) pollen in the conifer family Cheirolepidiaceae during the Triassic–Jurassic transition. *Proceedings of the Royal Society B: Biological Sciences,* 280(1768), 20131708.

Kürschner, W.M., Bonis, N.R., Krystyn, L. 2007. Carbon-isotope stratigraphy and palynostratigraphy of the Triassic–Jurassic transition in the Tiefengraben-section Northern Calcareous Alps (Austria). *Palaeogeography, Palaeoclimatology, Palaeoecology*, 244, 257–280.

Kürschner, W.M., Herngreen, G.W. 2010. Triassic palynology of central and northwestern Europe: A review of palynofloral diversity patterns and biostratigraphic subdivisions. *The Geological Society of London Special Publications*, 334(1), 263–283.

Kürschner, W.M., Mander, L., McElwain, J.C. 2014. A gymnosperm affinity for Ricciisporites tuberculatus Lundblad: implications for vegetation and environmental reconstructions in the Late Triassic. *Palaeobiodiversity and Palaeoenvironments,* 94(2), 295-305.

Kustatscher, E., Ash, S.R., Karasev, E., Pott, C., Vajda, V., Yu, J., McLoughlin, S. 2018. Flora of the late Triassic. *The Late Triassic World: Earth in a Time of Transition*, 545-622.

Leorri, E., Cearreta, A. 2009. Recent sea-level changes in the southern Bay of Biscay: transfer function reconstructions from salt-marshes compared with instrumental data. *Scientia Marina*, 73(2), 287-296.

Li, L., Wang, Y., Vajda, V., Liu, Z. 2018. Late Triassic ecosystem variations inferred by palynological records from Hechuan, southern Sichuan Basin, China. *Geological Magazine,* 155(8), 1793-1810.

Lindström, S. 2016. Palynofloral patterns of terrestrial ecosystemchange during the end-Triassic event–a review. *Geological Magazine,* 153 (2), 223–251.

Lindström, S., Callegaro, S., Davies, J., Tegner, C., van de Schootbrugge, B., Pedersen, G.K., Youbi, N., Sanei, H., Marzoli, A. 2021. Tracing volcanic emissions from the Central Atlantic Magmatic Province in the sedimentary record. *Earth-Science Reviews,* 212, 103444.

Lindström, S., Erlström, M., Piasecki, S., Nielsen, L.H., Mathiesen, A. 2017a. Palynology and terrestrial ecosystem change of the Middle Triassic to lowermost Jurassic succession of the eastern Danish Basin. *Review of Palaeobotany and Palynology,* 244, 65–95.

Lindström, S., Irmis, R.B., Whiteside, J.H., Smith, N.D., Nesbitt, S.J., Turner, A.H. 2016. Palynology of the upper Chinle Formation in northern New Mexico, USA: implications for biostratigraphy and terrestrial ecosystem change during the Late Triassic (Norian–Rhaetian). *Review of Palaeobotany and Palynology,* 225, 106-131.

Lindström, S., Sanei, H., Van De Schootbrugge, B., Pedersen, G.K., Lesher, C.E., Tegner, C., Heunisch, C., Dybkjær, K., Outridge, P.M. 2019. Volcanic mercury and mutagenesis in land plants during the end-Triassic mass extinction. *Science Advances*, 5(10), eaaw4018.

Lindström, S., Van De Schootbrugge, B., Dybkjær, K., Pedersen, G.K., Fiebig, J., Nielsen, H.N., Richoz, S. 2012. No causal link between terrestrial ecosystem change and methane release during the end-Triassic mass-extinction. *Geology*, 40, 531–534.

Lindström, S., Van De Schootbrugge, B., Hansen, K.H., Pedersen, G.K., Alsen, P., Thibault, N., Dybkjæra, K., Bjerrum, C.J., Nielsen, L.H. 2017b. A new correlation of Triassic–Jurassic boundary successions in NW Europe, Nevada and Peru, and the Central Atlantic Magmatic Province: a time-line for the end-Triassic mass extinction. *Palaeogeography, Palaeoclimatology, Palaeoecology,* 478, 80–102.

Litwin, R.J., Traverse, A., Ash, S.R. 1991. Preliminary palynological zonation of the Chinle Formation, southwestern USA, and its correlation to the Newark Supergroup (eastern USA). *Review of Palaeobotany and Palynology*, 68(3-4), 269-287.

Loboziak, S., Melo, J.H., Streel, M. 2005. Devonian Palynostratigraphy in Western Gondwana. In: Koutsoukos, E.A.M. (ed.), *Applied Stratigraphy, Springer Netherlands*, 73-99.

Lucas, S.G., Tanner, L.H., Donohoo-Hurley, L.L., Geissman, J.W., Kozur, H.W., Heckert, A.B., Weems, R.E. 2011. Position of the Triassic–Jurassic boundary and timing of the end- Triassic extinctions on land: data from the Moenave Formation on the southern "Colorado Plateau", USA. *Palaeogeography, Palaeoclimatology, Palaeoecology,* 302, 194-205.

Luis, L., 2007. Mirone: a multi-purpose tool for exploring grid data. *Computers & Geosciences,* 33, 31-41.

Lund, J.J. 2003. Rhaetian to Pliensbachian palynostratigraphy of the central part of the NW German Basin exemplified by the Eitzendorf 8 well. *Courier-Forschungsinstitut Senckenberg,* 241, 69-84.

Lund, J.J. 1977. Rhaetic to Lower Liassic palynology of the onshore south-eastern North Sea Basin. *Danmarks Geologiske Undersøgelse II. Række,* 109(2), 1-103.

Manuppella, G. 1992. Carta Geológica da região do Algarve, folha ocidental, na escala 1:100000. *Serviços Geológicos de Portugal*.

Manuppella, G., Marques, B., Rocha, R.B. 1988. Evolution tectono-sédimentaire du bassin de l'Algarve pendant le Jurassique. *In International symposium on Jurassic stratigraphy*, 2,, 1031-1046.

Martini, R., Cirilli, S., Saurer, C., Abate, B., Ferruzza, G., Lo Cicero, G. 2007. Depositional environment and biofacies characterisation of the Triassic (Carnian to Rhaetian) carbonate succession of Punta Bassano (Marettimo Island, Sicily): Palaeogeographic implications. *Facies*, 3, 53, 389-400.

Martini, R., Vachard, D., Zaninetti, L., Cirilli, S., Cornée, J.J., Lathuilière, B., Villeneuve, M. 1997. Sedimentology, stratigraphy and micropaleontology of the Upper Triassic reefal series in Eastern Sulawesi (Indonesia). *Palaeogeography, Palaeoclimatology, Palaeoecology,* 128, 157 – 174.

Martini, R., Zaninetti, L., Lathuillière, B., Cirilli, S., Cornée, J.J., Villeneuve, M. 2004. Upper Triassic carbonate deposits of Seram (Indonesia): palaeogeographic and geodynamic implications. *Palaeogeography, Palaeoclimatology, Palaeoecology,* 206, 75–102.

Martins, L.T. 1991. Actividade Ígnea Mesozóica em Portugal (Contribuição Petrológica e Geoquímica). PhD thesis, University of Lisbon, Portugal, 418 pp.

Martins, L.T., Madeira, J., Youbi, N., Munhá, J., Mata, J., Kerrich, R. 2008. Rift-related magmatism of the Central Atlantic magmatic province in Algarve, southern Portugal. *Lithos*, 101, 102-124.

Marzoli, A., Bertrand, H., Knight, K., Cirilli, S., Nomade, S., Renne, P., Vérati, C., Youbi, N., Martini, R., Bellieni, G. 2008. Comment on "Synchrony between the Central Atlantic magmatic province and the Triassic– Jurassic mass-extinction event? By Whiteside et al. (2007)". *Palaeogeography, Palaeoclimatology, Palaeoecology,* 262, 189–193.

Marzoli, A., Bertrand, H., Knight, K.B., Cirilli, S., Buratti, N., Vérati, C., Nomade, S., Renne, P.R., Youbi, N., Martini, R., Allenbach, K., Neuwerth, R., Rapaille, C., Zaninetti, L., Bellieni, G. 2004. Synchrony of the Central Atlantic magmatic province and the Triassic–Jurassic boundary climatic and biotic crisis. *Geology,* 32, 973–976.

Marzoli, A., Renne, P.R., Piccirillo, E.M., Ernesto, M., Bellieni, G., Min, A.D. 1999. Extensive 200-million-year-old continental flood basalts of the Central Atlantic Magmatic Province. *Science*, 284(5414), 616-618.

Mateus, O., Butler, R.J., Brusatte, S.L., Whiteside, J.H., Steyer, J. S. 2014. The first phytosaur (Diapsida, Archosauriformes) from the Late Triassic of the Iberian Peninsula. *Journal of Vertebrate Paleontology*, 34(4), 970-975.

Mazzullo, S.J. 2000. Organogenic dolomitization in peritidal to deep-sea sediments. *Journal of Sedimentary Research*, 70(1), 10-23.

McPhilemy, B. 1988. The value of fluorescence microscopy in routine palynofacies analysis: Lower Carboniferous successions from Counties Armagh and Roscommon, Ireland. Review of Palaeobotany and Palynology, 56, 345–359.

Mehdi, D., Cirilli, S., Buratti, N., Kamoun, F., Trigui, A. 2009. Palynological characterisation of the Lower Carnian of the Kea5 borehole (Koudiat El Halfa Dome; Central Atlas, Tunisia), *Geobios*, 42, 63-71.

Mendonça Filho, J.G., Araujo, C.V., Borrego, A.G., Cook, A., Flores, D., Hackley, P., Hower, J.C., Kern, M.L., Kommeren, K., Kus, J., Mastalerz, M., Mendonça, J.O., Menezes, T.R., Newman, J., Ranasinghe, P., Souza, I.V.A.F., Suarez-Ruiz, I., Ujiié, Y. 2010. Effect of concentration of dispersed organic matter on optical maturity parameters: interlaboratory results of the organic matter concentration working group of the ICCP. *International Journal of Coal Geology,* 84, 154–165.

Michalik, J., Biron, A., Lintnerova, O., Gotz, A.E., Ruckwied, K. 2010. Climate change at the Triassic/Jurassic boundary in the northwestern Tethyan realm, inferred from sections in the Tatra Mountains (Slovakia). *Acta Geologica Polonica*, 60(4), 535-548.

Mietto, P., Andreetta, R., Broglio Loriga, C., Buratti, N., Cirilli, S., De Zanche, V., Furin, S., Gianolla, P., Manfrin, S., Muttoni, G., Neri, C., Nicora, A., Posenato, R., Preto, N., Rigo, M., Roghi, G., Spötl, C. 2007. A candidate of the Global Boundary Stratotype Section and Point for the base of the Carnian Stage (Upper Triassic): GSSP at the base of the canadensis Subzone (FAD of Daxatina) in the Prati di Stuores/Stuores Wiesen section (Southern Alps, NE Italy). *Albertiana*, 36, 78-97.

Mietto, P., Mafrin, S., Preto, N., Rigo, M., Roghi, G., Furin, S., Gianolla, P., Posenati, R., Muttoni, G., Nicora, A., Buratti, N., Cirilli, S., Spötl, C., Ramezani, J., Bowring, S. A. 2012. The Global Boundary Stratotype Section and Point (GSSP) of the Carnian Stage (Late Triassic) at Prati Di Stuores/Stuores Wiesen Section (Southern Alps, NE Italy). *Episodes*, 35, 1051 414–430.

Miranda, J.P., Pina, B., Matos, V., Calhôa, A.M., Reis, R., Pimentel, N. 2010. Estudo das fácies de leque aluvial em afloramento do Triásico Superior de Coimbra. *e-Terra*, 21, 9.

Mishra, S., Aggarwal, N., Jha, N. 2018. Palaeoenvironmental change across the Permian-Triassic boundary inferred from palynomorph assemblages (Godavari Graben, south India). *Palaeobiodiversity and Palaeoenvironments*, 98(2), 177-204.

Morbey, S.J. 1975. The palynostratigraphy of the Rhaetian stage, Upper Triassic in the Kendelbachgraben, Austria. *Palaeontographica Abteilung B*, 152, 1-75.

Morbey, S.J. 1978. Late Triassic and Early Jurassic subsurface palynostratigraphy in northwestern Europe. *Palinologia*, 1 (special issue), 355-368.

Mouterde, R. 1971. Esquisse de l'évolution biostratigraphique de la Péninsule Ibérique au Jurassique. *Cuadernos Geologia Iberica*, Madrid, 2, pp. 21-31.

Nomade, S., Knight, K.B., Beutel, E., Renne, P.R., Verati, C., Féraud, G., Marzoli, A., Youbi, N., Bertrand, H. 2007. Chronology of the Central Atlantic Magmatic Province: implications for the Central Atlantic rifting processes and the Triassic–Jurassic biotic crisis. *Palaeogeography, Palaeoclimatology, Palaeoecology*, 244 (1–4), 326–344.

Oliveira, J.T. 1992. Carta Geológica de Portugal à escala 1:200 000, Notícia explicativa da folha 8, *Serviços Geológicos de Portugal*.

Oliveira, J.T., Wagner-Gentis, C.T. 1983. The Mértola and Mira Formation Boundary Between Dogueno and Almada de Ouro, Marine Carboniferous of South Portugal. *In Contributions to the Carboniferous geology and palaeontology of the Iberian Peninsula*, 1-39.

Orbell, G. 1973. Palynology of the British Rhaeto– Liassic. *Bulletin Geological Survey of Great Britain,* 44, 1-44.

Palain, C. 1976. Une série détritique terrigène les" Grès de Silves": Trias et Lias inférieur du Portugal. *Memória dos Serviços Geológicos de Portugal*, 25, 377.

Palain, C. 1979. Connaissances stratigraphiques sur la base du mésozoique portugais. *Ciências da Terra*, 5, 11-28.

Panfili, G., Cirilli, S., Dal Corso, J., Bertrand, H., Medina, F., Youbi, N., Marzoli, A. 2019. New biostratigraphic constraints show rapid emplacement of the Central Atlantic Magmatic Province (CAMP) during the end-Triassic mass extinction interval. *Global and Planetary Change*, 172, 60–68.

Parrish, J.T., 1993. Climate of the Supercontinent Pangea. *The Journal of Geology*, 10, 215–233.

Paterson N.W., Mangerud, G. 2015. Late Triassic (Carnian – Rhaetian) palynology of Hopen, Svalbard. *Review of Palaeobotany and Palynology*, 220, 98–119.

Paterson, N. W., Mangerud, G. 2020. A revised palynozonation for the Middle–Upper Triassic (Anisian–Rhaetian) series of the Norwegian Arctic. *Geological Magazine*, 157(10), 1568-1592.

Paterson, N.W., Mangerud, G., Mørk, A. 2016. Late Triassic (early Carnian) palynology of shallow stratigraphical core 7830/5-U-1, offshore Kong Karls Land, Norwegian Arctic. *Palynology*, 41(2), 230-254.

Pearson, D. L. 1984. Pollen/spore color "standard". Phillips Petroleum Company Exploration Projects Section (reproduced in Traverse, A., 1988. *Palaeopalynology*, Plate 1. Unwin Hyman, Boston).

Pedersen, K.R., Lund, J.J. 1980. Palynology of the plant-bearing Rhaetian to Hettangian Kap Stewart Formation, Scoresby Sund, East Greenland. *Review of Palaeobotany and Palynology*, 31, 1-69.

Pereira, Z. 1997. Palinologia e petrologia orgânica do sector Sudoeste da Zona Sul Portuguesa. Unpublished PhD Thesis. *Faculdade de Ciências, Universidade do Porto, Porto,* pp. 1-406.

Pereira, Z., Matos, J.X., Fernandes, P., Oliveira, J.T. 2008. Devonian and Carboniferous palynostratigraphy of the South Portuguese Zone, Portugal. *Comunicações Geológicas*, 94, 53-79.

Pérez-López, A., Cambeses, A., Pérez-Valera, F., Götz, A.E. 2021. Rhaetian tectono-magmatic evolution of the Central Atlantic Magmatic Province volcanism in the Betic Cordillera, South Iberia. *Lithos*, 396, 106230.

Playford, G., Dettmann, M.E. 1996. Spores. In: Jansonius, J. & Mcgregor, D. C. (Ed.) Palynology: Principles and aplications. *American Association of Stratigraphic Palynologists Foundation*, Vol. 1: 227-260.

Rasmussen, E.S., Lomholt, S., Andersen, C., Vejbak, O.V. 1998. Aspects of the structural evolution of the Lusitanian Basin in Portugal and the shelf and slope area offshore Portugal. *Tectonophysics,* 300, 199–255.

Raup, D.M., Sepkoski, J.J. 1982. Mass extinction in the marine fossil record. *Science,* 215, 1501-1503.

Reolid, M., Muñiz Guinea, F., Toscano, A., Belaústegui, Z. 2022. First record of fossil sauropterygians from the Upper Triassic of Southwestern Spain (Ayamonte, Huelva province). *Estudios Geológicos*, 78 (1), e145.

Riding, J.B., Warny, S. (Eds.). 2008. Palynological Techniques. Second Edition, *American Association of Stratigraphic Palynologists Foundation*, Dallas, Texas 137 pp.

Robbins, E.I. 1982. Fossil Lake Danville. Unpublished PhD Thesis, Pennsylvania State University, pp. 1- 400.

Robbins, E.I., Cuomo, M.C., Haberyan, K.A., Mudie, P.J., Chen, Y.Y., Head, E. 1996. Fecal pellets. *Palynology: principles and applications*, 3, 1085-1097.

Rocha, R.B. 1976. Estudo Estratigráfico e Paleontológico do Jurássico do Algarve Ocidental. *Ciências da Terra*, vol. 2, pp. 9-179.

Rocha, R.B., Mouterde, R., Soares, A.F., Elmi, S. 1987. Excursion A- Biostratigraphie et évolution séquentielle du Bassin au Nord du Tage au cours du Lias et du Dogger. *2nd International Symposium on Jurassic stratigraphy*, 1-84, Lisboa.

Roghi, G. 2004. Palynological investigations in the Carnian of the Cave del Predil area (Julian Alps, NE Italy). *Review of Palaeobotany and Palynology,* 132, 1–35.

Roghi, G., Gianolla, P., Minarelli, L., Pilati, C., Preto, N. 2010. Palynological correlation of Carnian humid pulses throughout western Tethys. *Palaeogeography, Palaeoclimatology, Palaeoecology*, 290 (1-4), 89-106.

Ruhl, M., Bonis, N.R., Reichart, G.J., Sinninghe, D.J.S., Kürschner, W.M. 2011. Atmospheric carbon injection linked to end-Triassic mass-extinction. *Science*, 333, 430–434.

Ruhl, M., Kürschner, W.M., Krystyn, L. 2009. Triassic–Jurassic organic carbon isotope stratigraphy of key sections in the western Tethys realm (Austria). *Earth and Planetary Science Letters*, 281, 169–187..

Ruiz-Martínez, V.C., Torsvik, T.H., van Hinsbergen, D.J.J., Gaina, C. 2012. Earth at 200 Ma: global palaeogeography refined from CAMP palaeomagnetic data. *Earth and Planetary Science Letters*, 331–332, 67–79.

Santos, A., Popovic, N., Mayoral, E. 2022. Palaeoecology of Late Triassic marine assemblages from the proto-Atlantic Basin (Ayamonte, SW Spain). *Proceedings of the Geologists Association*, 133(1), 47-66.

Schaller, M.F., Wright, J.D., Kent, D.V. 2011. Atmospheric P_{CO2} perturbations associated with the Central Atlantic Magmatic Province. *Science*, 331, 1404-1409.

Schaltegger, U., Guex, J., Bartolini, A., Schoene, B., Ovtcharova, M. 2008. Precise U–Pb age constraints for end-Triassic mass extinction, its correlation to volcanism and Hettangian post-extinction recovery. *Earth and Planetary Science Letters,* 267, 266–275.

Schneebeli-Hermann, E., Looser, N., Hochuli, P.A., Furrer, H., Reisdorf, A.G., Wetzel, A., Bernasconi, S.M. 2018. Palynology of Triassic–Jurassic boundary sections in northern Switzerland. *Swiss Journal of Geosciences,* 111 (1–2), 99–115.

Schobben, M., Van De Schootbrugge, B., Wignall, P.B. 2019. Interpreting the carbon isotope record of mass extinctions. *Elements*, 15 (5), 331–337.

Schoene, B., Guex, J., Bartolini, A., Schaltegger, U., Blackburn, T.J. 2010. Correlating the end-Triassic mass extinction and flood basalt volcanism at the 100ka level. *Geology*, 38, 387–390.

Schönfeld, J., Mendes, I. 2022. Benthic foraminifera and pore water carbonate chemistry on a tidal flat and salt marsh at Ria Formosa, Algarve, Portugal. *Estuarine, Coastal and Shelf Science,* 276, 108003.

Schulz, E., Heunisch, C. 2005. Palynostratigraphische Gliederungsmöglichkeiten des deutschen Keupers. *Stratigraphie von Deutschland. IV Keuper. Courier Forschungsinstitut Senckenberg*, 253, 43-49.

Schuurman, W.M. 1977. Aspects of Late Triassic Palynology. 2. Palynology of the “Grès et schiste àAvicula contorta” and “Argiles de levallois” (Rhaetian) of northeastern France and Southern Luxemburg. *Review of Palaeobotany and Palynology,* 23(3), 159-253.

Schuurman, W.M. 1979. Aspects of Late Triassic Palynology. 3. Palynology of latest Triassic and earliest Jurassic deposits of the northern Limestone Alps in Austria and southern Germany, with special reference to a palynological characterization of the Rhaetian Stage in Europe. *Review of Palaeobotany and Palynology*, 27(1), 53-75.

Scotese, C.R., Schettino, A. 2017. Late Permian-Early Jurassic paleogeography of western tethys and the world. In: Soto, J.I., Flinch, J.F., Tari, G. (Eds.), Permo-Triassic Salt Provinces of Europe, North Africa and the Atlantic Margins. *Elsevier*, 57–95.

Scott, R. A. 1982. Aspects of the Palynology of the Chinle Formation (Upper Triassic), Colorado Plateau, Arizona, Utah, and New Mexico. *United States Geological Survey, Open-File Report*, 82, 937, 1-19.

Sêco, S.L.R., Duarte, L.V., Pereira, A.J.S.C. 2015. Utilização da espectrometria gama na caracterização das unidades da base do Jurássico Inferior do sector norte da Bacia Lusitânica (Portugal): dados preliminares. *Comunicações Geológicas,* 102 (Especial I), 41–44.

Sellwood, B.W., Valdes, P.J. 2007. Mesozoic climates. In: Williams, M., Haywood, A.M., Gregory, F.J., Schmidt, D.N. (Eds.), Deep-time Perspectives on Climate Change: Marrying the Signal from Computer Models and Biological Proxies. *The Micropalaeontological Society, Special Publication,* 201–224.

Sepkoski, J.J. 1996. Patterns of Phanerozoic extinction: a perspective from global data bases. In *Global Events and Event Stratigraphy in the Phanerozoic: Results of the International Interdisciplinary Cooperation in the IGCP-Project 216* “*Global Biological Events in Earth History”*. *Berlin, Heidelberg: Springer Berlin Heidelberg*, 35–51.

Shinn, E. A. 1983. Tidal flat environment. In *Carbonate depositional environments. American Association of Petroleum Geologists*, Vol. 33, 171-210.

Smith, D.G. 1982. Stratigraphic significance of a palynoflora from ammonoid-bearing Early Norian strata in Svalbard. *Newsletters on Stratigraphy*, 11, 154-161.

Soares, A.F., Kullberg, J.C., Marques, J.F., da Rocha, R.B., Callapez, P.M. 2012. Tectonosedimentary model for the evolution of the Silves Group (Triassic, Lusitanian basin, Portugal). *Bulletin de la Société géologique de France*, 183 (3), 203–216.

Soares A.F., Marques, J.F., Rocha R.B., Sequeira, A.J.D., Sousa, M.B., Pereira, E. 2005. Carta geológica de Portugal – Folha 19-D Coimbra-Lousã. *Publicação do INETI*, Alfragide, Lisboa.

Soares, A.F., Marques, J.F., Sequeira, A. 2007. Carta Geológica de Portugal Folha 19-D (Coimbra-Lousã) à escala 1:50000. Notícia Explicativa da Folha 19-D (Coimbra-Lousã), *Instituto Nacional de Engenharia Tecnologia e Inovação, Lisboa.*

Soares, A.F., Rocha, R.B., Elmi, S., Henriques, M.H., Mouterde, R., Almeras, Y., Ruget, C., Marques, J.F., Duarte, L.V., Carapito, M.C., Kullberg, J.C. 1993. Le sous-bassin nord-lusitanien (Portugal) du Trias au Jurassique moyen: histoire d'un "rift avorté". *Comptes Rendus de l'Academie des Sciences*, *Paris*, (II), 317, 1659-1666.

Stampfli, G.M., Mosar, J., Favre, P., Pillevuit, A., Vannay, J.C. 2001. Permo-Mesozoic evolution of the western Tethys realm: the Neo-Tethys East Mediterranean basin connection. *Mémoires du Museum National d'Histoire Naturelle, Paris*, 186, 51–108.

Staplin, F.L. 1982. How to assess maturation and palaeotemperatures: Introduction. In: Staplin, F.L. (Ed.), How to Assess Maturation and Palaeotemperatures. *Society of Economic Paleontologists and Mineralogists*, pp. 1–5 Short Course No.7.

Suárez-Ruiz, I., Flores, D., Mendonça Filho, J.G., Hackley, P.C. 2012. Review and update of the applications of organic petrology: Part 1, geological applications. *International Journal of Coal Geology*, 99, 54–112.

Tanner, L.H., Lucas, S.G., Chapman, M.G. 2004. Assessing the record and causes of Late Triassic extinctions. *Earth-Science Review,* 65, 103–139.

Tanner, L.H., Smith, D.L., Allan, A. 2007. Stomatal response of swordfern to volcanogenic CO_2 and SO_2 from Kilauea volcano, Hawaii. *Geophysical Research Letters,* 34, L15807.

Teixeira, C. 1942. Notas sobre a geologia do Triássico português. *Boletim Sociedade Geológica Portugal,* Vol. 1, Fasc. III, 161–175.

Terrinha, P. 1998. Structural Geology and Tectonic Evolution of the Algarve Basin, South Portugal. Unpublished PhD Thesis, Department of Geology, Royal School of Mines, Imperial College, London, 430p.

Terrinha, P., Ribeiro, C., Kullberg, J.C., Lopes, C., Rocha, R., Ribeiro, A. 2002. Compressive episodes and faunal isolation during rifting, Southwest Iberia. *Journal of Geology*, 110, 101-113.

Terrinha, P., Rocha, R.B, Rey, J., Cachão, M., Moura, D., Roque, C., Martins, L., Valadares, V., Cabral, J., Azevedo, M.R., Barbero, L., Clavijo, E., Dias, R.P., Matias, H., Madeira, J., Silva, C.M., Munhá, J., Rebelo, L., Ribeiro, C., Vicente, J., Noiva, J., Youbi, N., Bensalah, M.K. 2006. A Bacia do Algarve: Estratigrafia, paleogeografia e tectónica. Geologia de Portugal no contexto da Ibéria, 1-138.

Terrinha, P., Rocha, R.B., Rey, J., Cachão, M., Moura, D., Roque, C., Martins, L., Valadares, V., Cabral, J., Azevedo, M.R., Barbero, L., Clavijo, E., Dias, R.P., Matias, H., Madeira, J., Silva, C.M., Munhá, J., Rebelo, L., Ribeiro, C., Noiva, J., Youbi, N., Bensalah, M.K. 2013. A Bacia do Algarve: Estratigrafia, paleogeografia e tectónica. Geologia De Portugal, Geologia Meso-Cenozóica De Portugal, II, 29–166.

Traverse, A. 2007. Paleopalynology, 2ª edição. In: Landman, N.H., Jones, D.S. (eds.), Topics in *Geobiology Series, American Association of Stratigraphic Palynologists Foundation, Springer, Dordrecht*, 28, 1-814.

Traverse, A. 2008. Paleopalynology. In: Landman, N.H., Jones, D.S. (Eds.), Topics in Geobiology 28. *Springer, Dordrecht*, 1–813.

Tverdokhlebov, V.P., Sennikov, A.G., Novikov, I.V., Ilyina, N.V. 2020. The youngest Triassic land vertebrate assemblage of Russia: Composition and dating. *Paleontological Journal*, 54, 297-310.

Tyson, R.V. 1993. Chapter 5: palynofacies analysis. In: Jenkins, D.G. (Ed.), Applied Micropaleontology. *Kluwer Academic Publishers, The Netherlands, Amsterdam*, 153–191.

Tyson, R.V. 1995. Sedimentary Organic Matter. Organic Facies and Palynofacies. *Chapman and Hall, London*, p. 615.

Van De Schootbrugge, B., Payne, J.L., Tomasovych, A., Pross, J., Fiebig, J., Benbrahim, M., Föllmi, K.B., Quan, T.M. 2008. Carbon cycle perturbation and stabilization in the wake of the Triassic–Jurassic boundary mass-extinction event. *Geochemistry, Geophysics, Geosystems*, 9 (4), 1–16.

Van De Schootbrugge, B., Quan, T.M., Lindström, S., Puttmann, W., Heunisch, C., Pross, J., Fiebig, J., Petschick, R., Rohling, H., Richoz, S., Rosenthal, Y., Falkowski, P.G. 2009. Floral changes across the Triassic Jurassic boundary linked to flood basalt volcanism. *Nature Geoscience*, 2 (8), 589–594.

Van Der Eem, J.G.L.A. 1983. Aspects of middle and late Triassic palynology. 6. Palynological investigations in the Ladinian and lower Karnian of the Western Dolomites Italy. *Review of Palaeobotany and Palynology*, 39(3–4), 189–300

Van Erve, A.W. 1977. Palynological investigation in the lower Jurassic of the Vicentinian Apls (Northeastern Italy). *Review of Palaeobotany and Palynology*, 23, 1 –117.

Van Gijzel, P. 1975. Polychromatic UV-fluorescence microscope-photometry of fresh and fossil plant substances with special reference to the location and identification of dispersed organic material in rocks. In: Alpern, B. (Ed.), Pétrographie de la matière organique des sédiments, relations avec la paleotemperature et le potentiel pétrolier. *Colloque International, Centre National de la Recherche Scientifique, Paris*, 67-91.

Van Gijzel, P. 1979. Manual of the Techniques and Some Geological Applications of Fluorescence Microscopy. *American Association of Stratigraphical Palynologists Foundation, Dallas*.

Verati, C., Rapaille, C., Féraud, G., Marzoli, A., Bertrand, H., Youbi, N. 2007. 40Ar/39Ar ages and duration of the Central Atlantic Magmatic Province volcanism in Morocco and Portugal and its relation to the Triassic–Jurassic boundary. *Palaeogeography, Palaeoclimatology, Palaeoecology*, 244(1-4), 308-325.

Vigran, J. O., Mangerud, G., Mørk, A., Worsley, D., Hochuli, P. A., 2014. Palynology and geology of the Triassic succession of Svalbard and the Barents Sea. Geological Survey of Norway, Special Publication no. 14, 247 pp.

Vilas-Boas, M., Paterson, N.W., Pereira, Z., Fernandes, P., Cirilli, S. 2022. The age of the first pulse of continental rifting associated with the breakup of Pangea in Southwest Iberia: new palynological evidence. *Journal of Iberian Geology*, 48(2), 181-190.

Vilas-Boas, M., Pereira, Z., Cirilli, S., Duarte, L.V., Fernandes, P. 2021. New data on the palynology of the Triassic–Jurassic boundary of the Silves Group, Lusitanian Basin, Portugal. *Review of Palaeobotany and Palynology*, 290, 104426.

Visscher, H., Brugman, W.A. 1981. Ranges of selected palynomorphs in the Alpine Triassic of Europe. *Review of Palaeobotany and Palynology*, 34(1), 115-128.

Visscher, H., Krystyn, L. 1978. Aspects of Late Triassic palynology. 4. A palynological assemblage from ammonoid-controlled Late Karnian (Tuvalian) sediments of Sicily. *Review of Palaeobotany and Palynology*, 26(1-4), 93-112.

Visscher, H., Looy, C.V., Collinson, M.E., Brinkhuis, H., van Konijnenburg-van Cittert, J.H.A., Kürschner, W.M., Sephton, M.A. 2004. Environmental mutagenesis during the end-Permian ecological crisis. *Proceedings of the National Academy of Sciences*, 101, 12952–12956.

Visscher, H., Schuurman, W.M.L., Van Erve, A.W. 1980. Aspects of a palynological characterization of Late Triassic and Early Jurassic 'Standard' units of chronostratigraphical classification in Europe. *Proceedings IV International Palynological Conference, Lucknow*, 2, 281–287.

Warrington, G. 2002. Triassic spores and pollen. In: Jansonius, J. & Mcgregor, D. C. (eds) Palynology: Principles and Applications. *American Association of Stratigraphic Palynologists Foundation*, 2nd edition, 2, 755-766.

Warrington, G., Cope, J.C.W., Ivimey-Cook, H.C. 2008. The St Audrie's Bay–Doniford Bay section, Somerset, England: updated proposal for a candidate global stratotype section and point for the base of the Hettangian Stage, and of the Jurassic System. *International Subcommission on Jurassic Stratigraphy Newsletter*, 35, 2-66.

Wellman, C., Gray, J. 2000. The microfossil record of early land plants. Philosophical *Transactions of the Royal Society of London,* serie B, 355, 717-732.

Whiteside, J.H., Olsen, P.E., Eglinton, T., Brookfield, M.E., Sambrotto, R.N. 2010. Compound-specific carbon isotopes from earth's largest flood basalt eruptions directly linked to the end-Triassic mass extinction. *Proceedings of the National Academy of Sciences,* 107(15), 6721-6725.

Whiteside, J.H., Olsen, P.E., Kent, D.V., Fowell, S.J., Et-Touhami, M. 2007. Synchrony between the Central Atlantic magmatic province and the Triassic–Jurassic mass extinction event?. *Palaeogeography, Palaeoclimatology, Palaeoecology*, 244, 345–367.

Wilson, M., Giraud, R. 1998. Late Permian to recent magmatic activity on the African–Arabian margin of Tethys. In: Macgregor, D., Moody, R., Clark-Lowes, D. (Eds.), Petroleum Geology of North Africa. *Geological Society, London, Special Publications,* vol. 132, pp. 231–263.

Wilson, R.C.L. 1975. Atlantic opening and Mesozoic continental margin basins of Iberia. *Earth and Planetary Science Letters*, 25(1), 33-43.

Wood, G.D., Gabriel, A.M., Lawson, J.E. 1996. Palynological techniques processing and microscopy. In: Jansonius, J., McGregor, D.C. (Eds.), Palynology: Principles and applications. 1. *American Association Stratigraphic Palynology Foundation*, 29-50.

Yaroshenko, O.P. 2007. Late Triassic palynological flora from Western Ciscaucasia. *Paleontological Journal,* 41, 1190-1197.

APPENDICES

Appendix 1: list of palynomorphs

This is a list of all palynomorphs taxa which were recovered from the material of both basins studied herein, or mentioned in the text, with full author citations. The taxa are listed alphabetically in three groups, spores, pollen and algae. Are also provided the reference to the plates where each taxon is illustrate in this work. Note the plates from the Appendix 2 are labelled with Roman numerals and appear after the plates presented in the chapters.

Spores:

Anapiculatisporites sp. [Plate V.II (18)]

Apiculatisporis sp.

Calamospora mesozoica Couper, 1958 [Plate V.II (11), (12); Plate III (6)]

Calamospora tener (Leschik 1955) Mädler, 1964 [Plate IV.I (1), (2); Plate V.II (13); Plate II (1)]

Calamospora sp. [Plate III.I (1)]

Camarozonosporites sp.

Carnisporites spiniger (Leschik) Morbey, 1975 [Plate IV.I (3); Plate V.II (19); Plate II (6)]

Carnisporites sp.[Plate II.IV (2); Plate IV.I (4); Plate II (2)]

Cibotiumspora sp. [Plate II.II (6); Plate IV.I (5); Plate II (8)]

Cingulatisporis sp.

Conbaculatisporites sp. [Plate III.I (2); Plate III (2)]

Converrucosisporites sp. [Plate III.I (3)]

Convolutispora sp. [Plate IV.I (11)]

Cyathidites sp. [Plate II.III (6); Plate II (3)]

Deltoidospora hallii Miner, 1935

Deltoidospora toralis (Leschick) Lund, 1977 [Plate V.II (15); Plate III (1)]

Deltoidospora sp. [Plate II.IV (1); Plate III.I (4); Plate IV.I (6); Plate V.II (16)]

Dictyophyllidites mortonii (de Jersey) Playford & Dettman 1965 [Plate II.II (5); Plate II (9)]

Dictyophyllidites sp.

Foveosporites foveoreticulatus Dring, 1965

Foveosporites sp.

Ischyosporites variegatus (Couper 1958) Schulz, 1967 [Plate II.II (4); Plate II.IV (3); Plate IV.I (7); Plate II (7), (10)]

Ischyosporites sp.

Kraeuselisporites reissingeri (Harris, 1957) Morbey, 1975 [Plate II.III (7), (8), (9); Plate IV.I (8), (9); Plate II (4), (5)]

Kraeuselisporites sp. [Plate V.II (20)]

Kyrtomisporis sp. [Plate IV.I (10); Plate V.II (21)]

?Klausipollenites sp. [Plate III.I (12)]

Leiotriletes directus Balme & Hennelly 1956

Leptolepidites argaenteaeformis (Bolkhovitina) Morbey, 1975 [Plate V.II (17)]; Plate III (5)]

Leptolepidites sp. [Plate II.IV (4)]

Lycopodiacidites rugulatus (Couper) Schulz, 1967 [Plate III.I (5); Plate III (4)]

Playfordiaspora sp. [Plate II.I (7); Plate V.II (14)]

Polypodiisporites sp. [Plate II.IV (8)]

Porcellispora longdonensis (Clarke) Scheuring emend. Morbey 1975 [Plate II.IV (9); Plate IV.I (12); Plate II (11)]

Retitriletes austroclavatidites (Cookson) Doring *et al*., 1963 in Krutzsch, 1963

Todisporites major Couper, 1958

Todisporites sp.

Trachysporites fuscus Nilsson, 1958

Trachysporites sp.

Uvaesporites sp.

Verrucosisporites sp. [Plate III.I (7)]

Pollen:

Alisporites diaphanus (Pautsch, 1958) Lund, 1977 [Plate V.I (5)]

Alisporites sp. [Plate II.II (3); Plate III.I (8); Plate V.I (4); Plate I (3)]

Araucariacites australis Cookson, 1947 [Plate V.I (18)]

Araucariacites sp. [Plate II.III (5); Plate IV.II (1); Plate V.I (19), (20)]

Aulisporites astigmosus (Leschik, 1956) Klaus, 1960 [Plate III.I (9); Plate III (9)]

Camerosporites secatus Leschik, 1956 emend. Scheuring, 1978 [Plate V.I (24); Plate III (19)]

Cerebropollenites macroverrucosus (Thiergart) Schulz, 1967 [Plate V.II (10); Plate III (20)]

Cerebropollenites sp. [Plate V.II (6), (7), (8), (9)]

Chasmatosporites sp.

Classopollis meyerianus (Klaus) de Jersey 1973 [Plate II.II (9); Plate II.V (7); Plate IV.II (2), (7); Plate V.II (1); Plate I (11)]

Classopollis torosus Reissinger 1950 [Plate II.III (3), (4); Plate II.V (4), (5), (6), (8); Plate IV.II (4); Plate V.II (3); Plate I (12)]

Classopollis sp. [Plate V.II (2)]

Cycadopites sp. [Plate II.III (1), (2); Plate III.I (10); Plate IV.II (3); Plate V.II (4)]

Duplicisporites granulatus Leschik, 1955 emend. Scheuring, 1970 [Plate II.II (2); Plate I (9)]

Ellipsovelatisporites sp.

Enzonalasporites vigens Leschik, 1956 emend. Scheuring 1970 [Plate II.I (5); Plate III.I (11); Plate V.I (9), (10); Plate I (6); Plate III (11), (12)]

Ephedripites sp. [Plate V.II (5)]

Eucommiidites sp.

Granuloperculatipollis rudis Venkatachala & Góczán emend. Morbey 1975 [Plate II.I (4); Plate I (7)]

Inaperturopollenites sp.

Lagenella martinii (Leschik, 1956) Klaus, 1960

Microcachrydites doubingeri Klaus 1964 [Plate II.I (8)]

Microcachrydites fastidioides (Jansonius) Klaus 1964 [Plate II.I (10)]

Microcachrydiites sp. [Plate V.I (2), (3)]

Monosulcites sp.

Nevesisporites cf. vallatus Jersey & Paten, 1964 [Plate III.I (6); Plate III (3)]

Ovalipollis ovalis Krutzsch 1955

Ovalipollis pseudoalatus Krutzsch, 1955 [Plate III.I (13); Plate III (8)]

Paracirculina quadruplicis Scheuring 1970 [Plate II.I (1), (2); Plate II.V (9); Plate V.I (15), (16), (17); Plate III (10)]

Paracirculina sp.

Patinasporites densus Leschik emend. Scheuring 1970 [Plate V.I (11), (12); Plate I (4); Plate III (17)]

Perinopollenites elatoides Couper 1958 [Plate II.IV (6), (7); Plate IV.II (6); Plate V.I (21), (22), (23); Plate I (8); Plate III (18)]

Pinuspollenites minimus (Couper) Kemp 1970 [Plate IV.II (5); Plate I (1)]

Praecirculina granifer (Leschik) Klaus 1960 [Plate II.I (11)]

?Protodiploxypinus sp. [Plate III.I (14)]

Rhaetipollis germanicus Schulz 1967 [Plate II.II (7), (8); Plate I (10)]

Samaropollenites speciosus Goubin, 1965 [Plate II.I (3): Plate III.I (15); Plate V.I (1); Plate I (2)]

Triadispora staplini (Jansonius) Klaus 1964 [Plate II.I (9)]

Triadispora sp. [Plate V.I (6), (7), (8); Plate III (7)]

Tulesporites briscoensis Dunay & Fischer, 1979 [Plate III.I (16), (17); Plate III (13), (14)]

Vallasporites ignacii Leschik, 1956 emend. Scheuring, 1970 [Plate II.II (1); Plate III.I (18), (19), (20); Plate V.I (13), (14); Plate I (5); Plate III (15), (16)]

Algae:

Algae sp. A [Plate V.III (7)]

Botryococcus sp. [Plate V.III (9)]

Leiosphaeridia spp. [Plate V.III (5)]

?Ourasphaira giraldae [Plate V.III (12), (13), (14)]

Ovoidites sp. [Plate V.III (6)]

Plaesiodictyon mosellanum ssp*. bullatum* Willie, 1970

Plaesiodictyon mosellanum ssp*. variable* Willie, 1970 [Plate V.III (1), (2), (3), (4)]

Plaesiodictyon sp.

Appendix 2: catalogue with the biostratigraphical significant palynomorphs

Selected palynomorphs from the Upper Triassic to Lower Jurassic (Carnian to Hettangian) of the Lusitanian and Algarve basins, are presented in the Plates I to IV and are organized by basin. This appendix aims to bring together the data obtained from the Lusitanian and Algarve basins, and represent through photographs, in a summarized form, the typical and most important taxa for the Triassic - Jurassic in Portugal. Plate I present pollen grains from Lusitanian Basin and Plate II illustrates spores from Lusitanian Basin. Plate III shows pollen grains and spores from the Algarve Basin and in Plate IV is presented aquatic material from both basins.

This species are housed in the collections of CIMA-UAlg, Faro, Portugal and LNEG (Portuguese Geological Survey), S. Mamede de Infesta, Portugal. The outcrop, sample number, slide number and microscope coordinates are provided. All the scale bars represent 50 μm.

Plate I. Selected pollen grains from the Silves Group in the Lusitanian Basin.

1. *Pinuspollenites minimus* (Couper) Kemp, 1970; Outcrop Lamas, sample LAM 8, slide 4, MC 1175-162.

2. *Samaropollenites speciosus* Goubin, 1965; Outcrop Parque de Campismo, sample PC2, slide 9, MC 1542-181.

3. *Alisporites* sp.; Outcrop Parque de Campismo, sample PC2, slide 9, MC 1478-20

4. *Patinasporites densus* Leschik emend. Scheuring, 1970; Outcrop Parque de Campismo, sample PC1, slide 7, MC 1149-50.

5. *Vallasporites ignacii* Leschik, 1955; Outcrop Parque de Campismo, sample PC1, slide 7,MC 1078-98.

6. *Enzonalasporites vigens* Leschik emend. Scheuring, 1970; Outcrop Parque de Campismo, sample PC2, slide 9, MC 1475-213.

7. *Granuloperculatipollis rudis* Venkatachala & Góczán emend. Morbey, 1975; Outcrop Alto de São João, sample ASJ2, slide 1, MC 1449-250.

8. *Perinopollenites elatoides* Couper, 1958; Outcrop Lamas, sample LAM 12, slide 4, MC 1420-80.

9. *Duplicisporites granulatus* Leschik, 1955 emend. Scheuring, 1970; Outcrop Parque de Campismo, sample PC2, slide 9, MC 1261-250.

10. Rhaetipollis germanicus Schulz, 1967; Outcrop Lordemão, sample LAG27b, slide 4, MC 1255-128.

11. *Classopollis meyerianus* (Klaus) de Jersey, 1973; Outcrop Lamas, sample LAM 6, slide 1, MC 1520-100.

12. *Classopollis torosus* Reissinger, 1950; Outcrop Lamas, sample LAM12, slide 3, MC 1370-215.

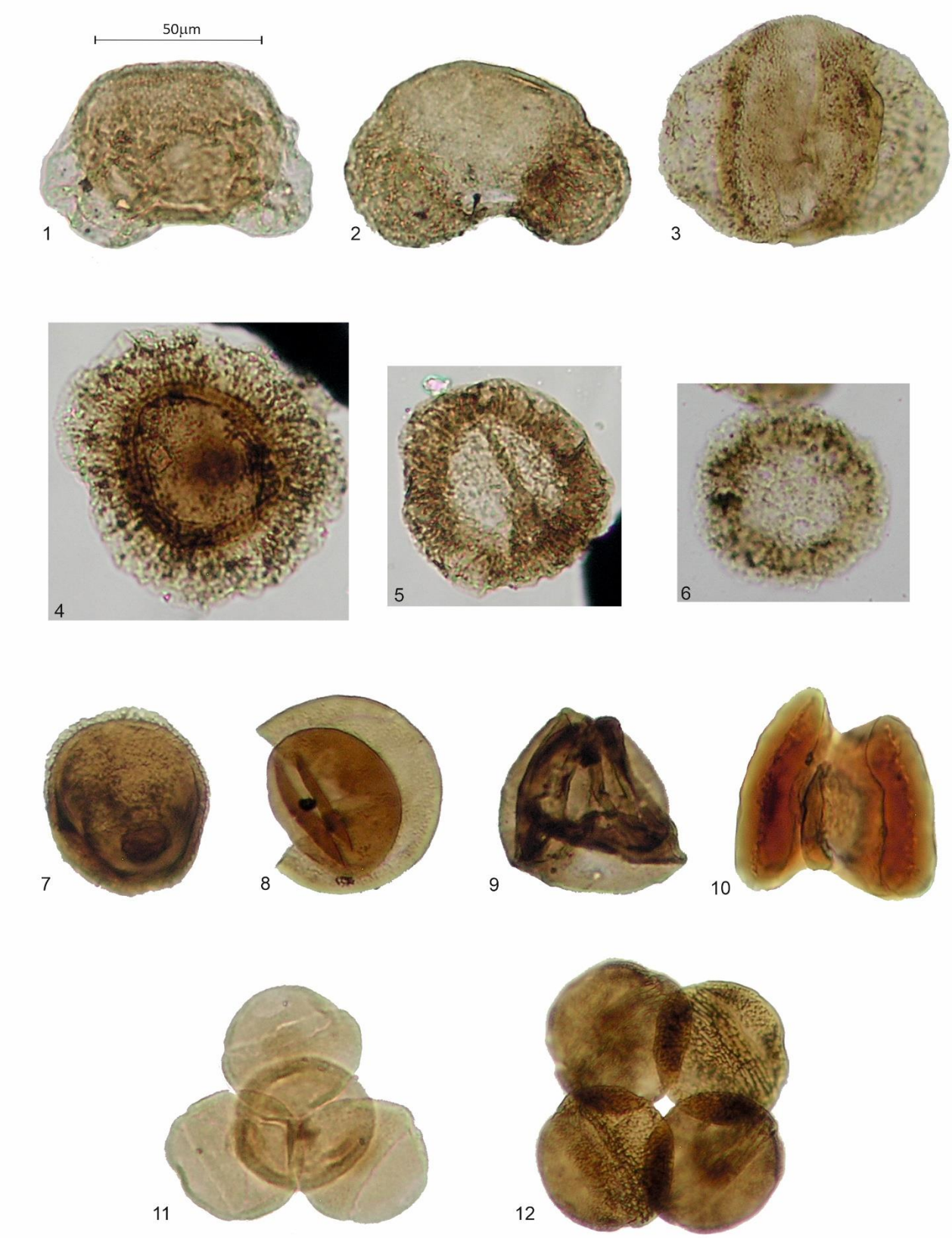

Plate I (caption in the previous page)

Plate II. Selected spores from the Silves Group in Lusitanian Basin.

1. *Calamospora tener* (Leschik) Mädler 1964, Outcrop Lamas II, sample LAM 1; slide 2, MC 1130-115.

2. *Carnisporites* sp.; Outcrop Lamas, sample LAM 12, slide 3, MC 1380-75.

3. *Cyathidites* sp.; Outcrop Lamas, sample LAM 1, slide 3, MC 1415-215.

4. *Kraeuselisporites reissingeri* (Harris, 1957) Morbey, 1975; Outcrop Lamas, sample LAM 6, slide 1, MC 1470-130.

5. *Kraeuselisporites reissingeri* (Harris, 1957) Morbey, 1975; Outcrop Lamas, sample LAM 12, slide 1, MC 1190-210.

6. *Carnisporites spiniger* (Leschile) Morbey, 1975 sp., Outcrop Lamas I, sample LAMAS 8/9; slide 1, MC 1309-1055.

7. *Ischyosporites variegatus* (Couper) Schulz, 1967; Outcrop Lordemão, sample LAG 27b, slide 7, MC 1339-156.

8. *Cibotiumspora* sp., Outcrop Lamas I, sample LAMAS 10/11; slide 1, MC 1281-209.

9. *Dictyophyllidites mortonii* (Jersey) Playford & Dettmann, 1965; Outcrop Lordemão, sample LAG 27b, slide 7,MC 1329-141.

10. *Ischyosporites variegatus* (Couper) Schulz, 1967; Outcrop Castelo Viegas II, sample CVII-3, slide 2, MC 1243-143

11. *Porcellispora longdonensis* (Clarcke) Scheuring emend. Morbey, 1975; Outcrop Carvalhais, sample CARVA 1B, slide 7, MC 1300-170.

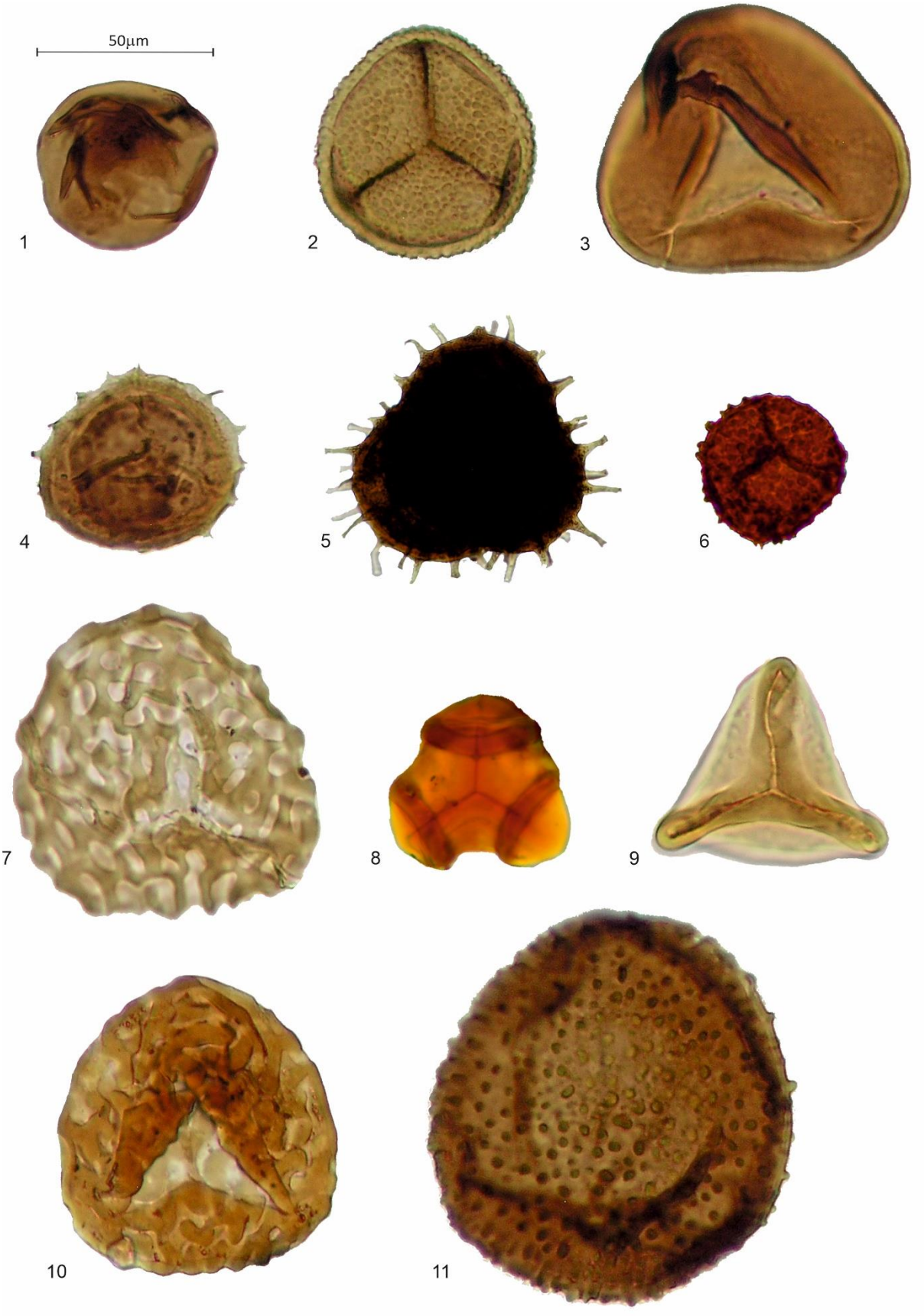

Plate II (caption in the previous page)

Plate III. Selected spores (1-6) and pollen grains (7-20) from the Silves Group in the Algarve Basin.

1. *Deltoidospora toralis* (Leschick) Lund, 1977, Outcrop Mina Sal-Gema, samples MSGvd7, slide 1F, EF T42.
2. *Conbaculatisporites* sp., Outcrop Autódromo, sample AUTO3, slide A, EF T47|3.
3. *Nevesisporites cf. vallatus* Jersey & Paten, 1964, Outcrop Autódromo, sample AUTO3, slide C, EF K36|1.
4. *Lycopodiacidites rugulatus* (Couper) Schulz, 1967, Outcrop Autódromo, sample AUTO3, slide B, EF R31.
5. *Leptolepidites argaenteaeformis* (Bolkhovitina) Morbey, 1975, Outcrop Mina Sal-Gema, samples MSGvd7, slide 1F, EF M27|2.
6. *Calamospora mesozoica* Couper, 1958, Outcrop Mina Sal-Gema, sample MSGvd6, slide F, EF L19.
7. *Triadispora sp.,* Outcrop Amorosa, sample Amorosa4(-20cm), slide 1, EF R28.
8. *Ovalipollis pseudoalatus* Krutzsch, 1955, Outcrop Autódromo, sample AUTO3, slide C, EF E51|2.
9. *Aulisporites astigmosus* (Leschik, 1956) Klaus, 1960, Outcrop Autódromo, sample AUTO3, slide c, EF J47|2.
10. *Paracirculina quadruplicis* Scheuring, 1970, Outcrop Amorosa, sample Amorosa4(-20cm), slide 1, EF N25.
11. *Enzonalasporites vigens* Leschik, 1956 emend. Scheuring, 1970, Outcrop Autódromo, sample AUTO3, slide A, EF D46|2.
12. *Enzonalasporites vigens* Leschik, 1956 emend. Scheuring, 1970, Outcrop Praia do Amado, sample AM15, slide 1Z, EF O16.
13. *Tulesporites briscoensis* Dunay and Fischer, 1979, Outcrop Autódromo, sample AUTO3, slide A, EF Q47.
14. *Tulesporites briscoensis* Dunay and Fischer, 1979, Outcrop Autódromo, sample AUTO3, slide A, EF J42|2.
15. *Vallasporites ignacii* Leschik, 1956 emend. Scheuring, 1970, Outcrop Autódromo, sample AUTOB5(+ 0,90), EF K30.
16. *Vallasporites ignacii* Leschik, 1956 emend. Scheuring, 1970, Outcrop Autódromo, sample AUTO3, slide A, EF Y41|2.
17. *Patinasporites densus* Leschik emend. Scheuring 1970, Outcrop Praia do Amado, sample AM16, slide 1Z, EF J46.
18. *Perinopollenites elatoides* Couper 1958, Outcrop Mina Sal-Gema, sample MSGvd6, slide 1F, EF M38|3.
19. Camerosporites secatus Leschik, 1956 emend. Scheuring, 1978, Outcrop Praia do Amado, sample AM15, slide 1, EF O22|3.
20. *Cerebropollenites macroverrucosus* (Thiergart) Schulz, 1967 Outcrop Mina Sal-Gema, sample 6, slide F, EF O20|3.

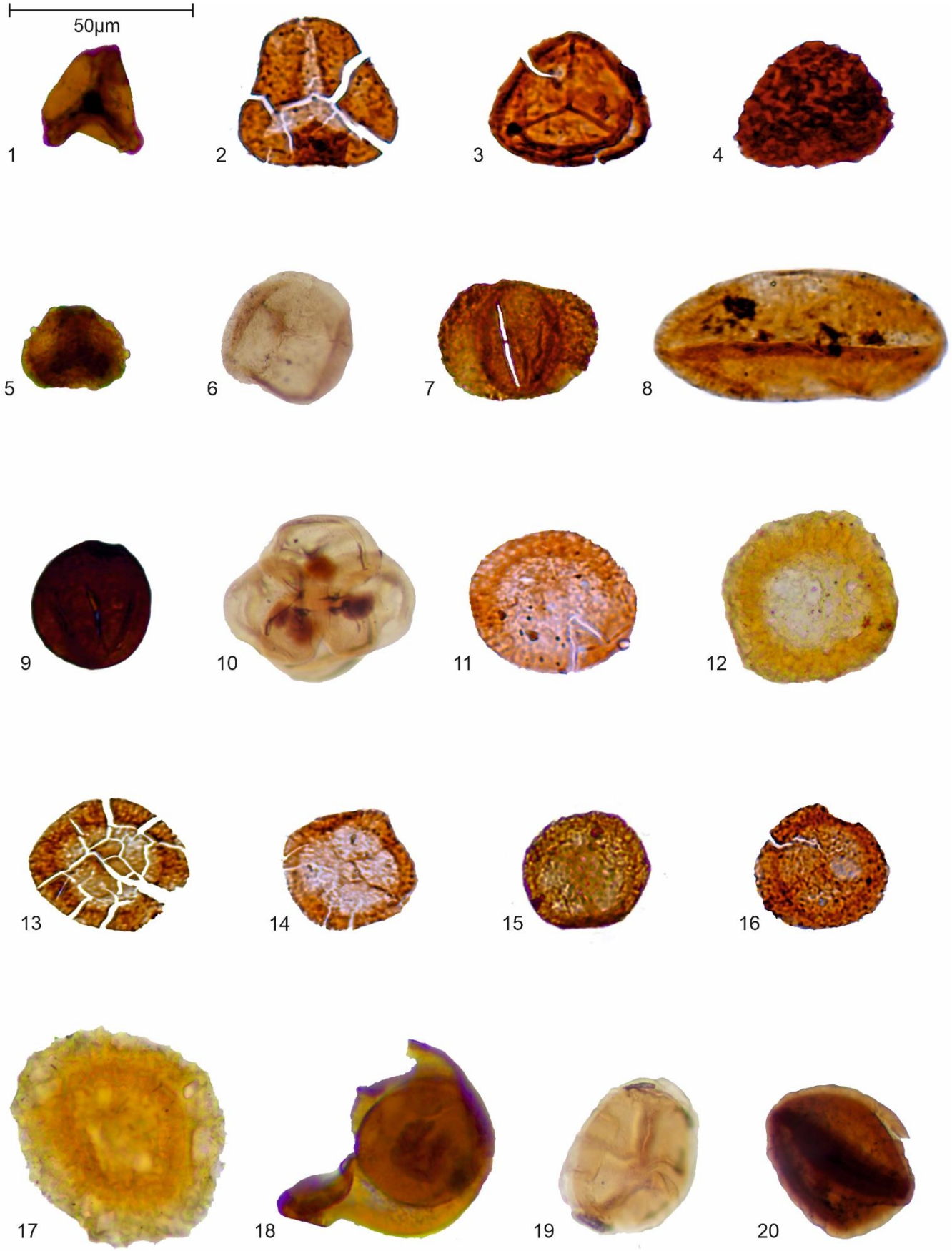

Plate III (caption in the previous page)

Plate IV. Selected aquatic palynomorphs from Lusitanian Basin (1-2) and Algarve Basin (3-11).

1. Foraminiferal lining, Outcrop Lamas I, sample LAMAS 10/11; slide 1 (1203-90).

2. Foraminiferal lining, Outcrop Lamas I, sample LAMAS 10/11; slide 1 (1201-171).

3. *Plaesiodictyon mosellanum* spp. *variable* Willie, 1970, Outcrop Praia do Amado, sample AM15, slide 1, EF O34.

4. *Plaesiodictyon mosellanum* spp. *variable* Willie, 1970, Outcrop Praia do Amado, sample AM15, slide 1Z, EF O37|3.

5. *Leiosphaeridia* sp., Outcrop Praia do Amado, samples AM15, slide 1, EF H17|4.

6. *Ovoidites* sp., Outcrop Praia do Amado, sample AM15, slide 1, EF P27.

7. Fungal Remains, Outcrop Praia do Amado, samples AM15, slide 1Z, EF T38|2.

8. Algae sp. A, Outcrop Praia do Amado, sample AM15, slide 1, EF K39|4.

9. ?*Ourasphaira giraldae* Loron, 2019, Outcrop Mina Sal-Gema, sample MSG1, slide 1, EF R28|1.

10. ?*Ourasphaira giraldae* Loron, 2019, Outcrop Mina Sal-Gema, sample MSG1, slide 1, EF L41|3.

11.?Scolecodont, Outcrop Praia do Amado, sample AM15, slide 1, EF E32.

12.?Scolecodont, Outcrop Praia do Amado, sample AM15, slide 1, EF M43.

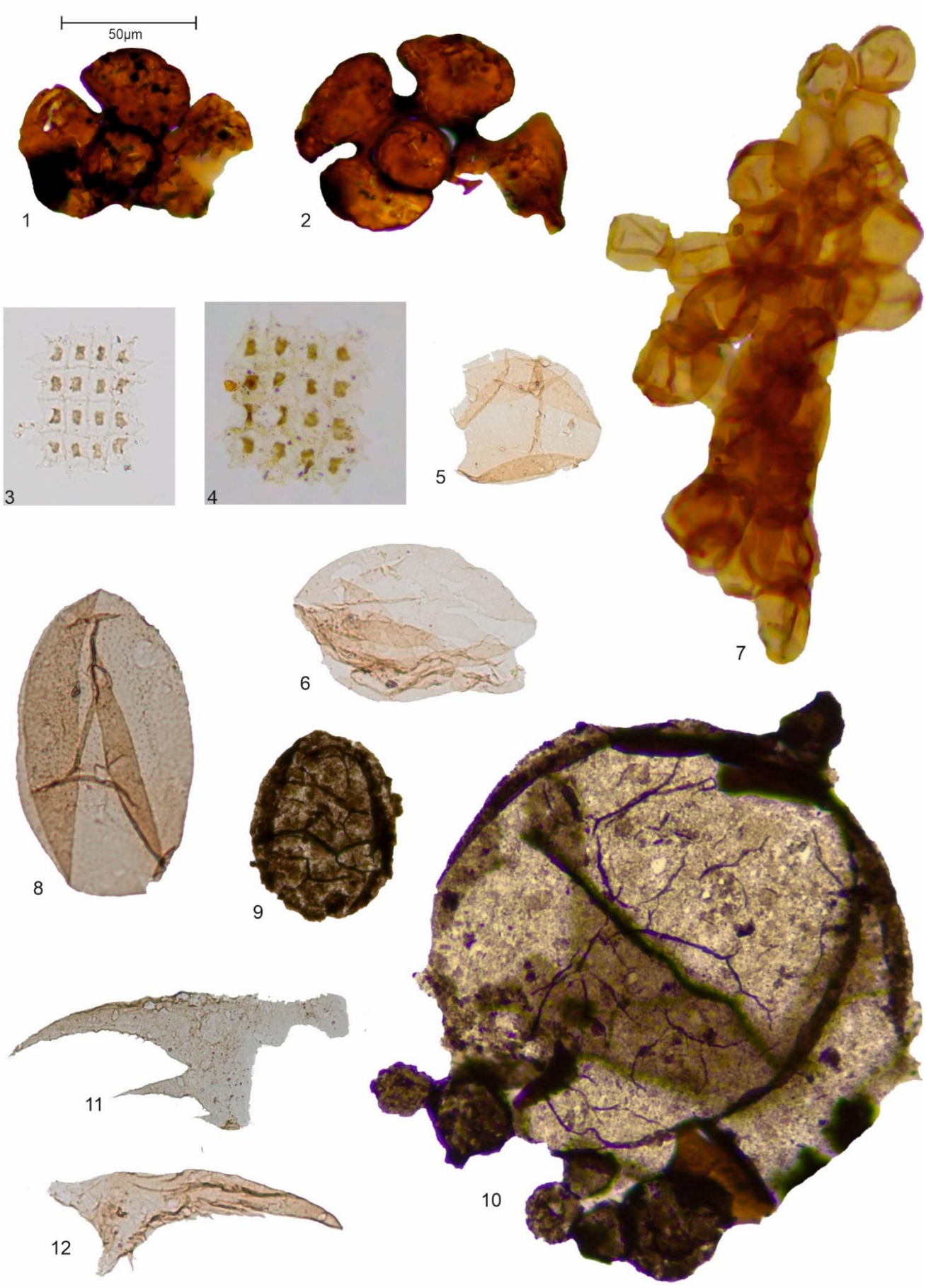

Plate IV (caption in the previous page)